National
Oceanography Centre
NATURAL ENVIRONMENT RESEARCH COUNCIL

National Oceanography Centre

Cruise Report No. 16

RRS *Discovery* Cruise 346

05 JAN – 19 FEB 2010

The 2010 transatlantic hydrography section at 24.5°N

Principal Scientist
B A King

Editor
D R C Hamersley

2012

National Oceanography Centre, Southampton
University of Southampton Waterfront Campus
European Way
Southampton
Hants SO14 3ZH
UK

Tel: +44 (0)23 8059 6438
Email: b.king@noc.ac.uk

DOCUMENT DATA SHEET

AUTHOR

KING, B A et al

PUBLICATION DATE 2012

TITLE

RRS *Discovery* Cruise 346, 05 Jan - 19 Feb 2010. The 2010 transatlantic hydrography section at 24.5°N.

REFERENCE

Southampton, UK: National Oceanography Centre, Southampton, 177pp. (National Oceanography Centre Cruise Report, No. 16)

ABSTRACT

A Hydrographic section was occupied at a nominal latitude of 24.5°N in the Atlantic Ocean during January - February 2010 on Cruise 346 of RRS *Discovery*. The primary objective of this cruise was to measure ocean physical, chemical and biological parameters in order to establish regional budgets of heat, freshwater and carbon, and to infer decadal variability.

A total of 135 CTD/LADCP stations were sampled, with two additional bottle blank stations. In addition to temperature, salinity and oxygen profiles from the sensors on the CTD package, water samples from a 24 x 20 litre rosette were analysed for salinity, dissolved oxygen and inorganic nutrients at each station. Water samples were collected from strategically selected stations and analysed onboard ship for SF_6, CFCs, DIC, alkalinity, and filtering. In addition, samples were collected from the ships' underway system to calibrate and compliment the data continually collected by the TSG (thermosalinograph). Full depth velocity measurements were made at every station by LADCP (Lowered Acoustic Doppler Current Profiler) mounted on the frame of the rosette. Throughout the cruise, velocity data in the upper few hundred metres of the water column were collected by the ship's VMADCP (Vessel Mounted Acoustic Doppler Current Profiler) transducers (75Hz and 150Hz) mounted on the hull. Meteorological variables were monitored using the onboard surface water and meteorological sampling system (SURFMET). Bathymetric data was collected using the EA600 echo sounder, which is attached to the hull. However, whilst steaming it was found that switching over to the fish instrument produced a cleaner dataset.

This report describes the methods used to acquire and process the data on board the ship during cruise D346.

KEYWORDS

ADCP, Atlantic Ocean, carbon, CFC, circulation, cruise D346 2010, CTD, Discovery, Lowered ADCP, Meridional Overturning Circulation, meteorology, MOC, nutrients, oxygen, shipboard ADCP

ISSUING ORGANISATION **National Oceanography Centre**
University of Southampton Waterfront Campus
European Way
Southampton SO14 3ZH UK
Tel: +44(0)23 80596116 Email: nol@noc.soton.ac.uk

Page intentionally left blank

Contents

List of Figures

List of Tables

Scientific Personnel

Name	Role	Affiliation
Brian King	Principal Scientist	NOCS
Gerard McCarthy	Physics	NOCS
David Hamersley	Physics	NOCS
Chris Atkinson	Physics	NOCS
Gavin Evans	Physics	NOCS
Helen Pillar	Physics	Oxford University
Ben Webber	Physics	UEA
Chris Banks	Physics	NOCS
Sinhue Torres Valdes	Nutrients & Oxygen	NOCS
Ekaterina Chernyavskaya	Nutrients & Oxygen	Arctic and Antarctic Research Institute, St. Petersburg
Claire Powell	Nutrients & Oxygen	UEA
Laura Casburn	Nutrients & Oxygen	NOCS
Helen Smith	Nutrients & Oxygen	NOCS
Francois-Eric Legiret	Nano-nutrients	NOCS
David Honey	Biology	NOCS
Ute Schuster	Carbon	UEA
Adriaan Louwerse	Carbon	UEA
Gareth Lee	Carbon	UEA
Oliver Legge	Carbon	NOCS
Marie-Jose Messias	CFC	UEA
Peter Brown	CFC	UEA
Stephen Woodward	CFC	UEA
Andrew Brousseau	CFC	UEA

NOCS = National Oceanography Centre Southampton
UEA = University of East Anglia
NMF= National Marine Facilities

Technical Personnel

Paul Duncan	Technician	NMF
Peter Keen	Technician	NMF
Alan Sherring	Technician	NMF
David Teare	Technician	NMF

Ships Personnel

Name	Rank
William Richardson	MASTER
John Leask	C/O

Iain Macleod	2/O
Richard Callender	3/0
Peter Griffin	CH/ENG
Stephen Bell	2/E
Gary Slater	3/E
Geraldine O'Sullivan	3/E
Dennis Jakobaufderstroht	ETO
Graham Bullimore	PCO
Greg Lewis	CPOD
John Smyth	ERPO
Mark Squibb	CPOS
Philip Allison	POD
John Brodowski	SG1A
Colin Birthwhistle	SG1A
Mark Duthie	SG1A
Philip Alford	SG1A
Mark Preston	H/CHEF
Lloyd Sutton	Chef
Jacqueline Waterhouse	STWD

Acknowledgments

It is a pleasure for the Principal Scientist to acknowledge the outstanding contributions by the ship's and scientific personnel. Over a long cruise, the Deck Officers efficiency in station keeping saves enough time for many extra stations; The deck crew managed overside operations with minimal interruptions, and the CPOS and CPOD ensured winch operations were smooth and efficient apart from the winch system failures documented elsewhere. The 2/E Officer and ETO kept the winch operational, without which the cruise could not have proceeded. While there were many important individual contributions on the technical side, none was more critical than Paul Duncan's simulation of the failed CLAM system, without which the cruise would have been terminated after less than a week. The Engineer Officers came up with an ingenious solution to the problem of waste management and local port regulations. This enabled *Discovery* to dock in Lisbon and use sea freight to transfer equipment to RRS *James Clark Ross*, thereby saving the logistical nightmare of transhipment by air freight. The combined effort of the entire scientific party enabled a complete dataset to be uploaded to the international data centre the day after the cruise ended. This is a unique achievement for a UK cruise of which all contributors should be proud, and was a result of the sustained efforts by sample analysts and data processors throughout. The Principal Scientist noted that the catering was of a high standard throughout, but particularly so on the occasion of his 50th birthday party. Finally the Principal Scientist is particularly indebted to David Hamersley, who assembled and edited this report, and to the Master, for his leadership, support and cooperation throughout his first major expedition with NERC.

Background and Objectives

RRS *Discovery* Cruise 346 was a repeat occupation of the Atlantic hydrographic section at a nominal latitude of 24.5°N. As such it will enable the study of decadal variability, of the present circulation, and the present transports of heat, freshwater, and biogeochemical tracers. The previous occupations of this line include *Discovery* Cruise D279 (2004), *Ronald H Brown* (1998) and *Hesperides* HE06 (1992). The cruise was a contribution to the CLIVAR/GO-SHIP repeat hydrography program, and end-of-cruise data have been submitted to the CLIVAR and Carbon Hydrographic Data Office (CCHDO).

The data collected during D346 came from four main scientific teams, physics, chemistry (nutrients and oxygen), carbon, and CFCs.

Summary

In total 137 CTDO (conductivity-temperature-depth-oxygen) stations were occupied. Two of these stations (assigned 200 and 202) were bottle blank stations run for the CFC team. Therefore, 135 stations comprised the principal data collected along the 24.5°N section.

A 24-bottle rosette, with 20 litre externally-sprung Niskin bottles, was used to take water samples at CTD stations. Samples were analysed for salinity, dissolved oxygen, inorganic and organic nutrients, carbon system and CFCs. Nanonutrient and biological samples were drawn and analysed as guest projects. A suite of instruments was mounted on the underwater package, including LADCP (Lowered acoustic Doppler current profiler), fluorometer, transmissometer, and altimeter for near-bottom detection. Those instruments not pressure rated below 6000m were removed for the duration of the deepest casts. Therefore data for certain parameters (LADCP, fluorometer and transmissometer) are unavailable for these stations. There were several problems with malfunctioning sensors (LADCPs, conductivity sensors, and an oxygen sensor), which are discussed in the CTD technicians' report (Section 1). In particular three out of four conductivity sensors failed before the midpoint of the cruise. In addition, the winch telemetry logging and display system (CLAM) failed early in the cruise so software had to be written in order to maintain a log and display of the wire-out and wire tensions. This is also discussed in further detail in Section 1 and Section 8.3. Continuous underway data were collected from the VMADCP (vessel mounted ADCP), thermosalinograph (TSG), the SURFMET system, multiple navigation sources, and the Simrad single-point precision echo sounder.

Itinerary and Cruise Track

Depart from Freeport, Bahamas, 5th January 2010 – arrive in Lisbon, Portugal, 19th February 2010.

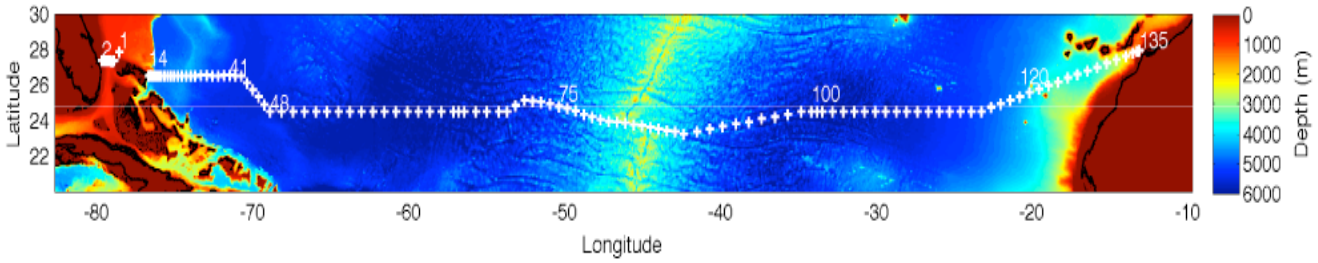

Figure 1: Station positions across the North Atlantic basin for Cruise D346 highlighted by white crosses.

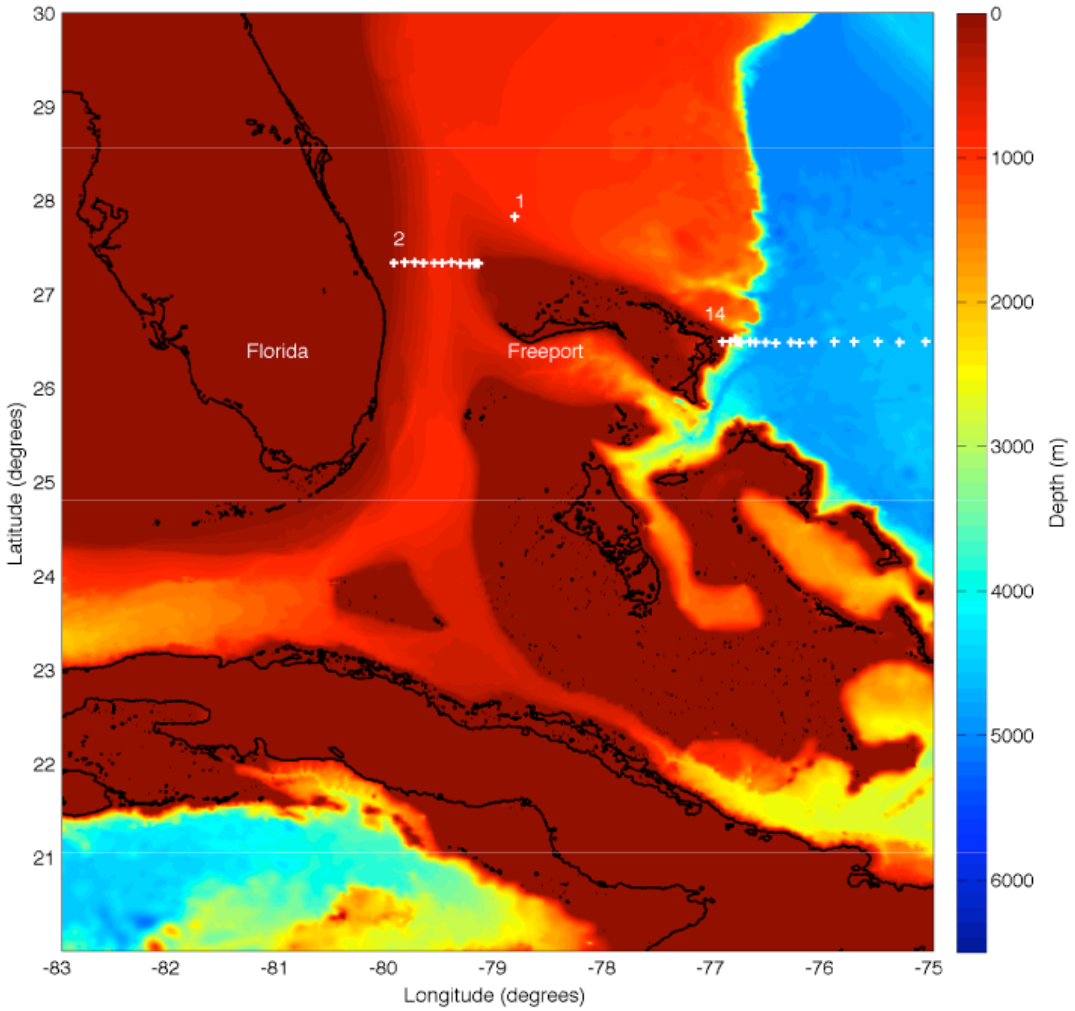

Figure 2: Western Boundary of the Atlantic Basin where Cruise D346 began

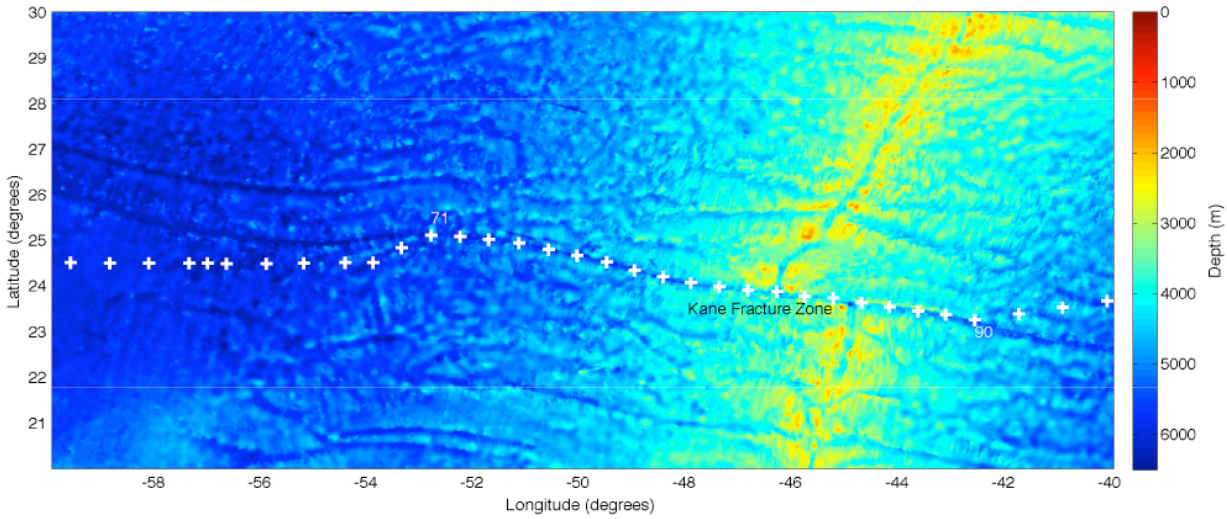

Figure 3: A focused view of the sampling scheme along the Kane Fracture Zone

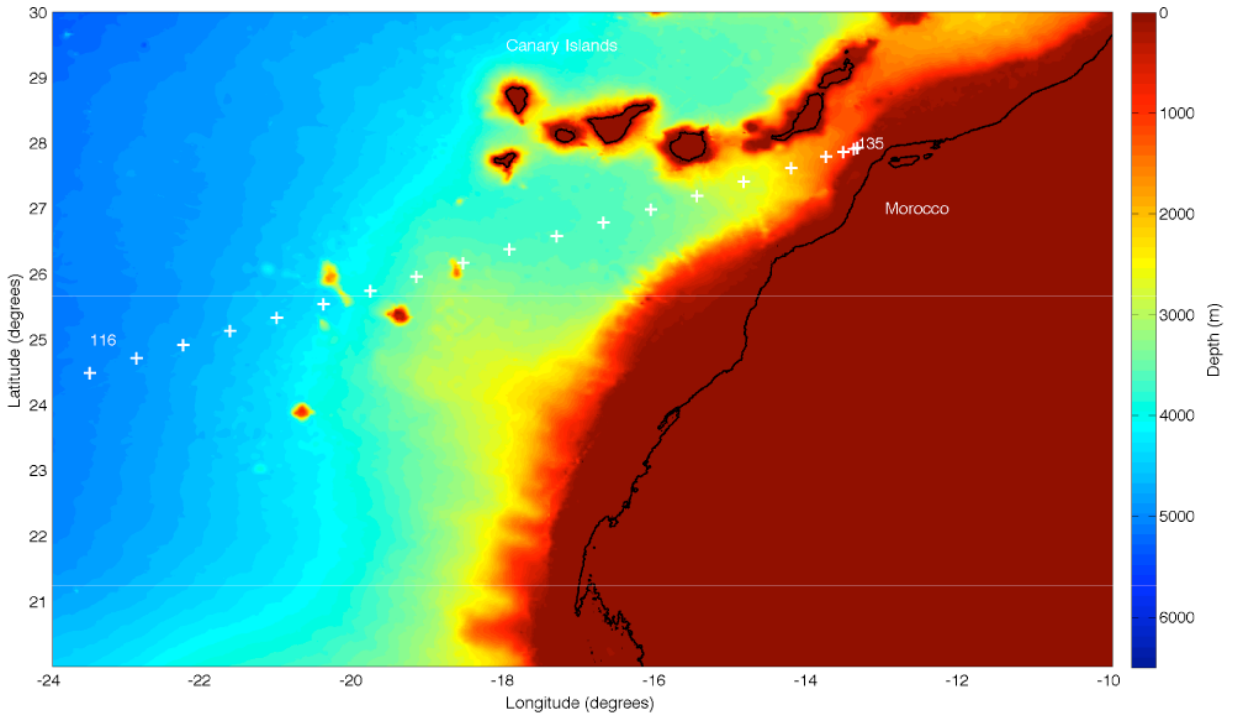

Figure 4: Eastern Boundary of the North Atlantic Basin where Cruise D346 finished

Diary

Fri 1 Jan (Local time is initially UTC-5).
Although some of the scientific party had taken a few days vacation in Freeport before the cruise, the majority had a very early start on New Years Day in the UK, arriving via Nassau.

Sat 2 Jan
The scientists arrived promptly at the ship to start mobilization. Most of the boxes had been made ready in the hangar, but there was no sign of the UEA Carbon and CFC containers. The Master had been pressuring the agent to get them brought over from the container port for some days. Continued pressure produced the improbable result that they arrived at about 17:00 on Saturday afternoon, to be swung on board immediately. Space was cleared to enable the installation and commissioning of the Liquid Nitrogen generator. It became apparent that despite frequent questions from the UK, the agent would be unable to secure a starting stock of LN_2 in the extra storage dewars brought for the purpose. It was therefore a great relief when the LN_2 generator started producing stock the next day.

It was discovered that there was neither a transmissometer nor a fluorometer for the CTD. This oversight apparently arose because the rest of the CTD equipment had been loaded for D344, for which these instruments were not required. When packing the small number of extra items required for D346, it was thought that the main instruments were already on board. The fluorometer was particularly important to provide context and to guide David Honey's measurements, and arrangements were put in place to have the instruments sent from NOC. It was agreed that UPS or an equivalent dispatch company could not guarantee their arrival and release from customs in a timely manner. The arrangement was therefore made for someone to fly to Freeport, bringing the items as accompanying baggage. Since a fluorometer was the most important instrument, it was agreed that two fluorometers and one transmissometer would be brought.

Sun 3 Jan (Local = UTC-5)
Container services were connected first thing, to enable the CFC and CO_2 teams to start mobilization. An early and major failure was the transformer for the power supply for the CFC analyzer. The ETO arranged a makeshift replacement, and while this enabled mobilization to start, it was considered a temporary repair. Mobilisation of other groups continued.

Mon 4 Jan
Mobilisation continued. Extensive enquiries confirmed that no spare transformer for the CFC analyzer was available in Bahamas. A correct spare was sourced in USA, to be shipped by overnight courier to Ft. Lauderdale. No US supplier could guarantee next-day shipment to Bahamas. The solution was to arrange for Andrew Brousseau to fly to Ft. Lauderdale to collect it. Andrew returned the next day via Miami after being bumped from his confirmed seat on the Ft. Lauderdale return flight. Back at NOC, John Wynar collected the missing instruments and was due to arrive late that evening after flying from LHR via Miami. Around mid afternoon, we received the unwelcome news that his flight from LHR to MIA had been cancelled due to

mechanical problems. He would instead arrive the following evening (5 Jan). It was agreed that sailing would be delayed to enable delivery of these instruments.

Tue 5 Jan
Sailing planned for midnight departure local time.

Andrew Brousseau returns early afternoon with CFC transformer, which was fitted by the ETO.

J Wynar arrives from LHR via MIA early evening, carrying one fluorometer and one transmissometer. A second fluorometer has been misdirected, even though it was collected and rechecked in MIA.

Wed 6 Jan
RRS *Discovery* moved away from berth for cruise D346 just after midnight local time, at 0519Z. Test station number 001, at 27°50'N, 78°50'W, was reached and a test station to 844dbar was conducted between 1649Z and 1758Z. The latitude of the Florida Current section will be 27°20'N. This allows access to shallow water while remaining outside the US 12 mile limit. We returned to that latitude at 2320Z. After a bathymetric survey into shallow water to the east to establish water depths for the subsequent CTD stations, a VMADCP survey with bottom tracking was conducted on a heading of 270° on that latitude.

Thu 7 Jan
The Florida Current section started in 100m water depth at 07/0420Z (Station 002).

Fri 8 Jan
The Florida Current section ended in 150m water depth at 08/0418Z (Station 013).

The ship steamed round to the north of Grand Bahama and Great Abaco Island to start the main section at 26°30'N, 76°56'W, arriving to start Station 014 at 1854Z. The station positions out to Station 43 (26°30'N, 71°00'W) follow those previously occupied on D279 in 2004, and in many other occupations by colleagues from Miami. The maximum station spacing was 20nm (nautical miles). Station 032 would be completed at 0343Z on 16 Jan.

While hauling Station 016 in water depth 1600m, the CLAM system failed at 09/0026Z, when the wire-out was 971m. After a pause the station was completed without the CLAM system, ending at 09/0130Z.

Sat 9 Jan
Subsequent investigation of the CLAM system revealed that the CLAM computer hard drive had failed and was unrecoverable. Stations continued without the CLAM, since the water depths meant that wire tension did not exceed the 5:1 Factor of Safety. It was agreed that a winch data logging system was needed to fulfill obligations of the agreement that allows NERC ships to operate wires with FoS less than 5:1. Inspection of tension data from D344 showed that this gave a practical operating limit of about 4000m, which would be exceeded on Station 020, which would occur about 12 hours later.

A spare CLAM computer was found in the tape store. However, this was ex-RRS *Darwin*, and did not have software for the RRS *Discovery* winch system. It had clearly been brought from the RRS *Darwin,* but had never been configured for RRS *Discovery*. No backup copy of the software on the failed hard drive was available on board. Documentation for the communication between the CLAM and the winch PLC was incomplete, mainly taking the form of the spec provided to Caley in advance of delivery, and not providing a complete description of the final system. The Caley PLC does not simply output serial data for logging. It requires to be polled by sending the correct characters to its serial port. After a certain amount of experimentation, Paul Duncan devised a system (subsequently referred to as CLAD) that enabled the winch PLC to be polled, with the output logged to a local and networked hard drive. The system consisted of the Windows PC borrowed from the PSO office, reconfigured to boot into Linux, with a 4-way USB/serial converter. A compiled 'C' program then generating polling characters (uppercase 'S') for the winch PLC at 5Hz. The return string of winch telemetry was logged to the local hard drive and also to the *Drobo* shared network drive. CLAD simulated all the RS232 serial ports of the CLAM, and enabled clock messages to be interspersed with the winch data in the logged file. Thus satisfied that we were fulfilling the winch logging obligations, we were able to proceed with Station 020 on schedule. The CLAD logging system came online during the downcast of Station 020 before the limiting tension was reached. A complete winch telemetry record has been kept from Station 021 onwards. The initial display was a scrolling text echo to the screen of the $CTD3 strings sent by the winch. Considering the non-negotiable necessity of a winch logging system, it is not an exaggeration to say that the assembly of this system rescued the cruise from a massive delay and setback and even possibly a premature end.

The second function of the CLAM system was to provide a data display for the winch drivers and the bridge. This includes a graphical display of tension data for recent minutes, as well as real-time digital display of tension, wire-out and haul/veer rate. In parallel with Paul Duncan's development of the CLAD logger, the PSO programmed a Matlab figure display comparable to the old CLAM display, updating the digital values and with a graphical display of 5 minutes of recent tension data. The CLAD display program ran on *NOSEA1*, pulling data in real time (up to 3 seconds delay) off the *Drobo* shared disk. The first version was available in time for Station 021. Initially, the CLAD Linux box had not been configured to run X windows displays, so the CLAD display was run on the PSO's laptop, feeding the video splitter box near the old CLAM system. Later, the CLAD Linux box was configured so that it could run remote X shells on *NOSEA1* and took over that function as well.

Mon 11 Jan
A short weather delay was experienced while waiting to start Station 026.

Wed 13 Jan
Further development of the CLAD had been difficult, since the machine was in regular use during stations with little time in between for experimentation. Station spacing at this stage was between 5 and 10 miles. Initial effort had been expended in trying to resurrect either of the original CLAM computers, but all efforts were thwarted by lack of correct software, even though some software had been sent from

NOC. The CLAM software was written in LabView, and we were unable to ascertain why it would not interrogate and then parse the return from the winch PLC. Colleagues at NOC were unable to tell us whether the replacement software sent to the ship worked correctly at NOC when offered simulated PLC output. However, by 13/1816Z, in time for Station 035, the CLAD output had been further modified so that it sent a correctly formatted serial output message on a port connected to the TECHSAS system, so TECHSAS logging was resumed. Logging to local drive (for security) and network drive (for CLAD display) continued. Files for Stations 021 to 034 were read into Matlab from the /*Drobo* data logs, and Mstar files produced equivalent to those taken from TECHSAS for other stations. The CLAD system continued in use for the remainder of the cruise.

Fri 15 Jan
Today it was noticed that primary conductivity sensor had failed, thus was consequently replaced with a spare.

Sat 16 Jan
Clocks advance on the night of 15 Jan, so ship time is now UTC-4.

Mon 18 Jan
The secondary conductivity sensor failed, but the decision was taken not to replace this as we only have one spare conductivity sensor remaining and the primary sensor is still working well so we will continue to use that for now.

Fri 22 Jan
Clocks advanced on the night of 21 Jan, so ship time is now UTC-3.

Sat 23 Jan
The LADCP and other units such as the fluorometer and transmissometer were removed before Station 64 as these instruments are not pressure rated to below 6000m.

After Station 064, a test station, referred to as number 200 to distinguish it from the main stations in the section, was undertaken for CFC bottle blanks. It commenced at 23/1120Z and ended at 23/1729Z. It reached 6349db, and all bottles were closed at the bottom of the cast. Shortly after starting to haul, at 6046db, the winch cut out. The compensator between the winch and the storage drum had reached the end of its travel and operated a stop. The winch remained stopped from 1320Z to 1455Z, while the 2nd Engineer and ETO investigated. No fault was found, and the conclusion was that the storage drum was struggling to provide sufficient back tension as required by the winch at high wire-outs. Accordingly, slower hauling speeds were used at high wire-outs in subsequent stations, to reduce the likelihood of a repeat. The wire was recovered on this station without further abnormal behaviour. A thorough investigation was carried out by the 2nd Engineer and ETO while steaming to Station 065, and on arrival the winch was declared fit for normal use, subject only to the limitation of lower haul rates at greatest depths.

Sun 24 Jan
Station 066 was the deepest station on the section. The maximum CTD depth was 6450m, at a pressure of 6592db. As far as we are aware, this is the greatest depth achieved with the present winch system. It slightly exceeds the depth of the equivalent station on D279. Bottom of the cast was reached at 24/0742Z and the cast ended at 24/1051Z. The maximum tension spike on this station was 2.86T, with a mean of 2.71T when first hauling from 6450m wire-out. This is well within the agreed SWL for the wire.

Ironically, the echo sounder was not working during this station. On arrival at station 066, the echo sounder was swapped from the PES fish to the starboard hull transducer, which was the custom throughout the cruise. The fish gave better data underway, but often gave poor or absent data whilst on station. It was supposed that this was due to trim of the fish being poor when stationary. Apparently when the swap was made, the plug may not have been properly seated in the socket, so when the echo sounder was reactivated it caused a failure of the system. Data were lost after 24/0442Z. Various replacement boards were tried without success. At 0535Z, Station 066 was commenced with the echo sounder u/s, relying solely on the CTD altimeter. The echo sounder had provided a reliable bottom depth before failing. The altimeter was used as normal, supplying height-off from a range of 97m, and the CTD approached to 10m off the seabed. During and following Station 066, the echo sounder was extensively investigated. Various boards (10kHz and 12kHz) were tried in the three operating slots available in the instrument. It was presumed that the original board had been damaged by being operated while the transducer selection plug was not properly seated. No obvious fault was found, and after various swaps the instrument was once again working. Mysteriously, it continued working when reassembled with the original boards in the original slots, and worked normally for the remainder of the cruise. We can only presume that multiple power cycling cleared whatever problem had originally occurred, where single power cycling had not.

A short weather delay was experienced while waiting to commence Station 067.

Tues 26 Jan
The original Aluminium-casing LADCP unit was replaced on Station 70 with a titanium-casing unit. This proved a bad move as the unit failed on Station 72. A very poor piece of equipment.

Wed 27 Jan
The termination failed early on the downcast of Station 073. The station was abandoned, the package was recovered and the wire re-terminated. A replacement Station 073 resumed at 27/1218Z

Thurs 28 Jan
The primary conductivity sensor, which had previously been replaced, failed, so we had to use our last remaining spare to replace it. It seems to have been a wise decision to save it for this moment; We must hope that this is a good one that behaves itself for the rest of the cruise.

Fri 29 Jan

The CTD was grounded at the bottom of Station 081, and approximately 200m of further wire paid out. A combination of poor depth echo, and no bottom return from either the pinger or the altimeter allowed the event to occur. No damage or loss occurred. The package evidently tipped over onto the seabed. Several Niskin bottles came back containing sediment. A detailed account of the events was prepared by the PSO and sent to NOC.

Sun 31 Jan
Clocks advance on the night of 30 Jan, so ship time is now UTC-2.

Thu 4 Feb (035)
The PSO's upcoming birthday on the 5th was marked with a BBQ. Strong winds underway between Stations 098 and 099 rendered outdoor cooking impossible, so the ship hove to between 35/2106Z and 35/2235Z so that most of the scientists and ships' personnel could enjoy an excellent selection of BBQ food prepared by the catering team, and anticipate the landmark of Station 100 due the following morning.

Fri 5 Feb (036)
A second CFC bottle blank station was conducted, designated 202 (since 201 had been reserved for use elsewhere), falling between Stations 100 and 101. This time the level chosen was 3500m. The station began at 36/1534Z and ended at 36/1738Z.

Mon 8 Feb (039)
Clocks advance on the night of 7 Feb, so ship time is now UTC-1.

Wed 10 Feb (041)
For the last run of stations the LADCP has been replaced with the original unit that started the cruise because this performed well.

Sun 14 Feb (045)
Clocks advance on the night of 14 Feb, so ship time is now UTC. This is the correct time zone for Lisbon.

Last station (number 135) completed

Fri 19th Feb (050)
We arrived in Lisbon early morning, approximately 06:30 UTC. Since finishing the sampling big efforts have been made by all the scientific teams to finish analysing the backlog of samples, write their sections of the cruise report and pack their equipment away. Today, both the ships' crew and the scientific contingent are working hard to finish packing away equipment for either freight back to the UK or to Montevideo for the ANDREX cruise scheduled to take place in 3 weeks time. Both Sinhue Torres and Andrew Brousseau will be taking part in ANDREX.

1. CTD Systems Operation

1.1. CTD and Sensors

The CTD system comprised of the following equipment:

- Seabird 911+ CTD with dual pumped temperature and conductivity sensor pairs
- Seabird SBE43 dissolved oxygen sensor
- Seabird SBE32 carousel with twenty-four OTE, externally sprung, twenty litre water bottles
- Downward looking RDI 300kHz workhorse ADCP
- Chelsea Instruments Alphatracka (transmissometer)
- Chelsea Instruments Aquatracka (fluorometer)
- Tritech P200 altimeter
- IOS 10kHz pinger
- Sonardyne location beacon

One pair of temperature\conductivity sensors were mounted on the stabilisation vane, the other pair, with the oxygen sensor, were mounted conventionally onto the CTD frame.

Overall the system worked well with only a small amount of time lost due to breakdowns. There were, however, a number of problems worthy of mention, these are listed below.

1. For the first half of the cruise the carousel repeatedly returned 'error, unsupported carousel message', this had been reported on the previous cruise. On several very early casts, bottles failed to fire, or fired but failed to return a valid code. The 11+ deck unit was changed which appeared to resolve the problem, although on one later cast the problem reappeared. After the sea cable was re-terminated the error message disappeared.

2. Near the end of the cruise there were several mechanical jams of the release levers. This was rectified by fitting "diverter" tie-wraps to provide a more direct pull on the levers. This problem is due to an alignment error between the release lever and the bottle position.

3. Three out of four conductivity sensors failed, due to cracking of the cells, at depths in excess of 5500m. After contacting Seabird it appears that a problem with the bonding of the cell to the unit is the cause. The cells will be replaced, free of charge, using the new bonding technique.

4. The original oxygen sensor was replaced due to an electronic error in the gain ranging.

The starting sensor configuration is as follows, with subsequent configuration files in the raw data directory.

T1 = 4872
C1 = 3258
P = 90573
T2 = 4381
C2 = 3052
Oxy = 1624
Alt = 6198.118171
Fluor = 088095
Trans = 161048

Salient cast and sensor changes are listed below.

Cast 36 Oxygen sensor 1624 swapped for 0621.
Cast 41 Conductivity sensor 3258 swapped for 3054.
Cast 50 Conductivity sensor 3052 failed but not replaced.
Cast 51 The physical position of the vane and CTD mounted sensors swapped. The channel allocation remained the same.
Cast 68 Suspect temperature sensor 4381 replaced with 2674.
Cast 69 Sensor 4381 checked ok, returned to replace 2674.
Cast 73 Sea cable terminated, carousel error messages disappeared.
Cast 77 Conductivity sensor 3054 failed, replaced with 2231.

1.2. LADCP

A single 300kHz Workhorse downward looking ADCP was operated on the frame in the lowered mode. Three units were available for this purpose and all were deployed at some point during the cruise. The ADCP was removed for casts deeper than 6000m. Instrument performance analysis on this cruise is dealt with in other reports though in general, two functioned reasonably well and one failed on its third cast. The unit which failed (s/n 13399) had had a small amount of water ingress through the main bulkhead connector, which came in contact with components on the top board where the main power supply comes in, causing these to short circuit.

1.3. 20L Niskin Bottles

Prior to commencement of the cruise the original silicon-fluoride O-rings were replaced with decontaminated 'Nitrile' O-rings. Decontaminated 'Viton' equivalents were also available and were substituted for the Nitrile versions where sealing of the bottle was considered an issue on the supposition that the Nitrile versions were too unyielding to affect a good seal.

As mentioned in the previous CTD section there were some issues early on associated with communications problems with the carousel leading to misfires on some of the earlier casts. This problem was eventually solved through re-termination of the cable. Later there were also problems with latches on the carousel hanging up, after returning a positive firing confirmation code, this being attributed to misalignment between the carousel and the rosette.

In addition to these problems there were frequent occasions where bottles did not seal properly or appeared to have closed at depths out of sequence with the order in which they were fired. Often this was revealed in anomalous temperatures when the bottle was being sampled. Records were kept of these occasions and are reported in detail elsewhere. Bottles that showed consistent failure were replaced. This amounted to changing three bottles over the course of the cruise.

David Teare, Peter Keen and Alan Sherring

2. CTD Data Processing and Calibration

2.1. Initial Processing Using SeaBird Programs

The files output by Seasave (Version 7.19) have the appendices: .hex, .HDR, .bl, .CON. The .CON files for each cast contain the calibration coefficients for the instrument. The .HDR files contain the information in the header of each cast file. The .hex files are the data files for each cast and are in hex format. The .bl files contain information on bottle firings of the rosette.

Initial data processing was performed on a PC using the Seabird processing software SBE Data Processing, Version 7.19. We used the following options in the given order:

Data Conversion - turns the raw data into physical units. It takes the .CON files and .hex files. The input files were named *D346_nnn.hex* where *nnn* refers to the three-digit station number.

Align CTD - takes the .cnv file and applies a temporal shift to align the sensor readings. The offsets applied were zero for the primary and secondary temperature and conductivity sensors as the CTD deck unit automatically applies the conductivity lag to the conductivity sensors. An offset of 5 was applied to the oxygen sensor.

Cell Thermal Mass - takes the .cnv files output from Align CTD and makes corrections for the thermal mass of the cell, in an attempt to minimize salinity spiking in steep vertical gradients due to a temperature/conductivity mismatch. The constants applied were; thermal anomaly amplitude $\alpha = 0.03$; thermal anomaly time constant $1/\beta = 7$.

Output files were copied to *NOSEA1* from *Drobo* using the UNIX exec *ctd_linkscript*. Symbolic links were created for each file named *ctd_di346_nnn_ctm.cnv*, where *nnn* is the station number.

As part of Data Conversion, an algorithm that attempts to reduce hysteresis between downcast and upcast oxygen measurements is available. This was initially applied to the oxygen data as part of routine processing using the default parameters recommended by SeaBird. Using this algorithm a noticeable reduction in upcast-downcast oxygen residuals was observed relative to data from cruise JC032 where processing was carried out using an earlier version of the SBE Data Processing suite where no hysteresis correction was available. To further tune the hysteresis parameters, a decision was taken to apply the SeaBird hysteresis algorithm to the oxygen data within the Mstar CTD processing suite. This eliminated the need for cumbersome reprocessing of data using the SBE Data Processing software each time a parameter change was tested. The final oxygen hysteresis correction was applied to 24Hz CTD files as part of Mstar CTD processing using the script *mctd_02b.m*.

2.2. Mstar CTD Processing

The entire Mstar software suite is written in Matlab and uses NetCDF file format to store all the data. There are four principal types of files:

- SAM files: store all information about rosette bottles samples, including upcast CTD data from when the bottles were fired. Data from chemistry samples corresponding with each bottle are uploaded into this file as well. Other information about the station is stored too.
- CTD files: store all data from CTD sensors. There are five CTD files: raw, 24Hz, 1Hz, psal and 2db. The program averages and interpolates the raw data until it has 2db resolution.
- DCS files: store information necessary to know CTD downcast (for e.g. start, bottom and end points of the cast). It is also used to merge in latitude and longitude.
- FIR files: keep information about CTD data in points when each rosette bottle was fired. Also stores information about winch work.

2.3. Processing Procedure Used on D346

After having converted CTD with the SBE processes, there were two ASCII files to work on: *ctd_di346_nnn_ctm.cnv* and *ctd_di346_nnn.bl*. The first one contains all raw CTD data including cast information. The other one contains information about the firing of each bottle on the cast.

To start the CTD data processing, *m_setup* was run in Matlab to add Mstar tools and information needed for the processing. The following scripts were then run:

msam_01: creates an empty sam file to store all information about rosette bottle samples. The set of variables are available in the */templates* directory and can be changed according to what it needs to store. This file, named as *sam_di346_nnn.nc*, stores data for each sample bottle, their flags, and some CTD data at firing time.

mctd_01: reads the raw data (*ctd_di346_nnn_ctm.cnv*) and stores it in a NetCDF file named *ctd_di346_nnn_raw.nc*, which becomes write protected.

mctd_02a: copies *ctd_di346_nnn_raw.nc* into *ctd_di346_nnn_24hz.nc* renaming the variables for the SBE sensor.

mctd_02b: using 24Hz data (*ctd_di346_nnn_24hz.nc*), applies oxygen hysteresis correction to variable oxygen_sbe to create new variable oxygen.

mctd_03: using 24Hz data (*ctd_di346_nnn_24hz*) it averages to 1Hz data. Then, using the 1Hz file (*ctd_di346_nnn_1hz*) it calculates salinity and potential temperature (*ctd_di346_nnn_psal*). This script also calls *mctd_sensor_choice.m*, which records the first choice CT sensor pair for each station. First choice sensor data is then stored in the variables temp and cond (which are subsequently used to calculate variables potemp and psal).

mdcs_01: creates an empty file named as *dcs_di346_nnn* to store information about the start, bottom and end of the cast.

mdcs_02: populates *dcs_di346_nnn* with information from the bottom cast. It takes the highest pressure point as bottom.

mdcs_03: selects and shows surface data < 20db (*ctd_di346_nnn_surf*) allowing the analyst to choose the positions of the start and end scan numbers.

The start is selected by scrolling from the top of data printed out by *mdcs_03.* The operator identifies where the CTD went from being on deck (zero/negative pressure) to roughly 10db and then the point where is it was brought back to the surface for the start of the downcast. The scan number at which the pressure begins to increase and temperature, salinity and oxygen data show reasonable values is selected as the start point of the downcast.

To find the end of upcast, the data were scrolled up from the bottom to identify where the CTD came back onboard. The operator chooses the last available point where sensor values are reasonable before an abrupt change in measurements occurs as the CTD is lifted out of the water.

mctd_04: using information on *dcs_di346_nnn* it selects the CTD downcast data from *ctd_di346_nnn_psal* file and averages it into 2db resolution (*ctd_di346_nnn_2db*).

mdcs_04: loads position from navigation file and merges it on the cast's points previously defined in *mdcs_03,* and stores it on *dcs_di346_nnn_pos.nc*.

mfir_01: extracts information about fired bottles from *ctd_di346_nnn.bl* and copies them into a new file named *fir_di346_nnn_bl.nc*.

mfir_02: using *fir_di346_nnn_bl* and *ctd_di346_nnn_1hz* it merges the time from the CTD using scan numbers and puts it into a new file (*fir_di346_nnn_time.nc*).

mfir_03: stores the CTD data at each bottle firing time in *fir_di346_nnn_ctd*. The CTD data are taken from *ctd_di346_nnn_psal* and selected according to the firing time information stored in *fir_di346_nnn_time*.

mfir_04: copies information of each bottle from *fir_di346_nnn_ctd* onto *sam_di346_nnn*.

mwin_01: creates a new file named *win_di346_nnn.nc* to store information about winch working (for e.g. angles, rate and tension).

mwin_03: using time stored in *fir_di346_nnn_time*, it selects wire-out from *win_di346_nnn* at each bottle firing location to *fir_di346_nnn_winch*.

mwin_04: pastes wire-out information from *fir_di346_nnn_winch* into *sam_di346_nnn.nc*.

mbot_01: creates a bottle file (*bot_di346_nnn*) to store information regarding the state of each Niskin bottle. It uses a text file named as *bot_di346_001.csv* (on BOTTLE_FILE/ directory) that must be always updated after each station with the number of the bottle, position on rosette, and a flag number.

mbot_02: copies information from *bot_di346_nnn* to *sam_di346_nnn.nc*.

mdep_01: applies the full water depth to all files. The depth is taken from the LDEO processing of the LADCP. Where this is not possible, *mdep_02* was used to create the full water depth using package depth combined with altimeter data or echo sounder data.

mdcs_05: applies positions from *dcs_di346_nnn_pos.nc* to all files. If a file on the set doesn't exist yet it won't be uploaded.

2.4. Sample Files

Chemistry and tracer data from the various groups were merged with CTD data to create master sample files. The sample files (*sam_di346_nnn.nc*) were created whilst processing each CTD station. These were, at this stage, filled with upcast conductivity, temperature, oxygen and pressure from both primary and secondary sensors coincident with bottle firings. Winch data were merged on, as were Niskin bottle flags.

Merging of these data took two steps for each tracer: the first step generated an Mstar file, which contained all the tracer data for a given station – these were the programs named *moxy_01*, *mnut_01*, *mcfc_01* and *mco2_01*. This step contains code specific to the format of the data received from the various groups. The files were named using similar format, e.g. *oxy_di346_nnn.nc* in the case of oxygen. The second step was to merge these individual Mstar files onto the master sam file for each station. This was performed by the programs *moxy_02*, *mnut_02* etc. For nutrient data, a further script, *mnut_03* was run to calculate organic nitrate and phosphate values from total nutrient and inorganic nutrient measurements and input these variables to the master sam file for each station. For oxygen data, a further script, *msam_oxykg* was run to convert bottle oxygen data from µmol/l to µmol/kg and input this variable to the master sam file for each station.

This approach provides a flexible method of assimilating data from the various teams contributing to D346. The sam files were periodically appended together to form the master file *sam_di346_all.nc*, which, along with the 2db CTD files, was used by *run_mgridp_ctd.m* to produce gridded and interpolated section data in NetCDF format. This gridded data was then plotted using *plot_cont_di346.m*. This allowed cruise progress to be continuously monitored and provided a useful first step for identifying bad data whose flags may need adjustment.

2.5. CTD files

Due to failure of the CLAM winch logging system during Station 16, some winch data was lost until a temporary solution was found. The introduction of the CLAD system from Station 36 onward allowed data to be logged again via the TECHSAS data streams. For Stations 1-16 and 36-135, winch data was therefore obtained using TECHSAS data using *mwin_01*. From Stations 17-20, no winch data was available. For Stations 21-35, winch data was saved in ASCII format before transformation to Mstar format by the script *mwin_00_get_time*.

Processed CTD sensor data was viewed using the script *mplotxy_ctdck.m*. This uses dcs, psal and 2db CTD files to allow CTD data to be viewed and compared with data from previous casts. Ideally, CTD data should be viewed immediately after each cast to identify any degradation in sensor performance so that a solution can be quickly found. Unfortunately, this system only became common practice several stations after initial degradation of the first oxygen sensor. This data was recovered following station-by-station calibration to bottle oxygen samples.

In addition to sensor degradation or failure, several minor spurious features were identified in the psal and 2db CTD and oxygen data. These included spikes associated with CTD telemetry failure, spikes at the start and end of a cast where bad start and end scan numbers were chosen in *mdcs_03*, unreasonable CT and oxygen values in the upper few decibars of a downcast relative to the surrounding water and bad CT and oxygen values where the pumps were temporarily switched off at the start of a downcast. Problems were solved on a case-by-case basis, either by adjusting start and end scan numbers in the *dcs_di346_nnn* files to omit bad data or by removing spikes using a median de-spiking routine to identify and set bad data to NaN values. In the latter case, corrections were made to the 24Hz files before re-processing CTD data through to the 2db stage.

Two CTD data corrections are highlighted. The first was to Station 81 where the CTD was temporarily grounded. Because the bottom of a downcast is identified using the deepest pressure value, several bad data scans were included in the downcast. The end downcast scan number was therefore edited in *dcs_di346_081* to exclude downcast data within 2db of the sea floor. The second was an anomalous TS spike generated by a pause in winching when switching to the autopilot during Station 12 (Figure 5). In this case water entrained in the wake of the CTD overtook the package leading to a warm and saline TS anomaly. The TS properties suggest the entrained water came from ~ 15m above the package and passed within ~20 seconds of the pause in winching. In this case bad scan values were set to NaN in the 24Hz files before re-processing CTD data through to the 2db stage. Whilst similar anomalies almost certainly exist in other files, these are difficult to identify in the final 2db CTD files that also retain some natural spikiness in TS space. Station 12 stood out as an interesting feature due to the clear kink produced in TS space and is highlighted here merely as a case study in wake effects generated by motion of the CTD package.

Final calibrated CTD sensor data for the Florida Straits and main 24°N section are shown in Figures 8-10.

2.6. Temperature-Conductivity Sensor

2.6.1. First Choice Sensor Data

The CTD used on D346 was equipped with two conductivity and temperature sensors. Initially the primary conductivity-temperature sensor was attached to the fin of the CTD and the secondary sensor was attached near the bottom of the main frame (Table 1). Both temperature sensors were found to compare well (< 0.001°C difference) and no evidence of significant upcast-downcast difference was found in either sensor. For Station 1-49, prior to failure, the secondary conductivity sensor was seen to possess less hysteresis between upcast and downcast (< 0.001 on potential temperature levels) and therefore was the initial sensor of choice.

The secondary conductivity-temperature sensor remained the first choice sensor to Station 49. During Station 50 the secondary conductivity sensor failed at the start of the upcast and was not replaced. From Station 50 onwards the (second) primary conductivity-temperature sensor therefore became the first choice sensor pair and from Station 51 onwards was swapped to a position on the bottom of the CTD frame. On Station 78 a new (third) primary conductivity sensor was installed following failure of the previous sensor at the start of the upcast on Station 77. Subsequently, the first choice temperature-conductivity sensor was positioned on the bottom of the main CTD frame for all stations except 50 (Table 1).

Due to no data being available from the secondary conductivity sensor on Station 77, upcast data were recovered by interpolation of downcast data on density surfaces. Four iterations on pressure, potential temperature, and potential density were carried out so that interpolations were successively less vulnerable to the broken conductivity sensor.

The primary conductivity sensors used from Stations 50-77 and 78-135 showed differing hysteresis properties to both the secondary conductivity sensor used for Stations 1-49 and to each other. However, in all cases the difference between upcast and downcast data on potential temperature levels was seen to be < 0.001 at pressures > 2000db.

Table 1: The position of primary and secondary conductivity-temperature sensors during D346 for Stations 1-135. Number in brackets denotes sensor number (this increments when a new sensor is fitted following failure of previous sensor). Stars denote the first choice sensor pair.

Frame	Fin	Stations
Secondary Sensor (1)*	Primary Sensor (1)	1-41
Secondary Sensor (1)*	Primary Sensor (2)* (Only for Station 50)	42-50
Primary Sensor (2)*	Secondary Sensor (1 – broken)	51-77
Primary Sensor (3)*	Secondary Sensor (1 – broken)	78-135

2.6.2. Conductivity Calibration

Upcast conductivity from the first choice sensors (Table 1), present in the SAM file at bottle depths as 'ucond', was calibrated against conductivity derived from bottle samples. Final calibrations were applied using *mcond_fix.m* to the 24Hz file conductivities before cascading through to 1Hz, psal, 2db and SAM files. As the calibration was applied at the transition between the raw files and the 24Hz files, it was necessary to do a conductivity (not salinity) calibration.

A multiplicative correction factor applied to conductivity is associated with a deformation of the conductivity cell. The ratio between conductivity derived from bottle samples and upcast conductivity was investigated at depths > 3000db where vertical salinity gradients are small and CTD-bottle comparison is less susceptible to bottle flushing issues. In the deep ocean (potential temperatures < 2°C) where horizontal salinity gradients are small, bottle salinities showed greater spread about the mean TS properties (std. dev. ~ 0.001-0.0015) than CTD salinities (std. dev. ~0.0005), which appeared to be more stable over time.

For the three first choice sensors used during D346, while bottle/CTD ratios were close to unity, offsets still existed for each sensor roughly equivalent to 0.001-0.002 in salinity. The final calibration ratios applied to the secondary, second primary and third primary conductivity sensors (Table 1) were 0.9999719, 1.0000574 and 1.0000285 respectively. For the second primary conductivity sensor, a small negative trend in conductivity ratio was observed over time (a change of ~ 0.00002 over 27 stations). However, only a mean ratio correction was chosen as calibration using a ratio trend introduced greater spread of CTD salinities about the mean TS curve in the deep ocean (potential temperatures < 2°C).

Following conductivity ratio calibration, bottle-CTD conductivity residuals showed some structure against pressure. The structure of the residuals was seen to be different for each sensor though in all cases offsets were equivalent to a maximum of ~ 0.001psu at pressures > 1500db. In the thermocline and surface-ocean, large gradients in temperature and salinity occur, and bottle-CTD residuals are of greater magnitude and less coherent with pressure. Bottle conductivities in this region often read lower than those of the CTD, which is partly interpreted as a bottle flushing issue. However, consistent bottle-CTD offsets observed in the surface mixed layer suggest some of the offset is related to sensor performance and therefore corrections against pressure were applied to the CTD sensor data throughout the water column. It is noted that although the pressure offsets are comparable in magnitude to the sensor downcast-upcast hysteresis, the structures against pressure are different and as such are considered a beneficial correction. No trends were noted in conductivity residuals against temperature or conductivity.

The calibration was applied by correcting conductivities using an additive factor decided by a pressure lookup table. The pressure lookup table was created for each sensor by calculating median offsets in pressure bins. Application of the calibration ratios and pressure corrections reduced rms offset of salinity offset from 0.00128, 0.00238 and 0.00202 to 0.00073, 0.00119 and 0.00064 for the secondary, second primary and third primary conductivity sensors respectively. Most of the remaining

offset is found in the upper ocean (< 1000db). Final offsets for all CTD-bottle pairs are shown in Figures 6 and 7.

Note that the performance of the third primary conductivity sensor was observed to be stable and calibration parameters calculated for Stations 78-106 were applied to all data from Stations 78-135.

2.7. Calibration of the Oxygen Sensor

The oxygen sensor was attached to the conductivity-temperature sensor on the CTD frame. Following a period of sensor degradation, the first oxygen sensor was swapped for a second oxygen sensor before Station 37. The second sensor was seen to perform well and remained stable for the rest of the cruise.

As discussed in section 1.1, a correction for downcast-upcast sensor hysteresis was made during Mstar processing by *mctd_02b*. This applies an algorithm provided by Sea-Bird for oxygen concentration values measured by the SBE 43 sensor.

The algorithm has the form:

$$Oxnew_{conc} = \left\{\left(Oxygen_{conc}(i) + \left(Oxnew_{conc}(i-1) \times C \times D\right)\right) - \left(Oxygen_{conc}(i-1) \times C\right)\right\} / D$$

Where:

$$D = 1 + H1 \times \left(\exp onential\left(P(i)/H2\right) - 1\right)$$

$$C = \exp onential\left(-1 \times \left(Time(i) - Time(i-1)\right)/H3\right)$$

i=indexing variable, P=pressure (db), Time=time (seconds), H1=amplitude of hysteresis correction function (default -0.033), H2=function constant or curvature function for hysteresis (default 5000), H3=time constant for hysteresis (seconds, default 1450) .

Following experimentation, values for H1, H2 and H3 of -0.028, 5000 and 2500 respectively were chosen for the first oxygen sensor. Values for H1, H2 and H3 of -0.037, 5000 and 1450 respectively were chosen for the second oxygen sensor. Downcast-upcast hysteresis was successfully reduced to typically a few μmol/kg by this procedure.

Following the hysteresis correction, upcast oxygen concentrations from each sensor was calibrated against oxygen concentrations derived from bottle samples. Final calibrations were applied using *moxy_fix.m* to the 24Hz file oxygen data before cascading through to 1Hz, psal, 2db and SAM files.

For the first oxygen sensor, bottle oxygen and CTD oxygen showed a clear linear relationship. As such a multiplicative correction factor calculated as the median ratio between bottle and CTD oxygen was applied to CTD oxygen. This was calculated and applied in bulk for Stations 1-22. For Stations 23-36, the correction was calculated and applied on a station-by-station basis to account for the gradual degradation in sensor performance over this period prior to removal of the sensor.

This reduced bottle-CTD residuals from > 10µmol/kg to ±5µmol/kg. After application of this correction, bottle-CTD residuals retained clear structure against pressure. Below 1500db, botoxy-CTD residuals were generally positive, whilst upper ocean residuals differed depending on the stage of sensor degradation. For Stations 1-22, upper ocean residuals were generally positive, for Stations 23-25, upper ocean residuals were nearer zero and for Stations 26-36 upper ocean residuals were typically negative. For each of the three groups of stations, an additive correction was made to CTD oxygen calculated using a third order polynomial fit of bottle-CTD residuals against pressure. Following this procedure, bottle-CTD residuals were reduced to ±2µmol/kg for the first oxygen sensor.

For the second oxygen sensor, bottle oxygen and CTD oxygen concentration offset was typically > 10µmol/kg however a linear relationship was less obvious than for the first sensor. In this case, bottle-CTD offset was reduced to ±2µmol/kg by applying a combined second order pressure and first order temperature dependent offset to all data with potential temperature < 7.5°C. The coefficients of the pressure-temperature offset function were calculated using a least-squares approach. For data with potential temperature > 7.5 °C, a simple offset of 7µmol/kg was added.

Final offsets for all CTD-bottle pairs are shown in Figure 7.

Note that the performance of the second oxygen sensor was observed to be stable, and that calibration parameters calculated for Stations 37-100 were applied to all data from Stations 37-135.

2.8. Addition of Metadata to the Mstar Files

Position, time and full water depth were added to the headers of all Mstar files including the sam and ctd_2db files.

Time: Time exists in Mstar files in seconds from the Mstar time origin. The Mstar time origin is parsed out from a UTC timestamp in the header of the SeaBird CTD files.

Position: Latitude and longitude were pasted into the files. The time corresponding to the bottom of the cast was found from the DCS files with the GPS4000 position merged on.

Water Depth: Water depth was added after processing of the LADCP was complete. The LDEO with CTD processing provides an estimate of full water depth by combining CTD depth with a height above the bottom estimate provided by the LADCP. A backup water depth was provided by a combination of the altimeter and depth of the package from the CTD data. This backup approach was used for Stations 1, 15, 16, 53, 64-70, 72, 100, 101 and 200. Depth from the echo sounder was used for Station 202 where distance between maximum package depth and the seafloor exceeded the range of both the LADCP and altimeter.

2.9. Niskin Bottles

The Niskin bottles, on the whole performed well, however, problems were identified with regards to sealing the bottles, possibly related to a change in the seals used. This resulted in dribbling from some of the bottles, which although thought not to contaminate the sample, was still undesirable due to losing a potentially substantial amount of water as the CTD is drawn upwards through the water column. The slight dripping can be related to both a sealing problem and a pressure effect, as it was continuously witnessed that shallower Niskin bottles displayed a greater tendency to dribble. Another problem that was sometimes encountered was when water leaked from the bottom tap, prior to the top valve being opened, indicating a slight break in the vacuum within the Niskin bottles with a potential increase in sample contamination. In order, to maximise the number of bottles sampled, and limit the probability of contamination, bottles with minor leaks were sampled and given a flag of 10. Bottles were only immediately rejected if they were seen to be leaking when the CTD was removed from the water (flag 3), or if the bottle did not fire (flag 4). The bottle was also rejected if the temperature measurement taken by the oxygen team revealed an unusually high temperature, conducive with the Niskin bottle failing to seal correctly at its original depth, but sealing fully higher up the water column (flag 4).

Table 2: Niskin bottle flags

Flags	
2	No Problems noted
3	Leaking profusely when taken from water
4	Bad Bottles from salinity/temp measurements
4	Did not fire
9	Samples not drawn from bottle
10	Slight drip/water leak when top valve opened

2.9.1. Bottle Performance

Bottles 1 and 15 were removed from the rosette on Station 87 and replaced with two spare Niskin bottles, labelled as bottles 25 and 26 respectively, due to a perceived higher failure rate. Bottle 19 was also removed from the rosette on Station 115 for exclusive use by the CFC group, and replaced with another unused bottle (bottle 27). On Station 121, bottle 18 was retained for exclusive CFC use, and replaced with bottle 19 for the remaining stations. Re-analysis of the results from the bottled salinity and bottled oxygen datasets revealed that Niskin bottles labelled with a flag of 10 were uncontaminated, because although there was a small dribble of water, there was no exchange of water as the bottle travelled through the water column. The total percentage of Niskin bottles during the cruise given a flag of 3 or 4 was ~4%.

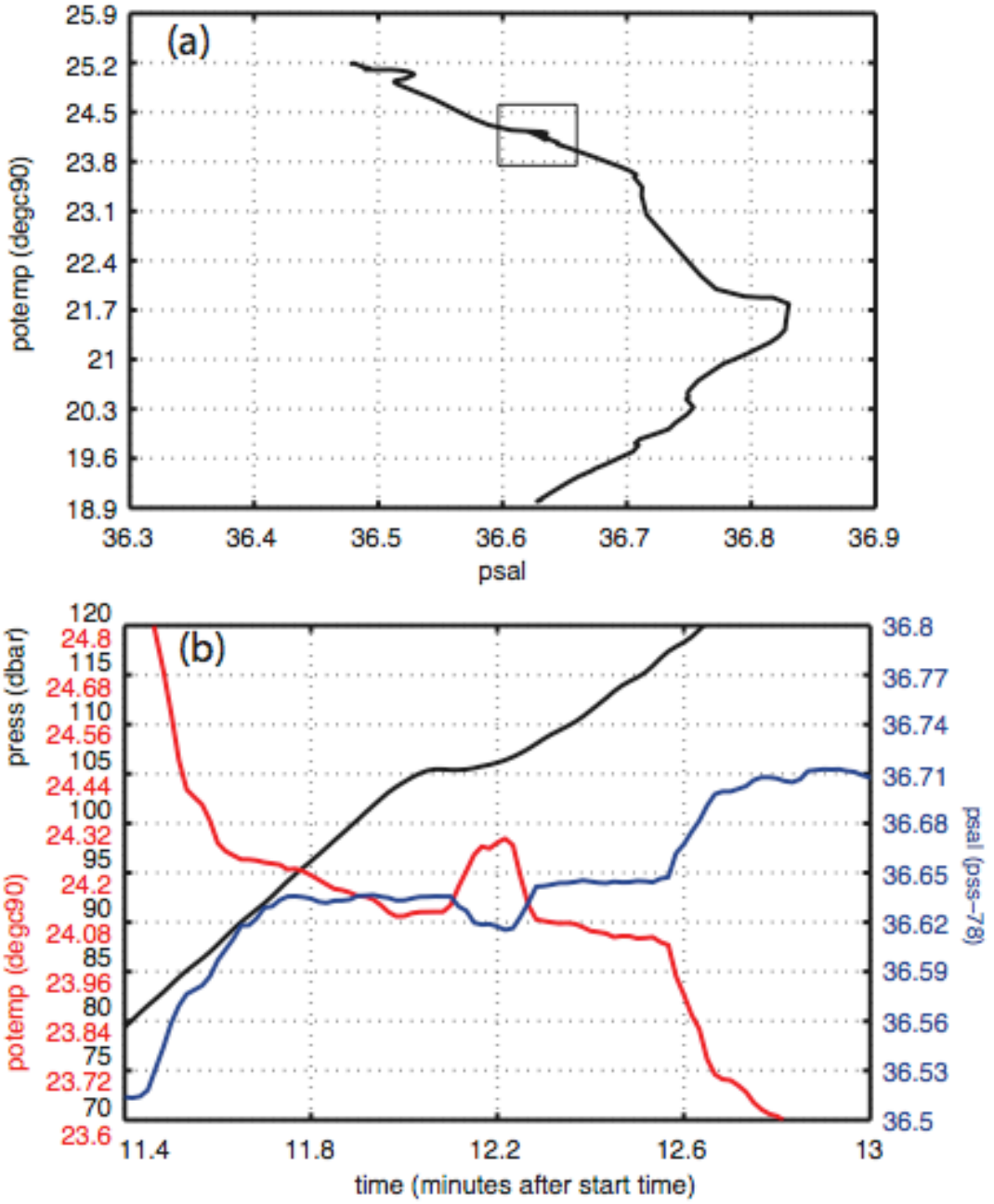

Figure 5: Θ-S anomaly during the Station 12 downcast resulting from a pause in winching (a) Θ-S anomaly (highlighted by rectangular box) (b) Θ-S-Pressure against time centred on the anomaly.

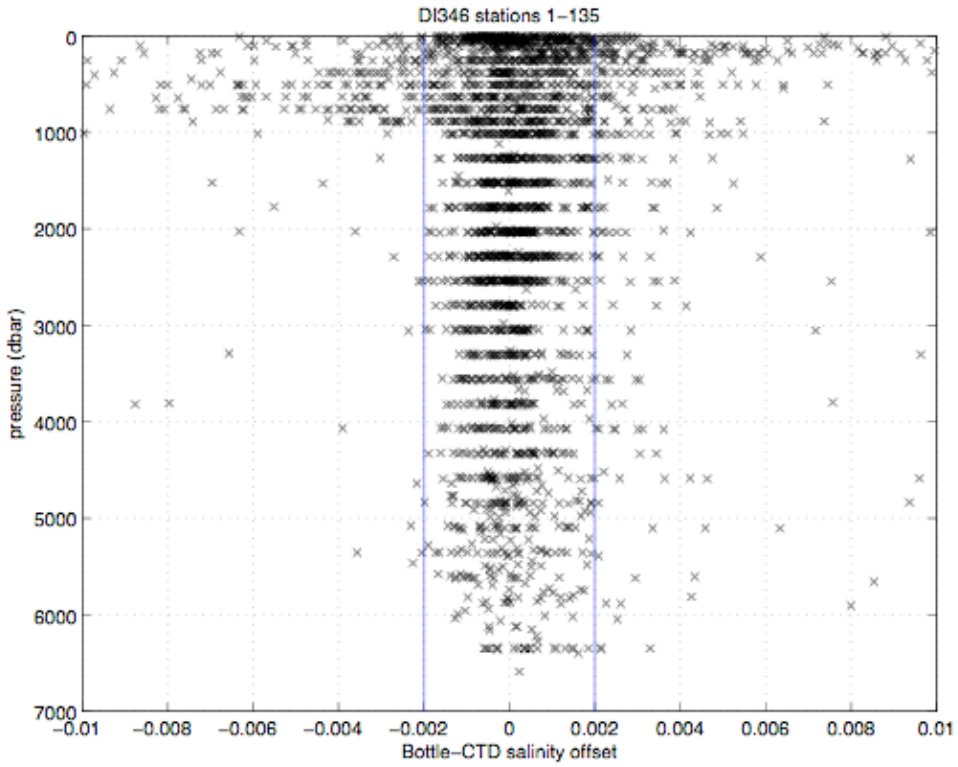

Figure 6: Final offsets between bottle salinities and calibrated CTD salinities for Stations 1-135 (also 200 and 202). Blue lines denote ±0.002 offset range.

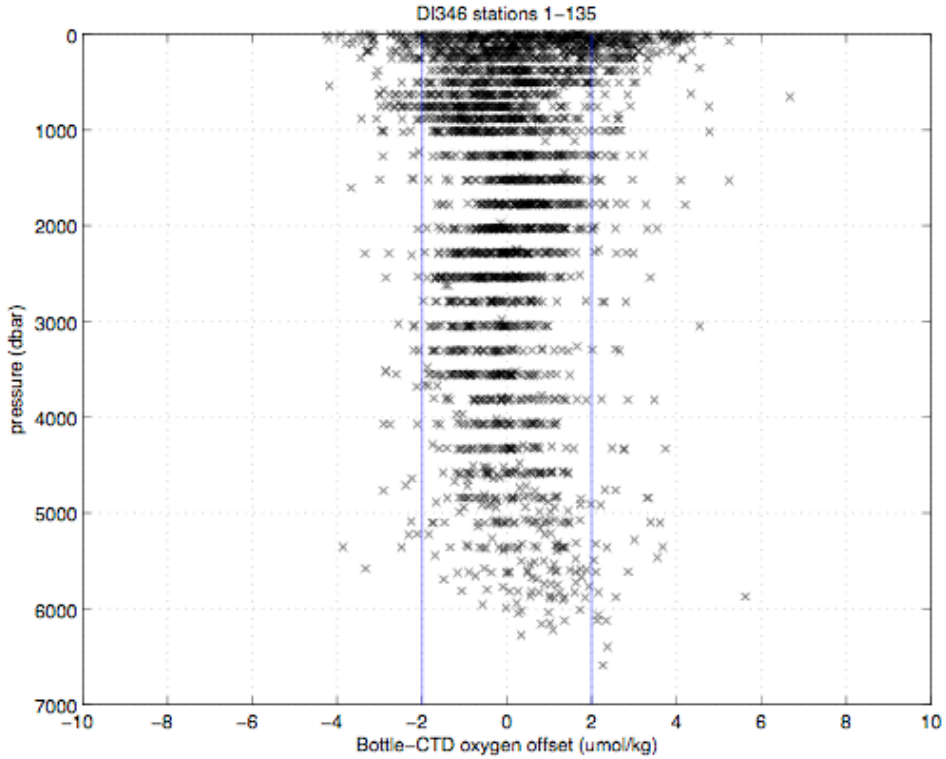

Figure 7: Final offsets between bottle oxygen and calibrated CTD oxygen for Stations 1-135 (also 200 and 202). Blue lines denote ±2µmol/kg offset range.

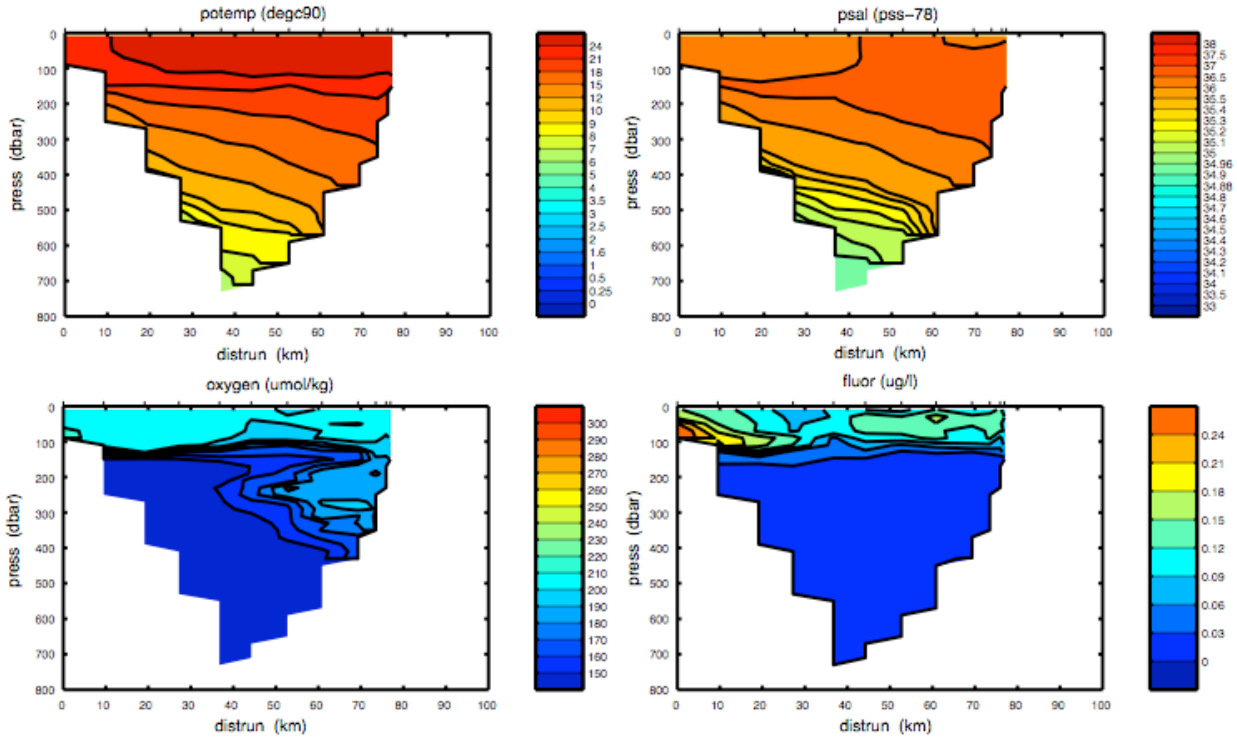

Figure 8: CTD potential temperature, salinity, oxygen and fluorescence across the Florida Straits transect.

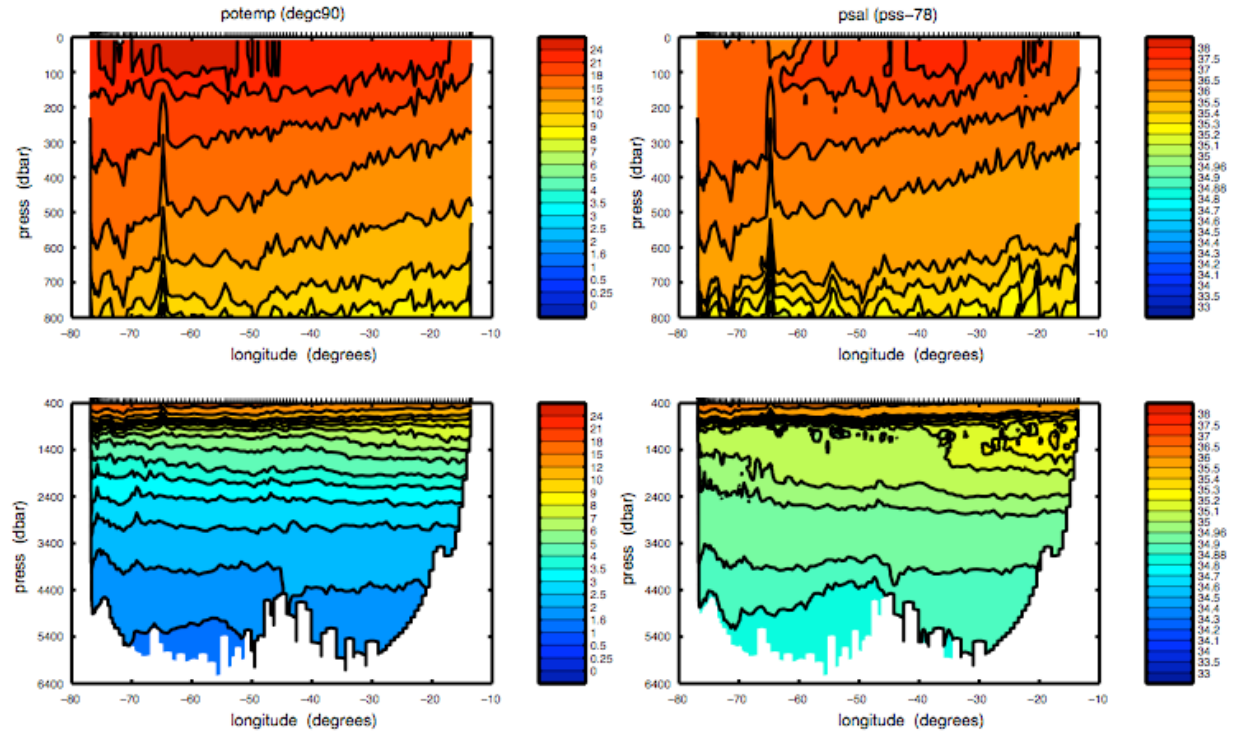

Figure 9: CTD potential temperature and salinity along the Atlantic 24°N hydrographic section.

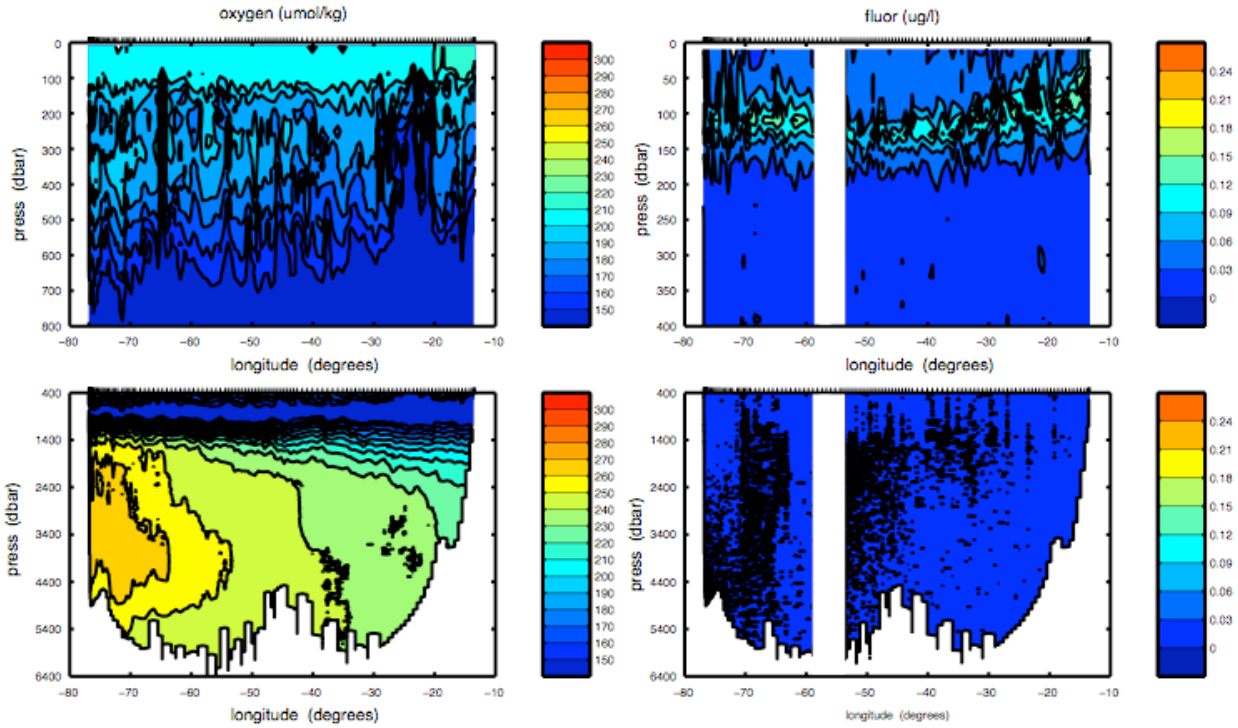

Figure 10: CTD oxygen and fluorescence along the Atlantic 24°N hydrographic section. White bands on fluorescence plots denote the deepest stations where the sensor was removed.

Chris Atkinson, Gerard McCarthy and Gavin Evans

3. Water Sample Salinity Analysis

3.1. Sampling

Bottle salinity sampling was undertaken as a secondary source of salinity measurements. Samples were collected in 200ml glass bottles from each Niskin bottle fired at each station. TSG samples were also collected at 4-hourly intervals and recorded within the watchkeeping logs. Ten crates were designated for general use and three crates for TSG. The standard procedure for sampling both the CTD and the TSG samples was to rinse the sample bottle and lid thoroughly three times using sample water from the appropriate Niskin bottle or using surface water from the TSG system. The sample water was then filled approximately to the neck of the glass bottle. The rim and inside of the lid was subsequently wiped using disposable paper towels to prevent salt crystals forming around the rim of the bottle and providing an artificial salinity enhancement. Each sample bottle was sealed with a disposable plastic stopper and its respective screw cap. After a station had been completed, the crate of salinity bottles was taken to the constant temperature (CT) laboratory and left for a minimum of 24 hours to allow for temperature equilibration. The time that the crate was left in the laboratory was recorded in UTC in order to readily identify it for later sample analysis.

3.2. Laboratory Setup

For the purpose of salinity analyses, two Guildline 8400B laboratory salinometers were used, serial numbers 68958 and 60839. The temperature of the laboratory was maintained at a temperature between 22-23°C for Stations 1-94, and between 20-21°C for Stations 94 onwards, therefore keeping the air temperature lower than the water bath temperature within the Autosal. The temperature of the CT laboratory was recorded as part of the watchkeeping logs.

3.3. Analysis

Autosal analysis of the salinity samples was shared between the members of the physics watch: Gavin Evans, Chris Atkinson, Gerard McCarthy, Benjamin Webber, David Hamersley and Helen Pillar. The methodology for using the Autosal was explained to each of the new analysts, so that the task of running salinity samples could be shared between the physics team members. The data-logging software for the most part provided good guidance to the analyst when recording salinities.

3.4. Initial Standardisation

The first two bottles of the test station were run as part of the standardisation process. A number of standard seawater samples were used to reaffirm the values produced by the salinometer. Initially, the values given for the standard seawater samples were fluctuating at an unacceptable level. However, after running four bottles of standard seawater through the Autosal, the Guildline conductivity ratio appeared to have stabilised. The conductivity ratio was set to be a little lower than the Autosal intended, to avoid the issue of alternation above and below the 2.0 suppression setting (i.e. 1.99973 in correspondence with the Autosal recommended 1.99994). A positive value of the suppression was needed for the Autosal software to be able to read it correctly. The test station crate was run as a practice to ensure that the Autosal was giving reasonable values.

3.5. Procedure

In order to use the Guildline 8400B salinometer for salinity samples, first the air pump system needs to be switched on so that the system is primed for drawing through the seawater samples. A standard sample of seawater is placed in the holding position on the Autosal with the intake tube inserted into the sample bottle. The tubing is handled using blue roll, to avoid unnecessary contamination. It is advisable to flush the system with old standard seawater samples before flushing three times using the new standard, in order to bring the salinity of the cell closer to that of the new sample.

To begin the analysis the peristaltic pump is switched on and draws water into the system, filling the cell. The system is then flushed three times whilst the read/standby knob is set to 'standby' mode. Once the three flushes are complete, seawater is drawn through the system a fourth time and the conductivity ratio of the sample is read. The standard number and bottle numbers were recorded on the salinometer logsheets, as well as automatically using the data logging software.

The conductivity ratio of the sample, as given by the Autosal was usually recorded within the 1.9-2.1 suppression range. To record the conductivity value the suppression dial on the Autosal is rotated to produce values within the correct suppression range, otherwise inaccurate results will be recorded. One potential improvement to the current software would be an on-screen warning to alert the user that the current suppression range is incorrect. After one value for the conductivity ratio of the sample is recorded, the system is flushed and another sample from the sample bottle is drawn through. The conductivity ratio of this sample is then recorded. The flush, draw and analyse process is repeated once more so that three values for the conductivity are obtained. The average of these three samples is then calculated automatically and recorded.

A sample of standard seawater must be run through the salinometer before and after every crate to ensure that there has not been any drift of the instrument and that the conductivities of the samples recorded are reliable. The standard seawater samples produced by Ocean Scientific Instruments Ltd. (OSIL), were used throughout the cruise- Batch number: P151, and K15 ratio: 0.99997, 2*K15: 1.99994. In the data

logging software, standards were recorded using a sequential numbering order. An ID number is given to the standard sample used using the naming convention '9' followed by the number of standard samples used i.e. the first standard sample used is referred to as '9001'.

3.6. Differences and Adjustments

The set procedure is to run a standardisation after each crate to ensure that the salinometer was not excessively skewing the conductivity ratio read-outs, and in order to remain within budgetary constraints given the cost of one sample of standard seawater. Each batch of standard seawater has a prescribed value for the conductivity ratio. The difference between twice the prescribed value and the actual value for the conductivity ratio recorded by the salinometer is known as the difference. The adjustment that is assigned as a result of the difference is done so as to smooth out any jumps in the salinometer readings. When applying adjustments, difficulty exists in assessing drift from the beginning of a crate to the end; therefore the adjustment is somewhat subjective. Once the adjustment is applied, the validity of the value chosen can be reaffirmed by comparing the bottle-measured conductivity with the CTD measured conductivity. The onboard CTD conductivity measurements appeared to show a high degree of structure, and hence a plot of the residuals of the bottled and CTD data could reveal a misjudged adjustment.

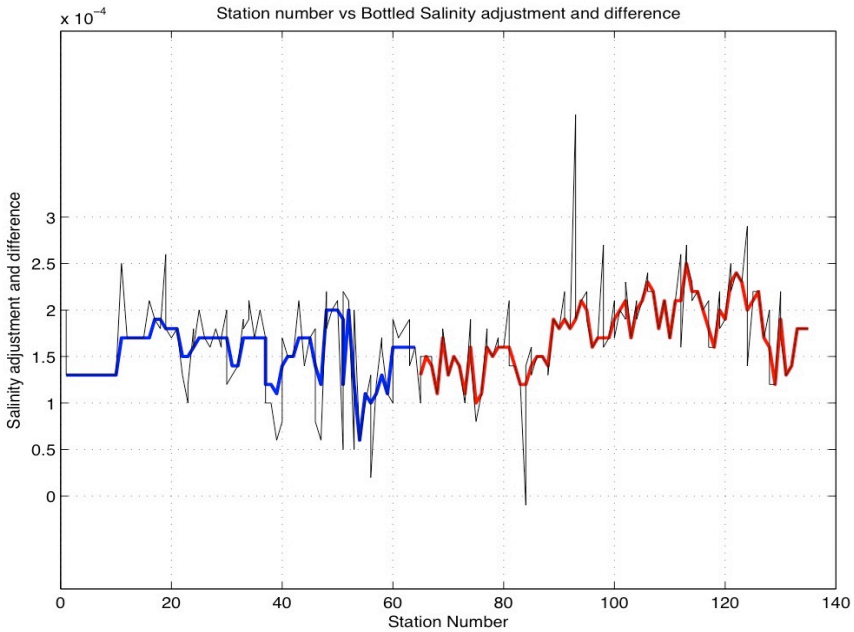

Figure 11: Salinity difference and adjustment for each station. The black line shows the difference given by the standard seawater samples that were analysed. The coloured lines show the adjustments that were applied i.e. blue line for the first Autosal/red line for the second Autosal.

3.7. Salinometer Performance

Initially the Guildline 8400B Autosal (Serial No: 68958) was used giving a robust performance for the first 40 stations. However, after witnessing an increasing spread in the residual dataset, the decision was made to change to the second Guildline 8400B (Serial No: 60839 at Station 65. This decision was based on analysis of the graph of the residuals of the bottle and CTD conductivities for each station. As the CTD conductivities were believed to be stable throughout this time period. The spread in the residuals was attributed to the bottle salinities. In order, to minimise the reasons for an increase in the distribution of the bottle salinities, a decision was made on the advice given by Brian King, to switch the peristaltic pump off when a reading was being taken. This was seen to limit the noise within the samples, and avoid any electrical bias that could be attributed to water being continually pumped through as the measurement is undertaken. All analysts reported a substantial difference in the conductivity values measured after changing to a 'pump-off' approach to measurement as opposed the readings before this change when the measurements could fluctuate by up to ~15 counts. A switch was added to the pump to improve the functionality for the analysts.

The change in Autosal and the technique of the analysts was seen to a make a genuine improvement in reducing the distribution of the residuals allowing it to be easier to apply an offset value to the CTD salinities. The offset would be different for the different salinometers, and the different conductivity sensors that were used on the CTD. The final plot of the conductivity residuals (Guildline ratio offset) is shown in Figure 11 for all samples collected deeper 3000dbar.

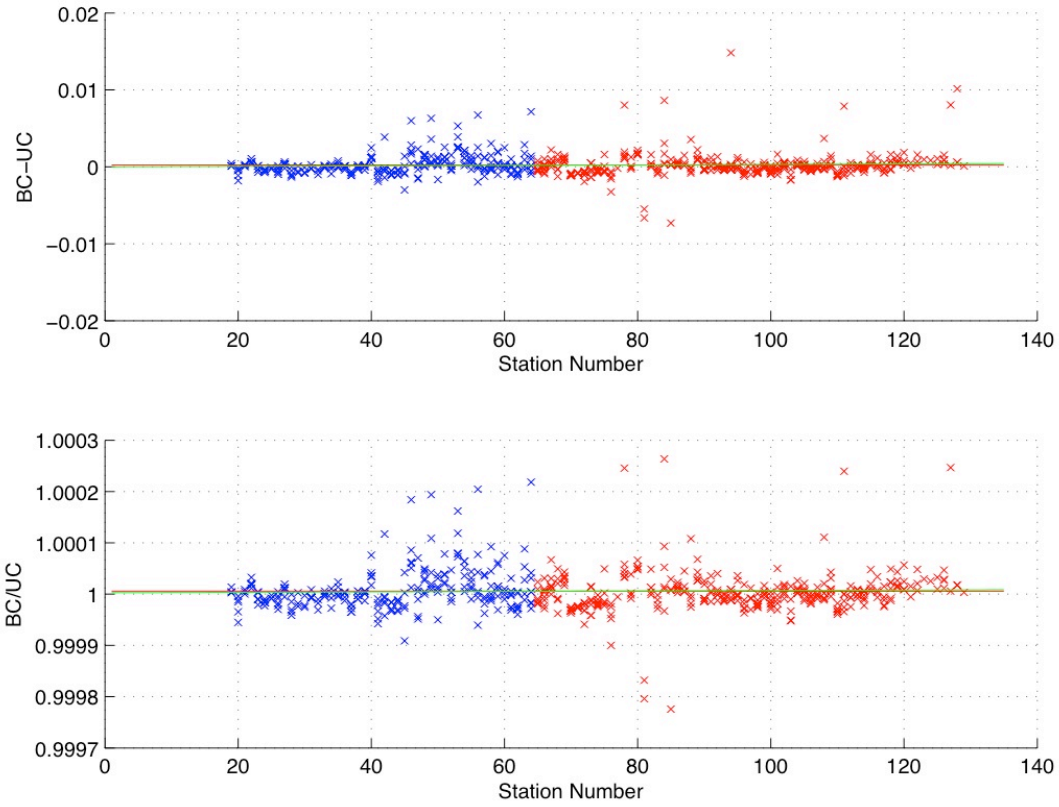

Figure 12: Residuals and ratio of the bottled and CTD conductivities for all points below 3000db for each station of the total 135 stations. The blue x show the first Autosal and the red x indicate the second Autosal.

The peristaltic pumps presented some issues, firstly due to bubbles forming within the cell of the Autosal, and also due to leaking from the plastic tubing. Formation of bubbles within the cell increases the analysis time, because additional flushing is required to remove the bubbles, and also bubbles have the potential to alter the conductivity readings. Leaks can reduce performance, further increasing analysis time. Three peristaltic pumps were used during the cruise and the tubing on two of them was changed due to leaks.

3.8. Secondary Standards

Secondary standards were briefly used to assess the stability of the second Autosal, to ensure reasonable residuals. A crate of 24 salinity bottles was drawn from one Niskin bottle (Niskin bottle 1) containing deep water (6146m) at Station 69. The secondary standards were run at the start, middle and end of each crate, accompanying the standards that were already being run.

The use of the secondary standards, Figure 13, seemed to provide no clear indication of a linear drift of the Autosal during an individual crate with a correlation coefficient of 0.1 between the primary and secondary standards for the test analysis.

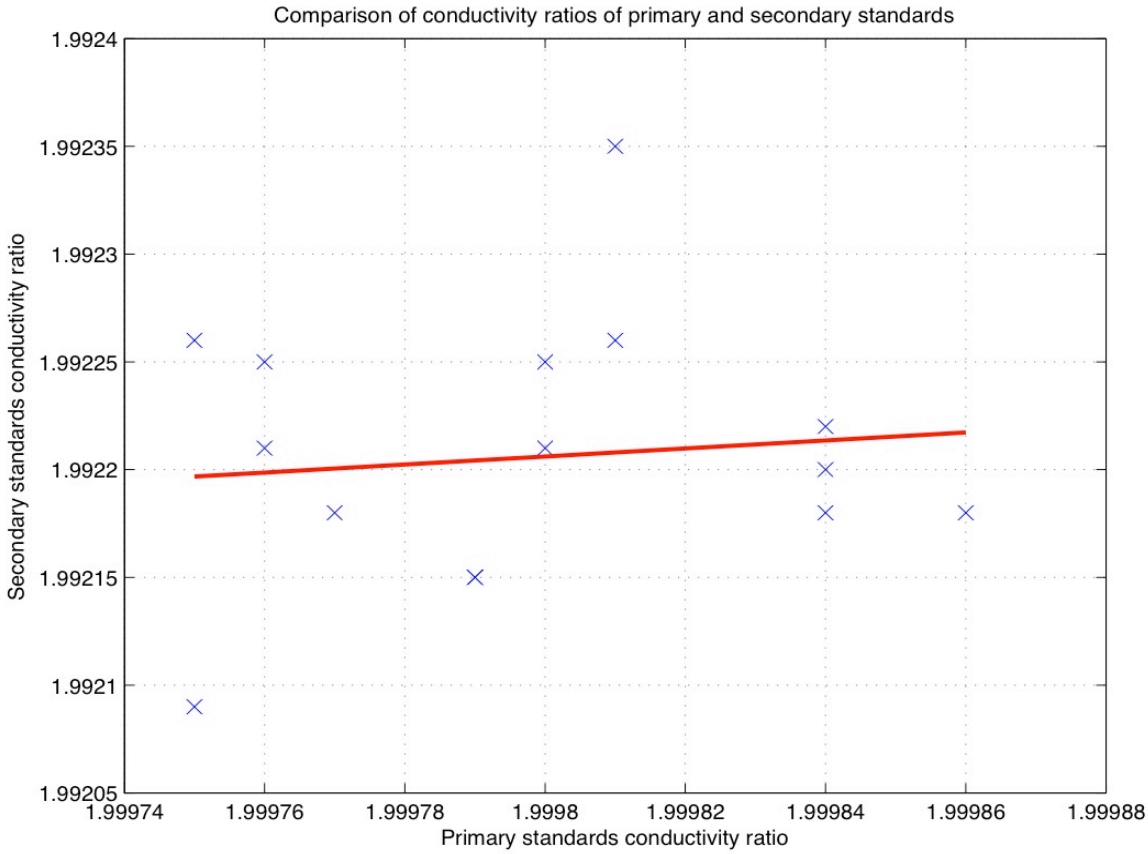

Figure 13: Guildline conductivity ratio for primary and secondary seawater standards for the same time period of Stations 69-75

Hence, a single adjustment value per crate is still the preferred method, as opposed to correcting for a linear drift of the Autosal during individual crates.

3.9. Processing

The data logging software outputs a Microsoft Excel spreadsheet containing the salinity of each sample. The spreadsheets were then manually edited. A sample number was assigned based on the station number and the position that the sample was taken from on the CTD rosette. For example, if the Niskin bottle in the first position was sampled at Station 32, the sample number would be 3201. Consultation of the CTD log sheets was required to account for any bottles that had failed to close or fire. The seawater standards were given an individual ID with one nine added to the sequential standard number (e.g. '9001', would be the sample number for the first standard used on the cruise). The TSG spreadsheets were edited to include a sample number based from the time at which the sample was taken, in the following format, '*ddhhmmss*'. After editing, the files were saved as comma delimited csv files for input into Matlab.

Using the adjustments chosen for each station and the data spreadsheets it was now possible to process the data using Matlab scripts: *msal_01.m* and *msal_02.m*. The adjustments are chosen based on the difference between the standard seawater sample measured by the Autosal and the actual conductivity ratio of the seawater. Adjacent difference values were also taken into account when deciding the adjustment. For the TSG, the Matlab script *mtsg_01_di346.m* was used. Similarly this requires an adjustment based on the standard seawater values.

Table 3: Bottle salinity analysis information

ID	Station	Crate	Run pos	Standard	Measured	Difference	Adjustment
9001	1	35	Before start	1.99994	1.99974	0.00020	0.00013
9002	1	35	End	1.99994	1.99981	0.00013	
9003	5	15	End	1.99994	1.99981	0.00013	0.00013
9004	7	19	End	1.99994	1.99981	0.00013	0.00013
9005	10	12	End	1.99994	1.99981	0.00013	0.00013
9006	11	24	Before start	1.99994	1.99969	0.00025	0.00017
9007	15	11	End	1.99994	1.99977	0.00017	0.00017
9008	15	11	End	1.99994	1.99977	0.00017	
9009	16	1	Before start	1.99994	1.99973	0.00021	0.00017
9010	17	40	Midway	1.99994	1.99975	0.00019	0.00019
9011	18	15	End	1.99994	1.99976	0.00018	0.00019
9012	19	19	Before start	1.99994	1.99970	0.00024	0.00018
9013	19	19	End	1.99994	1.99976	0.00018	
9014	20	35	End	1.99994	1.99977	0.00017	0.00018
9015	21	12	Before start	1.99994	1.99976	0.00018	0.00018
9016	22	24	End	1.99994	1.99981	0.00013	0.00015
9017	23	40	End	1.99994	1.99984	0.00010	0.00014
9018	TSG001	901	End	1.99994	1.99976	0.00018	0.00016
9019	23	40	End	1.99994	1.99982	0.00012	0.00015
9020	24	1	Before start	1.99994	1.99976	0.00018	0.00016
9021	24	1	End	1.99994	1.99978	0.00016	
9022	25	19	End	1.99994	1.99974	0.00020	0.00017
9023	26	15	End	1.99994	1.99977	0.00017	0.00017
9024	27	35	Before start	1.99994	1.99978	0.00016	0.00017
9025	27	35	End	1.99994	1.99978	0.00016	
9026	28	40	End	1.99994	1.99976	0.00018	0.00017
9027	29	11	Before start	1.99994	1.99978	0.00016	0.00017
9028	29	11	End	1.99994	1.99977	0.00017	0.00017
9029	30	12	Before start	1.99994	1.99974	0.00020	0.00017
9030	30	12	End	1.99994	1.99982	0.00012	
9031	31	21	End	1.99994	1.99981	0.00013	0.00014
9032	32	19	Before start	1.99994	1.99980	0.00014	0.00014
9033	33	1	End	1.99994	1.99975	0.00019	0.00017
9034	33	1	End	1.99994	1.99976	0.00018	
9035	34	10	Before start	1.99994	1.99975	0.00019	0.00017
9036	34	10	End	1.99994	1.99973	0.00021	
9037	35	15	End	1.99994	1.99977	0.00017	0.00017
9038	36	24	Before start	1.99994	1.99974	0.00020	0.00017
9039	37	11	End	1.99994	1.99977	0.00017	0.00017
9040	37	11	End	1.99994	1.99984	0.00010	0.00012
9041	38	12	End	1.99994	1.99984	0.00010	0.00012
9042	39	40	End	1.99994	1.99988	0.00006	0.00011
9043	40	1	Before start	1.99994	1.99986	0.00008	0.00014
9044	40	1	End	1.99994	1.99977	0.00017	
9045	TSG002	1	End	1.99994	1.99977	0.00017	0.00015
9046	41	19	End	1.99994	1.99979	0.00015	0.00015
9047	42	21	End	1.99994	1.99979	0.00015	0.00015

9048	43	24	Before start	1.99994	1.99973	0.00021	0.00017
9049	43	24	End	1.99994	1.99973	0.00021	
9050	44	15	End	1.99994	1.99980	0.00014	0.00017
9051	45	11	End	1.99994	1.99977	0.00017	0.00017
9052	46	40	Before start	1.99994	1.99980	0.00014	0.00014
9053	46	40	End	1.99994	1.99986	0.00008	
9054	47	19	End	1.99994	1.99988	0.00006	0.00012
9055	48	1	Before start	1.99994	1.99972	0.00022	0.00020
9056	48	1	End	1.99994	1.99976	0.00018	
9057	49	21	End	1.99994	1.99974	0.00020	0.00020
9058	50	12	End	1.99994	1.99973	0.00021	0.00020
9059	51	11	Before start	1.99994	1.99989	0.00005	0.00012
9060	51	11	End	1.99994	1.99972	0.00022	
9061	52	40	End	1.99994	1.99973	0.00021	0.00020
9062	53	19	Before start	1.99994	1.99989	0.00005	0.00012
9063	53	19	End	1.99994	1.99974	0.00020	
9064	54	15	End	1.99994	1.99988	0.00006	0.00006
9065	55	21	End	1.99994	1.99984	0.00010	0.00011
9066	56	12	Before start	1.99994	1.99984	0.00010	0.00011
9067	56	12	End	1.99994	1.99992	0.00002	
9068	57	10	End	1.99994	1.99982	0.00012	0.00011
9069	58	40	Before start	1.99994	1.99977	0.00017	0.00013
9070	58	40	End	1.99994	1.99978	0.00016	
9071	TSG003	901	Before start	1.99994	1.99978	0.00016	0.00013
9072	TSG003	901	End	1.99994	1.99977	0.00017	
9073	59	15	End	1.99994	1.99983	0.00011	0.00011
9074	60	1	Before start	1.99994	1.99984	0.00010	0.00016
9075	60	1	End	1.99994	1.99975	0.00019	0.00016
9076	61	24	End	1.99994	1.99977	0.00017	0.00016
9077	62	12	End	1.99994	1.99976	0.00018	0.00016
9078	63	21	Before start	1.99994	1.99975	0.00019	0.00016
9079	63	21	End	1.99994	1.99980	0.00014	
9080	64	19	End	1.99994	1.99978	0.00016	0.00016
9081	200	15	End	1.99994	1.99972	0.00022	0.00020
9082	65	11	Before start	1.99994	1.99984	0.00010	0.00013
9083	65	11	End	1.99994	1.99979	0.00015	
9084	66	40	End	1.99994	1.99979	0.00015	0.00015
9085	67	21	Before start	1.99994	1.99979	0.00015	0.00014
9086	67	21	End	1.99994	1.99980	0.00014	
9087	68	19	End	1.99994	1.99983	0.00011	0.00011
9088	69	12	Before start	1.99994	1.99977	0.00017	0.00017
9089	69	12	End	1.99994	1.99976	0.00018	
9090	70	10	End	1.99994	1.99981	0.00013	0.00013
9091	71	21	End	1.99994	1.99979	0.00015	0.00015
9092	TSG004	1	Before start	1.99994	1.99975	0.00019	0.00014
9093	TSG004	1	End	1.99994	1.99984	0.00010	
9094	72	11	End	1.99994	1.99980	0.00014	0.00014
9095	73	19	End	1.99994	1.99984	0.00010	0.00011

9096	74	12	Before start	1.99994	1.99975	0.00019	0.00016
9097	74	12	End	1.99994	1.99979	0.00015	
9098	75	24	End	1.99994	1.99986	0.00008	0.00010
9099	76	40	End	1.99994	1.99983	0.00011	0.00011
9100	77	10	Before start	1.99994	1.99976	0.00018	0.00016
9101	77	10	End	1.99994	1.99978	0.00016	
9102	78	21	End	1.99994	1.99979	0.00015	0.00015
9103	79	1	Before start	1.99994	1.99977	0.00017	0.00016
9104	79	1	End	1.99994	1.99978	0.00016	
9105	80	15	End	1.99994	1.99978	0.00016	0.00016
9106	81	40	Before start	1.99994	1.99973	0.00021	0.00016
9107	81	40	End	1.99994	1.99980	0.00014	
9108	82	24	End	1.99994	1.99980	0.00014	0.00014
9109	83	21	End	1.99994	1.99982	0.00012	0.00012
9110	84	10	Before start	1.99994	1.99995	-0.00001	0.00012
9111	84	10	End	1.99994	1.99980	0.00014	
9112	TSG005	901	End	1.99994	1.99982	0.00012	0.00012
9113	85	12	Before start	1.99994	1.99978	0.00016	0.00014
9114	85	12	End	1.99994	1.99981	0.00013	
9115	86	15	End	1.99994	1.99979	0.00015	0.00015
9116	87	40	End	1.99994	1.99979	0.00015	0.00015
9117	88	19	Before start	1.99994	1.99980	0.00014	0.00014
9118	88	19	End	1.99994	1.99981	0.00013	
9119	89	11	End	1.99994	1.99975	0.00019	0.00019
9120	90	35	End	1.99994	1.99976	0.00018	0.00018
9121	91	40	Before start	1.99994	1.99972	0.00022	0.00019
9122	91	40	End	1.99994	1.99975	0.00019	
9123	92	10	End	1.99994	1.99976	0.00018	0.00018
9124	93	12	Before start	1.99994	1.99953	0.00041	0.00019
9125	93	12	End	1.99994	1.99975	0.00019	
9126	94	11	End	1.99994	1.99973	0.00021	0.00021
9127	95	19	Before start	1.99994	1.99972	0.00022	0.00020
9128	95	19	End	1.99994	1.99975	0.00019	
9129	96	35	End	1.99994	1.99978	0.00016	0.00016
9130	97	15	End	1.99994	1.99977	0.00017	0.00017
9131	98	12	Before start	1.99994	1.99967	0.00027	0.00017
9132	98	12	End	1.99994	1.99978	0.00016	
9133	99	11	End	1.99994	1.99977	0.00017	0.00017
9134	100	21	Before start	1.99994	1.99973	0.00021	0.00019
9135	100	21	End	1.99994	1.99977	0.00017	
9136	TSG006	1	End	1.99994	1.99973	0.00021	0.00021
9137	101	19	End	1.99994	1.99974	0.00020	0.00020
9138	102	40	Before start	1.99994	1.99975	0.00019	0.00021
9139	102	40	End	1.99994	1.99971	0.00023	
9140	103	11	End	1.99994	1.99977	0.00017	0.00017
9141	104	24	Before start	1.99994	1.99973	0.00021	0.00020
9142	104	24	End	1.99994	1.99975	0.00019	
9143	105	12	End	1.99994	1.99973	0.00021	0.00021

9144	106	10	Before start	1.99994	1.99970	0.00024	0.00023
9145	106	10	End	1.99994	1.99972	0.00022	
9146	107	35	Start/End	1.99994	1.99972	0.00022	0.00022
9147	108	11	Before start	1.99994	1.99976	0.00018	0.00018
9148	109	24	End	1.99994	1.99973	0.00021	0.00021
9149	113	24	Before start	1.99994	1.99967	0.00027	0.00025
9150	113	24	End	1.99994	1.99969	0.00025	
9151	110	12	End	1.99994	1.99977	0.00017	0.00017
9152	111	21	End	1.99994	1.99973	0.00021	0.00021
9153	112	40	Before start	1.99994	1.99968	0.00026	0.00021
9154	112	40	End	1.99994	1.99978	0.00016	
9155	TSG007	901	End	1.99994	1.99973	0.00021	0.00021
9156	114	11	Before start	1.99994	1.99971	0.00023	0.00022
9157	114	11	End	1.99994	1.99973	0.00021	
9158	115	19	End	1.99994	1.99972	0.00022	0.00022
9159	116	24	End	1.99994	1.99974	0.00020	0.00020
9160	117	35	Before start	1.99994	1.99973	0.00021	0.00018
9161	117	35	End	1.99994	1.99978	0.00016	
9162	118	40	End	1.99994	1.99978	0.00016	0.00016
9163	119	10	Before start	1.99994	1.99972	0.00022	0.00020
9164	119	10	End	1.99994	1.99976	0.00018	
9165	120	15	End	1.99994	1.99975	0.00019	0.00019
9166	121	24	Before start	1.99994	1.99969	0.00025	0.00023
9167	121	24	End	1.99994	1.99972	0.00022	
9168	122	21	End	1.99994	1.99970	0.00024	0.00024
9169	123	35	End	1.99994	1.99971	0.00023	0.00023
9170	124	11	Before start	1.99994	1.99965	0.00029	0.00020
9171	124	11	End	1.99994	1.99980	0.00014	
9172	125	10	Before start	1.99994	1.99973	0.00021	0.00021
9173	125	10	End	1.99994	1.99972	0.00022	
9174	126	40	End	1.99994	1.99972	0.00022	0.00022
9175	127	15	End	1.99994	1.99977	0.00017	0.00017
9176	128	1	Before start	1.99994	1.99974	0.00020	0.00016
9177	128	1	End	1.99994	1.99982	0.00012	
9178	129	19	End	1.99994	1.99982	0.00012	0.00012
9179	130	21	Before start	1.99994	1.99972	0.00022	0.00019
9180	130	21	End	1.99994	1.99977	0.00017	
9181	131	35	End	1.99994	1.99981	0.00013	0.00013
9182	132	11	End	1.99994	1.99980	0.00014	0.00014
9183	133	10	End	1.99994	1.99976	0.00018	0.00018
9184	134/35	15/40	End	1.99994	1.99976	0.00018	0.00018
9185	TSG008	1	Before start	1.99994	1.99966	0.00028	0.00026
9186	TSG008	1	End	1.99994	1.99969	0.00025	

Gavin Evans

4. Inorganic and Total Nutrient Analysis

4.1. Method

Seawater was collected for analysis of micro-molar concentrations of dissolved nutrients; nitrate and nitrite (hereafter nitrate), phosphate and silicate. Samples for inorganic nutrient analysis were collected directly into either 30mL plastic pots or 60mL Sterilin pots. 60mL pots were used for collection of seawater for total nutrient analysis. The pots were rinsed with sample water at least three times before drawing the sample. When required, samples were stored in a fridge at approximately 4°C until analysis.

In general analyses were started within 1-4 hours of sample collection using a segmented continuous-flow Skalar San^{plus} autoanalyser set up for analysis and data logging with the Flow Access Software version 1.3.11. This system follows the method described by *Kirkwood* (1996), with the exception that the pump rates through the phosphate line were increased by a factor of 1.5, which improves the reproducibility and peak shape of the results.

For D346 the analysis was calibrated using the set of standards shown in Table 4. Table 4 shows target and actual standard concentrations. Target concentrations were values that were desired when preparing working standards (i.e., standards used everyday). Actual concentrations were values corrected by taking into account *i)* the weight of the dry chemical used to prepare a given standard (Table 4) and, *ii)* the calibrated volume of the pipettes used for diluting stock standards (i.e., high concentration standards).

5µmol L^{-1} stock standard solutions prepared in Milli-Q water were used to produce working standards. Working standards were prepared in a saline solution (40g NaCl in 1L of Milli-Q water, hereafter artificial seawater), which was also used as diluent for the analyses.

Total nutrients, total nitrogen (TN) and total phosphorus (TP), were measured as nitrate and phosphate, respectively, after photo-oxidation for 2 hours using a Metrohm 705 digester (*Sanders and Jickells, 2002*). The oxidation efficiency of the method was monitored using a Guanosine standard at two different N and P concentrations; i) 2 and 5µmol L^{-1} nitrogen, ii) 0.4 and 1µmol L^{-1} phosphorus, which produced i) 2±0.3 and 4.1±0.8 (efficiency higher than 80%) and ii) 0.2±0.3 and 0.8±0.2 (efficiency higher than 50%). The UV systems were installed inside the fume hood of the chemistry lab and a flow meter was attached in order to monitor the water flow for cooling.

Table 4: Set of calibration standards (*Std*) used for dissolved inorganic nutrient analysis. Bold numbers are target concentrations, otherwise actual concentrations. Concentration units are μmol L^{-1}.

	Nitrate		**Phosphate**		**Silicate**	
Std 1	**40**	40.80	**2.5**	2.54	**60**	61.22
Std 2	**20**	20.40	**2.0**	2.03	**40**	40.81
Std 3	**10**	10.10	**1.5**	1.52	**20**	20.41
Std 4	**5**	5.10	**1.0**	1.01	**10**	10.20
Std 5	**1**	1.02	**0.5**	0.51	**2.5**	2.55

Table 5: Compounds used to prepare stock standard solutions, weight dissolved in 1 L of Milli-Q water and molarity of the solution.

Compound	**Weight (g)**	**Molarity 1 L stock solution**
KH_2PO_4	0.6813	**5.0064**
Na_2SiF_6	0.9468	**5.0346**
$NaNO_3$	0.4278	**5.0332**
$NaNO_2$	0.3493	**5.0626**

4.2. Observations (inorganic and total nutrient analysis)

4.2.1. General observations

Prior to the cruise, all labware was washed with 10% HCl and rinsed with Milli-Q water several times. The labware was then rinsed again once onboard the ship.

The autoanalyser was washed through with 10% Deacon 90 then Milli-Q water for at least 30 minutes respectively after each run when the time between stations allowed, otherwise the autoanalyser was left with the reagent tubing connected ready for the next run. However, it was noticed that after each wash the baseline displayed a slight drift, with a decreasing trend as the run progressed. Therefore, the autoanalyser was usually left with the reagent tubing connected to avoid this problem. New pump tubing and lamps were fitted at the start of the cruise, along with a new cadmium column. After one and a half weeks the pump tubing was turned around to prevent the section in the pump from wearing out. By two and a half weeks, all tubing and lamps were replaced, and the cadmium column was replaced for the second half of the cruise. The new tubing was turned around at 5 weeks.

New batches of artificial seawater were prepared almost once a week and 2 sets of calibration standards were produced and used, with the first used up until CTD081 and the second from CTD082. Both artificial seawater and standards were analysed prior to use in order to check for contamination and consistency.

Time series of baseline, instrument sensitivity, calibration curve correlation coefficient and nitrate reduction efficiency were compiled to check the performance of the autoanalyser over the course of the cruise and are shown in Figures 14 to 20.

4.2.2. Autoanalysers

Originally two autoanalysers were set up to allow inorganic and total nutrient concentrations to be analysed separately. A second aim for a double setup was to test whether both instruments produced results consistent with each other. However, there was a communication issue very early on with the autoanalyser set up for inorganic nutrient analysis, which caused the calibration of nitrate to fail. The computer set for this autoanalyser crashed and it required reformatting, which caused the first couple of analysis files to be lost. The problem persisted even after the computer was reformatted, and it remains unclear whether the problem was related to the Flow Access software, a malfunction of the computer communication port, or a malfunction of the interface (integrator) between the light detectors and the computer. Samples for both inorganic and total nutrient analysis were therefore run through the same analyser for most of the cruise period, which also contributed to slowing down the turnover of sample processing and subsequently, of the results.

4.2.3. Total Nutrient Analysis

At the start of the cruise all samples from all stations were UV oxidised in duplicates. However, since the two UV units were first switched on, they started failing, despite being sent to the manufacturer (Metrohm) for maintenance prior to the cruise. This delayed the progress of the analysis and soon after the Florida Straits transect, these delays resulted in a large backlog of samples.

Ideally total nutrients should be analysed together with the respective inorganic fraction in the same autoanalyser run, but the large backlog prompted us to run all inorganic nutrient samples as soon as possible and the total nutrients as soon they became available upon UV oxidation (from Station 1 to Station 39). This suggested analysing total nutrients in separate runs.

In order to reduce the pressure on the lamps and clear the backlog of samples, it was decided to reduce the number of samples being analysed for total nutrient concentrations to every third station. From Station 39 and starting with Station 42, 1 out of 3 CTD casts were thus sampled for total nutrients. Whenever a Niskin bottle misfired, the available space on the UV unit racks was used for either a replicate or for the analysis of a Guanosine standard.

Once the backlog was cleared and the time between stations increased, it was decided that samples for total nutrient analysis should be taken from all casts again. However, this was not possible, due to the continuous failure of the UV systems.

Repeats of whole profiles were also run for a number of stations to check the reliability of the UV digester units and accuracy of the total nutrient concentrations. In the case of total nitrogen, repeats produced similar results, mostly within the error of the technique. However, results were not always consistent for total phosphorus concentrations. There were cases where the first run produced results inconsistent with the inorganic fraction, yet the results from the second run were consistent and vice versa. There were also cases where both runs produced either consistent or inconsistent results relative to the inorganic fraction. This suggests that the methodology may be flawed or is subject to error.

4.2.4. UV systems

UV digesters were unreliable throughout the duration of the cruise. Failure was originally due to the units overheating. It was discovered that the flow of the cooling system was insufficient to maintain the required temperature. Both UV units were initially washed out several times with 4M HCl and rinsed with Milli-Q, which improved the flow, indicating that the problem may have been accumulation of limescale inside the cooling system. However, the units soon became blocked again and so were washed out with 5M H_2SO4 followed by Milli-Q. This procedure was repeated frequently throughout the cruise to maintain a good flow through the cooling system. The pump unit was elevated to increase its efficiency. The units were also set to run for 1 hour at a time with a minimum of a 30 minutes cooling period between runs, thereby further reducing the potential for overheating and loss of the samples. In addition to the cooling system, a fan was used to improve airflow inside the fume hood and further reduce the potential of overheating.

The original bulbs fused early on and were replaced by brand new bulbs. However, the new bulbs also fused within a few uses. The melted end and surrounding glass were filed away to expose the undamaged connection wire. A copper disc was then placed at the base connection to provide the extra height needed for the lamp to reach the upper connection of the lamp unit. This fix functioned well, although the copper discs needed replacing every couple of days when the lamps were seen to fail more frequently than usual. The copper disc oxidised very quickly, most likely due to the high voltage passed though it when the unit is switched on. By the start of the fifth week of the cruise two of the UV bulbs were completely fused.

4.2.5. Performance of the Analyser

The performance of the autoanalyser was monitored by producing time series plots of the following parameters: standard concentrations, baseline, calibration slope (instrument sensitivity), calibration correlation coefficient, nitrate reduction efficiency, low nutrient seawater and bulk nutrient seawater. These are plotted against run/analysis number rather than date or station number given that runs sometimes included more than 2 stations and UV oxidised samples.

The precision of the method was determined by monitoring the variations of the complete set of standards measured throughout the cruise. Results of the standard measurements are summarised in Table 6 and shown in Figure 16. Triplicate analyses were performed on the first, mid and last sample of every station. This revealed the sample variability of replicates from a given mean concentration, which

was in general <0.8% (n=459). The limits of detection of this method were determined from the concentrations of lowest standard of each nutrient. The limits of detection of this method during D346 were 0.09µmol L^{-1} for PO_4^{3-}, 0.10µmol L^{-1} for NO_3^- and 0.14µmol L^{-1} for $Si(OH)_4$.

Table 6: Means and variations of all the standards measured, and the precision of the analysis at each concentration (µmol L^{-1}).

	NO_3^-	Prec.	PO_4^{3-}	Prec.	$Si(OH)_4$	Prec.
Std 1	40.8 ±0.3	0.1%	2.53 ±0.05	1.8%	61.4 ±0.4	0.7%
Std 2	20.4 ±0.2	0.9%	2.03 ±0.06	3.1%	40.9 ±0.3	0.7%
Std 3	10.1 ±0.9	8.8%	1.53 ±0.08	5.0%	20.6 ±1.8	8.7%
Std 4	5.0 ±0.1	1.6%	1.04 ±0.17	16.7%	10.2 ±0.1	0.7%
Std 5	1.1 ±0.05	4.6%	0.50 ±0.06	12.3%	2.6 ±0.1	2.7%

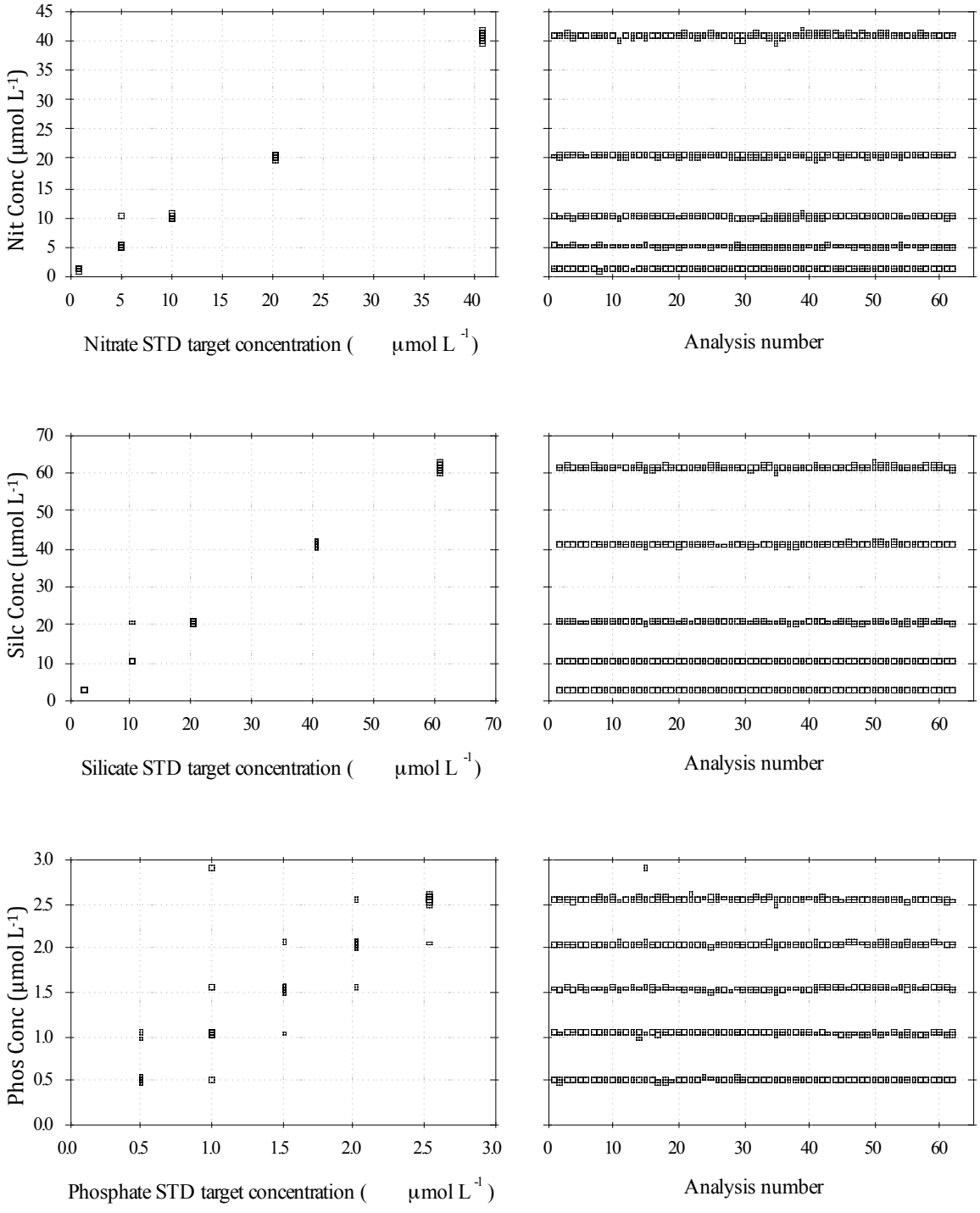

Figure 14: Complete set of 'measured' standards plotted against the 'prepared or intended' concentration (left side panels). 'Measured' standards plotted against respective analysis number (right side panels).

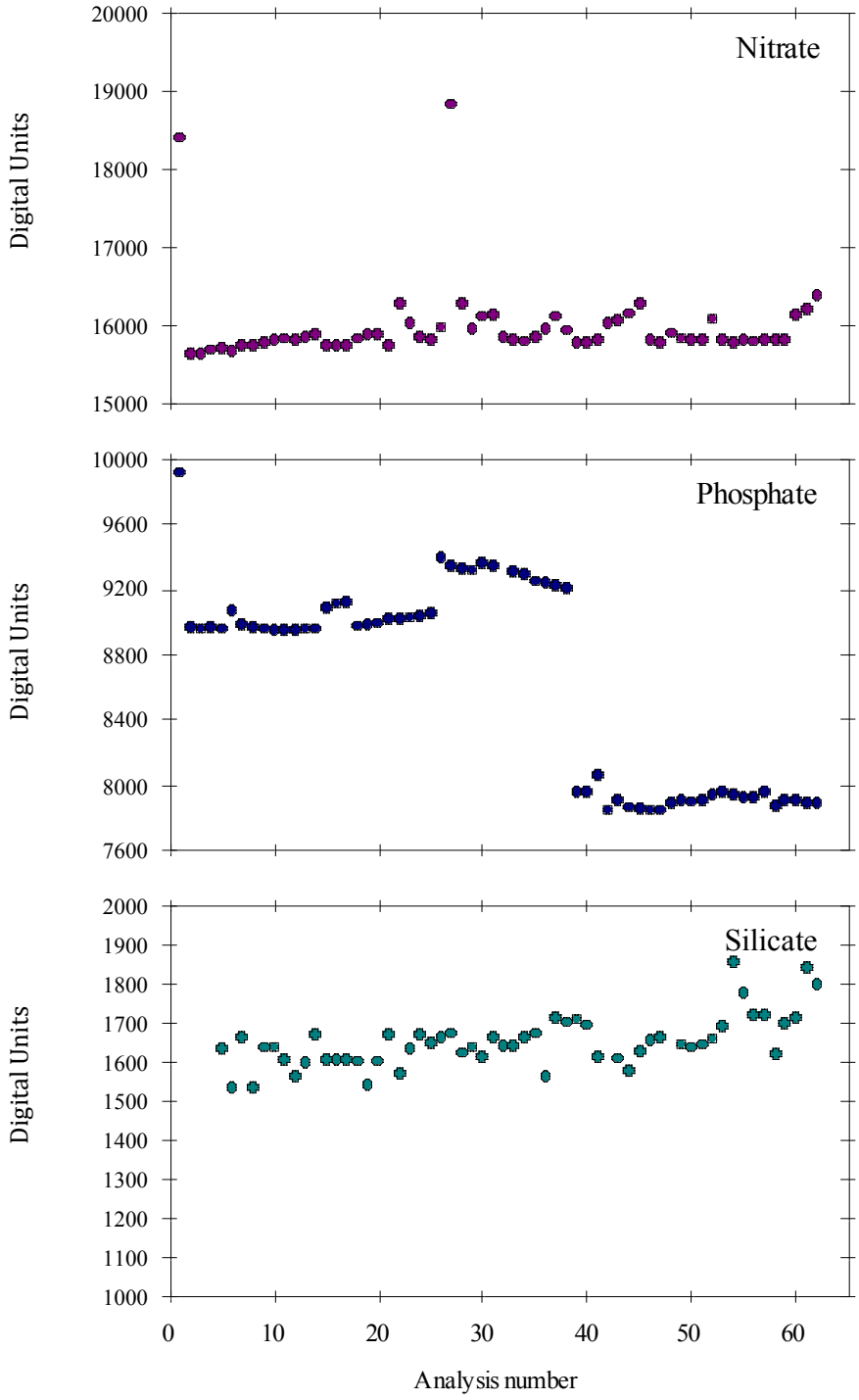

Figure 15: Baselines time series. The baseline for nitrate was fairly consistent all through the cruise. The phosphate baseline changed dramatically after changing the autoanalyser tubing and the silicate baseline shows a slight increased with time.

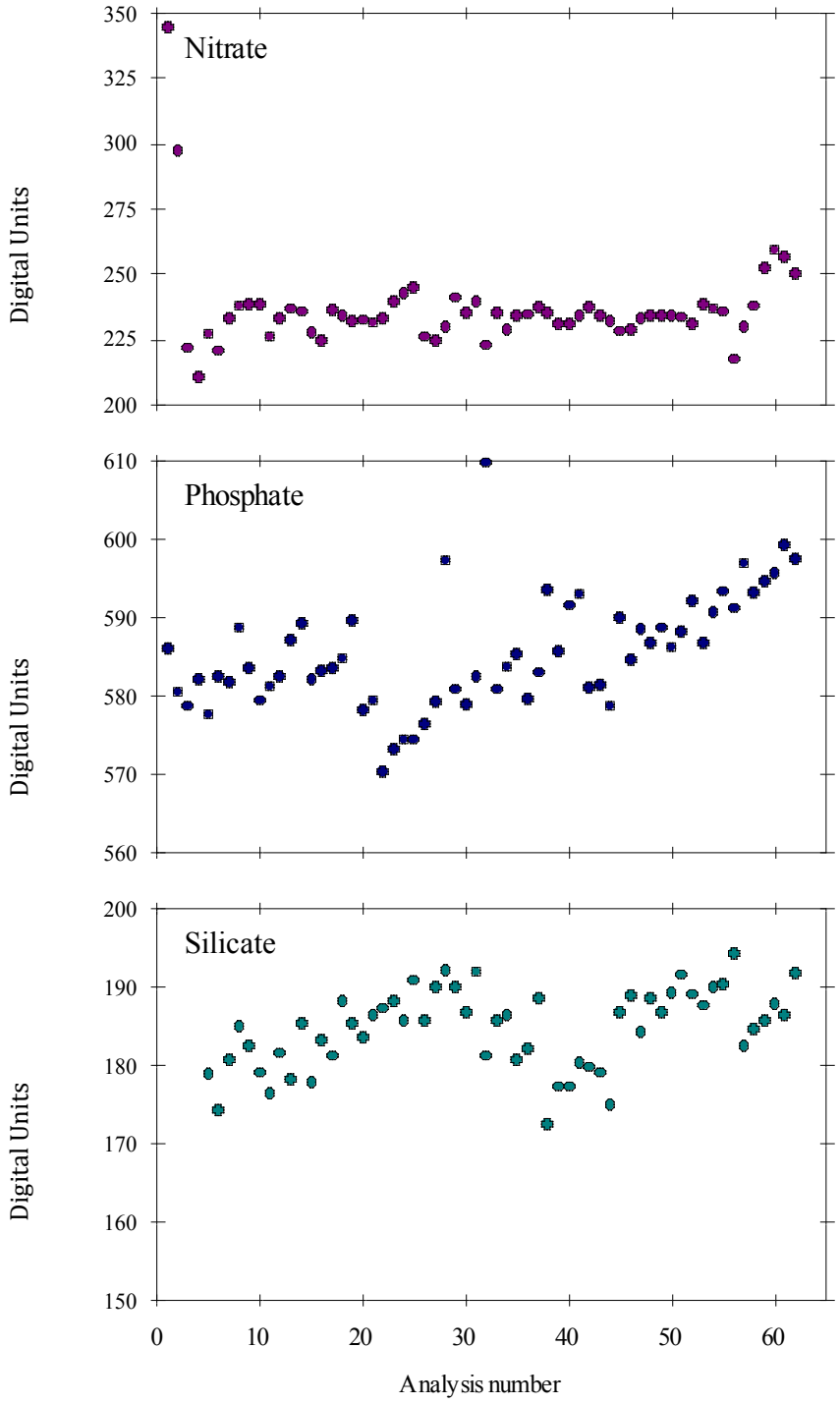

Figure 16: Calibration slope time series. These show the sensitivity of the three different autoanalyser channels (i.e., nitrate, silicate and phosphate), with increasing values (in digital units) indicating better sensitivity. The calibration slopes for nitrate and silicate remain fairly constant with time, with phosphate increasing towards the end of the cruise.

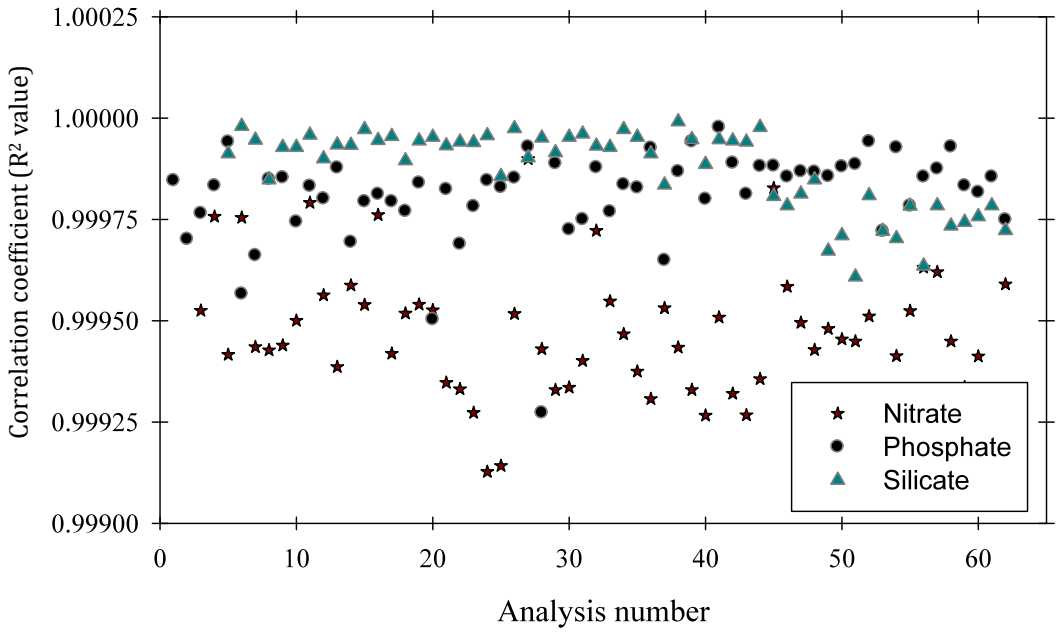

Figure 17. Calibration correlation coefficients. All r^2 were better than 0.999.

Low Nutrient Seawater: Certified Ocean Scientific International (OSIL) Low Nutrient Seawater (LNSW) was measured in duplicate in every run in order to test artificial seawater for contamination. LNSW has been also used as a quality control in order to check for the reproducibility of low nutrient concentrations.

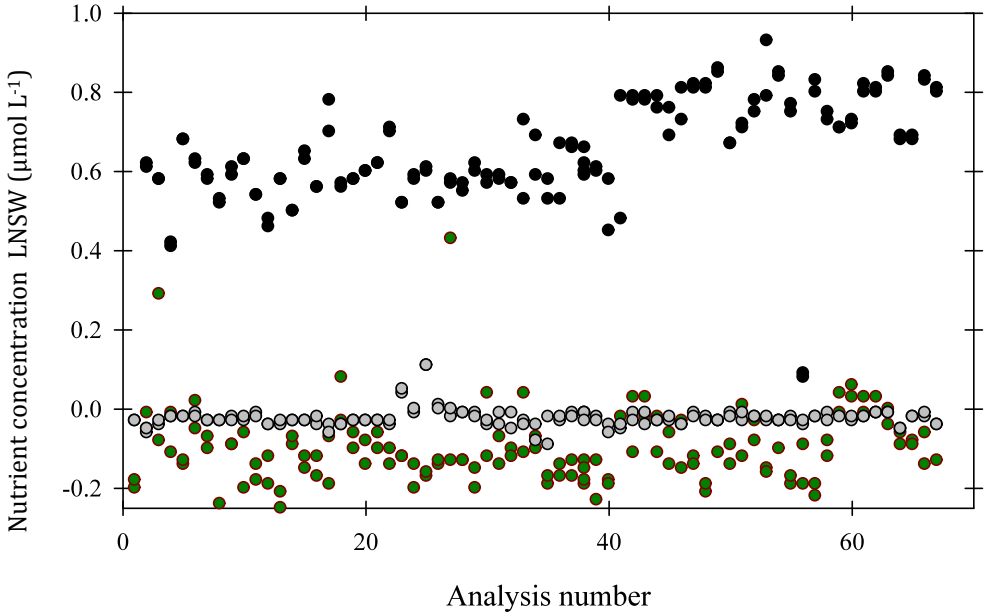

Figure 18: Low Nutrient Seawater (LNSW) time series. Black dots represent silicate, green dots represent nitrate and grey dots represent phosphate concentrations.

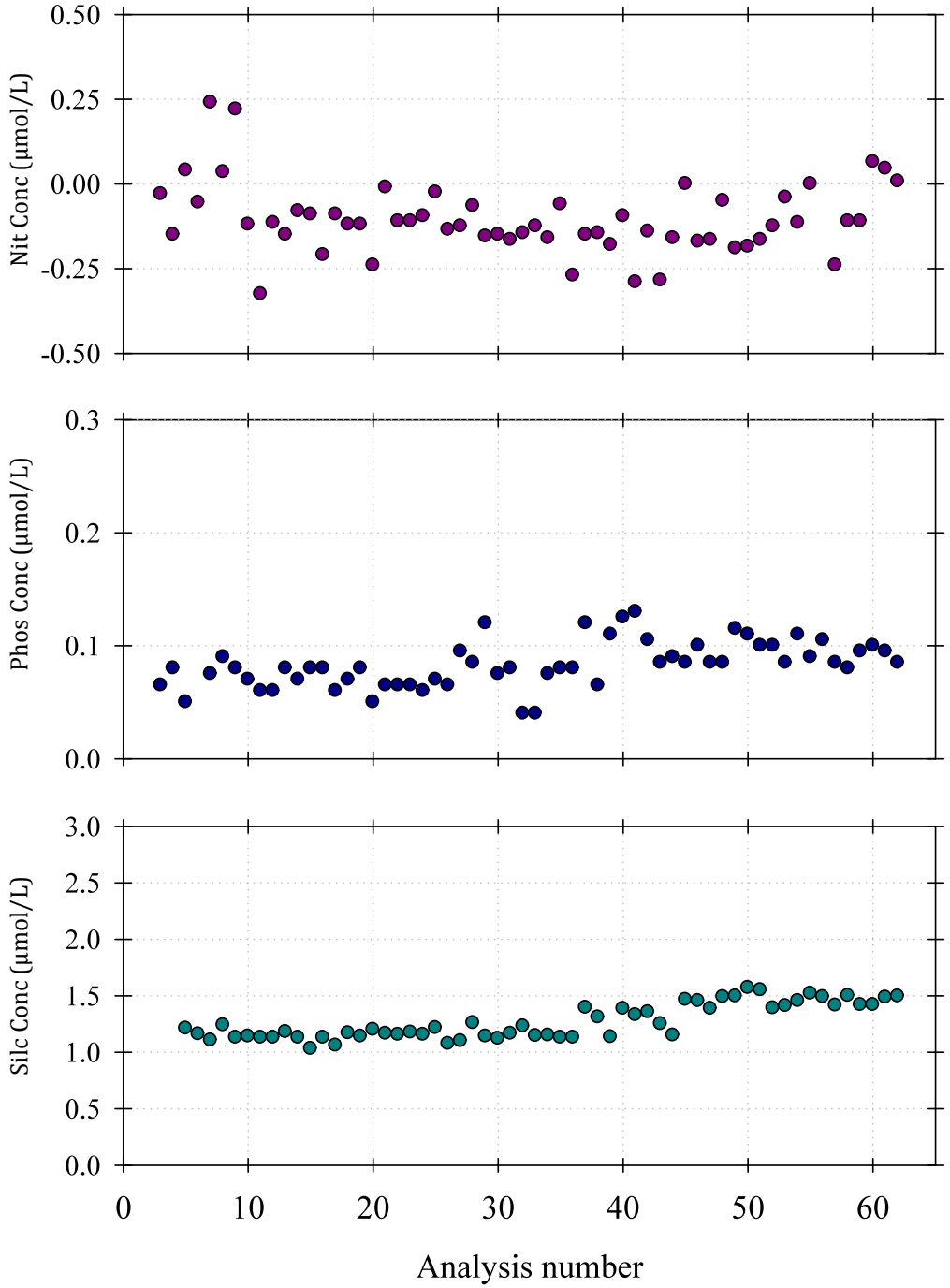

Figure 19: Time series of bulk nutrient seawater (from the South Atlantic Subtropical Gyre) concentrations. The average concentration was -0.14±0.1µmol L^{-1}, 1.26±1.2µmol L^{-1}, 0.08±0.08µmol L^{-1} for nitrate, silicate and phosphate respectively. Given the low nutrient concentration of the surface South Atlantic Subtropical Gyre, the negative concentration of nitrate and phosphate indicates this water has less nitrate and phosphate than the background levels of our artificial seawater solution.

Seawater collected in 2009 during the JC032 (24°S) cruise from the surface subtropical South Atlantic Ocean (henceforth referred to as Bulk Nutrients) was used as an additional 'Low Nutrient' standard. The purposes of measuring bulk nutrients are i) to test for the consistency of low nutrient measurements throughout the cruise and ii) to test artificial seawater (ASW) batches for contamination (i.e. by comparing these with the baseline produced by ASW).

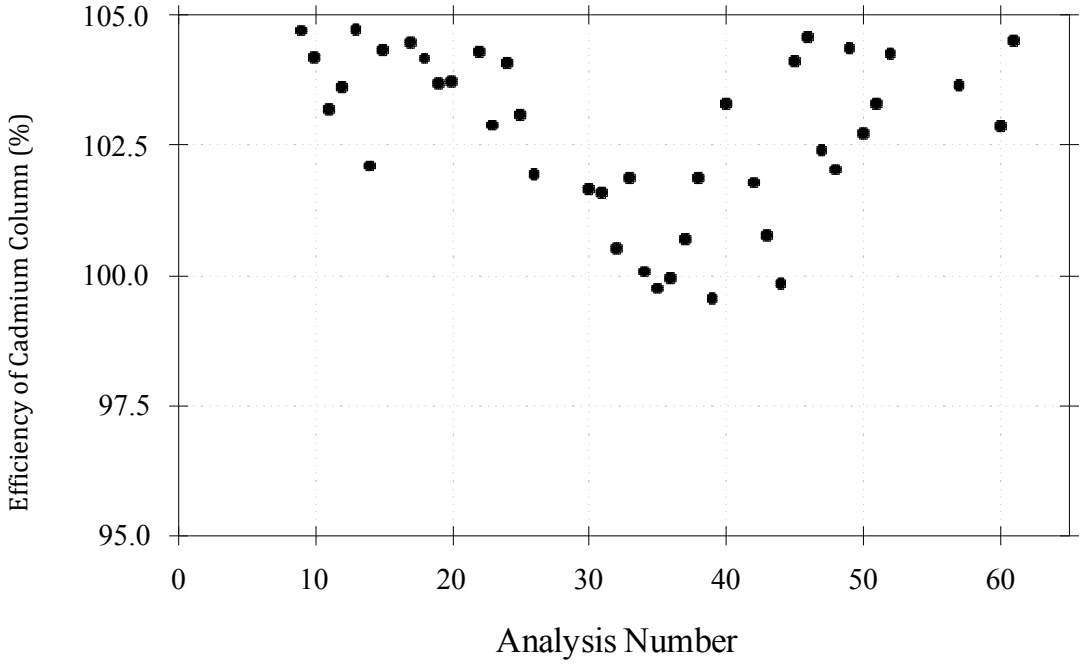

Figure 20: The efficiency of the cadmium column in reducing nitrate to nitrite is tested by measuring a nitrite standard of similar concentration to the top nitrate standard (40µmol L^{-1}). This figure shows the ratio of nitrate to nitrite for all analysis carried out. The nitrate standard though, was slightly lower than targeted, with an average concentration of 39.4µmol L^{-1}.

Sinhue Torres, Laura Casburn, Ekaterina Chernyavskaya, Claire Powell and Helen Smith

5. Dissolved Oxygen

All stations occupied during D346 were sampled for dissolved oxygen (DO) just after CFCs were sampled. Seawater was collected directly into pre-calibrated glass bottles using a Tygon® tube. Before the sample was drawn, the bottles were flushed with seawater for several seconds (for about 3 times the volume of the bottle) and the temperature of the water was recorded simultaneously using a handheld thermometer. The fixing reagents (i.e., manganese chloride and sodium hydroxide/sodium iodide solutions) were then added. Care was taken to avoid bubbles inside the sampling tube and sampling bottle, and a water seal was used after the sample was fixed. Samples were thoroughly mixed following the addition of the fixing reagents and were then kept in a dark plastic crate for 30-40 min to allow the precipitate to settle to <50% the volume of the bottle. Once the precipitate had settled all samples were thoroughly mixed for a second time in order to maximize the efficiency of the reaction. Analyses were carried out within 2 hours of sample collection.

5.1. Methods

DO determinations were made using a Winkler Ω-Metrohm titration unit (794 DMS Titrino) with an amperometric system to determine the end point of the titration (*Culberson and Huang, 1987)*. Chemical reagents were previously prepared at NOCS following the procedures described by *Dickson (1994)*. Recommendations given by *Dickson (1994),* and by *Holley and Hydes (1994)* were adopted. In general, thiosulphate calibrations were carried out every week using a 1.667µmol L^{-1} certified OSIL iodate standard. Calibration values are summarised in Table 7 and shown in Figure 21. Thiosulphate solutions were prepared by dissolving 50g of sodium thiosulphate in 1L of Milli-Q water. These solutions were left to stabilise for 24 hours and a new calibration was carried out before using it. Calculation of oxygen concentrations were facilitated by the use of an Excel spreadsheet provided by Dr. Richard Sanders (NOCS). This spreadsheet has been modified/corrected to include pipettes' calibrated dispensing volumes (i.e., reagents and iodate standard additions have been calibrated). Figure 22 shows a time series of replicates.

5.2. Observations

1. In general, replicate measurements of selected samples were carried out in order to test for reproducibility. At least one Niskin bottle was always sampled in duplicate, typically the deepest Niskin bottle. Any misfires were used to duplicate further Niskin bottles. The mean difference between replicates was 0.4±0.3µmol O_2 L^{-1}, results are shown in Figure 22.

2. In many cases the first oxygen measurement produced lower concentrations than expected (e.g., relative adjacent samples or replicate). In order to avoid this problem, a dummy sample was run previous to the analysis of samples. It seems the electrode needs to stabilise for some seconds inside the solution of seawater with the three different reagents mixed. It was also observed, that leaving the electrode inside the sample for some seconds before starting a titration also produced good results.

3. In addition to showing calibration results, Table 7 also indicates the station numbers where a given calibration was used to calculate oxygen concentrations. Three stocks of thiosulphate were prepared during the cruise (also shown in Table 5).

Table 7: D346 O_2 determinations; number of thiosulphate calibrations, dates on which calibrations were carried out, mean blank titre volume (BLK), standard titre volume (STD), STD minus BLK, molarity of thiosulphate solution and stations affected by each calibration (*new thiosulphate solution prepared).

Calibration number	Date	BLK (mL)	STD (mL)	STD-BLK	Thiosulphate Molarity	Used from CTD No.
1*	05/01/2010	0.0015	0.2556	0.2541	0.3970	1
2	11/01/2010	0.0022	0.2558	0.2536	0.3977	26
3	18/01/2010	0.0019	0.2558	0.2539	0.3972	51
4*	21/01/2010	0.0017	0.2567	0.2550	0.3956	59
5	28/01/2010	0.0021	0.2560	0.2539	0.3973	76
6*	06/02/2010	0.0011	0.2552	0.2541	0.3970	103
7	13/02/2010	0.0016	0.2552	0.2536	0.3977	124

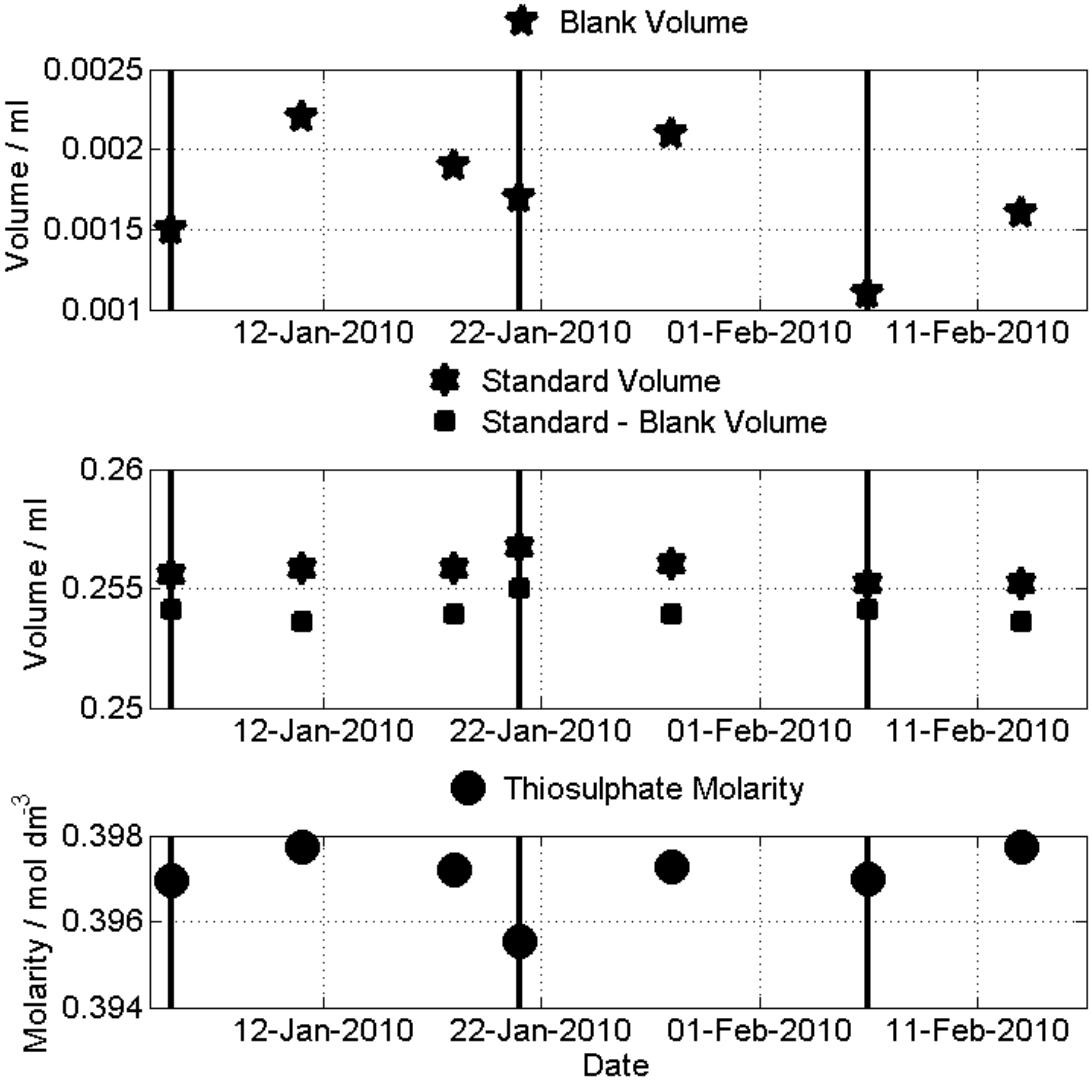

Figure 21: Calibrations for dissolved oxygen analysis. Blank volume titre (upper panel), standard volume titre, standard minus blank (middle panel) and thiosulphate molarity (lower panel). Black lines indicate when a new solution of thiosulphate was prepared. Values plotted here are shown in Table 7.

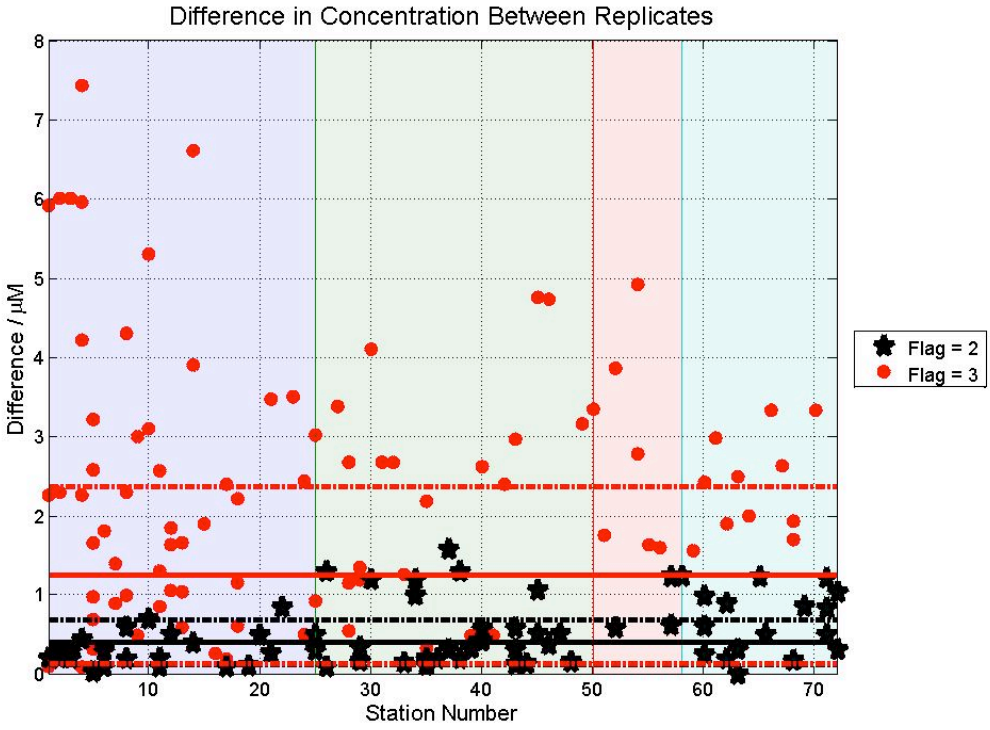

Figure 22: The absolute replicate difference for oxygen bottles in each CTD cast. The mean (0.4µmol L^{-1}) and the standard deviation (±1) are specified with solid and dash lines respectively. Black symbols show replicate values flagged as good and red symbols show all data, included values flagged as dubious or bad.

5.3. References

Culberson, C.H. and Huang, S. (1987), Automated amperometric oxygen titration. *Deep Sea Research*, 34, 875-880.

Dickson, A.G. (1994), Determination of dissolved oxygen in seawater by Winkler titration. Technical report, WOCE operations manual, WOCE report 68/91 Revision 1 November 1994.

Holley, S.E. and Hydes, D.J. (1994), Procedures for the determination of dissolved oxygen in seawater. Technical report, James Rennell Centre for Ocean Circulation.

Kirkwood, D. (1996), Nutrients: Practical notes on their determinations in seawater. ICES Techniques in marine environmental sciences. 17, 1-25.

Siedler, G., T. S. Müller, R. Onken, M. Arhan, H. Mercier, B. A. King and P. M Saunders (1996), The zonal WOCE sections in the South Atlantic. In: Wefer, G., W. H. Berger, G. Siedler and D. J. Webb (Eds). The South Atlantic: Present and Past Circulation. Springer-Verlag, Germany, pp 83-104.

Sinhue Torres, Laura Casburn, Ekaterina Chernyavskaya, Claire Powell and Helen Smith

6. Inorganic Carbon

The carbon parameter analytical equipment was set up in the seagoing laboratory container of the Laboratory for Global Marine and Atmospheric Chemistry (LGMAC), University of East Anglia (UEA), Norwich, UK. Discrete CTD samples were analysed for total inorganic carbon (DIC) and total alkalinity (TA).

6.1. Methods

6.1.1. CTD sampling strategy for inorganic carbon

Water samples for the determination of DIC and TA were drawn from the 20L Niskin bottles on the 24 Niskin CTD rosette and collected in 500ml and 250ml glass bottles according to the Standard Operating Procedure (SOP) #01 (*Dickson et al., 2007*), to avoid gas exchange with the air. All samples were poisoned with mercuric chloride (100µl per 500ml sample). Samples were stored in the dark until they were put into a 25°C water bath to bring the sample to an ambient temperature prior to analysis. In addition to station samples, 125 samples were taken for secondary standards from Stations 83, 85, and 86 and 2 stations used for tracer testing (Stations 200 and 202). Samples for DIC and TA were not taken from all depths at each station. Generally, 16 depths were sampled from each station, including the shallowest and deepest Niskins with the other depths selected to allow for optimum interpolation across the section. Initially, every station was sampled in 500ml bottles. However, this strategy proved unsustainable, as analysis could not keep pace with the frequency of the sampling. Therefore, from Station 34 until Station 129, every third station was sampled in 250ml bottles and initially stored. Stations sampled in 500ml bottles were analysed as a priority and once profiles for these stations had been obtained, selected 250ml bottles were analysed in order to strengthen areas of missing or suspect data. Whereas 500ml bottles allow both DIC and TA to be measured twice per sample (thereby providing information on the precision of measurements), 250ml bottles only allow one DIC and one TA measurement per sample. Therefore, four Niskins at each of the stations sampled with 250ml bottles were sampled in duplicate to provide a measure of consistency. Figure 23 shows the depth-longitude grid of samples analysed for DIC and TA during D346, for which values of both DIC and TA were available after the first shipboard quality control (1st QC).

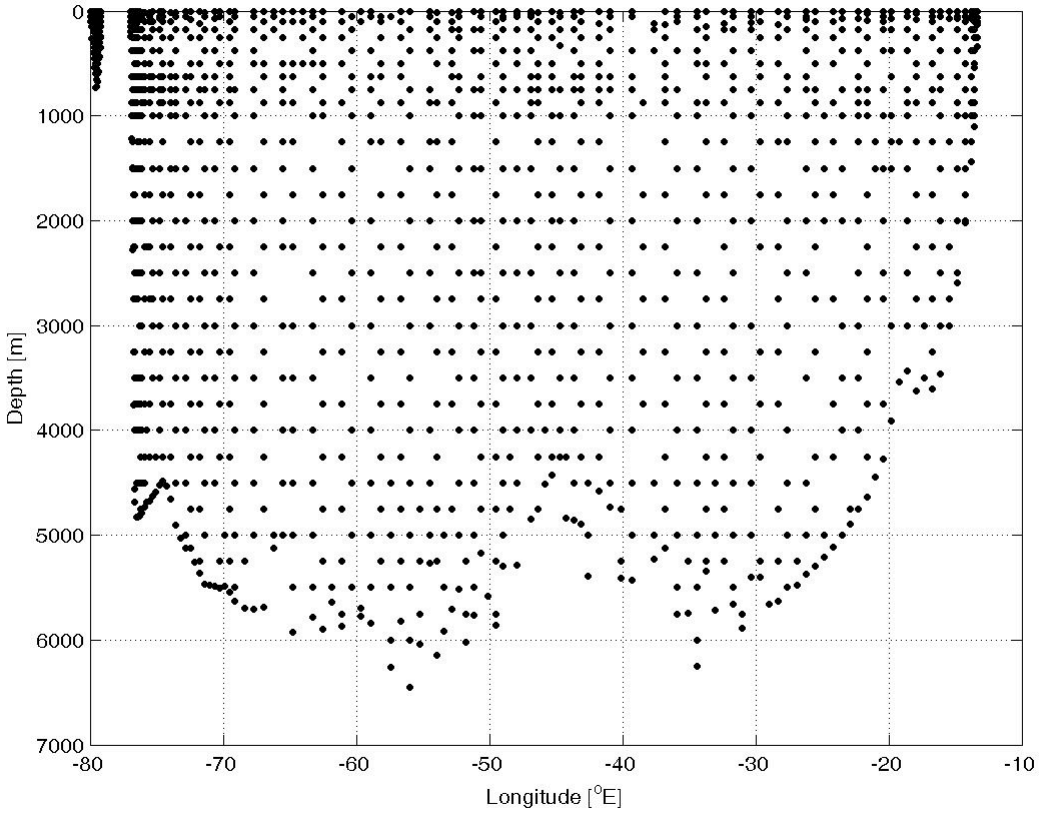

Figure 23: Depth-longitude grid of samples analysed for DIC and TA during D346, for which values of both DIC and TA were are available after shipboard first quality control (1st QC).

6.1.2. Dissolved Inorganic Carbon analyses

Water samples were first analysed for Dissolved Inorganic Carbon (DIC, also denoted as Total CO_2, TCO_2). Total inorganic carbon was analysed by coulometry (*Dickson et al. (2007)* SOP #02). All inorganic dissolved carbon is converted to CO_2 by addition of excess phosphoric acid (1M, 8.5%) to a calibrated volume of seawater sample. Oxygen-free-Nitrogen (OfN) gas, passed through soda lime to remove any traces of CO_2, is used to carry the evolving CO_2 to the coulometer cell, where all CO_2 is quantitatively absorbed, forming an acid that is coulometrically titrated.

DIC analysis was performed using two Versatile INstrument for the Determination of Titration Alkalinity (VINDTA version 3C, Marianda, Germany, SN # 004 and # 007, *Mintrop, 2004*), each connected to a coulometer (UIC, USA, model 5011). Samples were brought to 25°C prior to analysis, and the pipette (volume approximately 20ml), has a water jacket around it, keeping it at 25°C. Two replicate analyses were made on each 500 ml sample bottle and the coulometer counts were calibrated against Certified Reference Material (CRM, batch 97).

On 28th January, valve 11 on VINDTA #007 started leaking and had to be replaced, which affected the calibrated volume in the DIC pipette. The DIC pipette, having started to hold back drops of seawater on the inside, was also replaced and the volume of the new pipette was measured by dispensing Milli-Q water from the

pipette into 15 pre-weighed vials for weighing at the UEA. Between 5th and 7th February there was considerable downtime on VINDTA #007 due to electrical/mechanical problems. The fault was traced to a printed circuit board, which was replaced and sample analysis was resumed on 8th February 2010 (post-cruise QC will include the apparent shift in TA calibration on #007, see Figure 24(b)). Analysis was also interrupted on several occasions by power-cuts in the container.

Initial DIC calibration was done during the cruise for each instrument by correcting all sample data by the difference between the mean of all CRM measurements and the certified reference value of CRM batch 97 (2002.52µmol kg^{-1}; preliminary value in September 2009). Figure 24 shows these calibrated CRM values for (a) VINDTA #004 and (b) VINDTA #007, together with the mean, control limits and warning limits (*Dickson et al., 2007*). Whole-cruise CRM values varied by ±3.0µmol kg^{-1} for VINDTA #004 and by ±3.1µmol kg^{-1} for VINDTA #007 after on-board 1st QC.

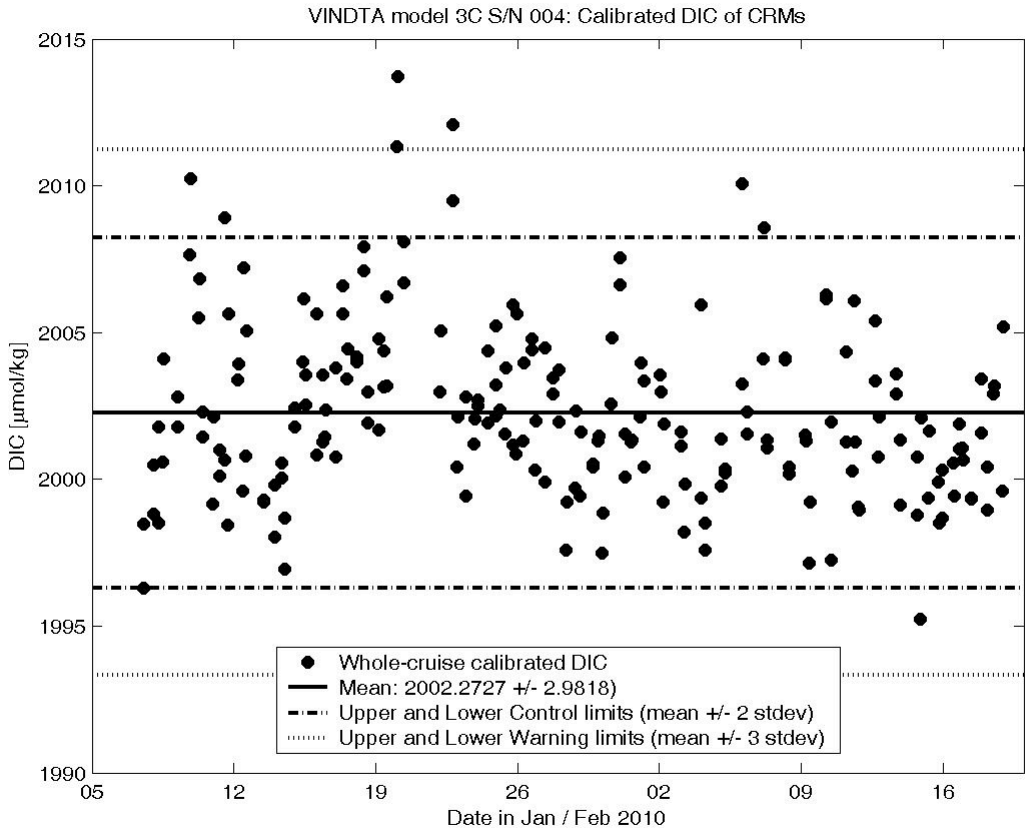

Figure 24 (a): Calibrated CRM-DIC values for the VINDTA #004, showing the mean, control limits and warning limits.

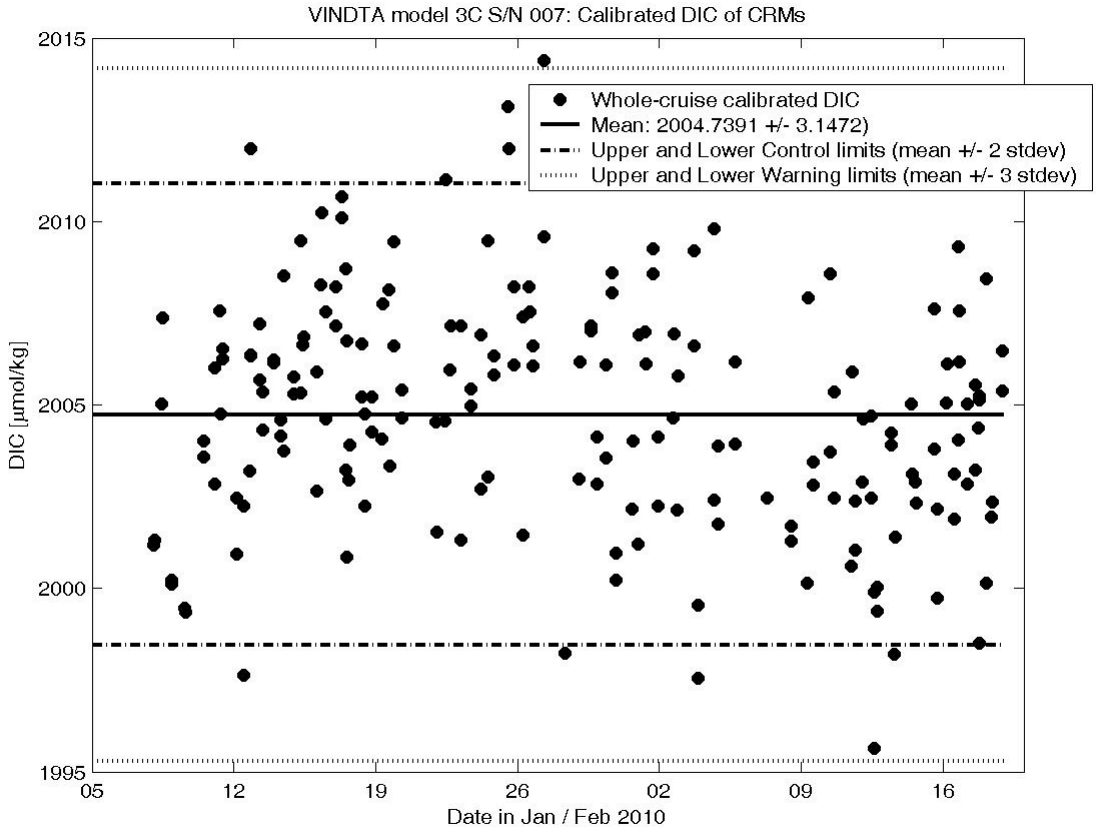

Figure 24 (b): Calibrated CRM-DIC values for the VINDTA #007, showing the mean, control limits and warning limits.

The differences between replicates of all samples analysed for DIC are shown in Figure 25 (a) for the VINDTA #004 and (b) for the VINDTA #007. The mean difference was 0.6µmol kg^{-1} and the precision was 1.9µmol kg^{-1} for the VINDTA #004, whilst the mean difference was 0.6µmol kg^{-1} and the precision was 2.4µmol kg^{-1} for the VINDTA #007.

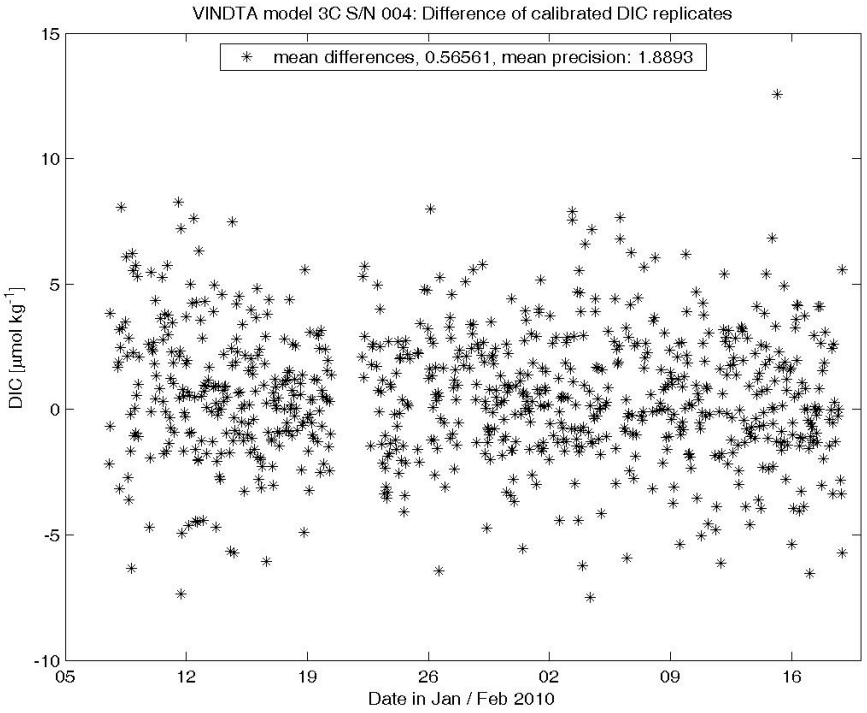

Figure 25 (a): Mean DIC difference and precision for the VINDTA #004.

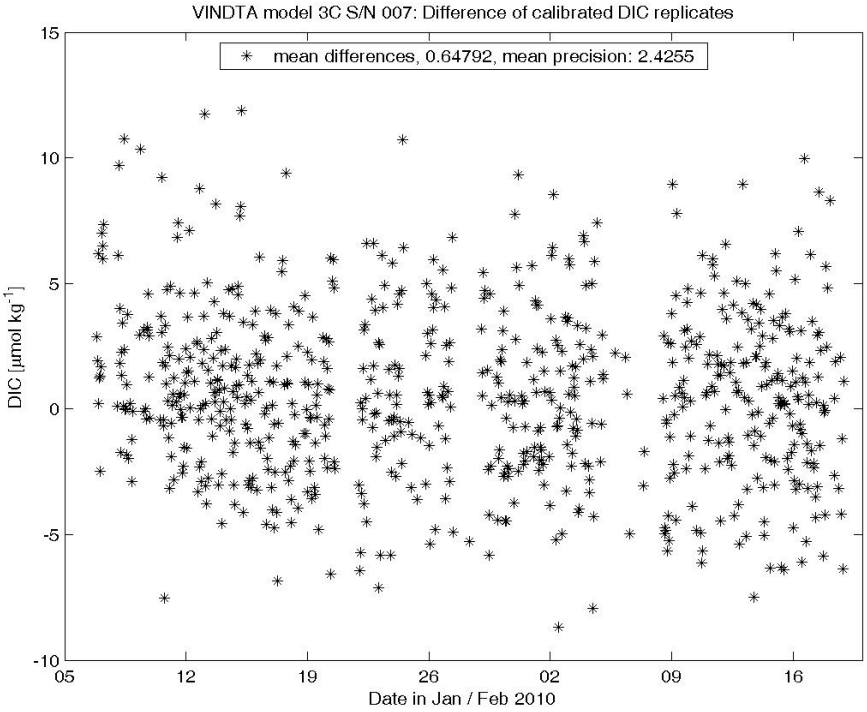

Figure 25 (b): Mean DIC difference and precision for the VINDTA #007.

Post-cruise data quality control will include calibration of the DIC readings for each coulometer cell used during D346, identification and removal of further outliers, and accounting for the instruments' drift during the cruise.

6.1.3. Titration Alkalinity analyses

The alkalinity measurements were made by potentiometric titration (*Dickson et al., 2007*) with two VINDTA instruments (model 3C, S/N #004 and #007) (*Mintrop, 2004*). The systems use a highly precise Metrohm Titrino for adding acid, an ORION-Ross pH electrode, a Metrohm reference electrode, and an auxiliary electrode. The pipette (volume approximately 100 ml), and the analysis cell have a water jacket around them, keeping them at 25°C. The titrant (0.1M hydrochloric acid, HCl) was made in the home laboratory; batch A used throughout the cruise. Replicate analyses were run for 500 ml samples brought to 25°C. Alkalinity values were calibrated using CRM batch 97 (certified at 2210.5µmol kg^{-1}, preliminary values September 2009).

As previously mentioned, between 5th and 7th February there was considerable downtime on VINDTA #007 due to electrical/mechanical problems. The fault was traced to a printed circuit board, which was replaced and sample analysis was resumed on 8th February 2010 (post-cruise QC will include the apparent shift in TA calibration on #007, see Figure 24(b)).

Figure 26 shows alkalinity CRM values recorded by (a) VINDTA #004 and (b) VINDTA #007, showing a whole-cruise variation of ±2.1µmol kg^{-1} on VINDTA #004 and ±3.1µmol kg^{-1} on VINDTA #007 after on-board 1st QC.

Post-cruise data treatment will include recalculation of alkalinities with CTD temperature, salinity, and nutrients, after recalibration of alkalinity pipettes' volume and temperature sensors. Post-cruise QC will then include identifying and removing further outliers, and accounting for drift in the instruments' alkalinity, especially the apparent drift in TA calibration on #007 after 8th Feb 2010.

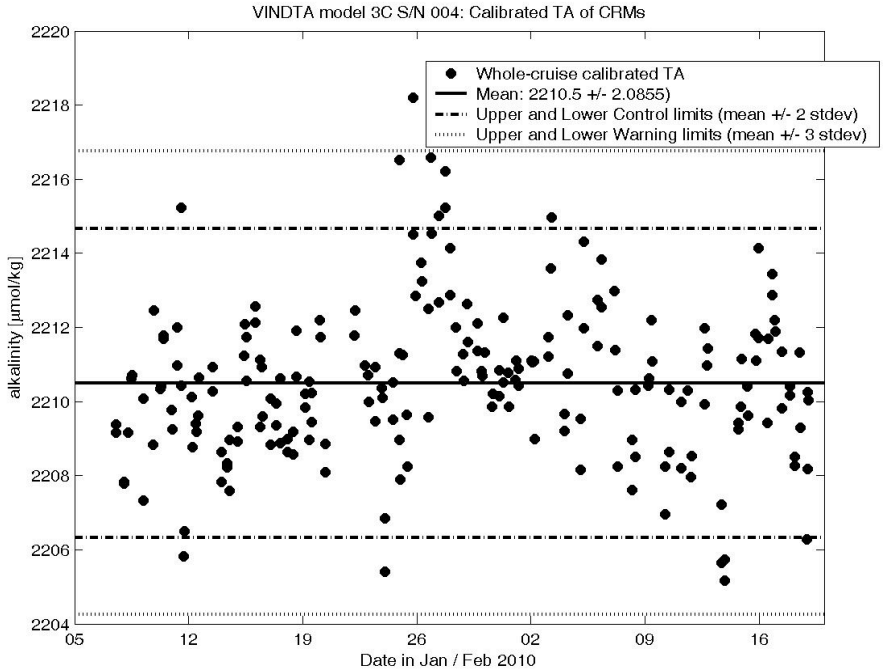

Figure 26 (a): Calibrated CRM-TA values for VINDTA #004. Mean, control and warning limits.

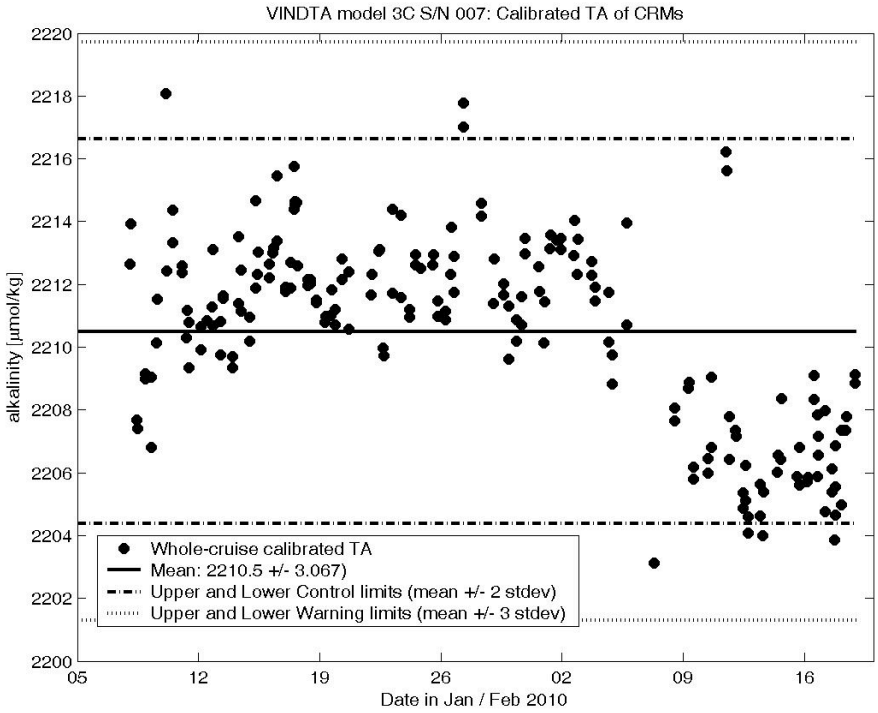

Figure 26 (b): Calibrated CRM-TA values for the VINDTA #007, showing the mean, control limits and warning limits.

The differences between replicates of all samples analysed for alkalinity are shown in Figure 27, (a) for the VINDTA #004 and (b) for the VINDTA #007. For the VINDTA #004 the mean difference was -0.2µmol kg^{-1} and the precision was 1.3µmol kg^{-1}, whilst for the VINDTA #007 the mean difference was -0.1µmol kg^{-1} and the precision was 1.1µmol kg^{-1}.

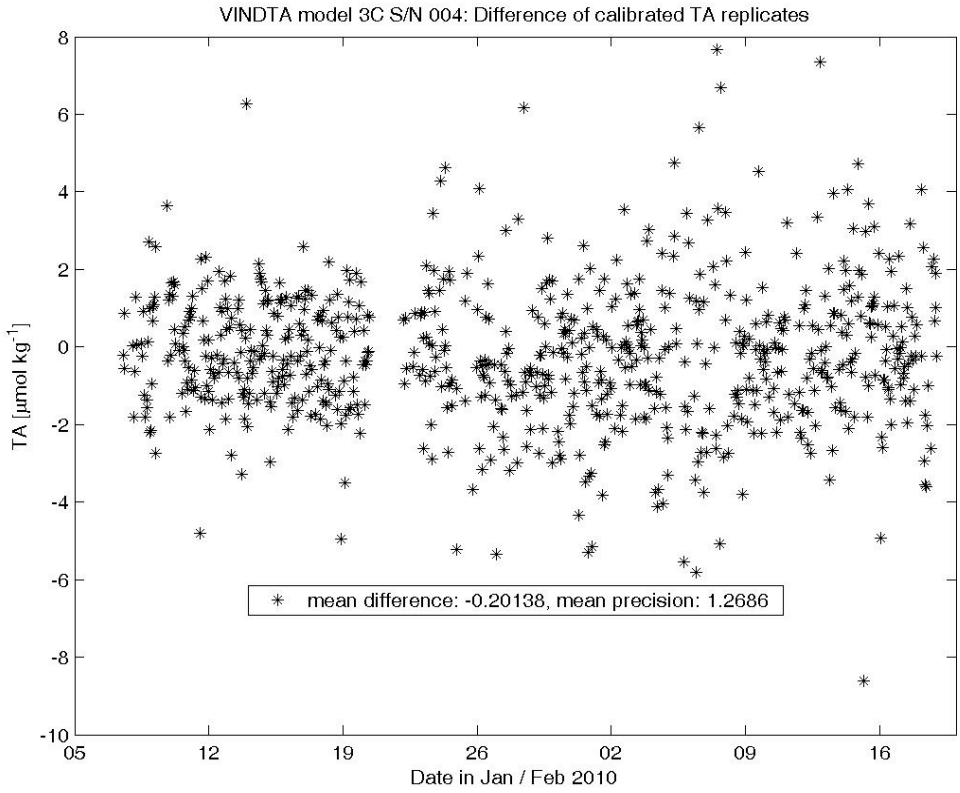

Figure 27 (a): Mean TA difference and precision for the VINDTA #004.

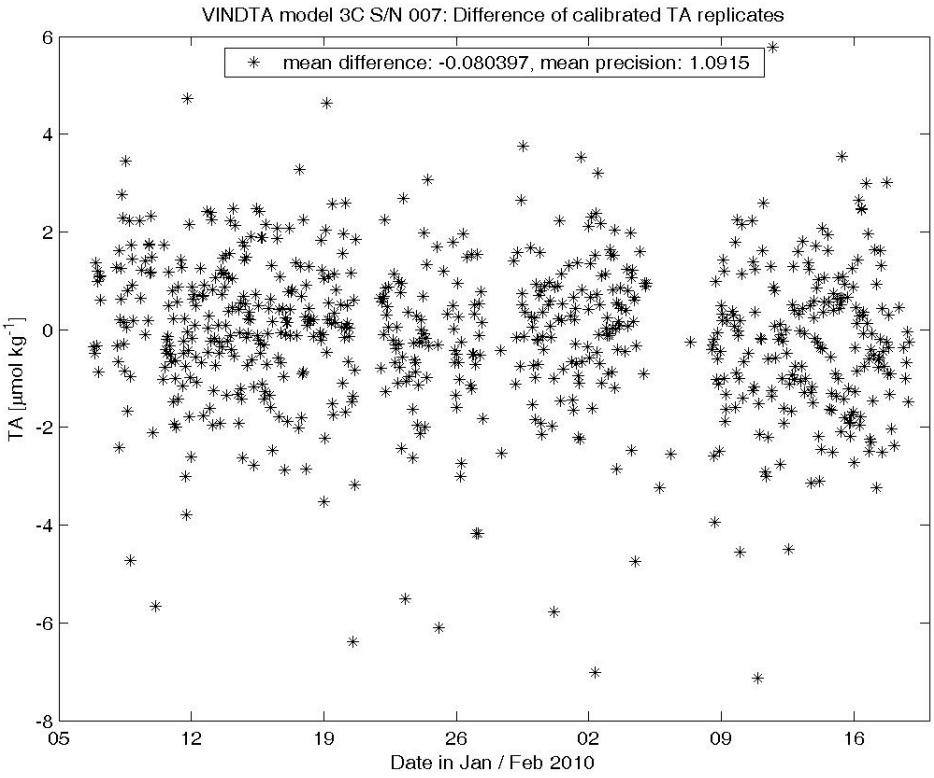

Figure 27 (b): Mean TA difference and precision for the VINDTA #007.

6.2. References

Dickson, A. G., Sabine, C. L., and Christian, J. R. (Eds.) (2007), Guide to best practices for ocean CO_2 measurements, PICES Special Publication 3, pp.191

Johnson, K. M., King, A. E., and Sieburth, J. M (1985), Coulometric TCO2 analyses for marine studies; an introduction, *Marine Chemistry*, 16, pp. 61-82

Johnson, K. M., Sieburth, J. M., Williams, P. J. l., and Braendstroem, L. (1987), Coulometric total carbon dioxide analysis for marine studies: automation and calibration, *Marine Chemistry*, 21, pp. 117-133

Johnson, K. M., and Wallace, D. W. R. (1992), The Single-Operator Multiparameter Metabolic Analyzer for total carbon dioxide with coulometric detection, DOE Res. Summary, 19, pp. 1-4

Johnson, K. M., Wills, K. D., Butler, D. B., Johnson, W. K., and Wong, C. S. (1993), Coulometric Total Carbon-Dioxide Analysis for Marine Studies - Maximizing the Performance of an Automated Gas Extraction System and Coulometric Detector, *Marine Chemistry*, 44, pp. 167-187

Ute Schuster, Arie Louwerse, Gareth Lee and Ollie Legge

7. Chlorofluorocarbons and Sulphur Hexafluoride measurements

7.1. Sample collection

As per WOCE protocol, seawater sample for Chlorofluorocarbons (CFCs) and Sulphur Hexafluoride (SF_6) measurements were the first samples drawn from the Niskin bottles.

The Nitrile 'O' rings of the Niskins were washed in isopropanol and baked in a vacuum oven for 24 hours prior to the cruise. The trigger system of the bottles was external stainless steel springs. Water samples were collected in 500 ml ground glass bottles. The bottles were rinsed with sample water, then filled from the bottom using Tygon® tubing. The bottles were overflowed at least twice before being stoppered and then stored in cool boxes containing seawater close to their sampling temperature (13˚C, 16˚C and 20˚C) until analysis was performed.

For air sampling, a ¼ inch OD Dekabon tubing was run from the analysis system to the mast of the ship. The air was pump through the line using a DA1 SE Charles Austen pump.

7.2. Equipment and technique

The samples were analyzed using an automated coupled CFC-SF_6 purge and trap system developed and built at the University of East Anglia from a design proposed by *Bill Smethie [LDEO, 2004, personal communication]*. This system has the advantage of simultaneous analysis of SF_6 and four chlorofluorocarbons, namely CFC-11, CFC-12, CFC-113, CCl_4 (carbon tetrachloride also classified as CFC-10) from the same water sample.

The system combines the LDEO CFC method (*W. Smethie et al., 2000*) and the PML SF_6 method (*Law et al., 1994*) with a common valve for the introduction of water samples. The samples were introduced to the system by applying nitrogen (N_2) pressure to the top of the sample bottles, forcing the water to flow through and fill a 25cm^3 calibrated volume for CFCs and a 300cm^3 calibrated volume for SF_6. The measured volumes of seawater were then transferred to a separate purge and trap circuit. Each purge and trap circuit was interfaced with an Agilent 6890 gas chromatograph equipped with an electron capture detector (GC-ECD). The compounds were extracted from the water by passing N_2 through the sparging chambers and then transferred at 85ml mn^{-1} to a Unibeads trap at -100°C for the CFCs and at up to 120ml mn^{-1} to a Porapak Q trap at -80°C for the SF_6. The headspace of liquid nitrogen was used to cool the traps. After 4 mins (3 mins for SF_6) of sparging, the traps were heated to 100°C for the CFCs and 65°C for SF_6 and injected into the respective gas chromatograph. The separation of the various CFCs was achieved using a 1m Porasil B packed pre-column and a 1.5m carbograph AC main column. The SF_6 separation was achieved using a molecular sieve packed 2m main column and 2m buffer column. The carrier gas was pure oxygen-free nitrogen, which was cleaned by a series of purifiers.

7.3. Calibration

The CFCs and SF_6 concentrations in air and water were calculated using an external gaseous standard. The standard supplied by NOAA (*Brad Hall, December 2009*) corresponds to clean dry air slightly enriched in SF_6, CFC-11 and CCl_4 in 29L Aculife-treated aluminum cylinders (SN AAL-072073). The calibration curves were made by multiple injections of different volumes of standard that span the range of tracers measured in the water. Examples of fitting calibration data are given in Figure 28. Calibration curves were made approximately every 2 days whereas the changes in the sensitivity of the system was checked by measuring a fixed volume of standard gas every 8 runs (Figure 29). The temporal drift of the ECD between two calibration curves was assumed to be linear in time. Particular difficulty was noted for CCl_4, where significant variation in standards was noted. In this report, dissolved CFCs and SF_6 are given in units of [pmol/l] and [fmol/l] respectively, calibrated on the NOAA 2009 scale. The final data set will be converted to mol/kg on the SIO-98 scale using NOAA's comparison tables.

7.4. Precision and accuracy

7.4.1. Precision or reproducibility

The precision of the measurements can be determined from duplicate samples drawn on the same Niskin bottles. 80 duplicate samples were analysed, from which we calculated the following precision, expressed as the square root of the variance of the duplicates differences.

Table 8: CFC precision table

SF_6	±1.05 %	for surface values
	±0.011 fmol/l	for values < 0.1 fmol/l
CFC-12	±0.95 %	for surface values
	±0.003 pmol/l	for values < 0.1 pmol/l
CFC-11	±1.1%	for surface values
	±0.006 pmol/l	for values < 0.1 pmol/l
CFC-113	±1.5%	for surface values
	±0.001 pmol/l	for values < 0.1 pmol/l
CCl_4	±3%	for surface values
	±0.015 pmol/l	for values < 0.3 pmol/l

7.4.2. Test stations and sample blank correction

The sample blank includes Niskin bottle blanks and other blanks associated with transferring, storing and analyzing the sample. This blank is best determined from analyses of CFC-free water. In order to assess the sample blank we tripped all the bottles in the lowest CFC water found of the two major basins crossed along the cruise-tract, respectively at 6300m in the western basin (Table 9, test Station 200) and at 3500m in the eastern basin (Table 10, test Station 202). We also took samples from a Niskin bottle sparged with nitrogen for up to 30 hours, until concentrations

had reached a steady-state value (Table 11). The comparison of the station tests with the samples from the sparged Niskin test shows that:

1- The CFC concentrations from test Station 200 are too high; the water appears to contain CFCs and those results are therefore not considered as a blank.

2- The CFC concentrations from test Station 202 are reasonably closed to the concentrations from the sparged Niskin test and those results are therefore considered as the blank concentration for the full cruise.

Table 9: Results of the test Station 200.

Niskin	SF6	F12	F11	F113	CCl_4
1	0.016	0.0726	0.1102	0.0152	0.5270
2	0.016	0.0637	0.1018	0.0143	0.5128
3	0.016	0.0728	0.1102	0.0150	0.5299
4	0.016	0.0676	0.1093	0.0147	0.5217
5	0.016	0.0651	0.1076	0.0124	0.5120
6	0.027	0.0643	0.1003	0.0129	0.4882
7	0.016	0.0624	0.1041	0.0120	0.4511
7	0.011	0.0624	0.0981	0.0113	0.3958
8	0.027	0.0671	0.1111	0.0137	0.4293
9	0.027	0.0699	0.1104	0.0141	0.4322
10	0.027	0.0677	0.1126	0.0145	0.4054
11	0.033	0.0665	0.1074	0.0121	0.4068
12	0.016	0.0658	0.1080	0.0118	0.4313
13	0.016	0.0643	0.1083	0.0116	0.4420
14	0.032	0.0711	0.1111	0.0124	0.4207
15	0.032	0.0693	0.1104	0.0126	0.4752
15	0.006	0.0682	0.1045	0.0131	0.3645
16	0.018	0.0714	0.1134	0.0137	0.4068
17	0.011	0.0655	0.1057	0.0125	0.3926
18	0.024	0.0714	0.1119	0.0127	0.4312
19	0.017	0.0695	0.1104	0.0142	0.4127
20	0.033	0.0631	0.1042	0.0118	0.4097
21	0.009	0.0690	0.1127	0.0137	0.4264
22	0.031	0.0706	0.1127	0.0158	0.3938
23	0.015	0.0682	0.1065	0.0123	0.3646
24	0.027	0.0683	0.1099	0.0121	0.4356
AVERAGE	0.0205	0.0676	0.1082	0.0133	0.4363
STDEV	0.0082	0.0032	0.0042	0.0013	0.0477

Table 10: Results of the test Station 202. The average and standard deviation of CCl_4 does not include the anomalously high concentration from Niskin 4.

Niskin	SF6	F12	F11	F113	CCl4
1	0.000	0.0083	0.0165	0.0056	0.0600
1	0.000	0.0107	0.0163	0.0050	0.0504
2	0.009	0.0124	0.0185	0.0069	0.0569
3	0.014	0.0092	0.0174	0.0043	0.0493
4	0.000	0.0086	0.0189	0.0079	0.2444
5	0.000	0.0055	0.0139	0.0055	0.0562
6	0.009	0.0074	0.0114	0.0052	0.0457
7	0.000	0.0074	0.0118	0.0053	0.0464
8	0.000	0.0071	0.0130	0.0049	0.0428
9	0.000	0.0060	0.0120	0.0040	0.0490
10	0.000	0.0074	0.0112	0.0061	0.0401
11	0.009	0.0072	0.0123	0.0051	0.0446
12	0.000	0.0069	0.0114	0.0048	0.0421
13	0.000	0.0102	0.0127	0.0059	0.0439
14	0.014	0.0083	0.0128	0.0039	0.0497
15	0.014	0.0086	0.0153	0.0054	0.0499
16	0.005	0.0099	0.0146	0.0052	0.0457
17	0.000	0.0081	0.0130	0.0058	0.0378
18	0.000	0.0078	0.0120	0.0028	0.0354
19	0.000	0.0085	0.0117	0.0034	0.0417
20	0.000	0.0072	0.0137	0.0048	0.0403
21	0.000	0.0064	0.0128	0.0050	0.0320
22	0.000	0.0088	0.0139	0.0039	0.0385
23	0.000	0.0094	0.0156	0.0040	0.0446
24	0.000	0.0100	0.0170	0.0037	0.0446
AVERAGE	0.0032	0.0082	0.0138	0.0051	0.0453
STDEV	0.0053	0.0016	0.0023	0.0011	0.0067

Table 11: Concentrations over time of the sparged Niskin test.

SAMPLING TIME	SF6	F12	F11	F113	CCl4
10/02/2010 08:00	0	0.0097	0.0179	0.0041	0.0549
10/02/2010 13:00	0	0.0102	0.0161	0.0047	0.0383
10/02/2010 18:00	0	0.0114	0.0192	0.0068	0.0264
11/02/2010 08:00	0	0.0114	0.0217	0.0049	0.0394
AVERAGE	0	0.0107	0.0188	0.0051	0.0398
STDEV	0	0.0009	0.0024	0.0012	0.0118

7.4.3. Sparging efficiency

The sparging efficiency was evaluated by re-stripping high concentration surface water samples and comparing the residual concentrations to the initial concentrations. The re-sparge values were approximately <2% of the initial sample concentration for CFC-12 and CFC-11 and below <7% for CFC-113 and CCl_4 for a sparging of 4 min at 85 mL/min. The SF_6 re-sparge value was zero for a 3 min sparging going up to 120mL/min. A fit of the re-sparging efficiency as a function of temperature and flow rate will be applied to the final data set.

7.5. Data

The contour plots for all 5 tracers are presented in Figure 30. A small number of water samples with anomalously high concentrations relative to adjacent samples are included in the sections but are given a quality flag of 3 or 4 in the data set. When not associated with anomalies in other parameters, it suggests that these samples were probably contaminated with CFCs during the sampling or analysis processes. This affected more often CFC-113 and CCl_4. Note that CFC-113 and CCl_4 were mostly not measured in the 200-500m depth range to save on analytical time.

As expected, the sections show high concentrations for all five tracers at the surface and within the North Atlantic Deep Water in the Western Basin. A puzzling feature is the high core of SF_6 above the Mid-Atlantic Ridge centred around 1500m, which is not associated with a CFC maximum. Another interesting feature is the invasion of CCl_4 in the deep eastern basin.

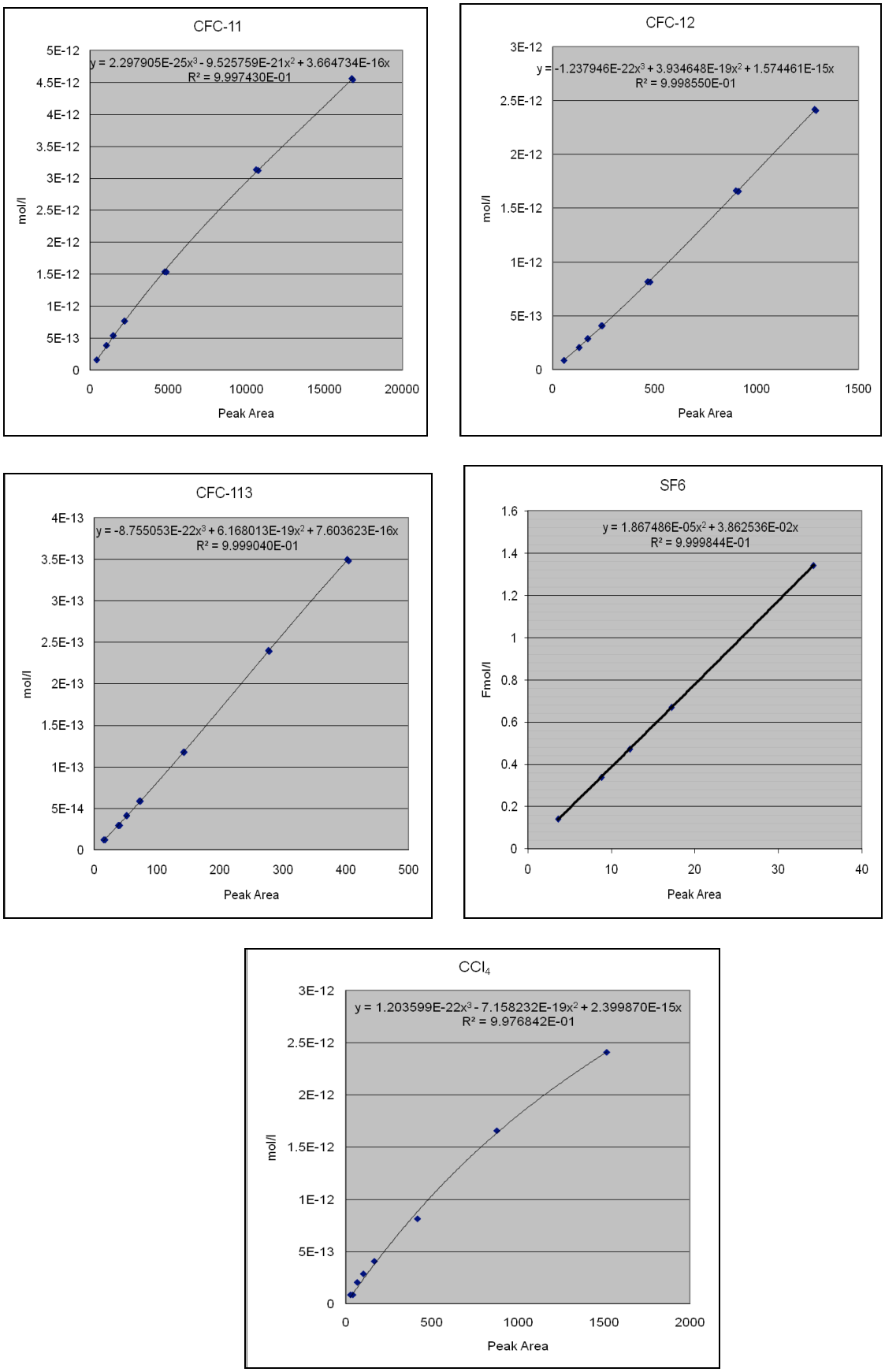

Figure 28: Example of calibration curves.

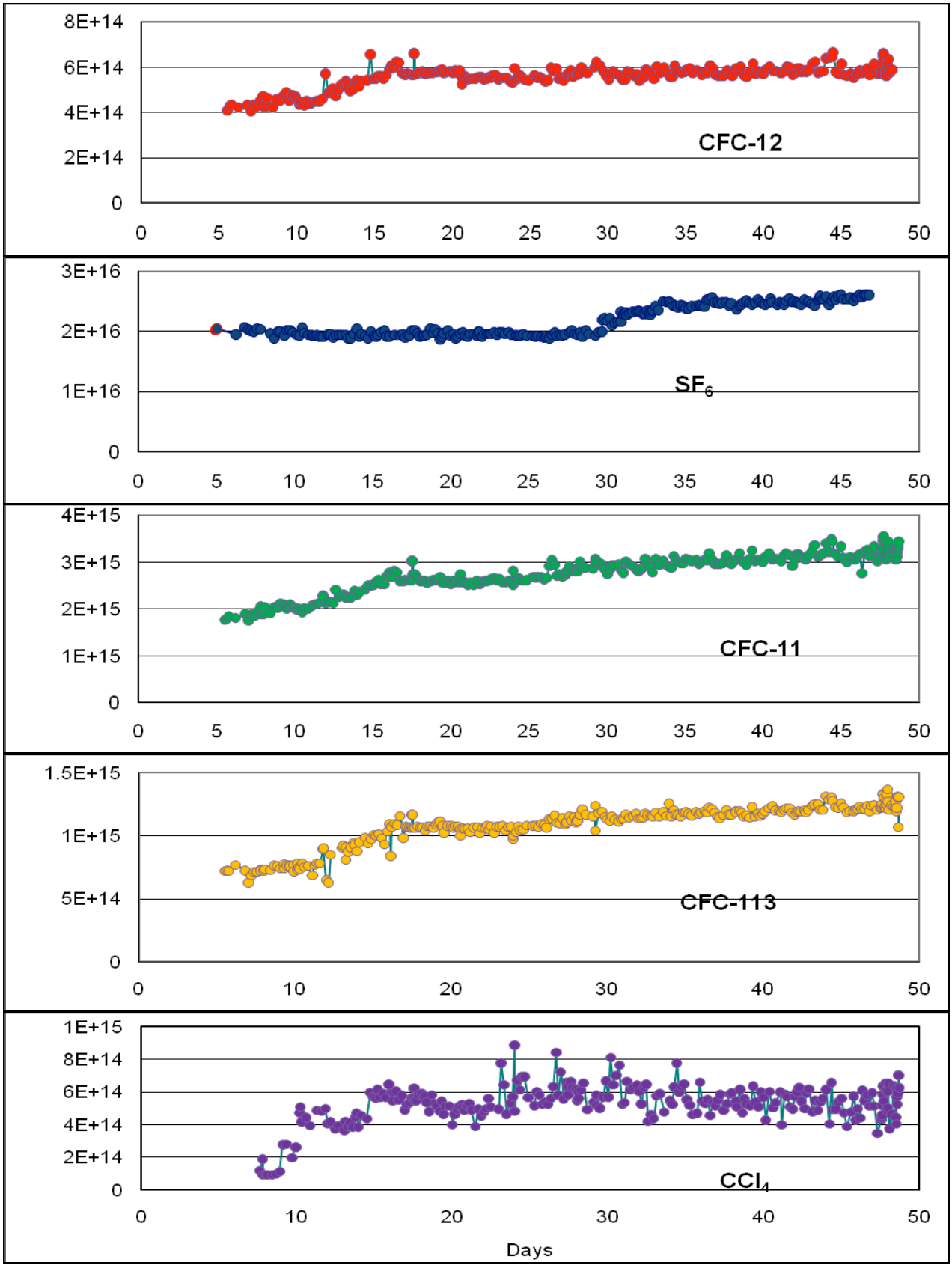

Figure 29: Sensitivity of the system over time expressed as the area divided by the amount of standard injected into a 1ml loop.

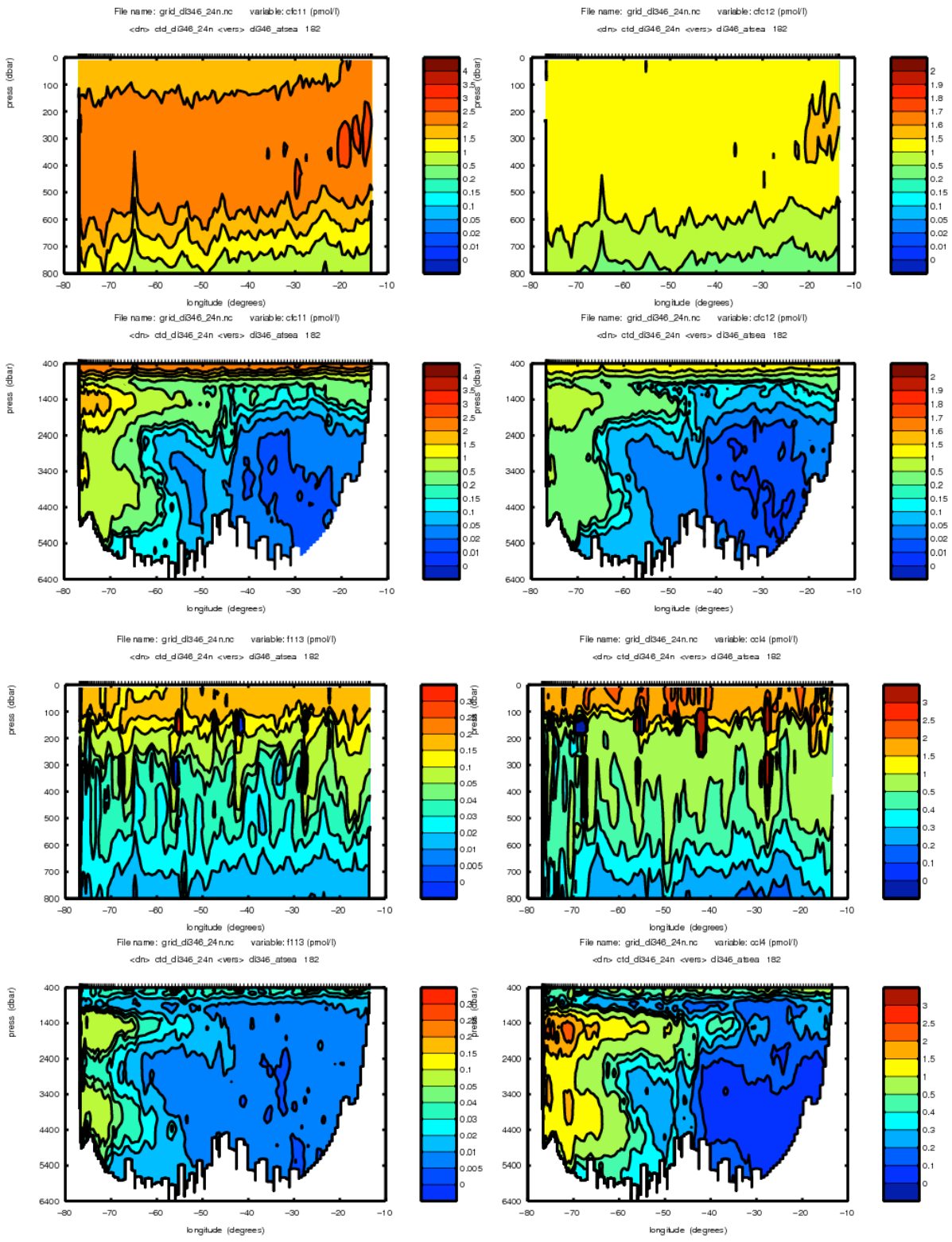
File name: grid_dl346_24n.nc variable: cfc11 (pmol/l)
<dn> ctd_dl346_24n <vers> dl346_atsea 182
File name: grid_dl346_24n.nc variable: cfc12 (pmol/l)
<dn> ctd_dl346_24n <vers> dl346_atsea 182
File name: grid_dl346_24n.nc variable: cfc11 (pmol/l)
<dn> ctd_dl346_24n <vers> dl346_atsea 182
File name: grid_dl346_24n.nc variable: cfc12 (pmol/l)
<dn> ctd_dl346_24n <vers> dl346_atsea 182
File name: grid_dl346_24n.nc variable: f113 (pmol/l)
<dn> ctd_dl346_24n <vers> dl346_atsea 182
File name: grid_dl346_24n.nc variable: ccl4 (pmol/l)
<dn> ctd_dl346_24n <vers> dl346_atsea 182
File name: grid_dl346_24n.nc variable: f113 (pmol/l)
<dn> ctd_dl346_24n <vers> dl346_atsea 182
File name: grid_dl346_24n.nc variable: ccl4 (pmol/l)
<dn> ctd_dl346_24n <vers> dl346_atsea 182
press (dbar)
longitude (degrees)

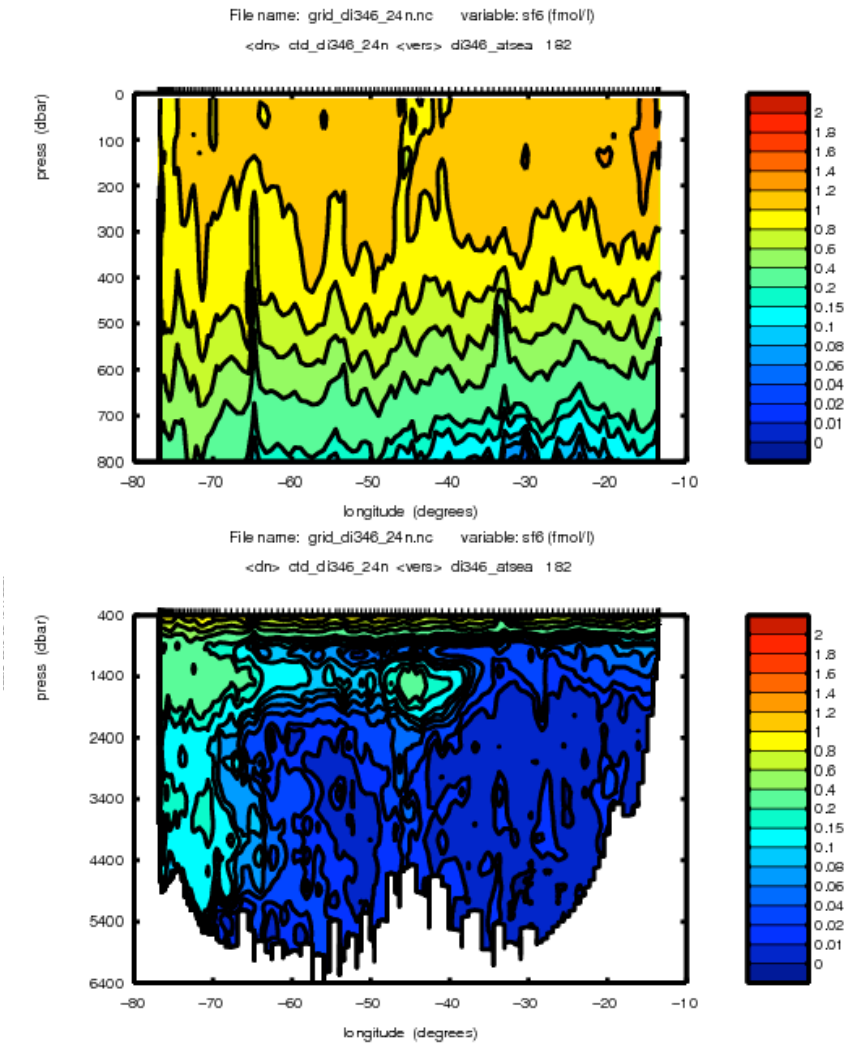

Figure 30: Countour plots of CFC-11, CFC-12, CFC-113, CCl_4 and SF_6 data from the main D346 24˚N transect.

7.6. References

Law C.S., Watson A.J. and Liddicoat M.I. (1994), Automated vacuum analysis of sulphur hexafluoride in seawater: derivation of the atmospheric trend (1970-1993) and potential as a transient tracer, *Marine Chemistry*, 48, pp. 57-69.

Smethie, W. M., Schlosser Jr., P., Bönisch G., and Hopkins T. S. (2000), Renewal and circulation of intermediate waters in the Canadian Basin observed on the SCICEX 96 cruise, *J. Geophys. Res*., 105(C1), 1105-1121.

Marie-José Messias, Andrew Brousseau, Peter Brown, and Stephen Woodward

8. Computing, Sea-Surface and Meteorological Instrumentation

8.1. Primary Logger – hardware and software

As in earlier cruises, the primary data logging is performed by IFREMER's TECHSAS data logging system.

At present the operating system is the third release of Red Hat's Enterprise Linux Workstation product. The reason for using this old version of the operating system is that the kernel it uses supports the National Instruments PCI serial cards used by the systems.

Chris Barnard has been doing some research with later kernels, and has also been communicating with National Instruments about the issue, and we hope to have a newer operating system, along with upgraded motherboards, processors, RAM in use in the near future. We are also hoping to switch over from an IDE-based hardware RAID solution, to one based on SATA drives.

8.2. Level C

The Level C software is still running on a Sun Blade 1500 SPARC-based workstation. The *fromtechsas* program is used to take data broadcast by the TECHSAS system over the ships' LAN, and then save it in individual data streams, which can then be examined in the graphical data editor, and/or have processing performed on them.

During the cruise, the graphical data editor was used to remove the worst of the spikes (including zero values) from the EA-500 bathymetry data, and the *prodep* program was then used to correct it for Carter Area. The *relmov/bestnav* navigation processing software was also run to create the bestnav and bestdrf streams. Finally the *windcalc* program was run to calculate the absolute wind speed and direction.

8.3. CLAM

The CLAM system, used to monitor and record data from the ships' winches, failed on the evening of Friday, 8th January.

Initial investigations revealed that the system's 3.4GB hard drive had failed. After all efforts to recover data from the drive had failed, the top was removed, and the drive head could be seen repeatedly travelling rapidly from the innermost area of the drive surface, to the outermost area.

Another CLAM system was located in the tape store, but unfortunately it was not identical to the system that had been in use. It had been used on *RRS Charles Darwin*, and had not been modified since. Therefore it had the wrong version of the

CLAM software, and could not be used to monitor the winch systems on RRS *Discovery*. It also had only a third of the RAM of the RRS *Discovery* CLAM system.

A version of the CLAM software was sent out from NOCS, and loaded onto the SBWR computer. A 4-port USB-serial converter was used to provide the necessary serial ports. We were unable to make this software read the data coming from the winch system.

Eventually, a system was cobbled together by taking the computer from the PSO's cabin, an Edgeport 4-port USB-serial converter. The computer's original hard disk was removed, and a spare hard drive (kept onboard for the TECHSAS systems) was put in its place. Ubuntu Linux was loaded, along with a terminal emulation program called Minicom.

Minicom was used to set the baud rate, parity, handshaking etc. on each port that the system needed to use. This was basically a cheat, to ease the programming load – the programs would simply use the serial ports in their last-used configuration.

It had been determined, through looking at the CLAM documentation and examining the CLAM code, that the Caley winch system was polled for data by sending an "S" character at 19,200 baud, about once every 200ms. Initially a shell-script was written that simply sent S characters to the serial port every second, whilst in a second terminal the UNIX tail -f command was used to read the responses from the winch. An example of these responses is shown below:

```
$CTD3, .69 , 1  224 , 52.0385 , 0 ,
$CTD3, .68 , 1  223 , 52.0385 , 0 ,
$CTD3, .67 , 1  222 , 52.0385 , 0 ,
$CTD3, .66 , 1  221 , 52.138 , 0 ,
$CTD3, .67 , 1  220 , 52.0385 , 0 ,
$CTD3, .68 , 1  220 , 52.0385 , 0 ,
```

Eventually a small C program was written to poll the winch at 200ms, read the date/time from the clock port, and write these data to the standard output, and also simulate the SMP message, which was sent to the TECHSAS logger. The output of this program was piped through the UNIX tee program to enable the winch data to be saved to the local hard disk, and also to some online disk storage.

The principal scientist wrote a program in Matlab, running on his *NOSEA1* Sun workstation that read the data from the online storage area and used it to generate a CLAM-like display on the PC. The video output from this PC was then hooked up to the video distribution system so that the winch cab and bridge had a good visual and numerical representation of the winch load, and also access to the wire-out and rate data.

8.4. Surfmet

The Surfmet system is used to log the following instrumentation:

- Seabird 45 (TSG) and Seabird 38 (sea surface temperature)
- WET Labs Fluorometer
- WET Labs Transmissometer
- Gill Windsonic sonic anemometer
- Vaisala HMP45 temperature/humidity sensor
- Vaisala PTB100A air pressure sensor
- 2 x Kipp & Zonen CMB6 total irradiance sensors
- 2 x Skye Photosynthetically Active Radiation (PAR) sensors

The Surfmet system provides an easy way to check on these instruments, with both graphical and numerical displays. In addition it also timestamps the data and sends it to the TECHSAS data loggers.

8.5. Simrad EA-500 Echo Sounder

Despite its age, this system worked fairly well until one of the transducers was improperly connected when switching over between the fish and the hull transducers. We initially thought that the transceiver board might have been blown, but after lots of playing around it came back to life.

The fish seems to be a little nose heavy, despite moving the weight in the tail boom fully aft. This caused problems with achieving good bathymetry data whilst the vessel was on station, and meant it was necessary to change over the transducers when arriving on and departing from stations.

8.6. Chernikeeff EM Log

For the past two cruises the EM Log has been reading quite high at the top end of the speed range.

The scientific party used the data from the ships' ADCP systems to derive new calibration data for the Chernikeeff. Once these were entered, the log gave a much more believable speed.

8.7. Printing

Both HP LaserJet 2605dn printers performed faultlessly throughout the cruise, with the only problem being a shortage of A4 paper towards the end of the cruise. Thankfully the UEA CFC team kindly donated three bags of paper, which helped a lot.

The DeskJet 1220C was only used briefly and worked fine, except that the colour cartridge ran out. The only other working colour cartridge on board was found in the other DeskJet 1220C in the technician's office.

When the DeskJet 1220C was found to be short of ink, an attempt was made to use the DesignJet 1055CM. Unfortunately this developed a fault in detecting the magenta ink cartridge. However, on 18th February it was turned on just to verify which ink cartridge was causing the problem, but was found to be working. Prior to this, this particular plotter must have been power cycled over a dozen times – some of them by the Master, who has used this plotter a lot in his previous post on cable ships. The plan is still to have it looked at by an HP service engineer during the coming rest period.

8.8. Backups

Two backups were performed every day. Firstly the Level C and TECHSAS files were backed up on the Level C's directly connected LTO2 drive. Secondly, the *NOSEA1* workstation was backed up over the network to a second LTO2 drive connected to the discovery3 workstation. Unfortunately, towards the end of the cruise, the LTO2 drive on discovery3 started to generate errors during the write process, even when the cleaning tape, and re-tensioning of the data tape were used. The intention is to replace this drive with a spare.

Paul Duncan

9. Lowered Acoustic Doppler Current Profiler (LADCP)

9.1. Instrument Setup and Performance

Three RDI 300kHz Workhorse LADCP units were available on D346: one aluminium cased unit and two titanium-cased units. The LADCP was configured to have a standard 16 x 10 m bins, and to ping in water track mode. There was also a 5m blank at the surface. Data were collected in beam co-ordinates and rotated to earth co-ordinates in post-processing. The instruments were mounted in a downward-looking orientation on the CTD frame.

Prior to each station the ADCP was connected to a laptop in the deck lab (via a serial port – USB adapter) for pre-deployment tests and the instrument was programmed. After each station the instrument was reconnected to the laptop for the retrieval of the data. The battery package was charged between stations.

The cruise began with the aluminium-cased unit mounted on the CTD frame. This instrument performed well. All beams were correlated and of similar strength (Figure 31). On cast 21, the instrument stopped and restarted itself halfway up the upcast, which led to two files for this station. Concatenating the two files together and then processing normally successfully processed these files. This instrument was removed after Station 63 as casts 64 – 69 were all deeper than 6000m and the LADCP is not depth rated beyond this depth.

At cast 70, the aluminium unit was replaced with one of the titanium-cased units, S/N 13399 (Figure 31). This unit was found to have one beam with a much greater strength than the others, however correlation between the beams was good. This unit failed on cast 72.

Another titanium-cased unit, S/N 13400, replaced it. This unit was found to have one beam weaker than the others. This beam was also not correlated with the others (Figure 31). In spite of this, this unit produced good data. It was replaced before Station 114 when the original instrument was put onto the frame again.

9.2. Data Processing

The data collected by the instrument were downloaded after each cast and stored as RDI binary files and corresponding text files in the directory */Drobo/D346/LADCP*.

The data were then processed using two different tools. Primarily a software package from the University of Hawaii (UH) was used to calculate absolute current velocities using the shear. This also provides information about the heading and tilt of the CTD package. The second piece of software originates from Lamont-Doherty Earth Observatory (LDEO). It calculates velocities using an inverse method and was also used for obtaining bottom track profiles and to monitor the beams of the instrument.

Data were collected in beam coordinates, as this is the recommended method of collection. The UH software handled this format with no modifications. The LDEO software required an updated version of their *loadrdi.m* program.

All the processing for the LADCP was carried out on the *NOSEA1* Linux terminal.

The sequence of the routine processing for the LADCP data is outlined below.

9.2.1. UH Processing

The initial stages of processing allow the user to examine the quality of the data and to calculate relative velocity profiles in the absence of CTD data.

1. After navigating to the directory *~/cruise/data/ladcp/uh*, ***source LADall*** sets up the paths required for the processing.
2. ***cd proc/Rlad***; ***linkscript*** creates symbolic links from the binary *.000 files to the real raw file. As processing was performed on the local disk of *NOSEA1*, the raw files were copied from the network and symbolic links were created to the required filenames. The UH software requires a filename of *dNNN_02.000*, where *NNN* is the station number. The LDEO software requires a filename of *D346_NNNm.000*. The suffix *02* refers to the LADCP being down-looking.
3. ***cd proc; perl –S scan.prl NNN_02*** to scan the raw data and create a station specific directory in the *proc/casts* directory. Data printed to screen should be checked to ensure the details of the cast (i.e. depth, downcast/upcast times) agree approximately with the CTD logsheet.
4. ***matlab; m_setup; putpos(NNN,02)*** gets position of the cast by accessing the TECHSAS data streams. ***magvarsm(NNN.02)*** applies the magnetic correction to the compass on the LADCP. Quit Matlab.
5. ***perl –S load.prl NNN_02*** loads the raw data, correcting for *magvar.tab* to start processing. It is very important that this step is only carried out once. If it needs to be repeated the database files (*~/proc/casts/dNNN_02/scdb*) must be deleted first.
6. ***perl –S domerge.prl –c0 NNN_02*** to merge the velocity shear profiles from individual pings into full upcast and downcast profiles. The option *–c0* refers to the fact that CTD data has not yet been included.
7. ***cd Rnav; matlab; make_sm*** makes a smoothed navigation file for the cast. Quit Matlab.
8. ***cd proc; matlab; plist = NNN.02; do_abs;*** calculates the relative velocity profiles. Check that these plots look sensible, i.e. reasonable agreement between downcast and upcast and that the vertical velocity changes sign between downcast and upcast (it may be necessary to rescale some of the plots).

Once the CTD data has been processed this can be incorporated into the LADCP processing to make more accurate estimates of depth and sound velocity and to obtain a final absolute velocity profile.

9. The inclusion of CTD data requires an ASCII file containing 1Hz CTD data for the station created in Matlab. If this is present ***cd proc; cd Rctd*** and open

a Matlab session. Run ***m_setup*** and the script ***mk_ctdfile(NNN).*** Quit Matlab.

10. ***cd proc/Pctd; ctd_in(NNN,02)*** will read the 1Hz CTD data in. ***plist=NNN.02; fd*** aligns the LADCP and CTD data sets in time. Quit Matlab.
11. ***cd proc; perl –S add_ctd.prl NNN_02*** adds the CTD data to the **.blk* LADCP files in the *scdb* directory.
12. ***perl –S domerge.prl -c1 NNN_02*** merges the single pings into corrected shear profiles. The *-c1* option now states that we have included CTD data.
13. ***matlab; plist=NNN.02; do_abs;*** calculates the velocities again with the merged pings.

9.2.2. LDEO Processing

As with the UH processing the LDEO processing can first be carried out without the CTD data to monitor the results and performance of the beams.

1. ***cd ladcp; cd ldeo/di1001;*** and start a Matlab session.
2. Type ***sp*** and when prompted enter the station number and the run letter *('noctd'* for no CTD data and *'wctd'* when CTD data are included).
3. Next type ***lp*** and this will run the processing scripts.

The steps above should then be repeated to include the CTD data after it has been processed. The format of the CTD data required is the same for both the LDEO and UH processing paths and when CTD data are available the processing will automatically use it.

The LDEO processing extracts the useful bottom track velocities. These velocities were not used to constrain the full velocity profile but existed as a method of verifying the reality of the near bottom velocities calculated by the standard LDEO inverse calculation.

The LDEO processing also extracts an estimate for the full ocean depth by combining the bottom ping with the CTD data. This was used to add to the headers of the CTD data. It was also used to add a better estimate of the full ocean depth to the *proc.dat* file in the *proc/* directory. The *domerge -c1* and the *do_abs* steps of the UH processing were rerun with this new *proc.dat* file to cut out sub-bottom pings.

9.3. M Formatting*

The data from both processing routes were read into M* files. Three M* files were created for each station: one for the UH profile, one for the full LDEO profile and one for the LDEO bottom track velocities. Three files were produced for ease of gridding. Figure 32 shows the gridded velocities from the LADCP through the Florida Straits.

9.4. Data Quality

Three main categories of profiles were observed. The first, evident in the survey of the Florida Straits and early profiles in the west of the section, was of the LDEO, UH, bottom track and VMADCP profiles all matching (Figure 33, top). Secondly, as the section moved over the abyssal plain and scatterers in the deep ocean diminished, profiles began to disagree (Figure 33 centre). Often the LDEO and UH would give different answers in the upper ocean and neither would agree with the bottom tracking velocities. The VMADCP was seen to agree more often with the UH software. Thirdly, using the third LADCP instrument which had a weak beam, the UH profile would drop out between 1000 and 1500 m (Figure 33, bottom). The LDEO gave a full profile but with often wild velocities of up to two or three metres per second. These profiles never agreed with the bottom track velocities. The VMADCP agreed much better with the UH processed data.

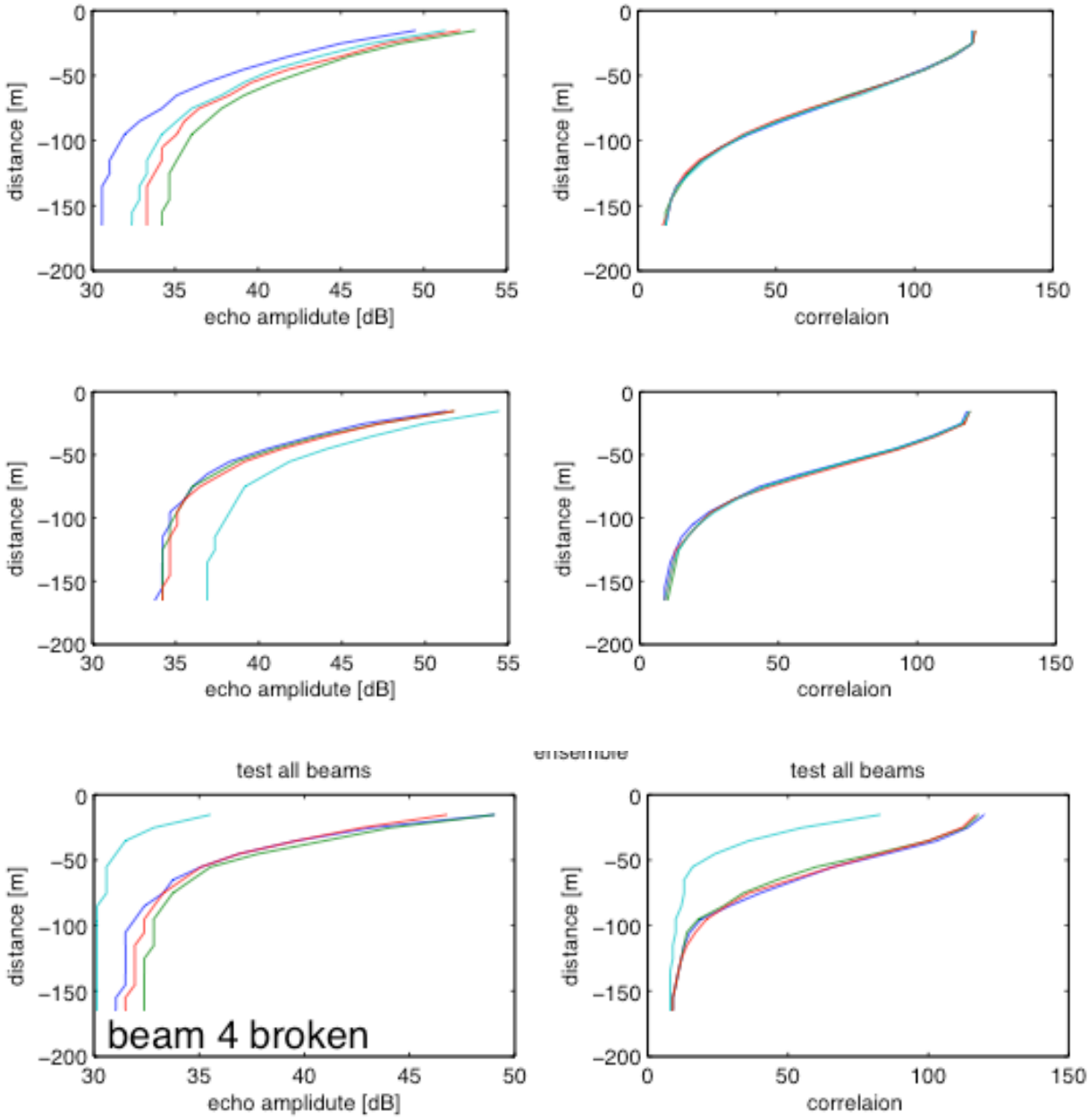

Figure 31: Instrument performance of the three LADCPs used on D346. From the top, the first instrument had four beams of similar strength and close correlation. The second had one beam stronger than the others but retained close correlation. The third had one beam weaker than the others and this beam had poor correlation with the other beams.

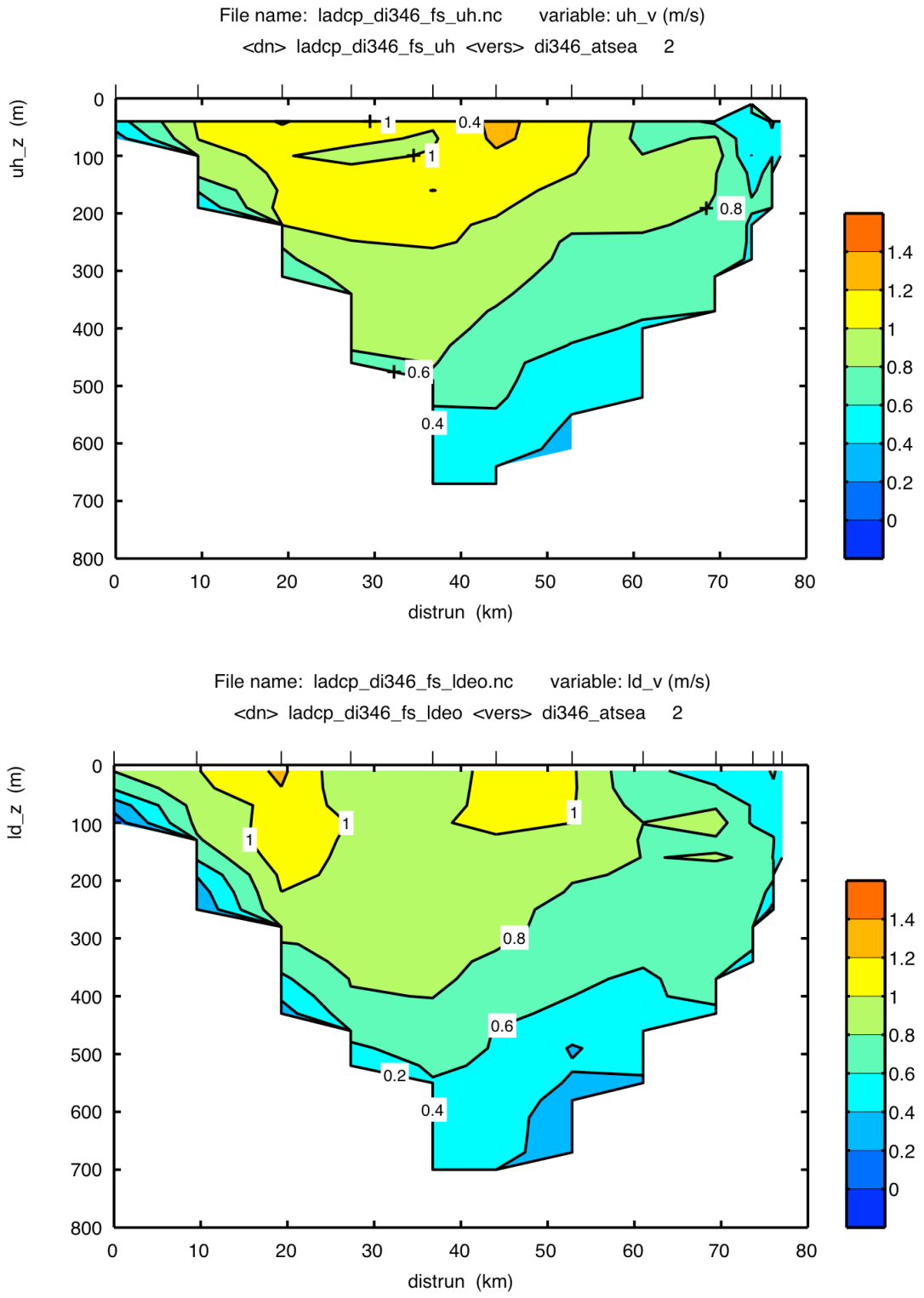

Figure 32. Gridded velocities through the Florida Straits from the UH software (upper) and the LDEO software (lower).

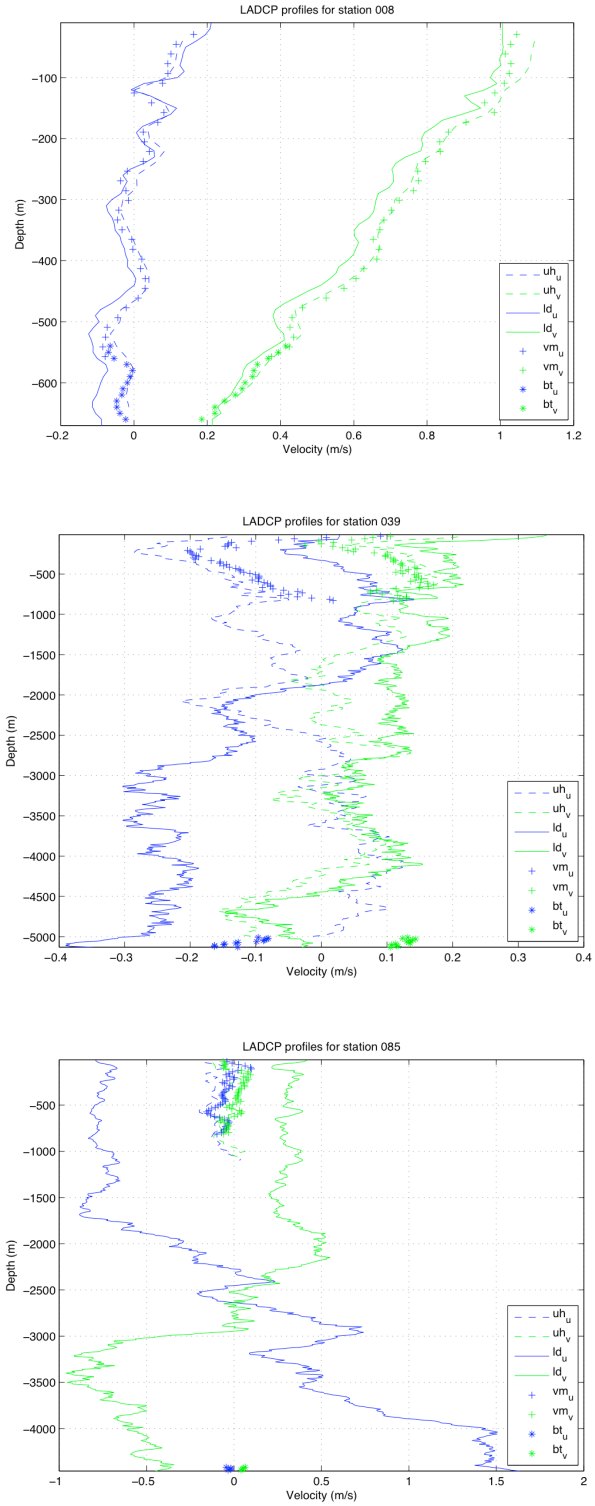

Figure 33: Three profiles illustrating different behaviour of the LADCPs used on D346: (top) Station 008, (centre) Station 039 and (bottom) Station 085.

Gerard McCarthy

10. Underway Temperature, Salinity, Fluorescence & Transmittance

10.1. Instrumentation

Near surface temperature, salinity, fluorescence and transmittance were measured throughout the cruise by instruments located in the non-toxic supply. The inlet for this supply is situated on the underside of the hull, close to the bow (Figure 34). The underway supply is pumped past a Seabird 38 temperature sensor (Figure 35), mounted within a few metres of the inlet, before reaching the fluorometer, transmissometer and thermosalinograph in the water bottle annex (WBA)/wetlab (Figure 36). Details of the instrumentation are given in Table 12.

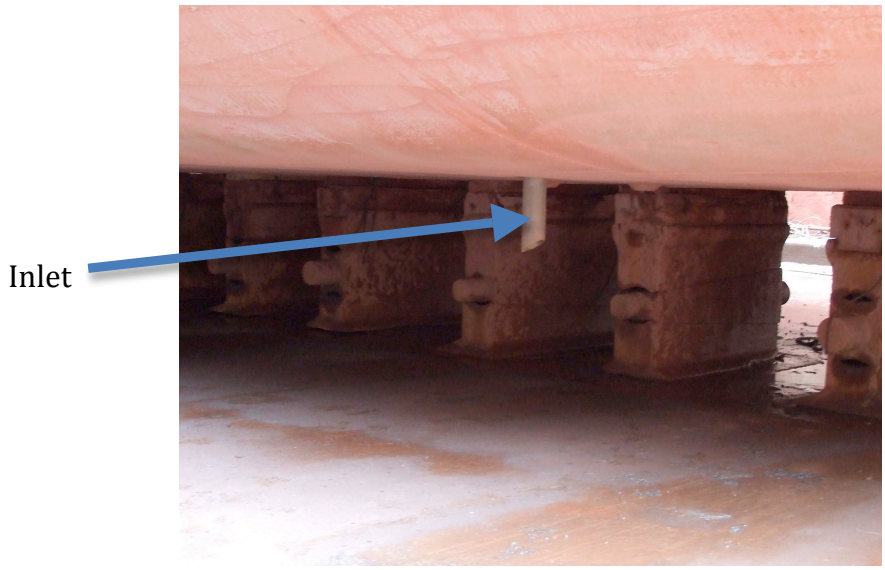

Figure 34: Location of RRS *Discovery* underway seawater supply (depth ~5-6 m).

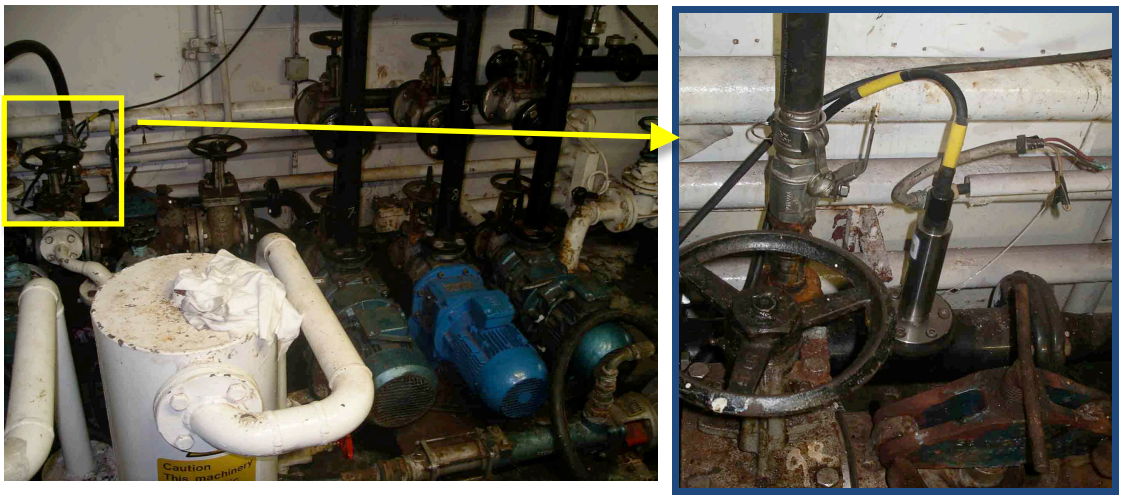

Figure 35: Non-toxic supply pumps in forward hold and enlargement showing temperature probe (estimated to be ~ 5 m from inlet).

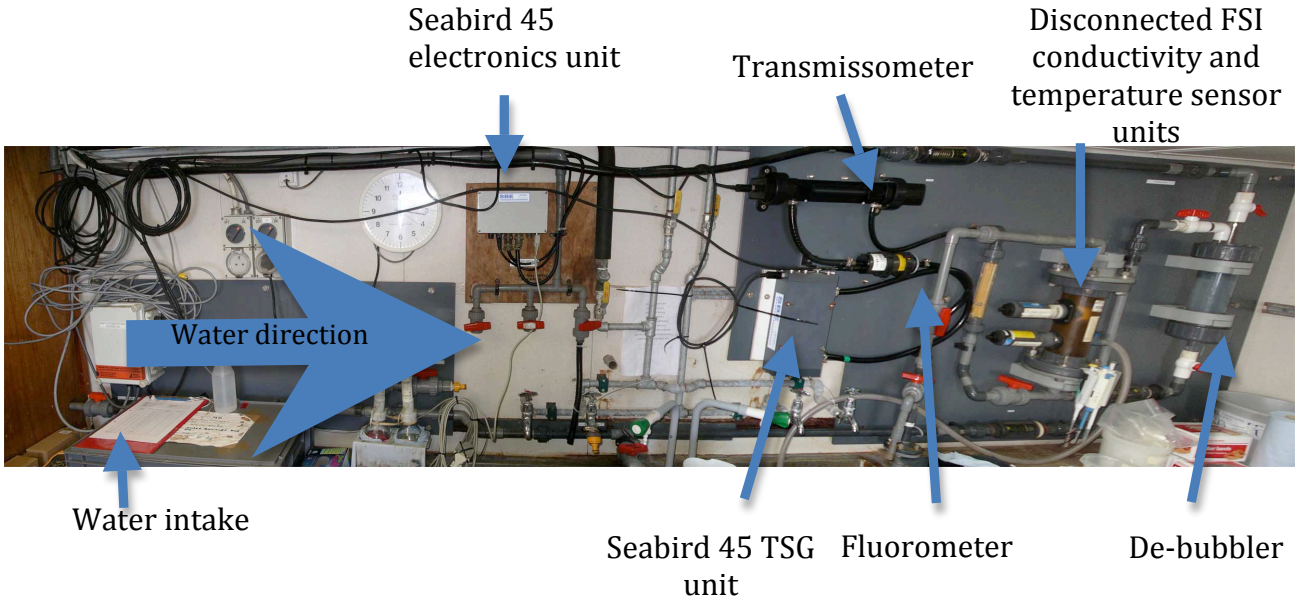

Figure 36: Photograph showing route of underway water supply through instruments located in Water Bottle Annex of RRS *Discovery*.

Table 12: Underway SST, SSS, fluorescence and transmittance instrument details.

Variable	**Instrument**	**Serial number**	**Sensor position**	**Accuracy**
Thermosalinograph - housing temperature	SBE45 MicroTSG	0229	Water bottle annex	
Thermosalinograph - conductivity	SBE45 Micro TSG	0229	Water bottle annex	
Sea surface temperature	SBE38 Digital Thermometer	0476	Near intake	
Fluorescence	Wetlabs Fluorometer	WS3S-247	Water bottle annex	± 0.66mV
Transmittance	Wetlabs Transmissometer	CST-112R	Water bottle annex	

10.2. Routine Processing

Data from the Seabird TSG was logged in both the *di346/data/met/surftsg* and *di346/data/tsg/* directories. The processing steps applied to the data in the two locations varied and are detailed below in the Surfmet Processing and TSG Processing sections respectively. Other variables were only processed in the Surfmet Processing only. Files were transferred from the onboard logging system

(TECHSAS) to the UNIX system on a daily basis using the script *mday_00_get_met.m*.

10.2.1. Surfmet Processing

The raw data (file extension *d***_raw.nc*) were copied to *d***_edit.nc* files for editing, using the function *mday_mk_met_edit.m*. Manual despiking of data was then performed using the Mstar function *mplxyed*.

Values of salinity were calculated in real-time in the *tsg/* directory but had to be computed from the conductivity and housing temperature (*temp_h*) variables in the *met/surftsg/* data stream. The logged conductivity ratio was converted to a salinity value by implementing the UNESCO algorithm of *Fofonoff and Millard (1983)* in *sw_salt.m*. The function *mavg_surftsg_di346.m* was used to call this script and average the data into 1-minute median bins. The smoothed output was saved with the extension *d***_avg.nc* and appended to the file *met_tsg_di346_01.nc* using the script *mapend_surftsg.m*.

10.2.2. TSG Processing

In order to utilise the daily despiked and averaged data, the individual NetCDF files were processed from */data/tsg/*. Navigation data are found using a similar naming convention (eg, *pos_di346_d006_raw.nc*) in */data/nav/gps4000.*

The Matlab program *mmerge* was used by specifying, for each day, the navigation file and the TSG file.

TSG data are stored in the *data/tsg* directory where the naming convention follows the following pattern:

tsg_di346_d006_edit.nc or *tsg_di346_d006_raw.nc*

<data type_cruise_Julian day _ either raw data or despiked data (edit)>. The raw version is that obtained from the TECHSAS data stream and the edit version is a copy of this used for processing.

Processing of the TSG data was achieved using the Mstar suite of packages. First, using *mplxyed.m*, the data were examined visually and any obvious and significant spikes removed. Spikes were removed in the two temperature records (inlet and water bottle annex), the conductivity record and the salinity record. Note that the sound speed values (the other variable available in the data files) were not despiked.

The working directory for the processing from this stage onwards is */data/cjb_work/cb_underway* where the next required Matlab script, *changenantemps2salin.m,* is located. This script recodes any value of salinity to be NaN if the temperature in the WBA was found to be NaN (i.e. as a result of the despiking exercise). A new variable, named *salin_mcalib,* is created and the original salinity values remain in the file. This script replaces the existing file with a new file of the same name, but containing a new variable.

The next script is *new_merge_all_tsg.m* and the first step is to combine (using *mapend.m*) all the TSG files (these are listed in *files_of_interest_bestnav*). When this stage is complete the data are merged (using *mmerge.m*) with the navigation data (taken from *data/nav/g12/bst_di346_01*). The resulting file is written to *data/tsg/tsgwithbestnav/tsg_merged*.

In order to ensure that all values of salinity that are NaN also represent cases where conductivity is NaN and *vice versa, changenantemps2nansalinv2.m* is run and produces two new variables (*salin_new* and *cond_new*).

The final processing stage in *new_merge_all_tsg.m* is to average the variables over a time span of two minute intervals using the *mavmed.m* function (i.e. the median values). The resulting file is written to *data/tsg/tsgwithbestnav/ tsg_merged_with_bestnav_smooth.nc*. At this stage the NetCDF files are also read into Matlab format using *mload.m*. Both smoothed and unsmoothed files are saved in *data_merged.mat* as the structures named *data_final* and *data_final_unsmoothed* respectively.

10.3 Calibration of Underway Sea Surface Salinity

Both of the above methodologies use the same calibration approach detailed here. Water samples from the TSG outflow pipe were collected in 200ml flat glass bottles at ~4 hour intervals throughout the cruise. Before each sample was taken, the hose connected to the outflow pipe was flushed for approximately 20 seconds to ensure that a fresh sample was drawn from the sea surface, and the sample bottles were rinsed thoroughly 3 times with the sample water. Bottles were filled halfway up the shoulder and the necks wiped dry to prevent contamination of the sample by salt crystallisation at the bottle opening. The bottles were then sealed using airtight, single-use plastic inserts before the bottle cap was refitted. The samples were stored in open crates and left in the controlled temperature laboratory for a minimum of 24 hours before analysis, ensuring full adjustment to the ambient temperature of the laboratory. A total of 193 TSG samples were taken during the cruise.

The conductivity ratio of each sample was measured using the salinometer, and the corresponding salinity value was calculated using the OSIL salinometer data logger software, and stored in a Microsoft Excel spreadsheet. The measured salinities of the samples were transferred to a text file, along with the date and time of collection. This file was converted to Mstar format, and the dates and times were converted into seconds since midnight on 1st January 2010 using *mtsg_01_di346.m*. This script appends data from successive processed crates to the file *tsg_di346.nc*.

The script *mtsg_02_di346.m* averaged the continuous TSG data onto the discrete bottle samples for calibration of the SBE45. For each bottle data point, the corresponding TSG salinity was determined as the 10-minute mean of the ~0.5Hz data stream, centred on the time that the bottle sample was drawn. This approach smoothes noise in the continuous data and accounts for the occasional uncertainty in the exact time that the bottle sample was collected. A comparison of the bottle and TSG salinities is plotted in Figure 37.

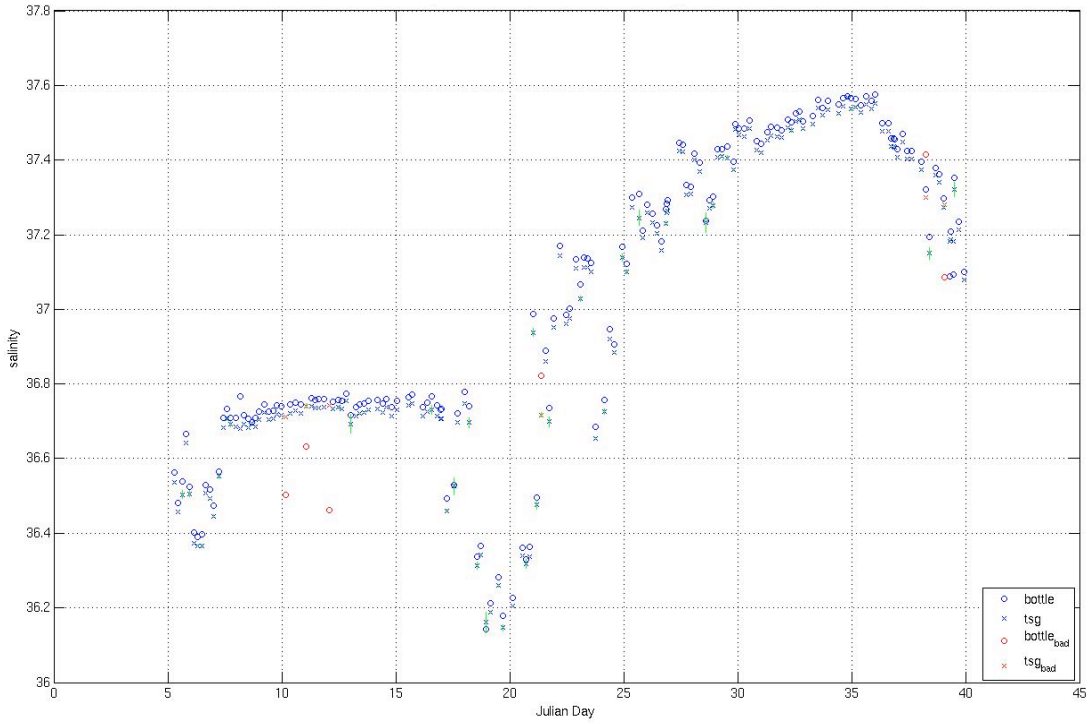

Figure 37: Comparison of Seabird TSG and bottle salinities during D346. The TSG error bars (plotted in green) are computed as the standard deviation of the 10-minute TSG data bin. Data points plotted in red exceeded the tolerated discrepancy between bottle and TSG data.

A maximum tolerated difference between the corresponding bottle and TSG salinities was set at 0.1 practical salinity units (psu). Six data points exceeded this difference and were subsequently omitted from the calibration calculation. The uncertainty (standard deviation of the 10 minute bin) associated with the discarded TSG data was not sufficiently large to account for the discrepancy in each case, suggesting a possible contamination of the bottle sample.

A first order calibration for the TSG salinity was employed to account for the constant offset of the Seabird sensor from the bottle samples and a small temporal drift:

$$TSG\_salinity\_calibrated = -3.412e\text{-}9 * time + 0.0291$$

The linear fit to the retained data is shown in Figure 38. The calibrated salinity is plotted in Figure 39.

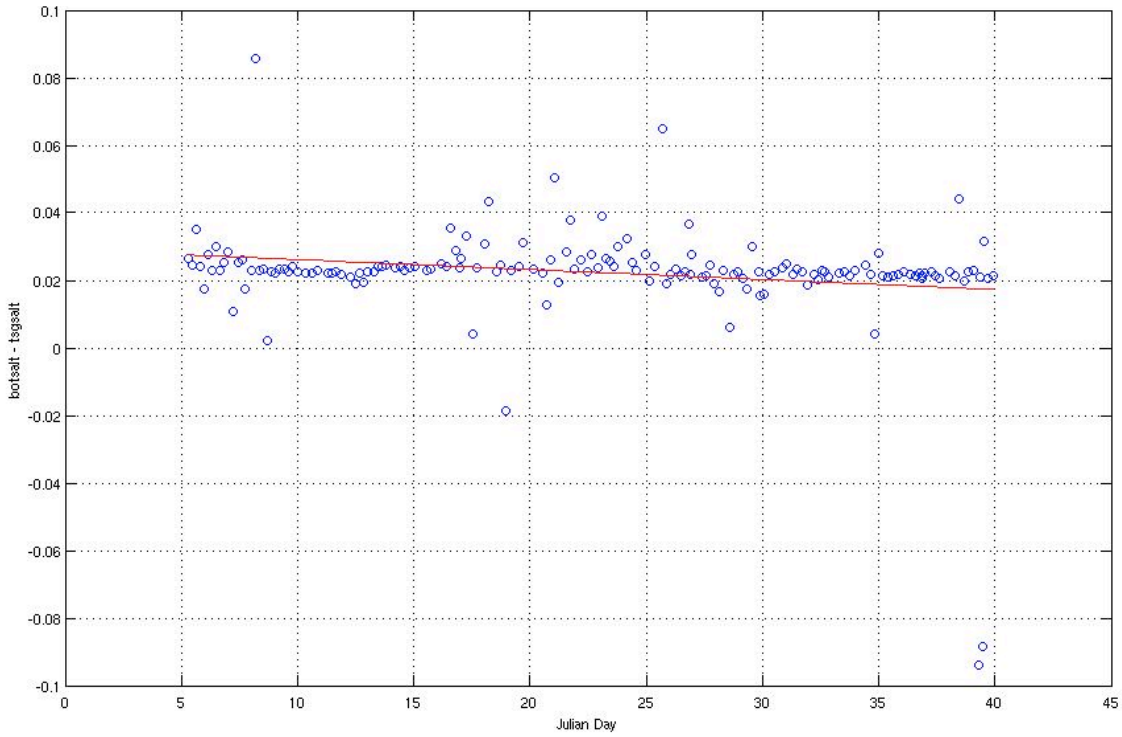

Figure 38: First order calibration of the TSG salinity sensor by comparison with the non-toxic water supply samples.

An independent calibration of the TSG can be performed by comparing the Seabird sensor in the inlet pipe, to temperature and salinity data from the instruments mounted on the CTD frame. During cruise D346, 135 CTD casts were taken between days 6 and 45. The script *mtsg_04_di346.m* selected the CTD temperature and salinity data logged between 5 and 6db (assumed to be the approximate depth of the remote temperature sensor in the inlet pipe) for each CTD cast. This region is assumed to be well mixed so that the depth difference between the level sampled by the CTD probe and the level of the inlet pipe is negligible. Data obtained during the 10m dip preceding each cast was discarded before averaging the TSG data onto the CTD sample times. For each CTD data point, the corresponding TSG salinity was determined as the 20-second mean of the ~0.5Hz data stream, centred on the time that the CTD probe sampled. This averaging bin is deliberately smaller than that selected for the TSG calibration with the bottle data, where the sample frequency was significantly lower and the collection time was rounded to the nearest minute.

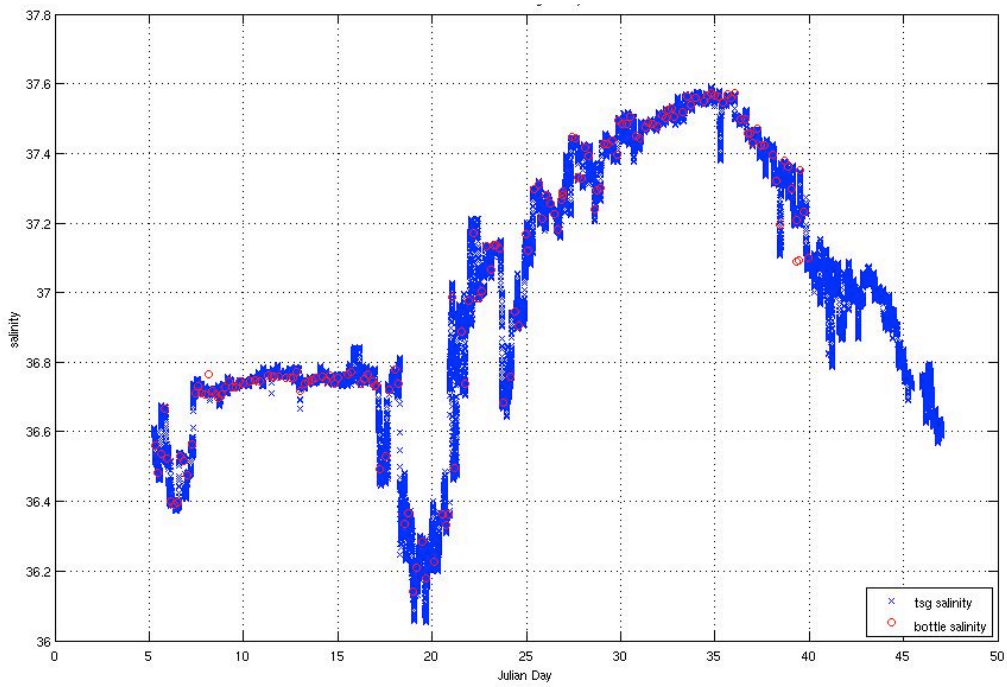

Figure 39: Calibrated TSG salinity plotted with bottle data used in calibration.

The SBE45 temperature and salinity sensors were found to have a small offset from the primary sensors mounted on the CTD. A comparison of the TSG and CTD temperatures is plotted in Figure 40. A first order calibration for the TSG temperature was employed to account for the discrepancy between the SBE38 digital thermometer and the superior CTD mounted probe:

TSG_temp_calibrated = 1.0268* TSG_temp_raw - 0.7512.

The calibrated TSG temperature is plotted in Figure 41.

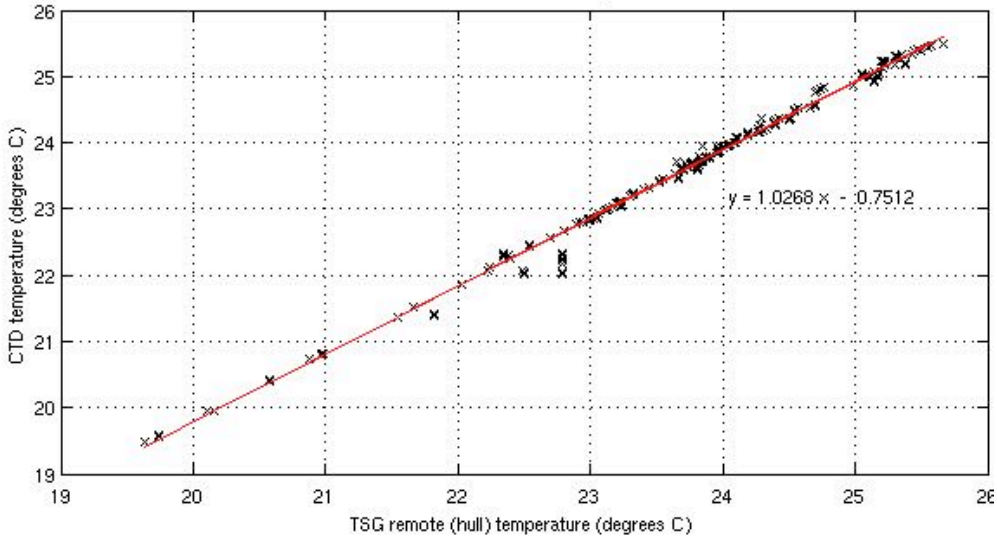

Figure 40: First order calibration of the TSG temperature sensor by comparison with the sensor mounted on the CTD frame.

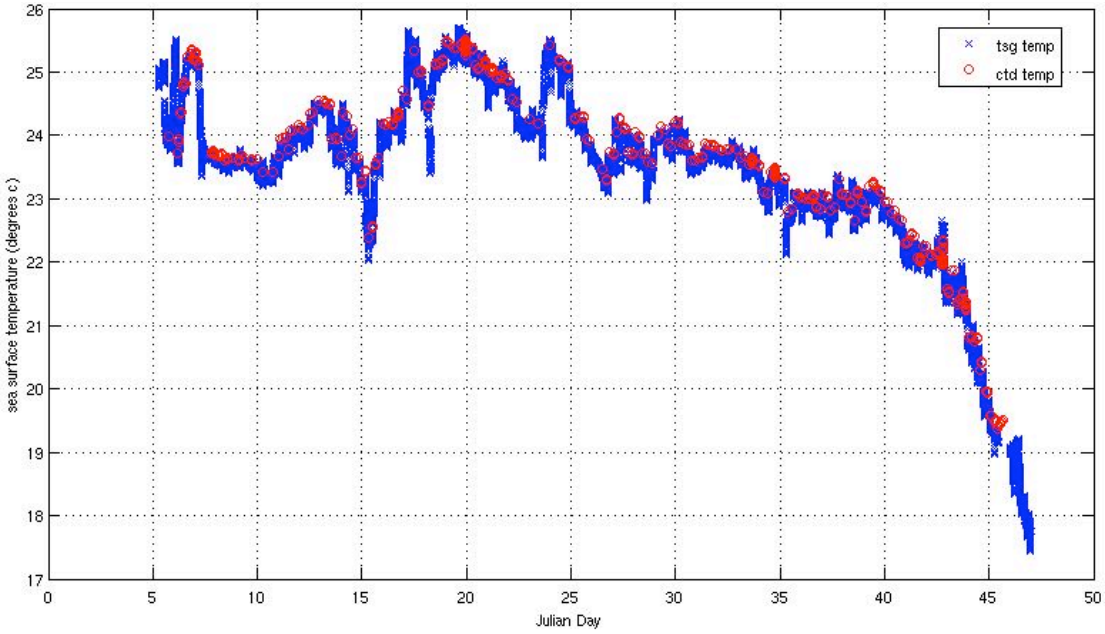

Figure 41: Calibrated TSG temperature plotted with CTD data used in calibration.

The SBE45 salinity measurements were also found to be weakly dependent on sea surface temperature (not shown). The Seabird TSG computes salinity using data from the temperature sensor collocated with the conductivity sensor in the water bottle annex. It is suggested the warmest SSTs were associated with the greatest ship-sea thermal contrast during D346. This contrast may have induced a more notable difference between the temperature read by the sensor in the hull and the sensor in the water bottle annex. However, the dominant uncertainty in the TSG salinity data was determined to be the instrument error previously accounted for by calibration with the bottle samples. As a result, no further adjustment to the salinity data was applied and the weak dependency on sea surface temperature was ignored.

Calibrated TSG salinity and temperature data averaged across 5km sections of the cruise track are shown in Figure 42 and Figure 43 below.

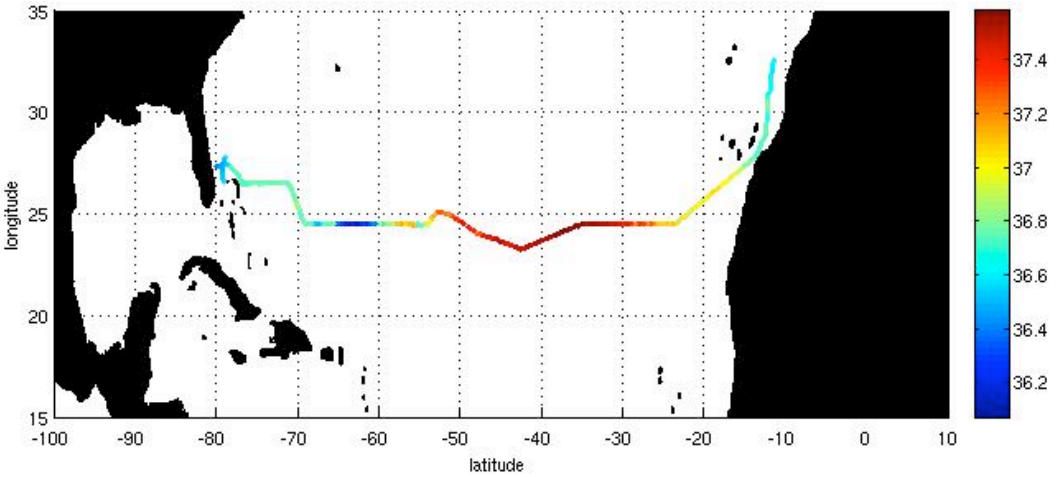

Figure 42: 5km mean calibrated TSG salinity during D346.

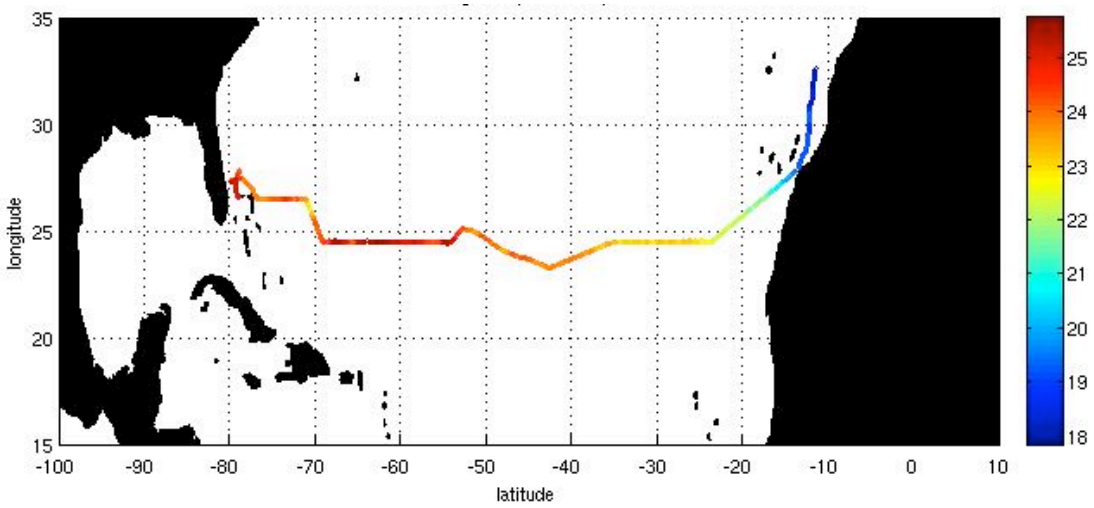

Figure 43: 5km mean calibrated TSG temperature during D346.

10.4. References

Fofonoff N. P. and Millard R. C., (1983), Algorithms for Computation of Fundamental Properties of Seawater, UNESCO Technical Papers in Marine Science 44.

Chris Banks and Helen Pillar

11. Surface Meteorological Sampling System (SURFMET)

11.1. Instrumentation

The RRS *Discovery* was equipped with a variety of meteorological sensors to measure air temperature and humidity, atmospheric pressure, total irradiance, photosynthetically active radiation, wind speed and wind direction throughout the cruise.

Table 13: Meteorological instrument details

Variable	Instrument	Serial number	Calibration $Y = C_0 + C_1x + C_2x^2 + C_3x^3$	Sensor position	Accuracy
Atmospheric Pressure	Vaisala PTB100A barometer	S3610008	C_0 = -1.17483 C_1 = 1.00152	Port Foremast	-
Dry bulb air temp + humidity	Vaisala HMP45A	B4950010	C_0 = 0.0 C_1 = 1.0	Port Foremast	Humidity ±1.5% Temp ±0.15°C
Wind speed + direction	Gill sonic anemometer	071123	C_0 = 0.0 C_1 = 1.0	Port Foremast	-
Total irradiance (TIR)	Kipp & Zonen CM6B (335 – 2200nm) pyranometer	994133	C_0 = 0.0 C_1 = 1.0	Port	9.60 μV/W/m^2
		962301	C_0 = 0.0 C_1 = 1.0	Starboard	9.76 μV/W/m^2
Photosynth-etically active radiation (PAR)	Skye energy sensor (400 – 700nm)	28557	C_0 = 0.0 C_1 = 1.0	Port	11.04 μV/W/m^2
		28556	C_0 = 0.0 C_1 = 1.0	Starboard	10.53 μV/W/m^2

The radiation and pressure variables were logged in the data/met/surflight directory. The remaining data was logged in /met/surfmet.

11.2. Routine Processing

Files were transferred from the onboard logging system (TECHSAS) to the UNIX system on a daily basis, using the script *mday_00_get_met.m*. The raw data files have extensions of the form *_di346_d***_raw.nc*, where *** represents the day number. These were copied *_di346_d***_edit.nc* files for editing using the script *mday_mk_met_edit.m*. The data were plotted using the scripts *mday_plot_surfmet.m*

and *mday_plot_surflight.m*, before being manually despiked using the function *mplxyed*. The data were then averaged into 1-minute (median) bins using *mavg_surfmet_di346.m* and *mavg_surflight_di346.m* and appended to the files *met_di346_01.nc* and *met_light_di346_01.nc* using the scripts *mapend_surfmet.m* and *mapend_surflight.m* respectively.

The barometer data was the only stream that required adjustment; a 1st order calibration, (as given in the instrument documentation) and a correction to account for the ~16m offset of the mounted barometer from the sea level. These adjustments were performed by running the script *mcal_atmpress.m*, which assumes the atmospheric boundary layer is both hydrostatic and well mixed (isothermal) between the surface and the instrument level. This is likely to be a reasonable assumption for the convective boundary layer (*Stull, 1988*) but may be unrepresentative of the nocturnal boundary layer in the absence of mechanical stirring. The corrected pressure was then averaged into 1-minute (median) bins and appended to *press_correct_di346_01.nc* using the scripts *mavg_press_di346.m* and *mapend_press.m* respectively.

Once the meteorology and navigation data had been processed, the true (Earth relative) wind speed and direction was computed from the cleaned, ship relative wind data using the script *mtruewind_di346.m* and saved in the file *met_di346_truewind.nc*. It is noted that ~19 hours of anemometer data was lost on 19/01/2010 when sustained spuriously high wind speeds were logged. The cause of this instrument error was not determined.

11.3. References

Stull, R.B. (1988), '*An Introduction to Boundary-Layer Meteorology'*, Kluwer, pp. 666

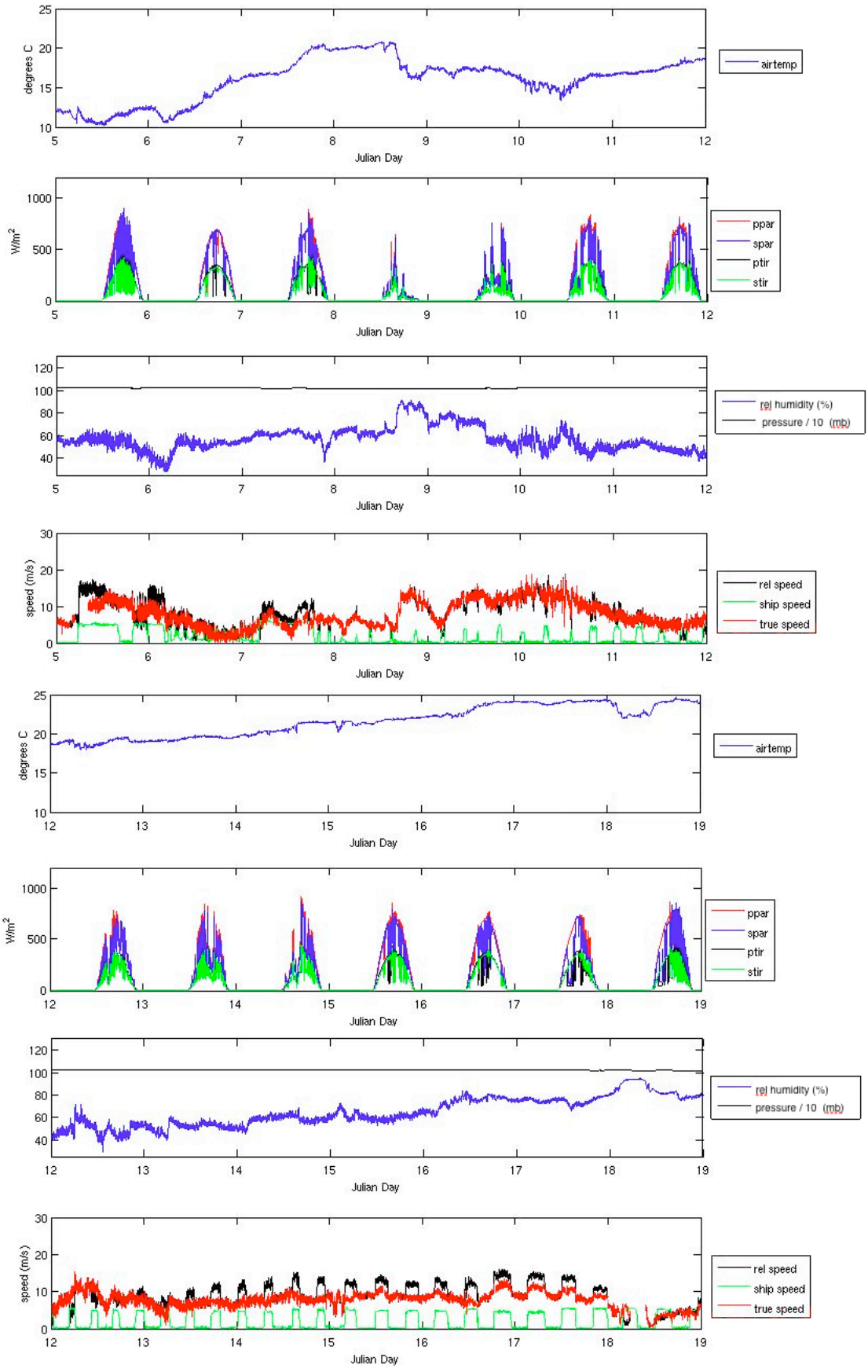
degrees C
Julian Day
airtemp
W/m^2
ppar
spar
ptir
stir
rel humidity (%)
pressure / 10 (mb)
speed (m/s)
rel speed
ship speed
true speed

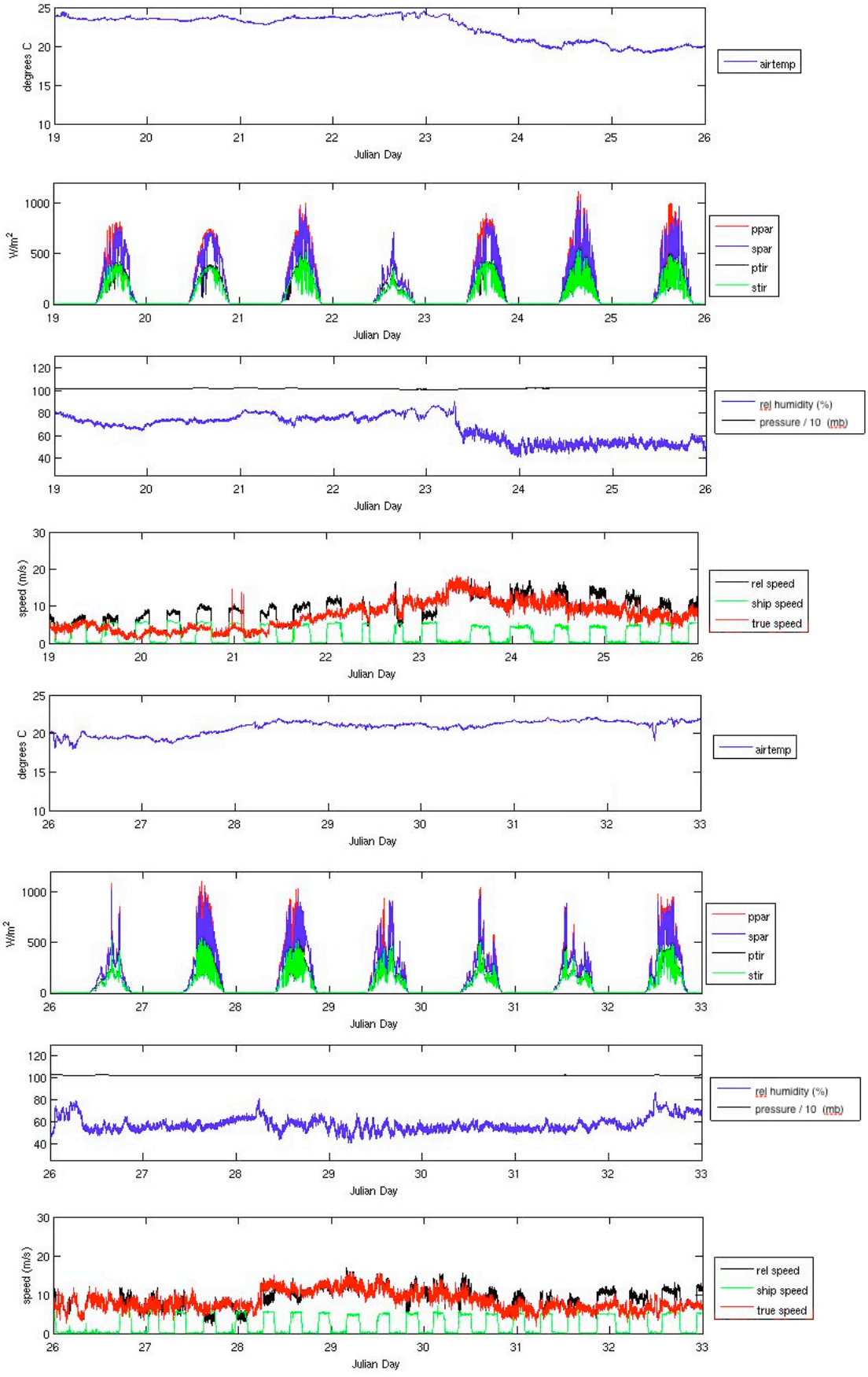
degrees C
Julian Day
airtemp
W/m2
ppar
spar
ptir
stir
rel humidity (%)
pressure / 10 (mb)
speed (m/s)
rel speed
ship speed
true speed

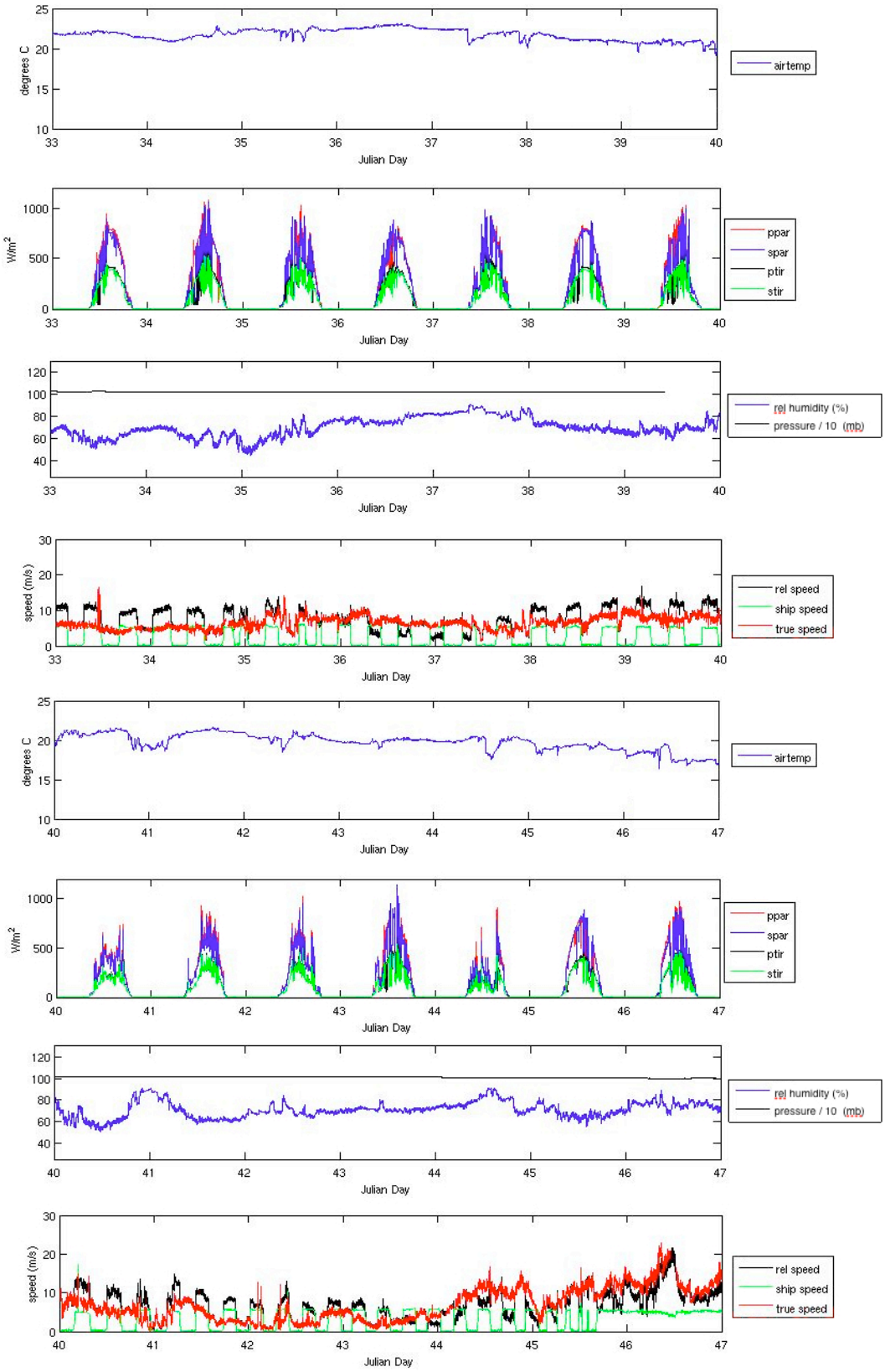

Figure 44: Time series of 1-minute (median) averages of the meteorological data for the duration of D346 (Julian day 5 – 47). The time annotation is completed decimal days, so the first panel begins at midnight at the end of day number 5 (5 Jan) and the last panel ends at midnight at the end of day number 47 (16 Feb)

Helen Pillar

12. Navigation

12.1. Navigation Summary

High quality navigation data were necessary to orientate all the measurements made during the cruise. In addition, accurate ship speed and heading were important for making accurate underway measurements of ocean currents as well as wind speed and direction, since small heading errors while steaming can lead to large anomalies when calculating absolute velocities from ship-relative measurements.

The *RRS Discovery* has three GPS receivers: the Trimble 4000, which is a differential GPS; the Ashtech; and the GPS G12. The ship also uses a gyrocompass and Chernikeeff Electromagnetic (EM) log to measure ship heading and speed. Data from the Trimble 4000 and G12 GPS streams as well as position and attitude data from the Ashtech GPS were processed daily as outlined below.

12.2. Comparison of GPS accuracy

A comparison of the position data produced by all three GPS streams was carried out (Figure 45). Differences in latitude and longitude were converted to metres for a more meaningful comparison. The G12 and the Trimble agree best; there is considerably more scatter in the comparisons of both with the Ashtech. However, there were several occasions during the cruise when the Trimble GPS froze, leading to gaps in the data. Therefore, the G12 was chosen as the most accurate and reliable GPS stream, and was used for creating the final 'bestnav' (*bst_di346_01.nc*) file.

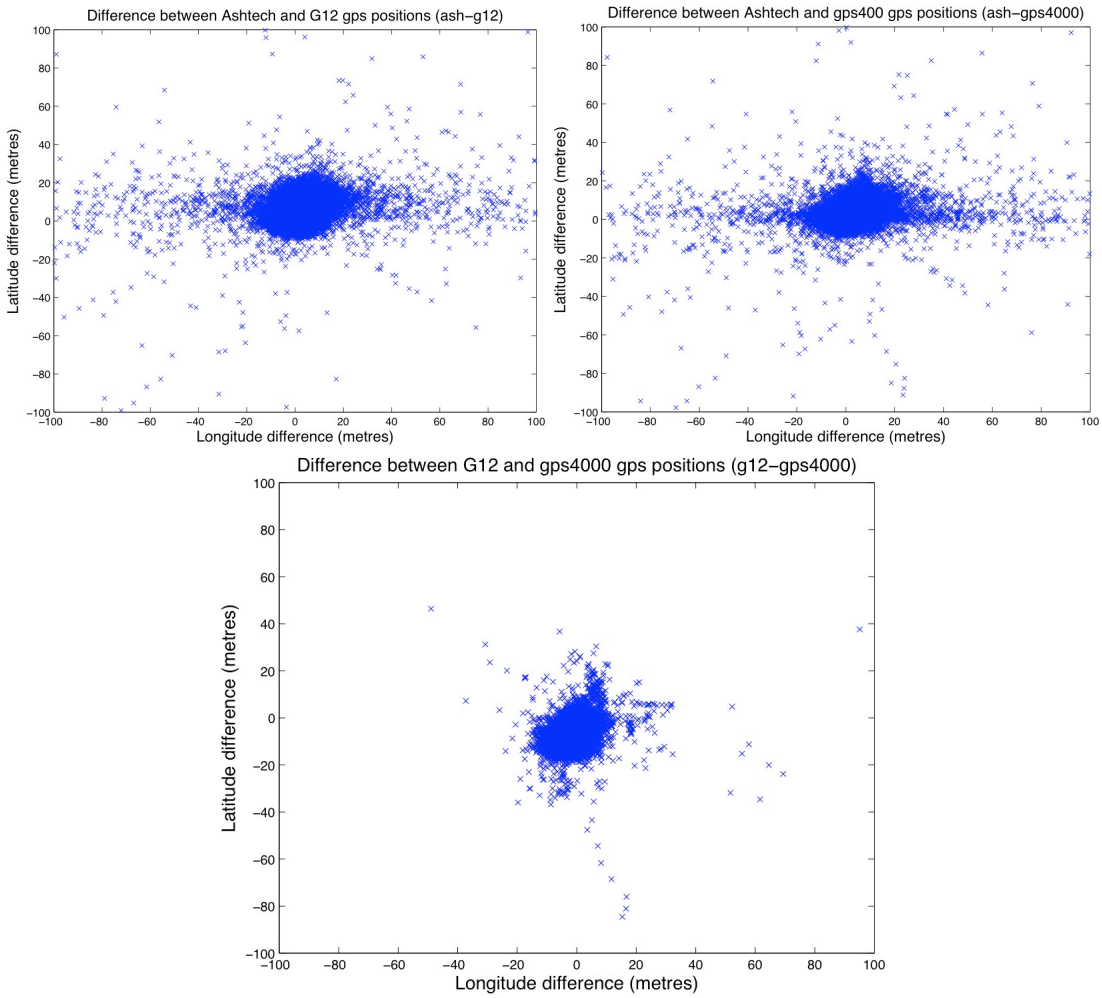

Figure 45: Comparisons between positions measured by (a) Ashtech and GPS G12, (b) Ashtech and GPS 4000, (c) GPS G12 and GPS 4000.

12.3. Gyrocompass

The ships' gyrocompass provides a reliable estimate of the ships' heading that is not dependent on transmissions external to the ship. However, the instrument is subject to latitude- and velocity-dependent errors and has an inherent oscillation following a change of heading. This is known as the Schuler oscillation with a period of approximately 86 minutes.

Because the gyrocompass calculates heading based on the rotation of the Earth, it needs to be configured for the ships' latitude and average speed. At the start of the cruise the primary gyrocompass failed at 05:45:12 GMT on 06/02/2010; the data stream was then changed to the secondary gyrocompass. However, this had not been correctly calibrated to the ships' latitude leading to a period of adjustment when the data were considered unreliable, until 06:43:48 GMT.

Although the gyrocompass is reliable, the time-dependent errors need to be corrected for using the less reliable but more accurate Ashtech Attitude Detection Unit (ADU) heading data. The data for both these systems and the heading correction were calculated in daily segments before being applied to calibrate the VMADCP data.

12.4. Ashtech 3DF GPS Attitude Detection Unit (ADU)

The Ashtech GPS comprises four antennae mounted above the bridge. Every second, the Ashtech calculates ship attitude (heading, pitch and roll) by comparing phase differences between the four incoming satellite signals. This is usually very accurate, but occasionally the Ashtech unit failed to pick up enough GPS signals to provide an accurate fix. These periods were usually identifiable by spikes in the heading, pitch and roll data. The largest of these spikes were automatically removed using the *mash_01* script as outlined below, and the rest were manually removed using the *mplxyed* function. This avoids allowing spurious Ashtech heading data to contaminate the ashtech-minus-gyro (a_minus_g) heading correction used in the calibration of the VMADCP.

12.5. Daily Processing Steps

Table 14: Navigation processing steps with descriptions of their function

<table>
<tr><td>mday_00_get_nav</td><td>Get all the navigation data and convert from techsas data into daily files of mstar data. The filenames were in the format <dataname>_di346_d???_raw.nc, where <dataname> refers to a three-letter string, e.g., ‘gyr’ for gyrocompass data.</td></tr>
<tr><td>mgyr_01</td><td>Remove non-monotonic times from the gyro data. Outputs gyr_di346_d???.nc files</td></tr>
<tr><td>mash_01</td><td>Merge the gyro heading into the ashtech data file then calculate the a-g heading correction.
Apply quality control using mdatpik such that data are removed outside the following limits:
<table>
<tr><td>head_ash</td><td>0</td><td>360</td></tr>
<tr><td>pitch</td><td>-5</td><td>5</td></tr>
<tr><td>roll</td><td>-7</td><td>7</td></tr>
<tr><td>mrms</td><td>0.00001</td><td>0.01</td></tr>
<tr><td>brms</td><td>0.00001</td><td>0.1</td></tr>
<tr><td>head_gyr</td><td>0</td><td>360</td></tr>
<tr><td>a_minus_g</td><td>-7</td><td>7</td></tr>
</table>
Apply 2 minute averaging to the data.

The output from this processing is in the ash_di346_d???.nc files.

Note that the purpose of this process is to provide reliable heading information to the VMADCP calculations. Therefore the emphasis is on removing bad data and smoothing over high-frequency variability. It is possible that the mdatpik stage removes good data, but it is expected that the amount of good data discarded will be relatively small.

Also note that although pitch and roll are carried through to the final files, the two-minute averaging means that these data should be extracted from the _raw.nc files instead.</td></tr>
</table>

mplxyed	The a_minus_g data were manually de-spiked using this interactive plotting command in mstar. Care was taken to remove spikes that were due to errors in the ashtech data but leave spikes due to sudden changes in ships' heading.
mday_00_run_nav	Append the daily data into a single *<dataname>_di346_01.nc* file for each data set.
mbest_all	Wrapper script for the mbest_01, mbest_02, mbest_03 and mbest_04 scripts. These scripts run 30-second averaging on the position (GPS_4000 and GPS_G12) and gyrocompass data and then calculates speed and groundcourse from the GPS data, before merging the GPS and gyro data into a *bst_di346_01.nc* file.

11.6. Chernikeeff Doppler Log Calibration

The Chernikeeff Doppler log records the ships' velocity through the water by measuring the voltage produced by seawater flowing through an alternating magnetic field. The velocities are measured in both the forward-aft and port-starboard directions. The amount of voltage produced is roughly 50 μV/Knot, and this signal is scaled to produce the 'measured' speed. However, because this relationship is not perfectly linear, it is necessary to calibrate the Chernikeeff to convert this measured speed into a 'true' speed for the ship. This calibration is typically done by steaming out and back over a measured distance at a set engine RPM and then taking the average velocity calculated from the two runs. This is repeated for multiple speeds to create an empirical look-up table as an approximation to the true calibration curve.

On cruise D346, it became apparent early on that the Chernikeeff was over-estimating the ships' speed considerably, especially at high velocities. It was decided that a practical solution would be to calibrate the Chernikeeff against the ships' velocity as measured by the VMADCP. The ships' forward-aft velocity from the second bin of the OS150 VMADCP was used for this purpose, corresponding to the ship-relative water velocity at approximately 16 m below the hull. It was assumed that any bias associated with calibrating between different depths would be negligible.

On examination of the previous calibration, it appeared that the reason for the Chernikeeff over-estimating the ships' speed was that the calibration value for the highest RPM was higher than would be expected from the previous points (Figure 46). Since the calibration is extrapolated from the last two points entered, any errors in this last point will be amplified at high speeds. When the Chernikeeff 'true' speed was plotted against the VMADCP measured speed, a kink was indeed evident at high speeds (Figure 47) that was assumed to be related to this apparent error.

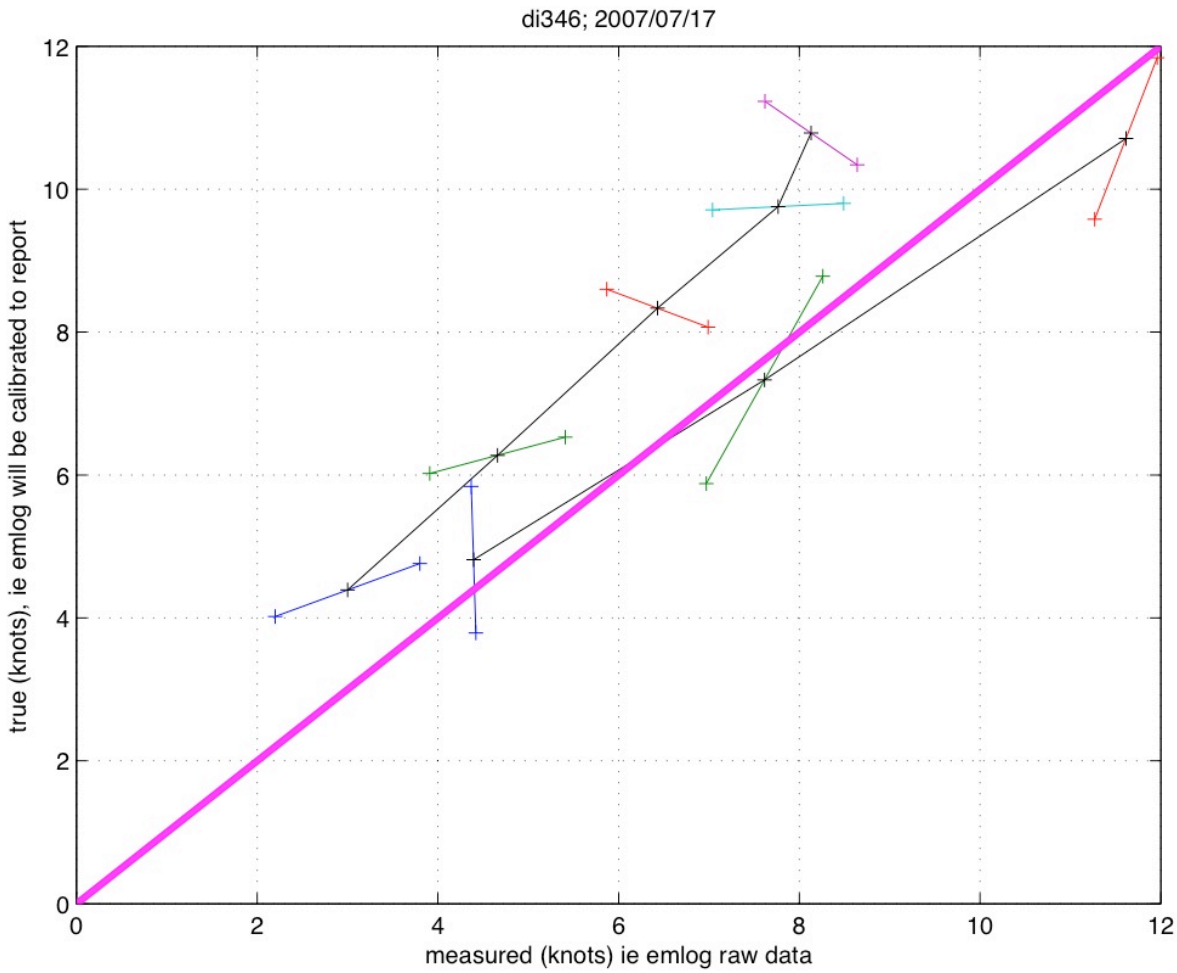

Figure 46: Calibration curves for the previous two calibrations of the Chernikeeff EM log on *RRS Discovery*. The upper curve is the most recent calibration, the lower curve a previous calibration with a linear relationship. The pink line represents a 1:1 relationship and is plotted for comparison only.

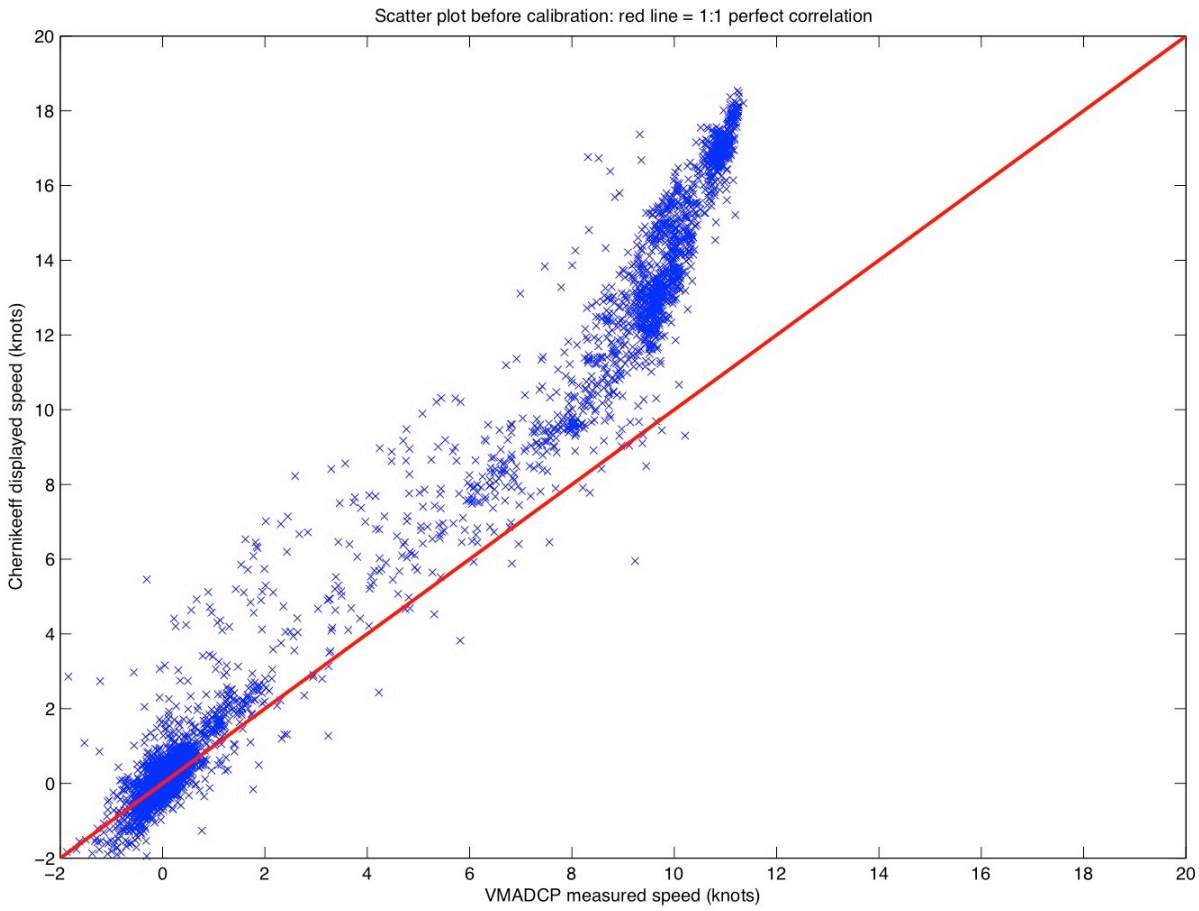

Figure 47: Scatter plot of Chernikeeff displayed speed against speed measured by the VMADCP second bin, before any calibration was applied.

Re-calibration of the Chernikeeff was performed by fitting a piecewise linear relationship with the VMADCP measured speed and using this best fit to adjust the values in the original look-up table. The values entered were adjusted by hand to make a smooth curve in the adjusted look-up table to reduce the possibility of inaccurate extrapolation from the final points. The resulting relationship between the Chernikeeff and the VMADCP is shown in Figure 48. It is apparent that the Chernikeeff was now under-estimating the velocities, but that the relationship was more linear than the previous. Thus a linear fit was applied to produce a third calibration, the result of which is shown in Figure 49. The gradient of the fit was now almost perfect, but there was a gradient in the cluster of points at high velocities. This appeared to be due to the value at around 9 knots being too low and the one at around 12 knots being too high. Thus these two values were adjusted by hand to give the final calibration, shown in Figure 50. There is some evidence that this final calibration may have been a slight over-correction for the gradient at high speeds in the previous calibration. However, given the relatively short period, during which rough weather was experienced, it is possible that this is not entirely representative. Further investigation on subsequent cruises may be worthwhile in order to establish additional improvements to this calibration.

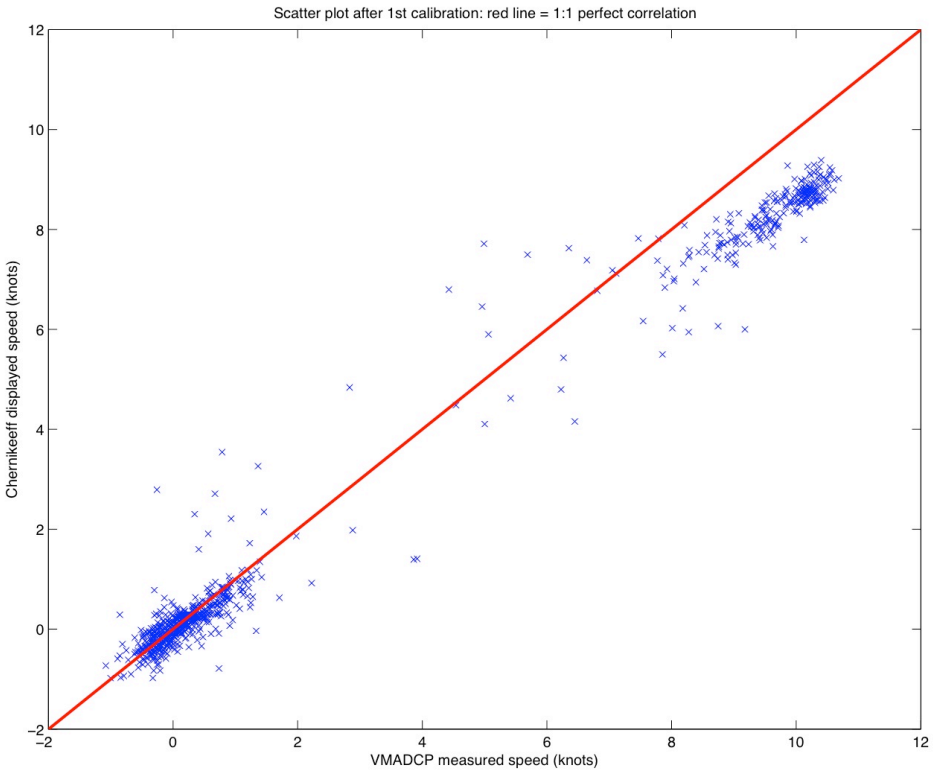

Figure 48: As Figure 47, but after first calibration

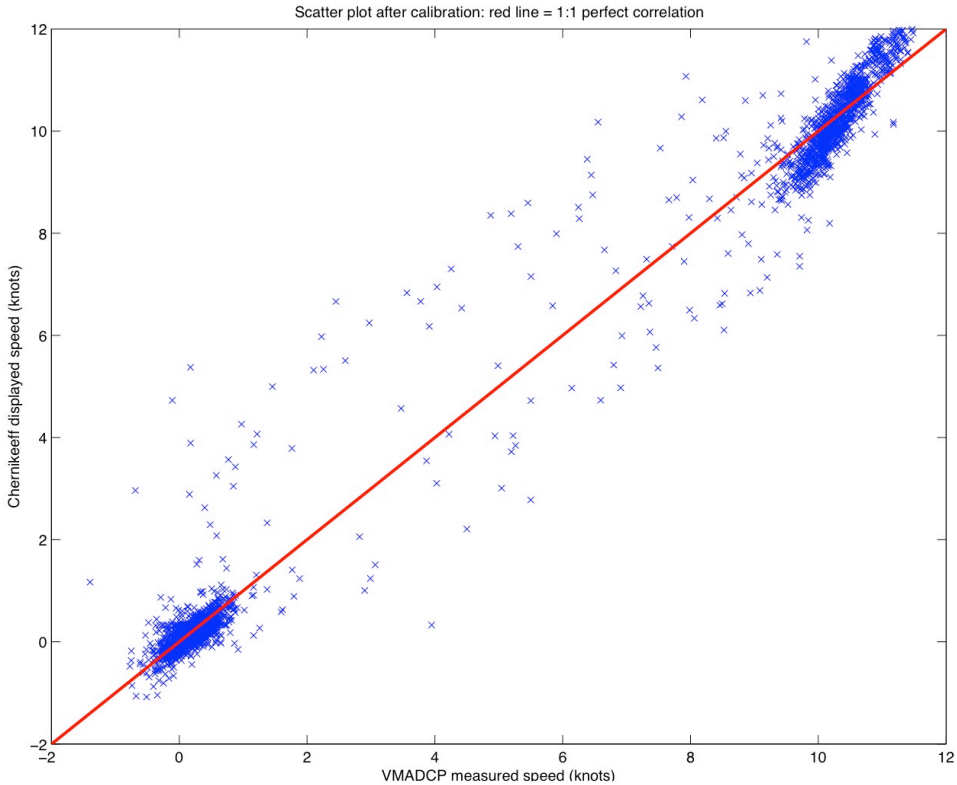

Figure 49: As Figure 47, but after second calibration

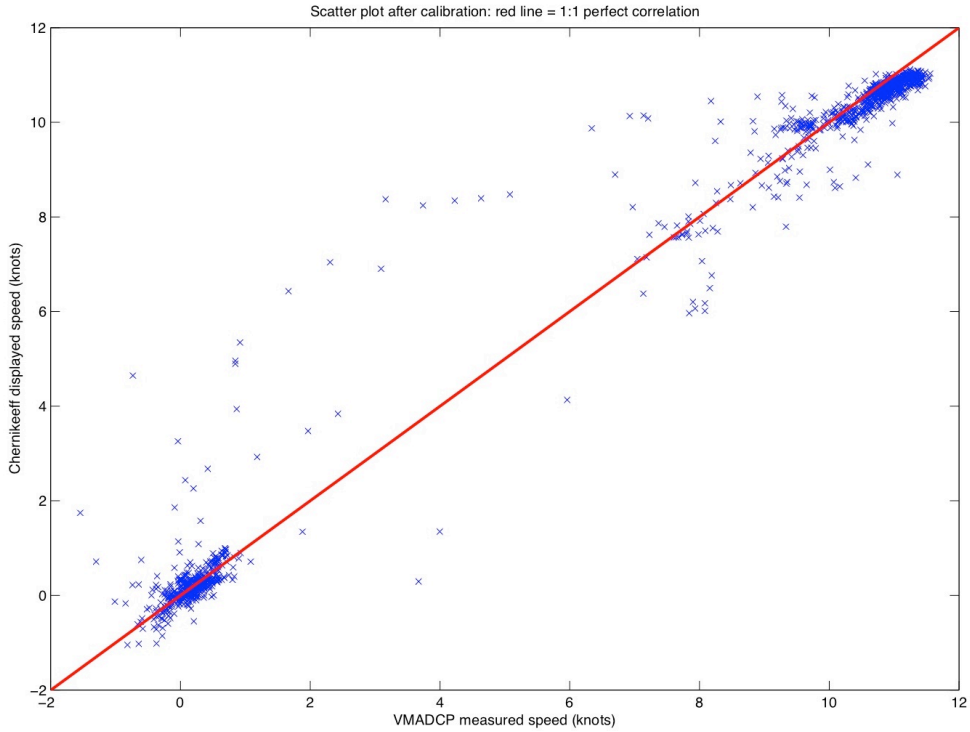

Figure 50: As Figure 47, but after final calibration

The look-up table with the original and new calibration values is shown below. Note that the Chernikeeff requires two tables to be entered for calibration (corresponding to the outbound and return legs of the trial runs), so the values in the final column are entered for both 'table 1' and 'table 2'.

Table 15: Calibration values entered into both 'table 1' and 'table 2' in the Chernikeeff EM log's calibration menu.

RPM	EM-log 'measured' speed	Original EM-log 'true' speed before calibration	VMADCP-calibrated true speed (after final calibration)
75	300	439	372
100	466	626	533
125	643	833	710
150	776	979	875
160	813	1079	980
180	1043		1133

Ben Webber

13. Bathymetry

13.1. Instrumentation

The RRS *Discovery* was equipped with a Simrad EA500 echo sounder (10.2/12.0kHz 'fish' and hull mounted system) to allow bathymetric profiling throughout the cruise. The estimated depth of the hull-mounted transducer was 5.3m. The Precision Echosounding (PES) transducer mounted in a 'fish' was towed at an estimated depth of 8.5m. Whilst steaming, the hull-mounted transducer was ineffective due to interference from bubbles generated by the ship propulsion. The PES fish transducer - towed at a lower depth - was used preferentially, proving less susceptible to this noise. At low towing speeds and whilst on station, the attitude and depth of the fish were less stable and the task of bathymetric profiling was switched to the hull-mounted transducer.

The measured depth was logged by the TECHSAS system and displayed on the Simrad visual display unit, informing decisions to change the preset range and gain of the signal. A hardcopy of this display was also produced on a colour printout. A uniform sound velocity of 1500m/s was assumed throughout the cruise.

13.2. Routine Processing

Files were transferred from the onboard logging system (TECHSAS) to the UNIX system on a daily basis using the Matlab function *mday_00('sim',day#)*. The raw data files have extensions of the form *_di346_d ***.nc* where *** is the number of the Julian day.

During the cruise, the echosounder often failed to detect the bottom and reported either zeros or spuriously large depths. The script *msim_01.m* was run to remove data outside a tolerated range and apply a 5-minute median despiking, outputting the file *sim_di346_d***_smooth.nc*. The script *msim_plot.m* copied the smoothed data to the file *sim_di346_d***_edited.nc* and called the function *mplxyed* to allow a manual removal of the remaining spikes. The paper record proved highly useful in detecting spurious depths resulting from side-echoes off steep topography and reflection off the CTD cable. Incorrect values for the bottom depth were also detected when the transmitted ping penetrated thick layers (up to ~200m) of soft sediment on the sea floor before being reflected by the underlying bedrock.

Following the manual edit of the smoothed data, the script *mapend_sim.m* was run to append all existing *sim_di346_d***_edited.nc* files to *sim_di346_01.nc*. Once a clean navigation file had been produced, *mmerge_sim_nav_di346.m* was run to merge the position and bathymetry data and correct for the variable speed of sound using Carter table climatologies. The corrected depths were saved in the file *sim_di346_01_withnav*. Finally, the data were averaged across 5km along-track intervals using *mavg_sim_di346.m*. This data was saved in the file *sim_di346_01_5km.nc* and is shown plotted against longitude in Figure 51 below. The most notable gap in the data is associated with discarded side-echoes generated whilst traversing the Abaco shelf.

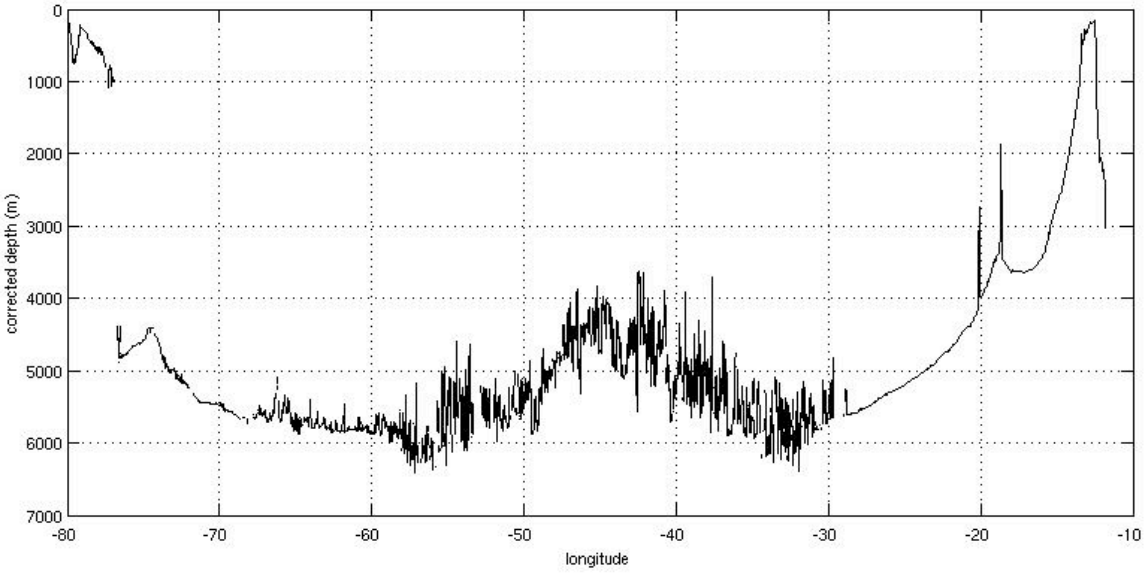

Figure 51: Bathymetry data averaged over 5km intervals of the distance run, plotted as a function of longitude for the duration of the cruise.

Helen Pillar

14. Vessel Mounted ADCP Instruments

14.1. Introduction

Two vessel-mounted Acoustic Doppler Current Profilers (ADCPs) onboard *RRS Discovery* were used throughout the cruise to measure the horizontal velocity field (cross-track and along-track). The 75kHz and 150kHz Ocean Surveyor (OS) instruments were supplied by Teledyne RD Instruments. Unlike *RRS James Cook*, *RRS Discovery* does not have retractable keels so these instruments are fitted to the hull of the ship. Cruise D345 did not have the 75kHz instrument fitted, so the transducer was installed by divers whilst docked in Freeport prior to D346. The depths of the transducers are 5.3m. Both transducers are phased-array, which means that they are made up of many elements each transmitting in different phase. This is advantageous, because it means that the accuracy of the velocities, derived from the Doppler shifted return signals, is not affected by speed of sound changes throughout the water column. However, the range and accuracy of the instruments has been observed in this cruise, as it has previously, to be affected by exposure to bubbles.

The different frequencies of the two instruments affect both their depth range and resolution. The 150kHz allows smaller depth bins and consequently higher vertical resolution, but the signal is more rapidly attenuated and typically only penetrates to approximately 400-500m. The 75kHz lacks such good vertical resolution but penetrates to approximately 800-1000m.

14.2. Real Time Data Acquisition

The data from the two instruments were acquired using the RD Instruments VmDas software package version 1.42. This software is installed on two PCs in the main laboratory, which control the 75kHz and 150kHz Ocean Surveyor instruments respectively. The software allows data acquisition in a number of configurable formats and performs preliminary screening and transformation of the data from beam to Earth coordinates.

In order to collect data in VmDas:

- Open VmDas from the Start Menu and click on “Collect Data” in the File Menu.
- Under Options, click “Edit Data Options” and then set the configurable parameters to the values outlined in the JC029 cruise report (Section 9.3.2). Under the ADCP setup tab, specify the relevant control file. It is important each time the ADCP is restarted to increase the number in the recording tab by 1; otherwise VmDas may overwrite previously written files.
- Recording commences by clicking the blue record button in the top left of the screen.
- Collection stops by pressing the blue stop recording button in the top left of the screen. Data collection was typically stopped and restarted with a new file number everyday during the cruise. Leaving it on the same file for too long

allows the files to become too large and post-processing in CODAS becomes slow.

14.2.1. Files Produced by VmDas

The files we produced have names of the form *os<inst>_di346<nnn>_<filenumber>.<ext>*, where *<inst>* is the instrument name (75 or 150), *<nnn>* is the file sequence number, *<filenumber>* is the number of the file in the sequence and *<ext>* is the extension. We set a new *<filenumber>* to occur every time a file size of 10Mb was reached. This was helpful, because it meant that if problems were encountered in the data processing, they were more likely to be contained within a single file number. If more than one file number was affected, then they could quite easily be processed together because of the same file sequence number.

The list of files produced is given below:

- .ENR files are the binary raw data files.
- .ENS files are binary ADCP data after being screened for RSSI and correlation and with navigation data included.
- .ENX files are ADCP single ping data and navigation data after having been bin-mapped, transformed to Earth coordinates and screened for error velocity and false targets.
- .STA files are binary files of short-term average ADCP data (**120s,** user-specified in VmDas).
- .LTA files are binary files of long-term average ADCP data (**600s**, user-specified in VmDas).
- .N1R files are ASCII text files of raw NMEA navigation data from the NMEA1 stream.
- .N2R files are ASCII text files of raw NMEA navigation data from the NMEA2 stream.
- .NMS files are binary files of navigation data after screening.
- .VMO files are ASCII text files specifying the option settings used for the data collection.
- .LOG files are ASCII text files logging all output and error messages.

These files were stored in the following directories:

/ADCP150/di346 (for 150kHz transducer data)
/ADCP75/di346 (for 75kHz transducer data)

14.2.2. Real Time Data Monitoring

The ‘R’, ‘S’ and ‘L’ tabs on the VmDas menu bar allow you to swap between graphical output from the .ENR, .STA and .LTA files. When in ‘R’ mode, the default upper left hand display in VmDas is the raw velocity parallel to each beam, but this can be difficult to interpret as it is shown in beam coordinates. A more useful plot can be made in either the ‘S’ or the ‘L’ mode, displaying the current at a specified depth level as a stick plot in Earth coordinates. To produce these plots, ensure ‘Ship

Track 1' and/or 'Ship Track 2' is ticked in the Chart menu. The bins used in the stick plot are specified within "Options", "Edit Display Options".

The data can also be inspected in real-time using the WinADCP software, which loads the .ENX, .STA or .LTA files and displays the output as contour plots. The Monitor Option should be switched on with a suitable time interval (120s), meaning the contour plot is regularly updated. Plots of *u* and *v* were routinely examined throughout the cruise to check the data stream and to inform the bridge of ADCP measurements as required on station.

Several other things were also regularly checked whilst the ADCPs were recording:

- We made sure the ensemble number in the real time display of VmDas was increasing during the 4 hourly watchkeeping log. Inspection of the navigation input to VmDas was identified as a necessary watchkeeping task after a 6-hour dropout of navigation data was noticed.
- We ensured that records of the files created are kept up-to-date.
- The .LOG file records any problems such as timeouts and navigation problems and was occasionally inspected.

14.2.3. Alignment

Zero offset for both sensors.

14.2.4. General Settings

During D346, we ran both instruments in narrowband single-ping mode. Where depth permitted, for the first few days of the cruise, we ran both instruments in bottom track mode to obtain the most accurate phase and amplitude calibrations. Typically, the instruments were switched between bottom tracking and water tracking close to 900m. A table of the bottom track phase and amplitude calibrations is given below.

Table 16: Bottom track calibration data for the OS75 instrument. The 'after tvrot' line is after applying the time-varying gyro minus ashtech correction. The 'final' line are data from the end of the cruise after applying the accepted adjustment of -2.88 for phase and 1.002 for amplitude.

File		Amplitude (median)	Amplitude (mean)	Amplitude (STD)	Phase (median)	Phase (mean)	Phase (STD)
di346005nbenx	Raw	1.0041	1.0034	0.0033	-4.1898	-4.1315	0.2493
	After tvrot	1.004	1.0032	0.0033	-2.8165	-2.8324	0.0733
di346006nbenx	Raw	1.0013	1.0015	0.0058	-2.6168	-2.7867	0.7168
	After tvrot	1.0012	1.0015	0.0053	-2.8837	-2.8806	0.2879
di346007nbenx	Raw	1.002	1.002	0.0037	-3.3616	-2.8444	1.5419
	After tvrot	1.0022	1.0021	0.26	-2.9398	-2.9308	0.244
di346008nbenx	Raw	1.0024	1.0027	0.0052	-3.6556	-3.8943	1.15
	After tvrot	1.0025	1.0024	0.0043	-2.8895	-2.9247	0.3157
di346009nbenx	Raw	1.005	1.0049	0.0021	-2.3513	-2.3066	0.7591
	After tvrot	1.0052	1.0049	0.0022	-2.8465	-2.8527	0.1366
di346050nbenx	Final	1.002	1.002	0.0021	0.0507	0.0768	0.2202

Table 17: Bottom track calibration data for the OS150 instrument. As table 16, but the accepted adjustments are -1.58 for phase and 1.005 for amplitude.

File		Amplitude (median)	Amplitude (mean)	Amplitude (STD)	Phase (median)	Phase (mean)	Phase (STD)
di346003nbenx	Raw	-	-	-	-	-	-
	After tvrot	-	-	-	-	-	-
di346004nbenx	Raw	1.0057	1.0038	0.0191	-1.215	-1.1278	1.4118
	After tvrot	1.0057	1.0021	0.0174	-1.6046	-1.5549	1.2753
di346005nbenx	Raw	1.0064	1.0059	0.0088	-1.965	-3.0424	4.8463
	After tvrot	1.0063	1.0062	0.0084	-1.6267	-2.7597	3.4155
di346006nbenx	Raw	1.0051	1.005	0.0031	-2.58	-2.5249	1.0367
	After tvrot	1.005	1.0051	0.0033	-1.5638	-1.5549	0.2815
di346007nbenx	Raw	NaN	NaN	NaN	NaN	NaN	NaN
	After tvrot	NaN	NaN	NaN	NaN	NaN	NaN
di346048nbenx	Final	1.001	1.0014	0.0028	-0.0079	0.0018	0.1504

The number of bins and the bin sizes on both instruments differed. On the OS75, 65 bins were used, with a bin size of 16m and for the OS150, 65 bins were used at a size of 8m. A blanking distance of 8 m was used for the OS75 and 6m for the OS150, in order to avoid ringing from the transmit pulse. Using the VmDas options the instruments were switched between bottom track and water track mode on decimal day 009 when the sea floor was out of range of bottom tracking. However, as can be seen in Table 17, file di346007nbenx on the OS150 does not contain any bottom track calibrations, because the seafloor was already out of range for this instrument. The means of the amplitude and phase values in each of the respective tables were used in the control files of each of the respective instruments.

Table 18: Water track calibration data for the OS75 instrument

File	Amplitude (median)	Amplitude (mean)	Amplitude (STD)	Phase (median)	Phase (mean)	Phase (STD)
di346010nbenx	1.001	1.001	0.0057	-3.1705	-3.1705	0.0969
di346011nbenx	1.007	1.0077	0.005	-2.485	-2.7927	0.5723
di346012nbenx	0.9995	1.0018	0.008	-2.6375	-2.7057	0.3126
di346013nbenx	0.9985	1.0001	0.0049	-2.9185	-2.9157	0.2907
di346014nbenx	1.003	1.0024	0.0036	0.001	0.0056	0.2453
di346015nbenx	1.0025	1.0015	0.004	-2.936	-2.9075	0.3469
di346016nbenx	1.004	1.0034	0.0055	-3.122	-3.1313	0.601
di346017nbenx	1.003	1.0013	0.0062	-2.842	-2.8988	0.3792
di346018nbenx	1.008	1.0068	0.0055	-2.6775	-2.823	0.4323
di346019nbenx	1.0015	0.9972	0.0132	-2.9095	-2.9732	0.7464
di346020nbenx	0.9995	0.9992	0.0064	-2.7945	-2.857	0.2657
di346025nbenx	1.001	1.0067	0.0136	-2.42	-2.011	1.1285
di346030nbenx	0.996	0.9946	0.0074	-0.092	0.0316	0.299
di346035nbenx	1.001	1.0018	0.0026	-2.8	-2.854	0.4182
di346040nbenx	0.998	0.998	0.0029	-0.165	-0.213	0.18
di346045nbenx	1.001	1.002	0.0093	0.146	0.2154	0.5141

Table 19: Water track calibration data for the OS150 instrument

File	Amplitude (median)	Amplitude (mean)	Amplitude (STD)	Phase (median)	Phase (mean)	Phase (STD)
di346010nbenx	1.002	1.0064	0.0145	-1.7625	-1.6661	0.5482
di346011nbenx	1.0025	1.0017	0.0044	-1.553	-1.6243	0.5724
di346012nbenx	1.007	1.0072	0.0067	-1.6725	-1.7828	0.5053
di346013nbenx	1.004	1.0045	0.0056	-1.738	-1.8077	0.544
di346014nbenx	1.007	1.0063	0.0071	-1.633	-2.0193	0.9957
di346015nbenx	1.01	1.0055	0.0098	-1.5875	-1.6335	0.2401
di346016nbenx	1.003	1.0046	0.0072	-1.3	-1.3826	0.2153
di346017nbenx	1.0055	1.0045	0.008	-1.802	-1.507	1.4555
di346018nbenx	0.996	0.9982	0.0053	-1.691	-1.6452	0.604
di346019nbenx	1.0045	1.0032	0.0034	-1.5385	-1.4968	0.2499
di346020nbenx	1.0035	1.0035	0.0034	-1.52	-1.471	0.3949
di346025nbenx	1.0045	1.0055	0.0048	-1.7605	-1.8502	0.6372
di346030nbenx	0.997	0.998	0.0058	-0.054	0.1974	0.4708
di346035nbenx	1.006	1.0047	0.0072	-1.3195	-1.3815	0.4863
di346040nbenx	1.001	0.9972	0.0066	-1.837	-1.7614	0.2914
di346045nbenx	1.001	0.9998	0.0069	0.261	0.1977	0.4863

14.2.6. Sound Speed Considerations

Measurements of *x* and *y* velocities are independent of the speed of sound for phased array ADCP instruments such as those used on D346. If the speed of sound changes in the vertical water column or in front of the transducer, the angle of the beam will consequently change. This change in beam angle change occurs in the same ratio as the Doppler shift equation, meaning that a change in the Doppler frequency shift of a particle moving parallel to the face is compensated entirely by the corresponding beam angle shift, cancelling out the change in the speed of sound. For a more in-depth account of speed of sound considerations when using ADCP units please refer to JC032 cruise report *(King et al., 2010)*.

14.3. Post-Processing

The final processing of the data was done using the CODAS (Common Ocean Data Access System) suite of software provided by the University of Hawaii. This suite of Unix and Matlab programs allows manual inspection and editing of bad profiles and provides best estimates of the required rotation of the data, either from water profiling or bottom tracking.

14.3.1. Transferring the Data

CODAS was run on the *NOSEA1* terminal, so the raw data files had to be copied over from the ADCP PCs. The raw data were moved into either the */vmadcp/di346_os75/rawdata* directory or the */vmadcp/di346_os150/rawdata* directory, depending on the instrument.

14.3.2. Setting Up the Directories and Using quick_adcp

Once loaded into the *rawdata* directory, the following steps were followed:

1. *movescript* was typed in the Unix command window. This creates a new directory called *rawdata<nnn>* (*nnn* denoting the file sequence) and moves the relevant data to this new location.

2. The command *adcptree.py di346<nnn>nbenx --datatype enx* was typed at the command window. This command sets up a directory tree for the CODAS dataset and an extensive collection of configuration files, text files and m files.

3. The directory was then changed to *di346<nnn>nbenx* using the *cd* command, and the control files *q_py.cnt*, *q_pyedit.cnt q_pytvrot.cnt* and *q_pyrot.cnt* were copied into that directory. We then used the command: '*quick_adcp.py --cntfile q_py.cnt',* which loads the data into the directory tree, performs routine editing and processing and makes estimates of both water track and (if available) bottom track calibrations. The raw ping files are also averaged into 5-minute periods. The calibration values are stored in the *adcpcal.out* and *btcaluv.out* files found in the *cal/watertrk* and *cal/botmtrk* directory respectively and are appended each time *quick_adcp.py* is run.

4. The files were usually left at this point of the processing for at least a day until the navigation processing had been completed for the appropriate period.

14.3.3. Calibration

The *quick_adcp.py* script estimates amplitude and phase corrections for each set of data. It is only by specifying a calibrated rotation in the *q_pyrot.cnt* file that accurate velocities could be obtained.

The best calibration estimates are obtained when the velocity data is collected using the seabed as a reference. However, bottom track calibration estimates are only obtainable when the water depth is within the ADCP profiling range. Bottom tracking was performed at the beginning of the section in the Bahamas from Julian day 006-009, and again when we reached the continental shelf of Morocco. The reason for running the ADCPs in bottom tracking mode at the end of the main section was to verify that the rotations applied to the data through the section had not changed since the first bottom tracking measurements obtained in the Bahamas. A table of the bottom tracking calibrations was created to calculate mean phase and amplitude of the instruments, which were then used as the rotation values in the *q_pyrot.cnt* control file. As can be seen from Tables 16 and 17 the final calibration check (highlighted in yellow) shows very little difference from the original rotations applied to the data and is well within acceptable limits (i.e. a tenth of a degree). The calibrations given were as follows: OS75 rotation angle = -2.88, amplitude = 1.002; OS150 rotation angle = -1.58, amplitude = 1.005.

Comparison with the water track rotations shows close similarity with the bottom track calibrations (Table 18 and 19). Here are the following means calculated from the water track data: OS75 rotation angle = -2.1194 amplitude = 1.0015; OS150 rotation angle = -1.4107, amplitude = 1.0032. The numbers are not identical, but this was not expected.

14.3.4. Applying the Rotation

Applying the rotations to the data required several different steps. Initially a heading correction file was created in Matlab by typing *m_setup* and running the script *make_g_minus_a(<os>,<nnn>)* in order to subtract the Ashtech heading from that of the shipboard gyro.

Back in Unix, the processing continued in the *cal/rotate* directory where the *rotate.tmp* file was edited using *vi* in order to provide the appropriate time angle file for data which was created in the previous processing step. To apply the rotation to the database the following command was typed; *rotate rotate.tmp*.

Using *quick_adcp.py --cntfile q_pytvrot.cnt* the time dependant heading correction was then run.

The final calibrations discussed above were applied to each file sequence using *quick_adcp.py --cntfile q_pyrot.cnt* in the *di346<nnn>nbenx* directory in the Unix terminal window. This rotates the data by the phase and amplitude specified by the

user in the control file *q_pyrot.cnt*. A recalculated calibration (after taking the first calibration into account) is printed to the **.out* file(s). The data were then checked in Gautoedit to ensure that any vertical striping associated with on/off station differences had been removed by application of the calibration. Any alterations that needed to be made to the files, for example due to bad profiles or bad bins were edited using Gautoedit.

14.3.5. Gautoedit

The Gautoedit package within CODAS allows the user to review closely the data collected by VmDas and flag any data that is deemed to be bad. These flags can then be passed forward and, using the *q_pyedit.cnt* control file, the data removed. Typically, the data were reviewed as follows:

1. Matlab was opened in the *di346<nnn>nbenx/edit* directory (for the portion of data we wished to process). In the command window, typing:

m_setup; codaspaths; gautoedit

An editing GUI, shown in Figure 52. The editing was done from here.

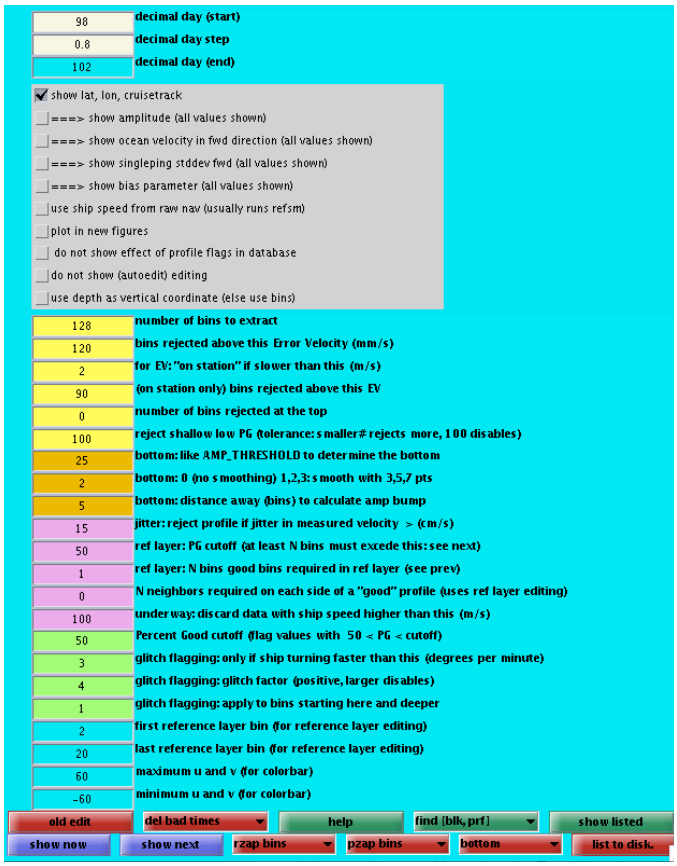

Figure 52: The Gautoedit window within the CODAS suite of programs in Matlab

2. Gautoedit was initially used after the first *quick_adcp.py* step to observe whether the ENX files had processed correctly. The start time of the ENX file was entered in the *decimal day (start)* box and the length of the dataset (in days) was entered in the *decimal day step* box. Upon pressing *Show Now*, two plots are displayed according to the default plot selections. One contains four subplots: the first displays the absolute east-west (U) velocity component, the second shows the absolute north-south (V) component, the third shows the percentage good parameter and the fourth shows the ship speed (in m/s) and an editing parameter called jitter. The second figure contains subplots of the ships' track and mean absolute velocity vectors at the reference layer. However, it was noted that throughout the duration of the cruise there was bug within this part of the software, as when show now was clicked, Gautoedit crashed during the plotting of the ships' track and velocity vectors. This did not present a problem to the processing because simply pressing show now once more succeeded in plotting the vectors. An error command will appear if there are no data in the selected time range. This initial review of the data allows the user to confirm the direction of steaming, identify the position of on-station and off-station parts of the file and spot any areas with low percentage good. It is also useful to identify the maximum and minimum values of *u* and *v* to allow a suitable colour bar to be used when examining the data more closely (by default -60 to +60 is used). To change this, use the *maximum u* and *v* and *minimum u* and *v* boxes.

3. To inspect the data more closely and to start applying edits, the data must be inspected in shorter time sections. Typically, we worked from the start of the data in 0.3 day portions as this allowed us to see the individual 5-minute bins. Once the edits were finished on one portion, the *List to Disk* option was selected to save the flags before using *Show Next* to advance onto the next 0.3 day section.

Routine editing for each section included:

- looking for bad profiles (i.e. those in which the *u* and/or *v* had a systematic offset over all depth levels). These were flagged using the *del bad times* command and choosing the select time range option.
- looking for bad levels. This is common at the bottom of profiles where the amplitude return is small and the profiles commonly have a low percentage good. These bad 'tails' are removed most easily using the *pzap bins* command, which allows the user to flag all data within a defined polygon.
- looking at the jitter parameter in the bottom subplot. A high level of jitter either indicates noise in the navigation and/or rapidly changing velocities. Generally, the default jitter threshold (set in the *Jitter: reject profile if jitter in measured velocity*) of 15cm/s seemed to be a reasonable value for flagging potentially bad profiles and did not need to be changed.

4. In particular, the presence of either enhanced scattering layers in the profiles or bubbles directly beneath the ship are known to bias the underway velocities in the affected layers in the direction of steaming**.** These biases are discussed further in Section 14.4.

- In an enhanced scattering layer (e.g. due to zooplankton) the bias parameter tends to have positive (red) values towards the top of the layer (as the anomaly increases with depth) and negative values below (as the anomaly decreases), though the sizes of these anomalies need not be symmetric. On station the parameter, by definition, has a value of zero. Positive values in the top two or three bins often indicate bias due to bubbles. The bias parameter is therefore a useful tool that can be used as a guide for identifying potential areas of velocity bias.
- If particularly bad bias in the along-track velocities on steaming sections could be found, the bad bins were flagged using *pzap bins*.

However, in both cases it was deemed unhelpful to remove these areas of data because the editing steps would remove the data in both the U and V components for the corresponding bins. We were unwilling to remove perfectly good data from one component just to remove potentially bad bins in the other component that spanned virtually the entire length of the dataset. Therefore, the scattering layers were left in.

5. Once satisfied with the changes made, the *List to Disk* option is selected which creates and updates *a*.asc* files in the *di346<nnn>nbenx/edit* directory.

14.3.6. Applying the Edits

Once the *a*.asc* files have been created, the edits are applied using the following command at the Unix terminal prompt from within the *di346<nnn>nbenx* directory:

quick_adcp.py –cntfile q_pyedit.cnt

The *q_pyedit.cnt* file has to have the correct *instname* command line (i.e. OS75 or OS150).

14.3.7. Creating the Output Files

Once the editing and rotations were completed, the final velocities were collated into Mstar files (*.nc) using the following commands in the *di346<nnn>nbenx* directory of a Matlab command window:

m_setup
mcod_01
mcod_02
(type the file number and instrument number when prompted to specify the input file).

The first command sets up the Mstar suite of programs and the relevant paths. The other two commands load in the final data for the file sequence and save it as two Mstar files. The first command produces a file of the form *os75_di346<nnn>nnx.nc* that includes the following variables:

- time - (in seconds since [2010 1 1 0 0 0])
- lon - (0 to 360)
- lat - (-90 to 90)
- depth - (of bin)
- uabs - (absolute *u* velocity in cm/s)
- vabs - (absolute *v* velocity in cm/s)
- uship - (*u* velocity of ship over ground)
- vship - (*v* velocity of ship over ground)
- decday - (decimal day of year)

The second file is of the form *os75_di346<nnn>nnx.nc* and includes, (in addition to the above variables):

- speed - (scalar water speed in cm/s)
- shipspd - (scalar ship speed over ground in cm/s).

The individual *os75_di346<nnn>nnx.nc* and *os150_di346<nnn>nnx.nc* files are then appended together into a single output file for the cruise using a script called *mcod_mapend*. This command relies on an input file containing the paths of all the individual files to be merged. These are to be found in the */di346_os75* and */di346_os150* directories and are named *nc_files*. This needed to be edited a number of times due to the bottle blank stations undertaken for the CFC team which were designated with file numbers 200 and 202. The reason this needed to be altered is because otherwise the files would have been appended in numerical order, which would have not placed them in the correct position in the appended file. The final output files are *os75_di346nnx_01.nc* and *os150_di346nnx_01.nc* which contain appended on-station and underway data.

In order to compare the vessel-mounted ADCP velocities on station with those derived from the lowered ADCP, the command *mcod_03* was run using the appended file as the input. A simple loop was usually written in the Matlab command window to automate this process. The *mcod_03* routine relies on an input file *stations.dat*, which contains the start and end times (in seconds since start of year) for each station. Usually when the mcod_03 step would not run, it meant that the *stations.m* file needed to be run again to update the *station.dat* file.

The output files from *mcod_03* contain individual on-station data of the form *os75_di346nnx_stn<nnn>.nc* where *<nnn>* denotes the station number.

Individual steaming sections (i.e. between two on-station sections) were created in a similar manner using the *mcod_04* script. The files created from this step were named accordingly, e.g. *os75_di346nnx_stn<nnn>_to_stn<nnn>.nc.*

Finally, the underway files created in mcod_04 were appended together with the *mcod_mapend_uway* script. This took the individual steaming sections listed in the input file *uway_nc_files* and appended them together to create the file *os75_di346nnx_uway_01.nc*.

14.4. Data Quality Issues

Whilst carrying out *Gautoedit* editing, several quality control issues were identified that warrant discussion.

14.4.1. Bubble Contamination and Bias

Two potential issues arise from the presence of bubbles immediately below the transducer face. Bubbles can prevent penetration of the transmit pulse and lead to truncated or bad quality profiles. This was not widely observed on cruise D346. It is also known that the high amplitude return from bubbles can cause anomalous velocities in the direction of ship steaming (i.e. towards the east on the main 24°N section). It is commonly identified by a relatively low percentage good in the top few bins, and a red surface stripe in the along-track bias parameter. It typically does not affect lower bins of the profile, which remain good.

There were relatively few incidences of bubble bias encountered on cruise D346 significant enough to warrant editing of the data. Figure 53 however, does show an incidence when it is thought that bubble bias may have been responsible for spurious high surface velocities. *Fischer et al, (2003)* relate an increase in bubble formation with increased inclement weather conditions, however this does depend on the location of the transducer on the ships' hull, as some areas may be more prone to bubble formation than others.

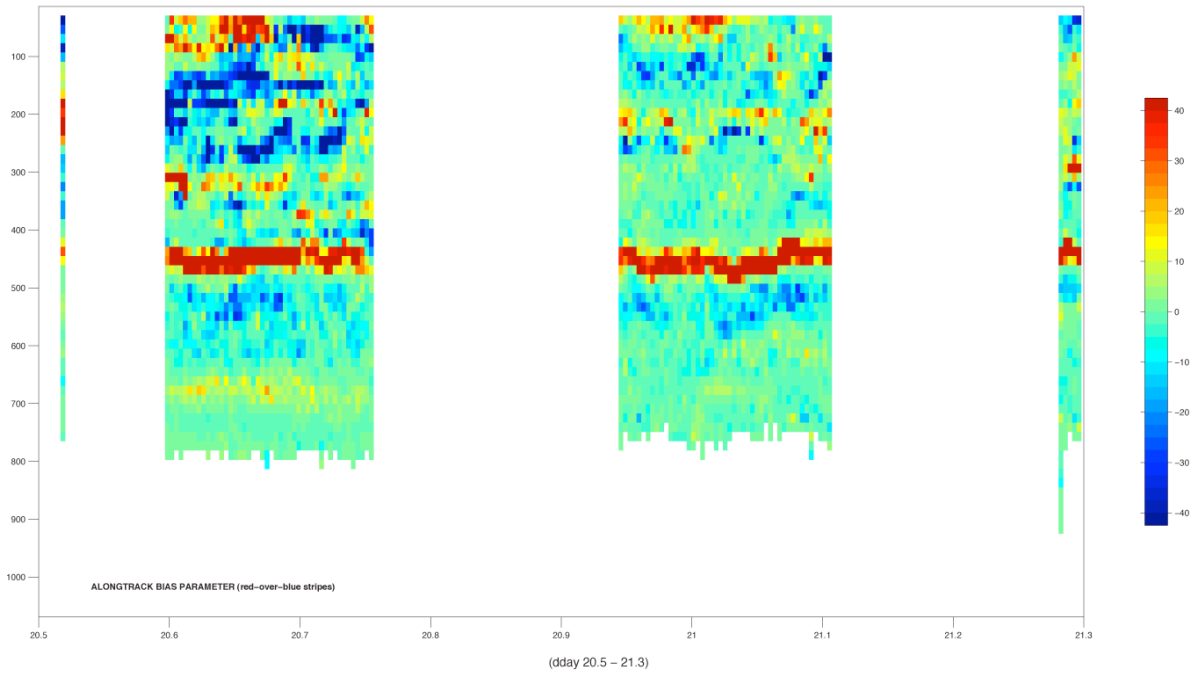

Figure 53: Example of scattering near the surface due to bubble contamination (approx. dday 20.65)

14.4.2. Anomalous Scattering Bias

A more extensive feature was the presence of anomalous scattering layers leading to along-track velocity bias. The presence of scatterers such as zooplankton in the water can cause severe bias in the direction of travel whilst the ship is steaming. This is observed as horizontal stripes in the velocity field, which disappear when the vessel is on station. If the layers are very strong, a layer of negative bias will also appear immediately below the scattering layer. Such features have been observed on previous subtropical cruises, such as Cruise 324 on *RRS Discovery* and Cruise JC032 on *RRS James Cook*.

On this cruise, a large anomalous scattering layer was found on the OS75 instrument between 460-660 metres across much of the section (see Figure 54; evidence of this scattering layer is also present in Figures 53 and 55). In Figure 53 this feature resulted in extensive red-over-blue striping in the along track bias parameter. The affected bins were not removed within Gautoedit because this would have also removed perfectly good data from the cross track parameter, which was deemed to be unwarranted. For much of D346, there was no obvious evidence for a diurnal cycle in the depth of this layer, as is commonly found in zooplankton layers. However, close examination of some days show an enhanced amplitude layer moving downwards during the day, before returning to its original level in the evening.

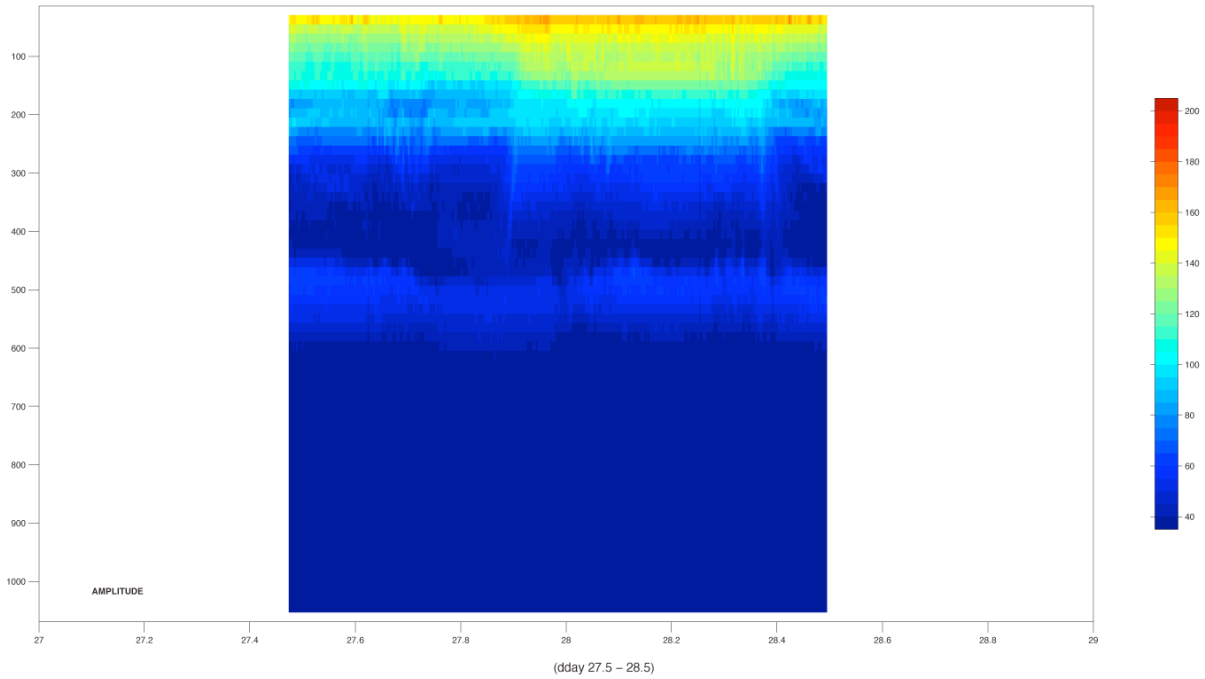

Figure 54: Example of the amplitude return for the OS75 instrument. The anomalously high scattering layer can be seen close to 500 metres.

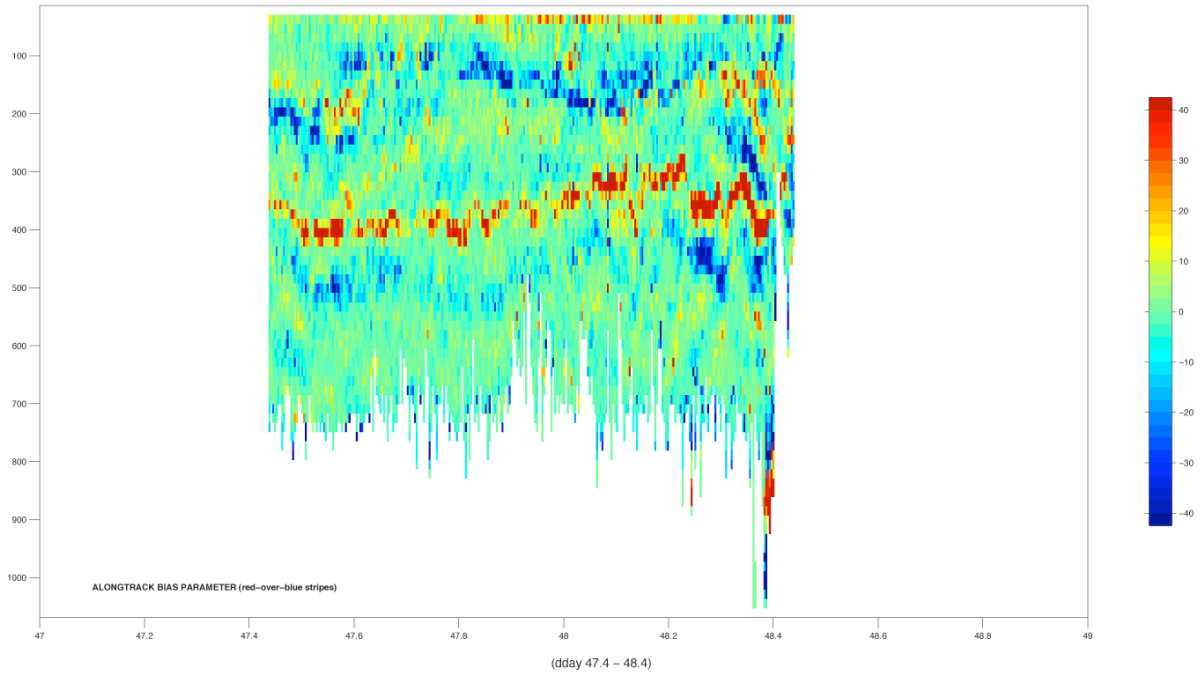

Figure 55: Note the strong red-over-blue striping during the steaming periods at a similar depth to the anomalous scattering layer. Note also the enhanced near-surface amplitude returns, most likely the result of bubbles below the ship.

Strong scattering layers are seen less frequently with the OS150. This is most likely because the beam does not penetrate as deeply as the OS75.

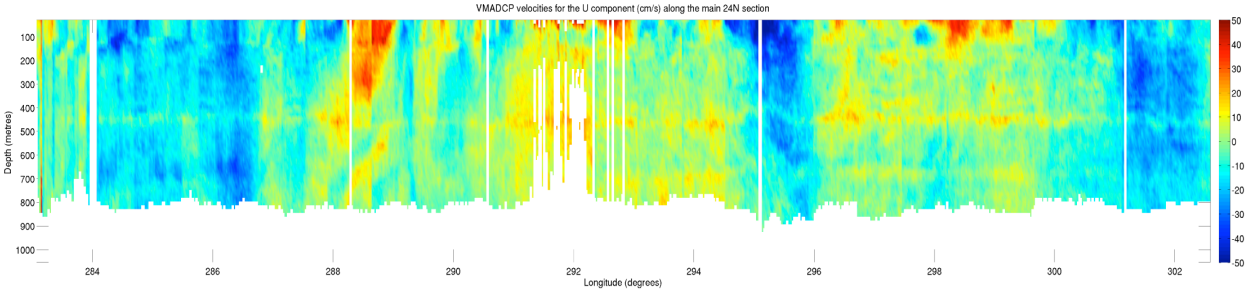

Figure 56: U component for the 24°N section. A strong scattering layer can be identified at approximately 500 metres, most likely a continuous zooplankton layer produces this feature.

14.4.3. Other Issues

A further departure from routine processing was the result of a failure in the input of the navigation data to the raw ENX files.

It was noticed from the CTD display that the navigation had dropped out. The problem was investigated and traced to a plug that had fallen out of a splitter box in the computer room. Paul Duncan fixed this problem, and as a result it was realised that the navigation was also not being fed to VmDas for the shipboard Dopplers. This meant that no headings for the data were available. The problem was found to have begun at 23:15 on Julian Day 028. The navigation data was still logged in the TECHSAS system however, so Brian King wrote a script entitled *fix_nav.m* to rescue

the navigation data and apply it to the VMADCP data using the ENS files instead of the ENX files.

On Julian day 28 the navigation source was switched over from the GPS4000 to the GPSG12 at approximately 23:20, and at approximately 23:30 the differential input for the GPS4000 was switched off. However, upon attempting to process the ENX files after this period it was found that there was no heading data in the files. Brian King was also responsible for fixing this problem, creating repaired raw data directories called *rawdata<nnn>_fixhead*. The following files were affected 026-029 for the OS150 and 029-032 for the OS75. This covers a period from approximately 23:20 on Julian day 028 until 14:54 on Julian day 030. At this point Paul Duncan switched the navigation input back to the GPS4000. Initially no NMEA1 messages were received and then it was realised that the baud rate needed changing back. The files for the OS75 and OS150 where thus started at ensemble 1414 (14:58) and ensemble 159 (15:00) respectively.

The affected files were processed using the ENS files, which meant that certain steps of the processing had to be altered. The control file *q_py.cnt* has to be altered to support ENS files instead of ENX files and the appropriate raw data directory selected (i.e. *rawdata<nnn>_fixhead*). Also it was necessary to add the line '*-- ens_halign 0*'. The *make_g_minus_a(<os>,<nnn>)* and *mcod_01* and *mod_02* files were also edited to accommodate the ENS files (i.e. *make_g_minus_a_ens(<os>,<nnn>), mcod_01_ens, mcod_02_ens*). To allow the *mcod_mapend* step to work properly, a symbolic link to the respective directory *di346<nnn>nbens* was created to parse the data through *di346<nnn>nbenx*. These data from these files were then available to be viewed, edited and appended just like any other ENX file.

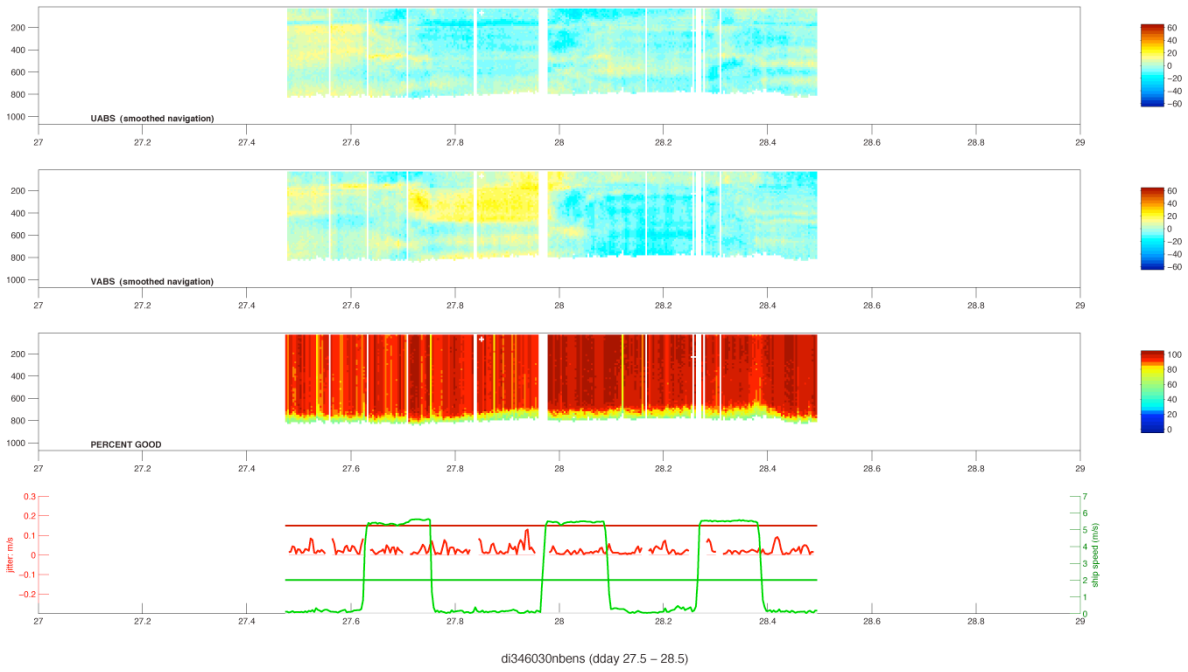

Figure 57: Here is an example of VMADCP data processed using ENS files instead of the ENX files

As a test, file 26 was processed using good ENX data and the repaired (heading added) ENS data and the velocities were then compared. They were found to be synchronous with differences in the standard deviation of ~0.01-0.02cm/s which is considered to be sufficiently good.

Due to a discrepancy between the PC clock and UTC time some files contained segments that would not process properly. CODAS keeps track of the offset between the time on the PC acquiring data and UTC in navigation messages. (The individual ensembles are timestamped with PC time, but if navigation messages are available with UTC then the offset is recorded within the ENX files). Each ENX file is processed using a single clock offset, because this is expected to vary slowly. Data from each ENX file are reduced to 5-minute averages, with single pings (at intervals of a few seconds) unused at the end of each ENX file carried over to be processed with the next ENX file. If the PC minus UTC clock offset has changed sufficiently between ENX files, this can create a backwards time jump between carried-over pings and the first ping in the next file. This causes quick_adcp.py to fail. The PC minus UTC clock difference varied in the range +/- 120 seconds. The solution is to process troublesome ENX files individually, rather than as a batch. It was found that once the individual ENX file was separated into its own *rawdata* directory (series 900 and following) and processed alone the processing ran smoothly and without problem. ENX files affected by this problem were recorded in a readme file in the OS75 and OS150 directories. Copies of these readme files can be found below in Table 20 and 21.

Another problem that was identified were anomalously high velocities found in the Florida Straits section. It was clear that these could not be true velocities so the data was investigated and it was realised in the end that the velocities were arising due to a doubling of the data. This occurred because of the existence of a bottom track directory that was created after the Florida Straits section in order to view the profile. Removing this directory, which was no longer needed, left only a single data source. Reprocessing this section of data after the removal of the redundant directory fixed the problem and yielded sensible velocities.

Table 20: OS75 filenames_readme

Directory number	ENX file numbers
701	os75_di346007_000001.ENX
900	All bottom track ENX files for OS75
901	os75_di346010_000001.ENX
902	os75_di346011_000002.ENX
903	os75_di346011_000004.ENX
904	os75_di346009_000001.ENX

Table 21: OS150 filesnames_readme

Directory Number	ENX File Numbers
901	os150_di346009_000000.ENX
902	os150_di346009_000001.ENX
903	os150_di346009_000002.ENX
904	os150_di346009_000003.ENX
905	os150_di346009_000004.ENX
906	os150_di346009_000005.ENX
907	os150_di346009_000006.ENX
910	os150_di346023_000001.ENX
911	os150_di346023_000003.ENX
912	os150_di346024_000002.ENX
913	os150_di346038_000001.ENX
914	os150_di346038_000003.ENX
915	os150_di346039_000001.ENX

On a couple of occasions along the 24°N transect, features such as those seen in Figure 58 were identified. This is a cold core eddy. This was better defined using the OS75 due to the greater range of the instrument. Eddies born from the Gulf Stream as it travels northwards can have warm or cold cores. These can also be identified by observing satellite images of sea surface temperature. The eddy identified in Figure 58 is rotating in an anticlockwise direction, which means that it has a cold core. Eddies usually retain properties that differ from those of the surrounding water mass. For example the occurrence of this feature coincided with a drop in the surface mixed layer and surface layer salinity.

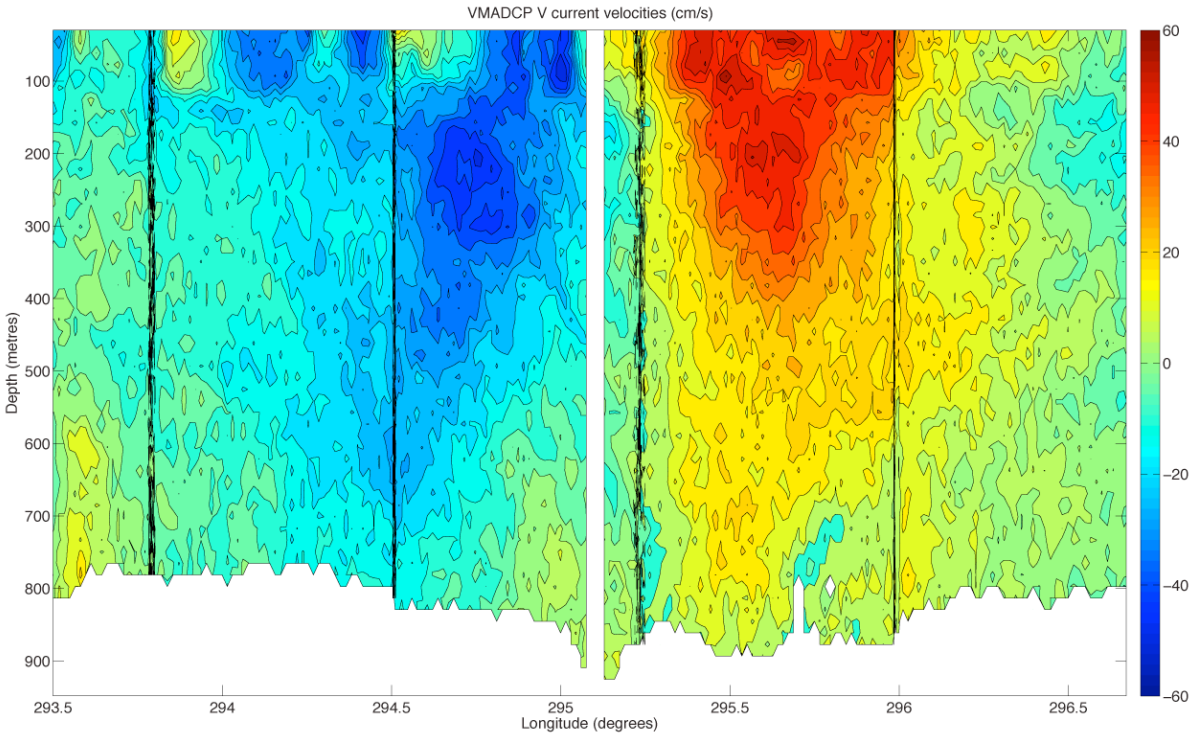

Figure 58: A cold core eddy identified using the OS75 VMADCP instrument.

Another interesting feature was revealed earlier in the cruise as a result of our passage across the Florida Straits. *RRS Discovery* performed two transects of the Florida Straits along the same latitude, which allowed us to collect sufficient data to produce profiles of the Gulf Stream. Figure 59 illustrates our first uninterrupted pass along the Florida Straits, whereas Figure 60 is created from the underway data of various durations appended together to compare the two sections. It is interesting to note the spatial changes in water transport velocity that occur over such a short timescale. The timescale between these figures is approximately 4-5 days maximum.

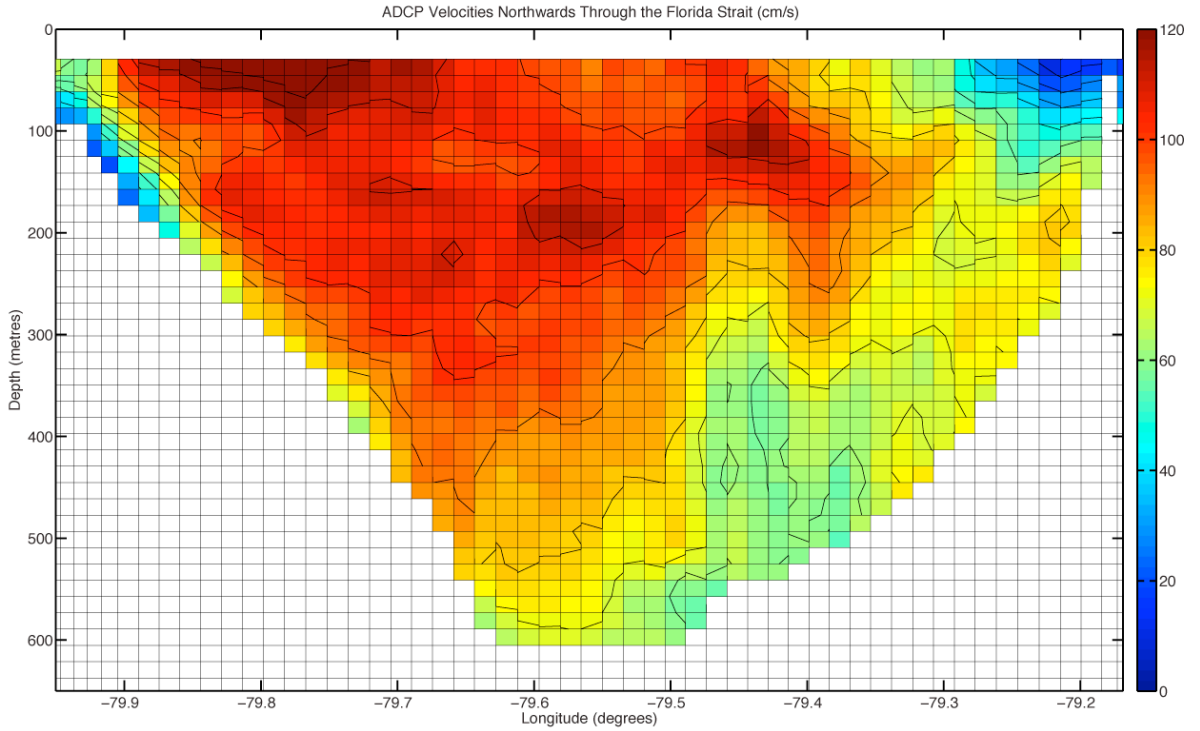

Figure 59: A profile of the first transect across the Florida Straits using data from the OS75 instrument

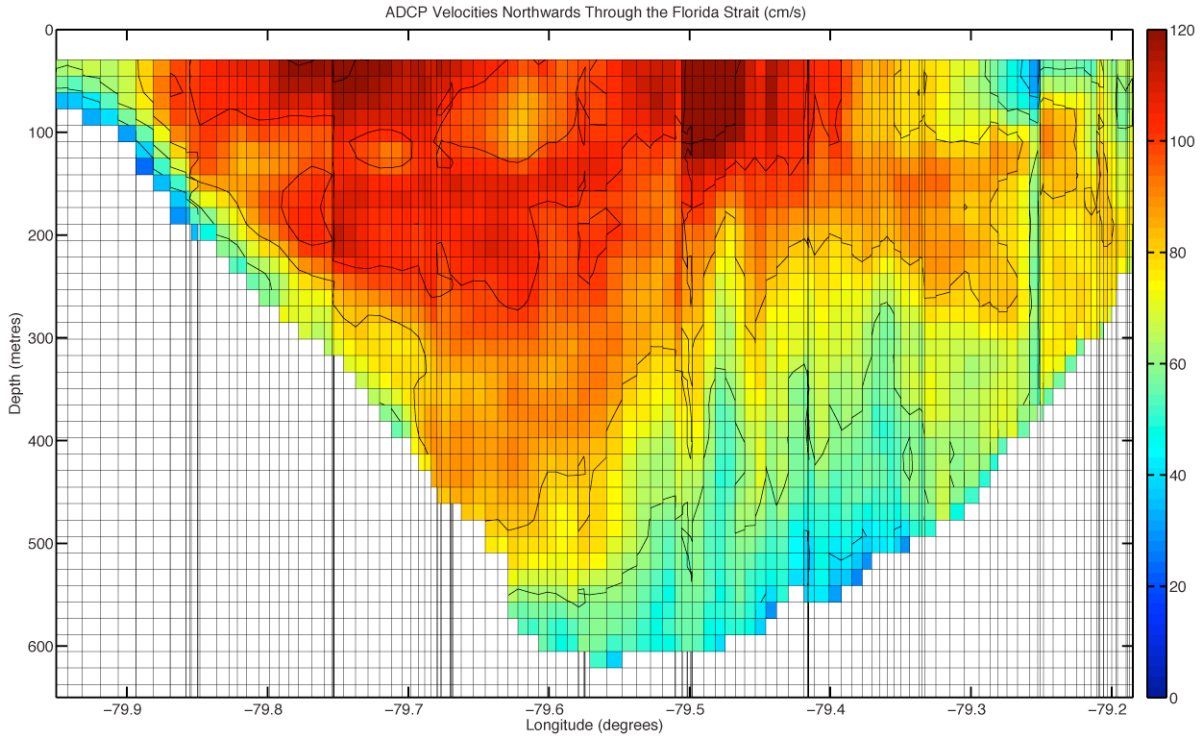

Figure 60: A profile of the return transect across the Florida Straits using data from the OS75 instrument

Table 22: The sequence log of the OS150 instrument.

ENX File Number	Start Date	Start Time	End Ensemble	End Date	End Time	BT/WT	Notes
1	6			6		In Port	In Port
2	6	05:36	2032	6	07:31	BT	Bad Gyro
3	6	07:31	1600	6	09:08	BT	Bad Gyro
4	6	09:09	12416	6	21:03	BT	
5	6	21:04	17175	7	13:03	BT	
6	7	13:03	27892	8	13:50	BT	
7	8	13:51	18355	9	05:16	BT	
8	9	05:17	57051	10	12:58	BT	
9	10	12:59	43648	11	13:14	WT	
10	11	13:14	43122	12	13:12	WT	
11	12	13:13	43549	13	13:24	WT	
12	13	13:24	43148	14	13:23	WT	
13	14	13:23	42735	15	13:08	WT	
14	15	13:09	722	16	13:15	WT	
15	16	13:16	40894	17	11:59	WT	
16	17	12:00	45262	18	13:08	WT	
17	18	13:09	47425	19	15:30	WT	
18	19	15:32	37014	20	12:04	WT	
19	20	12:05	43427	21	12:12	WT	
20	21	12:13	41955	22	11:31	WT	
21	22	11:33	42920	23	11:23	WT	
22	23	11:23	45000	24	12:24	WT	
23	24	12:24	43253	25	12:28	WT	
24	25	12:28	43270	26	12:31	WT	
25	26	12:31	41316	27	11:29	WT	
26	27	11:29	42861	28	11:18	WT	
27	28	11:18	44366	29	11:57	WT	GPSG12
28	29	11:58	45837	30	13:26	WT	

29	30	13:26	2621	30	14:54	WT	
30	30	14:54	36290	31	11:04	WT	GPS4000
31	31	11:05	41969	32	10:23	WT	
32	32	10:25	42391	33	09:57	WT	
33	33	09:59	43632	34	10:12	WT	
34	34	10:12	43950	35	10:38	WT	
35	35	10:39	43984	36	11:05	WT	
36	36	11:06	41518	37	10:09	WT	
37	37	10:10	42618	38	09:51	WT	
38	38	09:52	30930	38	01:19	WT	
39	39	01:21	16053	39	10:16	WT	
40	39	10:17	42028	40	09:38	WT	
41	40	09:39	42822	41	09:26	WT	
42	41	09:27	42600	42	09:07	WT	
43	42	09:08	43665	43	09:24	WT	
44	43	09:25	43737	44	09:43	WT	
45	44	09:43	42364	45	09:15	WT	
46	45	09:16	43343	46	09:21	WT	
47	46	09:21	8943	46	14:23	WT	
48	47	14:23	9206	46	22:54	BT	
49	46	22:54	24387	47	12:27	WT	
50	47	12:28	39279	48	10:17	WT	
51	48	10:18	43755	49	10:36	WT	
52	49	10:36	14227	49	18:31	WT	END

Table 23: The sequence log of the OS75 instrument

ENX File Number	Start Date	Start Time	End Ensemble	End Date	End Time	BT/WT	Notes
1	6		1062	6		In Port	In Port
2	6	05:36	343	6	06:03	BT	Bad Gyro
3	6	06:03	14	6	06:23	BT	Bad Gyro
4	6	06:23	949	6	07:34	BT	Bad Gyro
5	6	07:35	993	6	09:09	BT	
6	6	09:09	7527	6	21:00	BT	
7	6	21:02	11078	7	13:01	BT	
8	7	13:02	16603	8	13:46	BT	
9	8	13:47	5112	9	05:15	BT	
10	9	05:15	40091	10	12:57	WT	
11	10	12:57	30651	11	13:11	WT	
12	11	13:12	30319	12	13:09	WT	
13	12	13:10	30622	13	13:21	WT	
14	13	13:22	30348	14	13:20	WT	
15	14	13:20	30056	15	13:05	WT	
16	15	13:06	723	16	13:10	WT	
17	16	13:15	28759	17	11:58	WT	
18	17	11:59	31866	18	13:09	WT	
19	18	13:10	790	19	15:31	WT	
21	19	15:31	25960	20	12:04	WT	
22	20	12:06	30552	21	12:14	WT	
23	21	12:14	29504	22	11:33	WT	
24	22	11:33	30248	23	11:27	WT	
25	23	11:28	31606	24	12:26	WT	
26	24	12:27	30378	25	12:27	WT	
27	25	12:27	30390	26	12:28	WT	
28	26	12:28	29065	27	11:27	WT	
29	27	11:27	30156	28	11:17	WT	
30	28	11:17	31195	29	11:56	WT	GPSG12
31	29	11:57	32197	30	13:22	WT	

32	30	13:23	1843	30	14:51	WT	
33	30	14:51	25568	31	11:03	WT	GPS4000
34	31	11:03	29610	32	10:27	WT	
35	32	10:28	29771	33	09:59	WT	
36	33	10:00	30683	34	10:14	WT	
37	34	10:14	30917	35	10:40	WT	
38	35	10:40	30929	36	11:06	WT	
39	36	11:07	29187	37	10:10	WT	
40	37	10:10	29967	38	09:51	WT	
41	38	09:53	30804	39	10:13	WT	
42	39	10:13	29556	40	09:34	WT	
43	40	09:35	30125	41	09:23	WT	
44	41	09:24	29973	42	09:05	WT	
45	42	09:05	30711	43	09:21	WT	
46	43	09:22	30766	44	09:40	WT	
47	44	09:40	29789	45	09:12	WT	
48	45	09:13	30565	46	09:22	WT	
49	46	09:23	8943	46	14:23	WT	
50	46	14:23	6222	46	22:55	BT	
51	46	22:55	17130	47	12:28	WT	
52	47	12:28	27613	48	10:18	WT	
53	48	10:18	30749	49	10:36	WT	
54	49	10:38	10005	49	18:32	WT	END

14.5. References

Fischer, J., P. Brandt, M. Dengler, M. Müller, and D. Symonds, (2003), Surveying the Upper Ocean with the Ocean Surveyor: A New Phased Array Doppler Current Profiler. *J. Atmos. Oceanic Technol.*, **20**, pp. 742–751.

McDonagh, E.L., et al, Hamersley, D.R.C. and McDonagh, E.L. (eds.) (2009), *RRS James Cook Cruise JC031, 03 Feb-03 Mar 2009. Hydrographic sections of Drake Passage.* Southampton, UK, National Oceanography Centre Southampton, 170pp. (National Oceanography Centre Southampton Cruise Report, 39)

David Hamersley

15. Iron, Nitrogen Fixation and Filtering

15.1. Background and cruise objectives

Cruise D346 provided the perfect opportunity to sample an area of specific interest to my PhD, the tropical North Atlantic, with respect to the influence of iron (Fe) on nitrogen fixation. Despite the vast abundance of molecular nitrogen (N_2) in the atmosphere, fixed sources of nitrogen (nitrates, nitrites, ammonia, etc) in the oceans can often be in short supply. This is related to the strong triple bond between the two atoms of N, which results in its relatively inert behaviour. This can induce a limitation on biological production as nitrogen provides the fundamental building blocks of life, including DNA. The tropical North Atlantic is an area known to exhibit high levels of nitrogen fixation and the project aims to investigate the role Fe has to play in this system.

Organisms that are able to biologically fix nitrogen are known as diazotrophs and the most commonly known are from the genus *Trichodesmium*. The enzyme responsible for this reaction is nitrogenase, which has a high Fe requirement. It is believed that the marine diazotrophs provide a significant proportion of fixed nitrogen to the oceans. The term heme (or haem) refers to the Fe-porphyrin complex that acts as the prosthetic group for a wide range of Fe proteins, also known as the hemoproteins. However, it should be noted that hemes are not directly involved in the nitrogenase enzyme. There are 3 specific heme structures commonly represented in biology: hemes *a*; *b*; and *c*. Heme *b* (also referred to as protoheme IX) is considered the most versatile form and is associated with globins, cytochrome P_{450}, catalases, peroxidases and *b*-type cytochromes (*Caughey (1973)*). Therefore, hemeoproteins and nitrogenase could potentially highlight the allocation of Fe within these nitrogen-fixing organisms.

It is undeniable that Fe plays a significant role in mediating phytoplankton blooms and, therefore, potentially influences carbon sequestration to the oceans. However, it has also been argued that the availability of nitrate (NO_3^-, classical 'biological' view) and/or phosphate (PO_4^{3-}, 'geochemical' view) could exclusively or co-limit biological growth and phytoplankton biomass (*Smith (1984), Codispoti (1989), Tyrrell (1999)*). In addition, it has been hypothesised that fluctuations in oceanic nitrogen concentration influence the atmospheric CO_2 concentration over large time scales (i.e. 10^4 years) (*McElroy (1983)*). Therefore, in addition to the obvious interest of CO_2 variation and climate change, it is interesting to note the significant relationship between Fe (including heme complexes) and the nitrogen cycle. It is hoped that results collected from the cruise will provide an insight regarding the allocation of Fe in the region, either to the photosynthetic apparatus (heme) or nitrogen fixation (nitrogenase).

15.2. Sampling and methods

Samples from the surface, chlorophyll maximum and one further 'near-surface' depth (usually between the surface and chlorophyll maximum) were collected from the CTD which were then filtered onto GF/F's for heme, chlorophyll and nitrogenase, as

well as POC using ashed-GF/F's. All filters were then stored in the -80°C freezer for analysis post-cruise. In addition, waters from surface and chlorophyll maximum depths were 'spiked' with $^{15}N_2$ and incubated at sea-surface temperature for 24 hours, before also being filtered onto ashed-GF/F's and dried in an oven at 50°C for a further 24 hours. All incubation filters were stored in a dry place for analysis post-cruise. In order to measure total Fe, a GOFLO was deployed once a day throughout the main section of the cruise to collect samples from 20m and 40m. Clean concentrated nitric acid was then added to the samples in preparation for analysis post-cruise.

15.2.1. Heme

Heme samples were taken from the CTD at three depths per station (surface, chlorophyll maximum and one further 'near-surface' depth). Up to 4000ml of seawater was filtered onto GF/F filters. Filters were then folded into eppendorfs and kept in the -80ºC freezer. Analysis will be conducted at NOCS, UK using the High Performance Liquid Chromatography (HPLC) with diode array spectrophotometry technique described by *Gledhill (2007)*. In total, 388 heme samples were collected from 133 stations.

15.2.2. Chlorophyll-a

Chlorophyll-*a* samples were taken from the CTD at three depths per station (surface, chlorophyll maximum and one further 'near-surface' depth). 500ml of seawater was filtered onto GF/F filters. Filters were then folded into eppendorfs and kept in the -80ºC freezer. Analysis will be conducted at NOCS using a Turner fluorometer. In total, 401 chlorophyll-*a* samples were collected from 133 stations.

14.2.3. POC

POC samples were taken from the CTD at three depths per station (surface, chlorophyll maximum and one further 'near-surface' depth). Up to 4000ml of seawater was filtered onto pre-ashed GF/F filters. Filters were then folded into eppendorfs and kept in the -80ºC freezer. Filters are to be processed and dispatched to Proudman Marine Laboratory (PML) for analysis. In total, 374 POC samples were collected from 133 stations.

15.2.4. Nitrogenase

Nitrogenase samples were taken from the CTD at three depths per station (surface, chlorophyll maximum and one further 'near-surface' depth). Up to 3000ml of seawater was filtered onto GF/F filters. Filters were then folded into eppendorfs and kept in the -80ºC freezer. When sampling for nitrogenase, it was always filtered immediately (i.e. before heme, POC and chlorophyll) and then immediately placed in the -80ºC freezer in an attempt to minimise the degree of degradation of the enzyme. Analysis will be conducted at NOCS. In total, 110 nitrogenase samples were collected from 38 stations.

15.2.5. Nitrogen fixation incubations

Once per day, samples were taken from the CTD at two depths (surface and chlorophyll maximum) for the preparation of nitrogen fixation incubations. 4½L clear bottles were filled with sample water and spiked (injected) with 4ml of $^{15}N_2$ through a septum closure. Filter film was used to adjust light levels: surface = 1 x blue; chl max = 1 x blue, 1 x black. The bottles were then placed in an incubator on the aft deck using water from the non-toxic underway supply, keeping them at approximately surface temperature. After 24 hours, the bottles were removed and the contents filtered onto pre-ashed GF/F filters. Filters were then folded into eppendorfs and placed in a drying oven (50°C) for a further 24 hours. Once complete, the eppendorfs were stored in a dry place. Analysis will be conducted at NOCS. In total, 78 nitrogen fixation incubations were conducted from 39 stations.

15.2.6. Trace metal analysis

The GOFLO bottle was used to collect water samples that would not be contaminated with Fe from the CTD (cable and rosette) or the ship (*RRS Discovery*). The 2L GOFLO was attached to climbing rope (thoroughly rinsed with seawater before use) and deployed to 20m and 40m whilst on station. These depths were chosen as the first (20m) was sufficiently away from the ship to avoid contamination, but to also provide a deeper sample (40m) somewhat closer to the chlorophyll maximum. As the instrument was entirely deployed by hand, it was not practical to allow the GOFLO to be lowered to greater depths. The added counter weight that would be required and possible water currents would make the operation too dangerous; especially considering it was conducted on the starboard aft-deck only 20m from the CTD. Once recovered, the bottle tap was rinsed with Milli-Q. Trace metal clean tubing was attached to direct the water samples into previously prepared trace metal clean bottles (60ml). 50µl of clean concentrated nitric acid was added to the samples in the fume cupboard to allow them to be analysed post-cruise at NOCS, UK. In total, trace metal samples were collected from 32 stations.

15.3. Evaluation

In general, the cruise was extremely successful with over 3000L of water filtered across the transect, as well as numerous nitrogen fixation incubations and GOFLO samples collected. However, a few small issues were raised during the cruise.

15.3.1. -80°C freezer

One major problem that was apparent throughout the cruise was the reliability of the -80°C freezer. Roughly once a week, the temperature would rise to approximately -30°C, obviously causing much concern for the affect on the samples it contained. The temperature would generally rise extremely quickly (50°C in around 2-3 hours) before recovering back to a more suitable temperature where it still regularly fluctuated (between -70°C and -80°C). A few theories were discussed for this including the warm temperature of the hold area where the freezers are stored (next to the engine room and incinerator), but also that the freezer was not particularly full

(eppendorfs containing GF/F's utilise little space and it was only used for this purpose during the cruise) reducing the efficiency. The heme, chlorophyll and POC samples would not have been greatly affected by the temperature change as they can be stored at -20°C (albeit for differing time periods). However, the nitrogenase samples are fairly unstable once filtered and difficult to sample at the best of times, so are required to be keep at -80°C until analysis. It was decided that the freezer would be regularly monitored (every 4 hours) to ensure it was still working adequately; a task carried out by the physics team during their 4 hourly watchkeeping log. The instrument needs to be properly checked once back in port.

15.3.2. Fume cupboard

Ideally, a fume cupboard was required to add the clean concentration nitric acid to the samples taken from the GOFLO bottle. This would allow the procedure to be undertaken safely (removes fumes) and reduces the risk of contamination. However, the fume cupboard was out of action and could not be repaired during the cruise. The problem was sorted by ensuring the acid was added in a well-ventilated area and extra precautions were taken to avoid contact with sources of contamination (i.e. Fe).

15.3.3. Volume of water available

At certain stations, not enough water was available to filter at the 3 target depths (i.e. surface, chlorophyll maximum and one further 'near-surface' depth). Ideally, up to 4L each would be filtered for heme, POC and nitrogenase, 0.5L for chlorophyll as well as setting up an incubation, which requires another 4 ½L. Obviously, it cannot be expected that 17L will be made available for this sole purpose from 20L Niskin bottles. However, at times only 5L remained once all the other teams had sampled which left very little opportunity to adequately filter for these measurements. The situation was rectified by asking others to be less wasteful with the water, although it was understood that thorough rinsing was required (e.g. CFC, oxygen, carbon). In addition, specific bottle depths were replicated whenever possible (only at shallower stations) to ensure plenty of water was available.

15.4. References

Caughey WS (1973), Iron porphyrins - hemes and hemins. In: Eichham GL (ed) Inorganic Biochemistry. Elsevier, Amsterdam, pp 797-831

Codispoti LA (1989), Phosphorus vs. nitrogen limitation of new and export production. In: Berger WH, Smetacek VS, Wefer G (eds) Productivity of the ocean: Past and present: Report of the Dahlem workshop. John Wiley and Sons, New York, pp 377-394

Gledhill M (2007), The determination of heme b in marine phyto- and bacterioplankton. *Marine Chemistry*, 103, pp. 393-403

McElroy MB (1983), Marine biological controls on atmospheric CO_2 and climate, *Nature*, 302, pp. 328-329

Smith SV (1984), Phosphorus versus nitrogen limitation in the marine environment, *Limnology and Oceanography*, 29, pp. 1149-1160

Tyrrell T (1999), The relative influences of nitrogen and phosphorus on oceanic primary production, *Nature*, 400, pp. 525-531

Table 24: List of Samples collected for nitrogen fixation and filtering

Station	Sample	Bottle	Depth	Filtered Volume (L)				N_2 Fix Incubation	GOFLO
				Heme	POC	Chlorophyll	Nitrogenase		
1	1	24	10	1.5	1.5	0.5	0.0	No	No
	2	21	50	1.5	1.5	0.5	0.0	No	
	3	18	180	2.0	2.0	0.5	0.0	No	
2	1	21	5	1.5	1.5	0.5	0.0	No	No
	2	13	50	1.0	1.0	0.5	0.0	No	
	3	4	101	1.0	1.0	0.5	0.0	No	
3	1	20	5	1.5	1.5	0.5	0.0	No	No
	2	14	50	1.5	1.5	0.5	0.0	No	
	3	8	150	1.5	1.5	0.5	0.0	No	
4	1	22	5	2.0	2.0	0.5	0.0	No	No
	2	18	50	1.5	1.5	0.5	0.0	No	
	3	14	100	2.0	2.0	0.5	0.0	No	
5	1	23	5	2.0	2.0	0.5	0.0	No	No
	2	20	50	2.0	2.0	0.5	0.0	No	
	3	16	150	2.5	2.5	0.5	0.0	No	
6	1	23	10	2.0	2.0	0.5	0.0	No	No
	2	21	50	2.0	2.0	0.5	0.0	No	
	3	16	200	3.0	3.0	0.5	0.0	No	
7	1	24	5	2.5	2.5	0.5	0.0	No	No
	2	21	50	2.5	2.5	0.5	0.0	No	
	3	18	150	2.5	2.5	0.5	0.0	No	
8	1	23	10	2.0	2.0	0.5	2.0	No	No
	2	21	50	2.0	2.0	0.5	2.0	No	
	3	19	100	3.0	3.0	0.5	2.0	No	
9	1	24	5	2.0	2.0	0.5	0.0	No	No
	2	21	50	2.0	2.0	0.5	0.0	No	
	3	18	150	1.5	1.5	0.5	0.0	No	
10	1	22	10	2.0	2.0	0.5	0.0	No	No
	2	18	50	2.0	2.0	0.5	0.0	No	
	3	14	100	2.5	2.5	0.5	0.0	No	
11	1	21	5	2.5	2.5	0.5	0.0	No	No
	2	17	50	2.5	2.5	0.5	0.0	No	
	3	14	150	2.5	2.5	0.5	0.0	No	
12	1	24	10	2.0	2.0	0.5	0.0	No	No
	2	14	50	2.0	2.0	0.5	0.0	No	
	3	9	100	1.5	1.5	0.5	0.0	No	
13	1	23	5	2.0	2.0	0.5	0.0	No	No
	2	10	50	2.0	2.0	0.5	0.0	No	
	3	2	166	2.0	2.0	0.5	0.0	No	
14	1	24	5	2.0	2.0	0.5	0.0	Yes	No
	2	21	25	2.0	2.0	0.5	0.0	Yes	
	3	18	50	1.5	1.5	0.5	0.0	No	
15	1	24	5	2.0	2.0	0.5	0.0	No	No
	2	21	25	3.0	3.0	0.5	0.0	No	
	3	20	50	2.0	2.0	0.5	0.0	No	
16	1	24	5	2.0	2.0	0.5	0.0	No	No
	2	21	50	2.0	2.0	0.5	0.0	No	
	3	19	100	2.0	2.0	0.5	0.0	No	
17	1	24	5	2.0	2.0	0.5	0.0	No	No
	2	21	50	2.0	2.0	0.5	0.0	No	
	3	19	100	2.0	2.0	0.5	0.0	No	

18	1	-	-	0.0	0.0	0.0	0.0	No	No
	2	-	-	0.0	0.0	0.0	0.0	No	
	3	-	-	0.0	0.0	0.0	0.0	No	
19	1	24	5	3.0	3.0	0.5	0.0	No	No
	2	22	50	2.5	2.5	0.5	0.0	No	
	3	20	100	2.5	2.5	0.5	0.0	No	
20	1	24	5	1.5	1.5	0.5	0.0	Yes	20m
	2	23	50	1.5	1.5	0.5	0.0	Yes	
	3	22	100	2.0	2.0	0.5	0.0	No	
21	1	24	5	3.0	2.5	0.5	2.0	No	No
	2	23	50	3.0	3.0	0.5	2.0	No	
	3	22	100	2.5	2.0	0.5	2.0	No	
22	1	24	5	3.0	3.0	0.5	0.0	No	No
	2	23	50	3.0	3.0	0.5	0.0	No	
	3	22	100	3.0	3.0	0.5	0.0	No	
23	1	24	5	2.0	2.0	0.5	2.0	Yes	No
	2	23	50	3.0	3.0	0.5	3.0	No	
	3	22	100	2.5	2.5	0.5	3.0	Yes	
24	1	24	5	2.0	2.0	0.5	3.0	No	No
	2	22	120	3.5	3.0	0.5	3.0	No	
	3	21	175	3.0	3.0	0.5	3.0	No	
25	1	24	10	3.0	3.0	0.5	0.0	No	No
	2	23	50	3.0	3.0	0.5	0.0	No	
	3	22	105	3.5	3.5	0.5	0.0	No	
26	1	24	10	2.0	2.0	0.5	2.0	Yes	No
	2	23	50	2.5	2.5	0.5	3.0	No	
	3	22	100	2.5	2.0	0.5	3.0	Yes	
27	1	24	10	3.0	3.0	0.5	3.0	No	No
	2	23	50	3.0	3.0	0.5	3.0	No	
	3	22	100	3.0	1.5	0.5	3.0	No	
28	1	24	10	3.0	3.0	0.5	0.0	No	No
	2	23	50	3.0	3.0	0.5	0.0	No	
	3	22	100	3.0	3.0	0.5	0.0	No	
29	1	24	10	3.0	3.0	0.5	0.0	No	No
	2	22	50	3.0	3.0	0.5	0.0	No	
	3	20	100	3.0	3.0	0.5	0.0	No	
30	1	24	5	0.0	0.0	0.5	0.0	Yes	No
	2	23	50	3.0	3.0	0.5	0.0	No	
	3	22	100	2.0	2.0	0.5	0.0	Yes	
31	1	24	5	3.0	3.0	0.5	3.0	No	20m, 40m
	2	22	100	3.0	3.0	0.5	3.0	No	
	3	21	175	4.0	3.0	0.5	3.0	No	
32	1	24	5	3.0	3.0	0.5	0.0	No	No
	2	23	50	3.0	3.0	0.5	0.0	No	
	3	21	100	3.0	3.0	0.5	0.0	No	
33	1	24	5	3.0	3.0	0.5	0.0	No	No
	2	22	50	3.0	2.5	0.5	0.0	No	
	3	21	100	3.0	3.0	0.5	0.0	No	
34	1	24	10	3.0	3.0	0.5	0.0	No	No
	2	22	100	3.0	3.0	0.5	0.0	No	
	3	21	175	3.0	3.0	0.5	0.0	No	
35	1	24	10	0.0	0.0	0.5	2.0	Yes	20m, 40m
	2	22	100	0.0	0.0	0.5	2.0	Yes	
	3	21	175	3.0	3.0	0.5	3.0	No	
	1	24	10	3.0	3.0	0.5	0.0	No	No

36	1	24	10	3.0	3.0	0.5	0.0	No	No
	2	23	50	3.0	3.0	0.5	0.0	No	
	3	22	100	3.0	3.0	0.5	0.0	No	
37	1	24	5	3.0	3.0	0.5	0.0	No	No
	2	23	50	3.0	3.0	0.5	0.0	No	
	3	22	130	3.0	3.0	0.5	0.0	No	
38	1	24	5	2.5	2.5	0.5	2.0	No	No
	2	23	50	2.5	2.5	0.5	3.0	No	
	3	22	100	3.0	3.0	0.5	3.0	No	
39	1	24	5	2.5	0.0	0.5	2.0	Yes	No
	2	23	50	3.0	3.0	0.5	3.0	No	
	3	22	80	3.0	3.0	0.5	3.0	Yes	
40	1	24	5	3.0	3.0	0.5	0.0	No	No
	2	23	50	3.0	3.0	0.5	0.0	No	
	3	22	120	3.0	3.0	0.5	0.0	No	
41	1	24	5	3.0	3.0	0.5	0.0	No	No
	2	23	50	3.0	3.0	0.5	0.0	No	
	3	22	100	3.0	3.0	0.5	0.0	No	
42	1	24	10	1.25	0.0	0.5	0.0	Yes	20m
	2	22	100	3.0	3.0	0.5	3.0	Yes	
	3	21	175	3.0	2.5	0.5	3.0	No	
43	1	24	5	3.0	3.0	0.5	0.0	No	No
	2	23	50	3.0	3.0	0.5	0.0	No	
	3	22	100	3.0	3.0	0.5	0.0	No	
44	1	24	5	3.0	3.0	0.5	0.0	No	No
	2	23	50	3.0	3.0	0.5	0.0	No	
	3	22	75	3.0	3.0	0.5	0.0	No	
45	1	24	5	2.0	2.0	0.5	0.0	Yes	20m, 40m
	2	23	50	3.0	3.0	0.5	0.0	No	
	3	22	100	3.0	3.0	0.5	0.0	Yes	
46	1	24	5	3.0	3.0	0.5	0.0	No	No
	2	23	50	3.0	3.0	0.5	0.0	No	
	3	22	100	3.0	3.0	0.5	0.0	No	
47	1	24	5	3.0	3.0	0.5	0.0	No	No
	2	23	50	3.0	3.0	0.5	0.0	No	
	3	22	100	3.0	3.0	0.5	0.0	No	
48	1	24	5	0.0	0.0	0.5	0.0	Yes	20m
	2	23	50	3.0	3.0	0.5	3.0	No	
	3	22	100	2.5	2.5	0.5	2.0	Yes	
49	1	24	5	3.0	3.0	0.5	0.0	No	No
	2	23	50	3.0	3.0	0.5	0.0	No	
	3	22	110	3.0	3.0	0.5	0.0	No	
50	1	24	5	3.5	3.5	0.5	0.0	No	No
	2	23	50	3.0	3.0	0.5	0.0	No	
	3	22	100	3.5	3.5	0.5	0.0	No	
51	1	24	5	2.5	2.0	0.5	0.0	Yes	No
	2	23	50	3.0	3.0	0.5	0.0	No	
	3	22	100	2.5	2.5	0.5	0.0	Yes	
52	1	24	5	3.0	3.0	0.5	3.0	No	No
	2	23	50	2.5	2.0	0.5	3.0	No	
	3	22	100	3.0	3.0	0.5	3.0	No	
53	1	24	5	3.0	3.0	0.5	0.0	No	No
	2	23	50	3.0	3.0	0.5	0.0	No	
	3	22	100	3.0	3.0	0.5	0.0	No	
	1	24	5	2.5	0.0	0.5	0.0	Yes	20m,

54	1	24	5	2.5	0.0	0.5	0.0	Yes	40m
	2	22	100	1.5	0.0	0.5	0.0	Yes	
	3	21	175	3.0	3.0	0.5	0.0	No	
55	1	24	5	3.0	3.0	0.5	0.0	No	No
	2	23	50	3.0	3.0	0.5	0.0	No	
	3	22	100	3.0	3.0	0.5	0.0	No	
56	1	24	5	3.0	3.0	0.5	0.0	No	No
	2	23	50	3.0	3.0	0.5	0.0	No	
	3	22	100	3.0	3.0	0.5	0.0	No	
57	1	24	5	2.0	2.0	0.5	0.0	Yes	20m, 40m
	2	23	50	3.0	3.0	0.5	0.0	No	
	3	22	100	2.0	2.0	0.5	0.0	Yes	
58	1	24	5	3.0	3.0	0.5	0.0	No	No
	2	23	50	3.0	3.0	0.5	0.0	No	
	3	22	100	3.0	3.0	0.5	0.0	No	
59	1	24	5	3.0	3.0	0.5	0.0	Yes	No
	2	22	100	3.0	3.0	0.5	0.0	Yes	
	3	21	175	3.0	3.0	0.5	0.0	No	
60	1	23	50	3.0	3.0	0.5	3.0	No	No
	2	22	100	3.0	3.0	0.5	3.0	No	
	3	21	175	3.0	3.0	0.5	3.0	No	
61	1	24	5	3.0	3.0	0.5	0.0	No	No
	2	23	50	3.0	3.0	0.5	0.0	No	
	3	22	100	3.0	3.0	0.5	0.0	No	
62	1	24	5	0.0	0.0	0.5	0.0	Yes	No
	2	23	50	3.0	3.0	0.5	0.0	No	
	3	22	100	3.0	3.0	0.5	0.0	Yes	
63	1	23	50	3.0	3.0	0.5	0.0	No	20m, 40m
	2	22	100	3.0	3.0	0.5	0.0	No	
	3	21	175	3.0	3.0	0.5	0.0	No	
64	1	24	5	3.0	3.0	0.5	0.0	No	No
	2	23	50	3.0	3.0	0.5	0.0	No	
	3	22	100	3.0	3.0	0.5	0.0	No	
65	1	24	5	3.0	3.0	0.5	0.0	No	No
	2	23	50	3.0	3.0	0.5	0.0	No	
	3	22	100	3.0	3.0	0.5	0.0	No	
66	1	24	5	3.0	3.0	0.5	0.0	No	No
	2	23	50	3.5	4.0	0.5	0.0	No	
	3	22	100	3.0	3.5	0.5	0.0	No	
67	1	24	5	2.5	0.0	0.5	0.0	Yes	No
	2	23	50	3.0	3.0	0.5	0.0	No	
	3	22	100	2.5	0.0	0.5	0.0	Yes	
68	1	24	5	3.0	3.0	0.5	0.0	No	No
	2	23	50	3.0	3.5	0.5	0.0	No	
	3	22	100	3.5	3.5	0.5	0.0	No	
69	1	24	10	1.75	0.0	0.5	0.0	Yes	No
	2	22	100	2.5	2.5	0.5	0.0	Yes	
	3	21	175	3.0	3.0	0.5	0.0	No	
70	1	24	5	3.0	3.0	0.5	3.0	No	No
	2	23	50	3.0	3.0	0.5	3.0	No	
	3	22	100	3.0	3.0	0.5	3.0	No	
71	1	24	10	2.0	2.0	0.5	0.0	No	No
	2	23	50	3.0	3.0	0.5	0.0	No	
	3	22	100	3.0	0.0	0.5	0.0	No	
	1	24	5	3.0	0.0	0.5	2.0	Yes	20m,

72	1	24	5	3.0	0.0	0.5	2.0	Yes	40m
	2	23	50	3.0	3.0	0.5	3.0	No	
	3	22	100	3.0	3.0	0.5	3.0	Yes	
73	1	24	5	0.0	0.0	0.4	0.0	Yes	20m, 40m
	2	23	50	3.5	3.5	0.5	0.0	No	
	3	22	100	3.0	0.0	0.5	0.0	Yes	
74	1	24	5	3.0	3.0	0.5	3.0	No	No
	2	22	100	3.0	3.0	0.5	3.0	No	
	3	21	175	3.0	3.0	0.5	3.0	No	
75	1	24	5	3.0	3.0	0.5	0.0	No	No
	2	23	50	3.0	3.0	0.5	0.0	No	
	3	22	100	3.0	3.0	0.5	0.0	No	
76	1	24	5	3.0	3.0	0.5	3.0	Yes	20m, 40m
	2	22	50	3.0	3.0	0.5	3.0	No	
	3	21	100	2.25	0.0	0.5	2.0	Yes	
77	1	24	5	3.0	3.0	0.5	0.0	No	No
	2	22	100	3.0	3.0	0.5	0.0	No	
	3	21	175	3.0	3.0	0.5	0.0	No	
78	1	24	5	3.0	3.0	0.5	0.0	No	No
	2	23	50	3.0	3.0	0.5	0.0	No	
	3	21	100	3.0	3.0	0.5	0.0	No	
79	1	24	5	3.0	3.0	0.5	0.0	Yes	20m, 40m
	2	22	50	3.0	3.0	0.5	0.0	No	
	3	21	100	3.0	3.0	0.5	0.0	Yes	
80	1	24	5	2.5	2.5	0.5	2.0	No	No
	2	23	25	3.0	3.0	0.5	3.0	No	
	3	21	100	3.0	3.0	0.5	3.0	No	
81	1	-	-	0.0	0.0	0.0	0.0	No	No
	2	-	-	0.0	0.0	0.0	0.0	No	
	3	-	-	0.0	0.0	0.0	0.0	No	
82	1	24	5	3.0	3.0	0.5	0.0	No	No
	2	23	25	3.0	3.0	0.5	0.0	No	
	3	22	50	3.0	3.0	0.5	0.0	No	
83	1	24	10	2.0	1.75	0.5	0.0	Yes	20m, 40m
	2	22	100	2.25	2.0	0.5	0.0	Yes	
	3	21	175	3.0	3.0	0.5	0.0	No	
84	1	24	5	0.0	3.0	0.5	3.0	No	No
	2	23	25	3.0	3.0	0.5	3.0	No	
	3	21	100	2.0	2.0	0.5	3.0	No	
85	1	24	5	3.0	3.0	0.5	0.0	No	No
	2	23	50	3.0	3.0	0.5	0.0	No	
	3	22	100	3.0	3.0	0.5	0.0	No	
86	1	24	10	3.0	3.0	0.5	3.0	Yes	20m, 40m
	2	22	50	3.0	2.25	0.5	3.0	No	
	3	21	100	2.5	2.0	0.5	3.0	Yes	
87	1	24	5	3.0	3.0	0.5	0.0	No	No
	2	22	50	3.0	3.0	0.5	0.0	No	
	3	21	100	3.0	3.0	0.5	0.0	No	
88	1	24	5	3.0	3.0	0.5	0.0	No	No
	2	23	50	3.0	3.0	0.5	0.0	No	
	3	22	100	3.0	3.0	0.5	0.0	No	
89	1	24	5	2.5	2.5	0.5	0.0	Yes	20m, 40m
	2	23	50	3.0	3.0	0.5	0.0	No	
	3	22	100	2.0	2.0	0.5	0.0	Yes	
	1	24	5	3.5	3.5	0.5	0.0	No	No

90	1	24	5	3.5	3.5	0.5	0.0	No	No
	2	23	50	3.5	3.5	0.5	0.0	No	
	3	22	100	3.5	3.5	0.5	0.0	No	
91	1	24	5	3.5	3.5	0.5	0.0	No	No
	2	23	50	3.5	3.5	0.5	0.0	No	
	3	22	100	3.5	3.5	0.5	0.0	No	
92	1	24	5	0.0	0.0	0.5	0.0	Yes	20m, 40m
	2	23	50	3.5	3.5	0.5	0.0	No	
	3	22	100	3.5	3.5	0.5	0.0	Yes	
93	1	24	5	3.5	3.5	0.5	3.0	No	No
	2	23	50	3.5	2.5	0.5	3.0	No	
	3	21	175	3.5	3.0	0.5	3.0	No	
94	1	24	5	3.5	3.5	0.5	0.0	No	No
	2	23	50	3.5	3.5	0.5	0.0	No	
	3	22	100	3.5	3.5	0.5	0.0	No	
95	1	24	5	0.0	0.0	0.4	0.0	Yes	20m, 40m
	2	23	50	3.5	3.5	0.5	0.0	No	
	3	22	100	2.0	0.0	0.5	0.0	Yes	
96	1	24	5	3.5	3.5	0.5	0.0	No	No
	2	23	50	3.5	3.0	0.5	0.0	No	
	3	22	100	3.5	3.5	0.5	0.0	No	
97	1	24	5	3.5	3.5	0.5	0.0	No	No
	2	23	50	3.5	3.5	0.5	0.0	No	
	3	22	100	3.5	3.5	0.5	0.0	No	
98	1	24	5	3.0	3.0	0.5	3.0	Yes	20m, 40m
	2	22	50	3.0	2.5	0.5	0.0	No	
	3	21	100	3.0	3.0	0.5	3.0	Yes	
99	1	24	5	3.5	3.5	0.5	0.0	No	No
	2	23	50	3.5	3.5	0.5	0.0	No	
	3	22	100	3.5	3.5	0.5	0.0	No	
100	1	24	5	3.5	3.5	0.5	0.0	No	No
	2	23	50	3.5	3.5	0.5	0.0	No	
	3	21	175	3.5	3.5	0.5	0.0	No	
101	1	24	5	2.5	2.0	0.5	0.0	Yes	20m, 40m
	2	23	50	3.5	3.5	0.5	0.0	No	
	3	22	100	3.0	1.75	0.5	0.0	Yes	
102	1	24	5	3.5	3.5	0.5	0.0	No	No
	2	23	50	3.5	3.5	0.5	0.0	No	
	3	22	100	3.5	3.5	0.5	0.0	No	
103	1	24	5	0.0	0.0	0.5	3.0	Yes	20m, 40m
	2	23	50	3.5	3.25	0.5	3.0	No	
	3	22	100	3.5	3.0	0.5	3.0	Yes	
104	1	24	5	3.5	3.5	0.5	0.0	No	No
	2	23	50	3.5	3.5	0.5	0.0	No	
	3	22	88	3.5	3.5	0.5	0.0	No	
105	1	24	5	3.5	3.5	0.5	0.0	No	No
	2	23	50	3.5	3.5	0.5	0.0	No	
	3	22	130	3.5	3.5	0.5	0.0	No	
106	1	23	5	3.5	3.5	0.5	3.0	Yes	20m, 40m
	2	22	50	3.5	3.5	0.5	3.0	No	
	3	20	100	3.5	3.5	0.5	3.0	Yes	
107	1	24	5.0	3.5	3.5	0.5	0.0	No	No
	2	23	50	3.5	3.5	0.5	0.0	No	
	3	22	100	3.5	3.5	0.5	0.0	No	
	1	24	5	3.5	3.5	0.5	0.0	No	No

108	1	24	5	3.5	3.5	0.5	0.0	No	No
	2	23	50	3.5	3.5	0.5	0.0	No	
	3	22	77	3.5	3.5	0.5	0.0	No	
109	1	24	5	3.5	0.0	0.5	0.0	Yes	20m, 40m
	2	23	50	3.5	3.5	0.5	0.0	No	
	3	22	100	3.5	0.0	0.5	0.0	Yes	
110	1	24	5	3.5	3.5	0.5	0.0	No	No
	2	23	50	3.5	3.5	0.5	0.0	No	
	3	22	100	3.5	3.5	0.5	0.0	No	
111	1	24	5	3.5	3.5	0.5	3.0	No	No
	2	23	50	3.5	3.5	0.5	3.0	No	
	3	22	100	3.5	3.5	0.5	3.0	No	
112	1	24	5	3.5	0.0	0.5	0.0	Yes	20m, 40m
	2	23	50	3.5	3.5	0.5	0.0	No	
	3	22	85	3.5	3.5	0.5	0.0	Yes	
113	1	24	5	3.5	3.5	0.5	0.0	No	No
	2	23	50	3.5	3.5	0.5	0.0	No	
	3	22	100	3.5	3.5	0.5	0.0	No	
114	1	24	5	2.5	2.25	0.5	0.0	Yes	20m, 40m
	2	22	65	3.5	3.5	0.5	0.0	Yes	
	3	21	175	3.5	3.5	0.5	0.0	No	
115	1	24	5	3.5	3.5	0.5	0.0	No	No
	2	23	50	3.5	3.5	0.5	0.0	No	
	3	22	100	3.5	3.5	0.5	0.0	No	
116	1	24	5	3.5	3.5	0.5	0.0	No	No
	2	22	75	3.5	3.5	0.5	0.0	No	
	3	21	100	3.5	3.5	0.5	0.0	No	
117	1	24	5	3.5	3.5	0.5	3.0	No	No
	2	23	50	3.5	3.5	0.5	3.0	No	
	3	22	100	3.5	3.5	0.5	3.0	No	
118	1	24	5	2.25	2.0	0.5	0.0	Yes	20m, 40m
	2	23	50	3.5	3.5	0.5	0.0	No	
	3	21	100	3.5	3.5	0.5	0.0	Yes	
119	1	24	5	2.5	2.25	0.5	3.0	No	No
	2	23	25	3.5	3.0	0.5	3.0	No	
	3	21	100	3.5	0.0	0.5	3.0	No	
120	1	24	5	3.5	3.5	0.5	0.0	No	No
	2	21	75	3.5	3.5	0.5	0.0	No	
	3	20	100	3.5	3.5	0.5	0.0	No	
121	1	24	5	3.5	3.5	0.5	0.0	Yes	20m, 40m
	2	22	50	3.5	3.5	0.5	0.0	No	
	3	21	100	2.0	0.0	0.5	0.0	Yes	
122	1	24	5	3.5	3.5	0.5	3.0	No	No
	2	20	75	3.0	2.25	0.5	3.0	No	
	3	19	100	3.5	3.5	0.5	3.0	No	
123	1	24	5	3.5	3.5	0.5	3.0	No	No
	2	22	25	3.5	3.5	0.5	3.0	No	
	3	20	100	3.5	3.5	0.5	3.0	No	
124	1	24	5	3.5	3.5	0.5	0.0	No	No
	2	21	50	3.5	3.5	0.5	0.0	No	
	3	19	100	3.5	3.5	0.5	0.0	No	
125	1	24	5	3.5	3.5	0.5	0.0	Yes	20m, 40m
	2	19	100	0.0	0.0	0.5	0.0	Yes	
	3	18	175	3.5	3.5	0.5	0.0	No	
	1	24	5	3.5	3.5	0.5	3.0	No	No

126	1	24	5	3.5	3.5	0.5	3.0	No	No
	2	21	75	3.5	3.5	0.5	3.0	No	
	3	20	100	3.5	3.5	0.5	3.0	No	
127	1	24	5	3.5	3.5	0.5	0.0	No	No
	2	22	50	3.5	3.5	0.5	0.0	No	
	3	20	75	3.5	3.5	0.5	0.0	No	
128	1	24	5	3.5	3.25	0.5	3.0	No	20m, 40m
	2	23	25	3.5	3.5	0.5	3.0	No	
	3	21	80	3.5	3.5	0.5	3.0	No	
129	1	24	5	3.5	3.5	0.5	3.0	Yes	20m, 40m
	2	21	50	3.5	3.5	0.5	3.0	No	
	3	19	95	3.5	3.5	0.5	3.0	Yes	
130	1	24	5	3.5	3.5	0.5	3.0	No	No
	2	22	25	3.5	3.5	0.5	3.0	No	
	3	19	100	3.5	3.5	0.5	3.0	No	
131	1	24	5	3.5	3.5	0.5	3.0	No	No
	2	20	60	3.5	3.5	0.5	3.0	No	
	3	17	175	3.5	3.5	0.5	3.0	No	
132	1	24	5	3.0	3.0	0.5	3.0	Yes	20m, 40m
	2	19	75	2.5	2.25	0.5	0.0	Yes	
	3	18	100	3.0	3.0	0.5	3.0	No	
133	1	24	5	3.0	3.0	0.5	0.0	No	No
	2	19	75	3.0	3.0	0.5	0.0	No	
	3	18	100	3.0	3.0	0.5	0.0	No	
134	1	24	5	3.0	3.0	0.5	3.0	No	No
	2	20	50	3.0	3.0	0.5	3.0	No	
	3	14	100	3.0	3.0	0.5	3.0	No	
135	1	24	5	3.0	3.0	0.5	3.0	Yes	20, 20m, 40m
	2	20	40	3.0	3.0	0.5	3.0	Yes	
	3	13	100	3.0	3.0	0.5	3.0	No	

David Honey

16. Inorganic Nitrate and Phosphate at Nanomolar Concentrations

16.1. Cruise objectives

My main objective for cruise D346 was to measure nanomolar concentrations of nitrate and phosphate. This will be the first time that accurate nutrient measurements at the surface are achieved.

16.2. Method

Gas-segmented continuous-flow colorimetric method was used for both phosphate and nitrate. The chemical methods are described by *Grasshoff et al., (1983)*. The autoanalyser is coupled with liquid waveguide capillary cells (LWCC) to achieve nanomolar levels of detection following the methods described by *Patey et al. (2008)*.

Blanks were measured with Milli-Q and low nutrients seawater (LNSW), this water being aged several months in the lab at room temperature and with light. Standards were measured in Milli-Q and LNSW to correct for the salt effect from the seawater matrix.

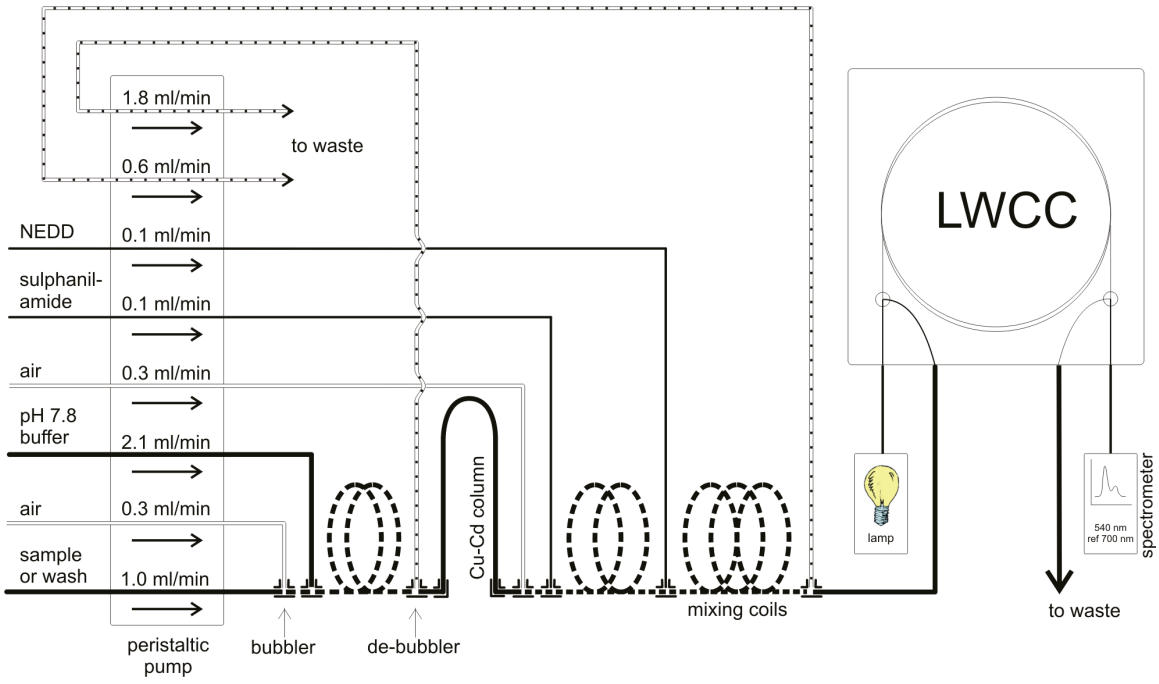

Figure 61: The nitrate+nitrite SCFA-LWCC system below the phosphate system. The glass coils used are 1.6-mm ID.

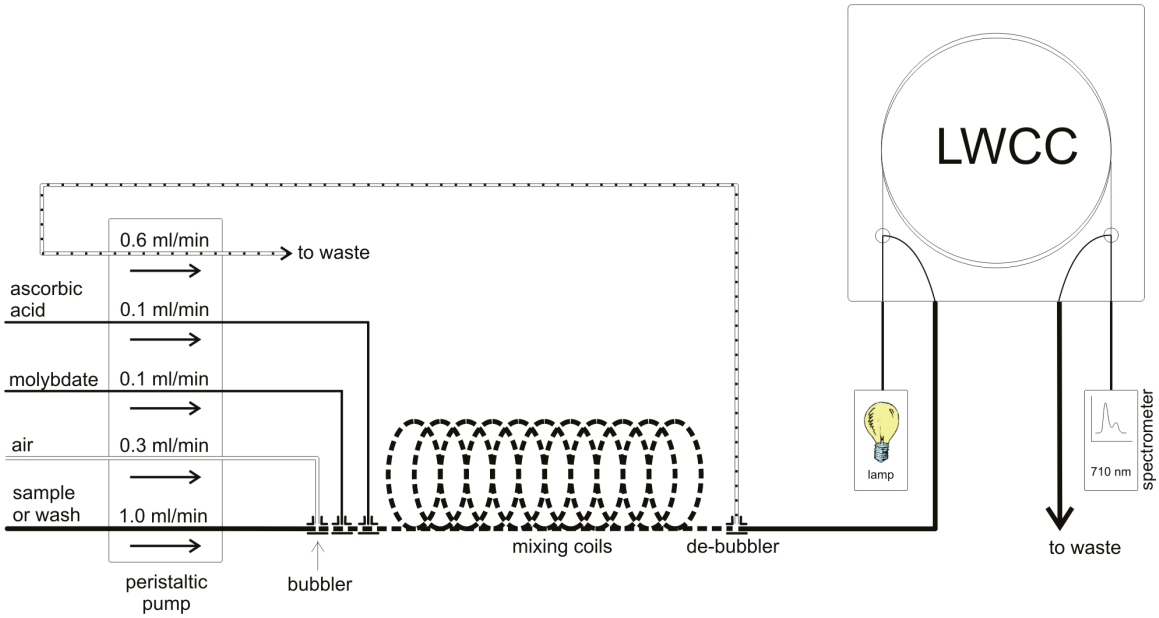

Figure 62: The Phosphate SCFA-LWCC system. The glass coils used are 1.6-mm ID.

16.3. System

Samples were drawn from Niskin bottles on the CTD into 10% HCl clean 60ml LDPE bottles from Nalgene and kept refrigerated at approximately 4^{o}C until analysis.

An auto-sampler from Skalar has been added ahead of the system. Sampling time was 150 seconds and the wash time was 150 seconds leading to 1:1 ratio.

Analysis was undertaken on a modified Burkard Autoanalyser with one main peristaltic pump and reaction channels, one for phosphate and one for nitrate.

The detection cells were Liquid Core Waveguide Capillary Cells (LWCC) of 2m in length, from WPI instruments. Spectrophotometric detection was achieved using tungsten lamps as light sources and 2 spectrometers. These devices were linked with fiber-optic connections. All of this equipment was supplied by OceanOptics.

Data acquisition was undertaken using the software Spectrasuite in 2 steps. First the spectrum of the coloured complex provides a value of the signal intensity for each wavelength. The absorbance of the signal is measured for the wavelength of interest for each compound. The selected wavelengths for nitrate and phosphate are respectively 540nm and 710nm.

16.4. Performance

The general performance of the analyser is monitored via the following parameters: sensitivity, baseline value, intensity of the signal, regression coefficient of the calibration curve and cadmium column efficiency. The efficiency of the cadmium column was checked and cleaned if required. The sensitivity of the analyser stayed relatively constant throughout the cruise.

NB: Channels were washed daily with 10% triethanolamine, methanol and 2M HCl.

Several problems have been encountered:

- The first was with the software's capability to read both channels simultaneously. The software does not support the function of being given two references, one for each channel. We had to add a reference monitor required for the second acquisition.

- The second problem was due to contamination of samples in the lab. This problem had been anticipated so a bag, flushed with oxygen-free nitrogen, was successfully set around the sampler to prevent any contamination from the air. The first sample read was repeated at the end of the run to make ensure there was no contamination.

16.5. Results

Overall 135 stations were sampled from the surface down to a depth of 300m. System calibrations enabled us to validate the quality of the signal.

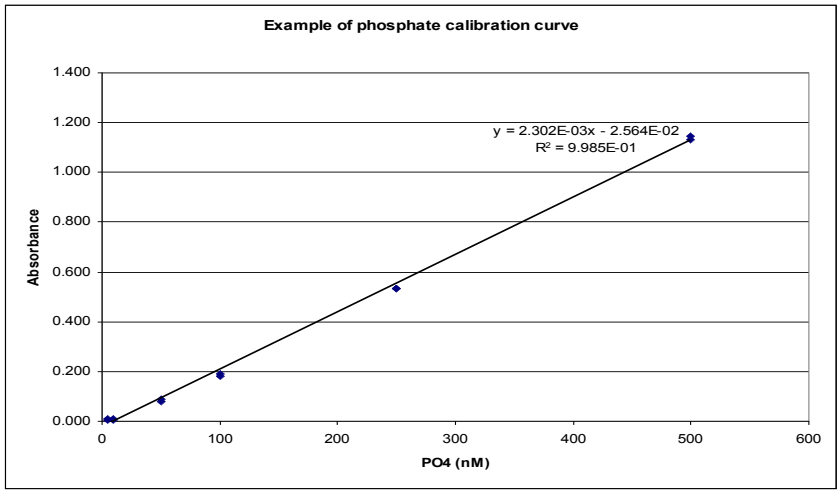

Figure 63: Phosphate calibration curve

Further cross-linked analysis of this new dataset with parameters measured on the cruise will be conducted.

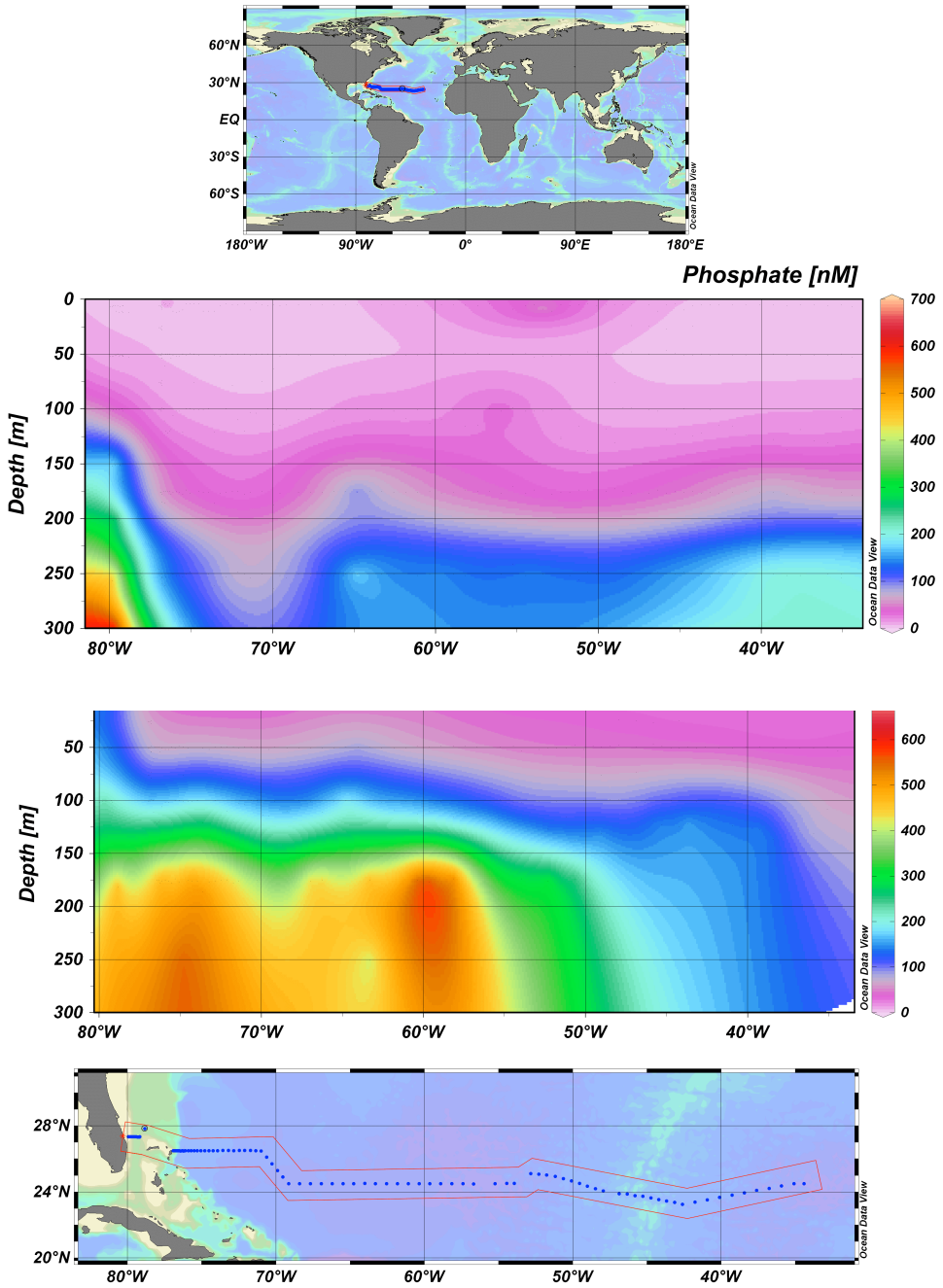

Figure 64: Contour plots of nitrate and phosphate concentrations in the upper layer along the transect

16.6. References

Grasshoff, K., Ehrhardt, M., and Kremling, K., (1983) Methods of Seawater Analysis, Verlag Chemie, Weinheim.

Patey, M. D., Rijkenberg, M.J.A., Statham, P.J., Mowlem, M., Stinchcombe, M.C. and Achterberg, E.P. (2008) Determination of nitrate and phosphate in seawater at nanomolar concentrations, TrAC Trends in Analytical Chemistry, **27** (2): 169-182.

François-Eric Legiret

17. Near-surface and Sea Surface Salinity Study for SMOS Cal/Val

17.1. Introduction

In November 2009, ESA launched the Soil Moisture and Ocean Salinity satellite (SMOS). The payload of SMOS is the Microwave Imaging Radiometer using Aperture Synthesis (MIRAS) and this instrument is the first attempt to measure ocean salinity and soil moisture from space. Using complex cross-correlations of the 69 receivers, SMOS will provide global coverage of ocean salinity every three days with an estimated accuracy of ~1psu (pixel size 35-50km). This accuracy can be improved to ~0.1psu by combining data over 10 days and 200 x 200km, or 30 days and 100 x 100km.

As part of the calibration and validation (Cal/Val) of the SMOS satellite the National Oceanography Centre, Southampton is studying the salinity of the North Atlantic during the initial data collection phase. In particular, data from the underway conductivity and temperature sensors during D346 is of importance. However, the salinity as measured by SMOS relates to the top few centimetres rather than the ~5.5m depth of the underway water inlet (or the depths of a few metres gathered by other underway systems, buoys or floats). Additional data have been gathered throughout the cruise with an aim of understanding salinity variability in the top 10m likely to impact on differences between SMOS and other measurement systems.

Two main approaches have been used for this purpose in addition to data from the underway system and CTDs. The first method comprised a handheld CT probe, and the second used a tethered buoy system both intended to look at variability at different depths. The two approaches are discussed in the following sections and the preliminary results are presented.

17.2. Handheld CT sensor

The lower 5m of the cable of the YSI 30 handheld conductivity (salinity), temperature (CT) probe was marked at 1-metre intervals using different coloured tape. This probe provides salinity and temperature values to 1 decimal place and was calibrated just before being air freighted for D346. During occupation of some CTD stations the probe was lowered into the water from the starboard side and values of salinity and temperature were noted on the way down and the way up for each of the intervals. In addition, an effort was made to hold the sensor as close to the surface as possible and this represented the surface value. Later on in the cruise (from 19th January), the number of markings and maximum depth were increased to 10m.

In order to reduce the depth at which surface salinity was measured (i.e. the top few cm), the probe was attached to a piece of wood using reusable cable ties from 26th January onwards. To prevent the cable sinking the sensor, an empty drink bottle was attached approximately 1m from the probe. This arrangement was deployed at the same time as the measurements to 10m depth.

17.3. Tethered buoy system

In order to investigate the near surface salinity, it was planned to deploy a system of CT sensors vertically on a buoy tethered to the ship during the occupation of CTD stations. NOCS, in collaboration with the School of Electronics and Computer Science, University of Southampton, are developing a new 'lab-on-a-chip' salinity-temperature sensor and eight of these sensors were obtained for the purposes of the SMOS Cal/Val project. In addition, D346 provided an opportunity for deployment of the sensors in an oceanic rather than laboratory setting.

The sensors are mounted at one end of a cylindrical pot (Figure 65) with a removable fixing disc at the other end. The sensors are held inside by screwing on the lid (with an integral guard to protect the sensor head) and sealed against the plate (Figure 65a) with an 'o' ring. The fixing disc has a channel into which the rope is placed and then held in place by attaching to the pot with four screws (Figure 65).

Shortly before the cruise, whilst the sensors were still in the UK, a problem was noted with the temperature sensor. To provide a working solution for the purposes of the cruise a thermistor was added to the arrangement by drilling through the plate holding the sensor (see Figure 65a).

a)

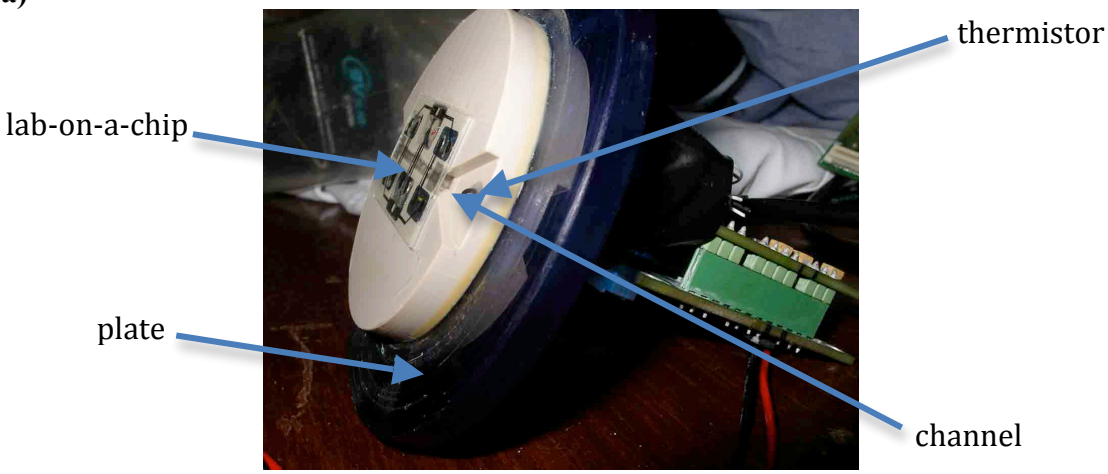

b)

c)

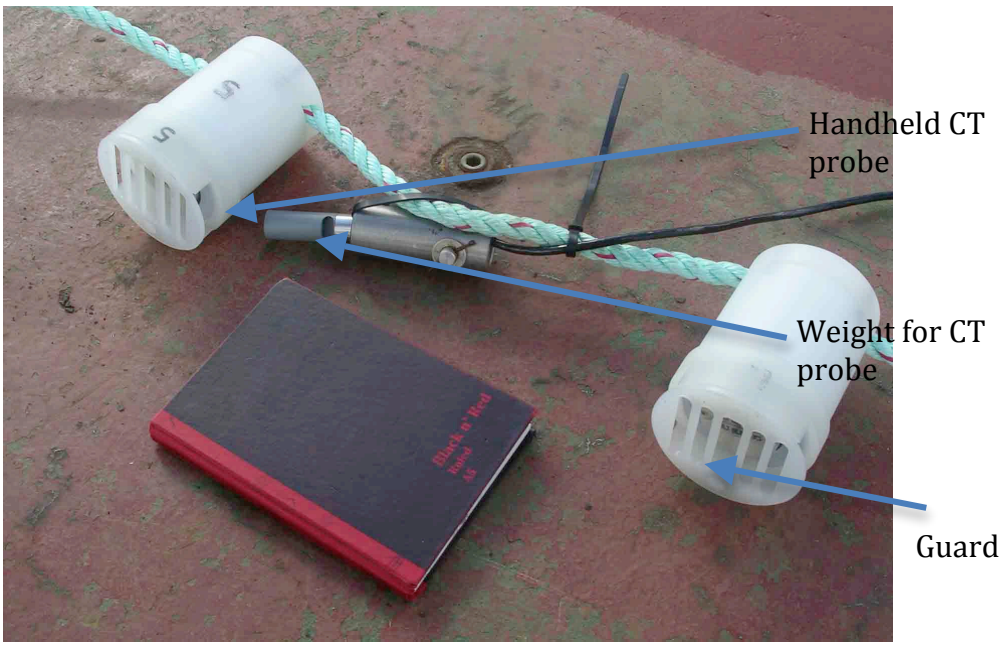

Figure 65: Photographs showing a) internal arrangement of sensor 'pot'; b) sensor attached to buoy and c) close up of sensors on rope (also showing handheld CT probe)

In order to test the sensors, they were placed in a bucket being replenished by the non-toxic seawater supply on 6th January. After downloading the data it became clear that there were issues with the calibration of the sensors. In addition, one of the pots had leaked allowing seawater in. Other pots also leaked when the system was tested over the starboard side to a depth of ~5m.

One possible reason was that the difficulties were caused by the presence of bubbles in the channel (Figure 65a). Two of the sensors were then weighted down and then left to operate inside a coolbox in the Constant Temperature (CT) laboratory ensuring (by shaking and close inspection) that all bubbles had been removed. However, this failed to solve the issue and the temperature values, not dependent on the channel, were also incorrect.

As the thermistors were added after the calibration it was suggested that the calibration should be repeated. By using the coolbox in the CT laboratory with various salinity values, a calibration exercise was carried out using the four remaining sensors that had not leaked over the next few days. Unfortunately, one of the pots leaked during the calibration exercise leaving three working sensors.

On 18th January, two sensors were attached to a tethered buoy and deployed off the stern during CTD Station 51. Upon recovery, one of the pots had leaked and so the battery was disconnected and the electronics rinsed thoroughly in deionised water. The temperature measured by the remaining instrument was approximately -60ºC. However, by taping the battery to the terminals the problem of the instrument resetting itself with the slightest loss in voltage was removed.

The two remaining instruments (#4 and #5) were now producing consistent values of salinity and temperature. The tethered system was deployed at 20 subsequent CTD stations, at depths varying between ~0.3 – 3.0m. However, they will require an extensive post-cruise calibration and as such no values of SSS and SST are reported here.

Also developed throughout the cruise were a variety of different approaches to tethering the sensors to the ship. Initially the setup was simply a tether from the ship to a single Polyform A2 buoy weighted with a length of chain and the sensors attached onto the rope holding the chain. However, in order to reduce the snatch from the ship, as it moved relative to the sensors, a chain between buoys was used so that any movement of the ship was first taken up in the chain as the chain tended to sink and pull the buoys together. Two variations of the system are shown in Figure 66 and the final setup of the system is shown in Figure 67.

Figure 66: Photographs of showing the development of the near surface salinity buoy system showing a) 2 sensors mounted on initial 5m long chain-weighted rope; b) and c) showing later shallower, lighter system.

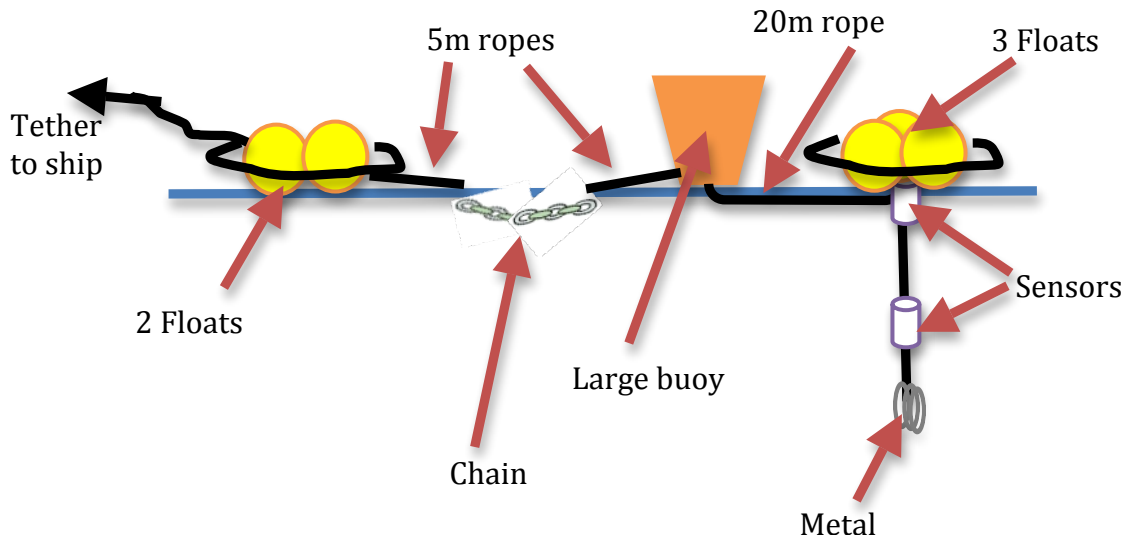

Figure 67: Diagrammatic representation of final system for near surface salinity measurements.

17.4. Validation using the non-toxic supply

As the sensors were observed to be taking some time to equilibrate with the temperature of the sea, it was decided to place them in a bucket being replenished with the underway sea water supply. This had the additional benefit of providing useful validation data as the temperature and salinity of this supply are constantly monitored (see Section 10).

As there was limited variability in the temperature (and salinity) encountered on the trans-Atlantic section the sensors were left in the bucket for the northward leg of the cruise towards Lisbon. These data will provide additional useful validation of the sensors as they show the T/S properties of the surface water from 13:20 on 15th February (27º54.7N, 13º24.6W) to 15:33 on 17th February (35º10.8N, 10º35.8W).

17.5. Results of near surface salinity investigations

The summary data for the handheld CT sensor investigations are detailed in Table 25 for both salinity and temperature. The salinity and temperature values given as 0-10m represent the mean (and standard deviation) of all measurements from surface to 10m depth (but not floater measurements). As such, these values provide a basis of comparing near surface salinity with surface salinity as measured by the floater.

The relationship between the two estimates of SSS and SST from the handheld and that from the ships' underway TSG are shown in Figure 68. The underway TSG data in these plots represent the mean SST or SSS measured in a 20 minute interval either side of the time of the deployment of the handheld sensor. As the handheld system was only deployed when the ship was on station, the values from the TSG effectively remain constant (on the level of precision measured by the handheld probe, i.e. to 1 decimal place).

The values of salinity and temperature of the water in the water bottle annex (WBA) as measured by the underway system and sensors #4 and #5 during the northward cruise between 15th and 17th February are plotted in Figure 67. Whilst the values of temperature seem to be in general agreement, there clearly needs to be further investigation of the new sensors response to salinity.

Table 25: Times, dates, locations and summary data for deployment of handheld CT sensor during D346

Time and Date		CTD Station	Lon	Lat	S float	T float	Salinity 0-10m	Salinity surface	Temperature 0-10m	Temperature surface
1920	08/01/2010	14	76º55.83W	26º30.03N	-	-	36.6±0.0	-	23.8±0.0	-
1415	13/01/2010	34	74º14.71W	26º29.82N	-	-	36.8±0.0	-	24.3±0.1	-
1900	13/01/2010	35	73º56.26	26º30.17	-	-	36.9±0.1	-	24.6±0.0	-
2050	14/01/2010	39	72º27.83W	26º30.15N	-	-	36.8±0.0	-	23.9±0.0	-
1840	15/01/2010	42	71º21.63	26º29.76	-	-	36.9±0.1	-	23.7±0.0	-
1735	16/01/2010	45	70º15.93W	25º42.20N	-	-	36.9±0.0	-	23.7±0.0	-
1730	17/01/2010	48	-68.85	24.5º	-	-	36.9±0.0	-	24.4±0.0	-
1738	18/01/2010	51	66º56.25	24º29.97	-	-	36.9±0.1	-	25.1±0.0	-
1130	19/01/2010	53	65º29.39	24º30.03	-	-	36.5±0.0	-	25.1±0.0	-
1730	19/01/2010	54	64º46.02	24º29.94	-	-	36.5±0.1	-	25.2±0.0	-
1125	20/01/2010	56	63º17.53	24º29.74N	-	-	36.4±0.1	-	25.4±0.0	-
1820	20/01/2010	57	62º33W	24º30N	-	-	36.3±0.0	-	25.4±0.1	-
1225	21/01/2010	59	61º5.38W	24º30.1	-	-	36.5±0.1	-	25.1±0.0	-
1820	21/01/2010	60	60º21	24º30	-	-	36.4±0.0	-	25.2±0.1	-
1300	22/01/2010	62	58º53.55W	24º29.98	-	-	37±0.0	-	24.9±0.0	-
1945	22/01/2010	63	58º9.21W	24º29.89N	-	-	37.1±0.0	-	25±0.0	-
1150	23/01/2010	200	57º3.13077	24º29.8716	-	-	37±0.0	-	24.3±0.0	-
1254	26/01/2010	71	52º50.43W	25º6.91N	37.4	24.3	37.4±0.0	37.4	24.3±0.0	24.3
1800	26/01/2010	72	52 17.37W	25º4.58N	37.2	24	37.3±0.0	37.2	24±0.0	24
1300	27/01/2010	73	51º44.42W	25º1.12N	37.3	23.4	37.3±0.0	37.3	23.5±0.0	23.4
2130	27/01/2010	74	51º11.11W	24º56.20N	37.4	23.7	37.3±0.0	37.4	23.8±0.0	23.7
1205	28/01/2010	76	50º5.37W	24º40.09	36.5	24	37.5±0.0	36.5	24.2±0.0	24
1850	28/01/2010	77	49º32.06W	24º31.25N	37.4	23.7	37.4±0.1	37.4	23.8±0.0	23.7
1130	29/01/2010	79	48º28.42W	24º11.77	37.2	23.7	-	37.2	#DIV/0!	23.7
1720	29/01/2010	80	47º56.10W	24º3.93N	37.3	23.6	37.4±0.1	37.3	23.6±0.0	23.6
1625	30/01/2010	83	46º20.06W	23º52.4N	37.2	23.9	37.4±0.1	37.2	23.9±0.0	23.9
1510	31/01/2010	86	44º43.94W	23º39.98N	37.5	23.8	37.5±0.0	37.5	23.9±0.0	23.8
2005	31/01/2010	87	44º12.39W	23º32.19N	37.1	23.6	37.5±0.0	37.1	23.7±0.0	23.6
1145	01/02/2010	89	43º8.35W	23º22.24N	37.5	23.8	37.5±0.0	37.5	23.9±0.0	23.8
1835	01/02/2010	90	42º35.96W	23º14.96N	37.5	23.8	37.5±0.0	37.5	23.9±0.0	23.8
0900	02/02/2010	92	40º56.30W	23º31.03N	37.6	23.8	37.5±0.0	37.6	23.8±0.0	23.8
1900	02/02/2010	93	40º6.22W	23º40.00N	37.5	23.9	37.5±0.0	37.5	23.9±0.0	23.9
1230	03/02/2010	95	38º25.96W	23º56-05N	37.7	23.6	37.6±0.0	37.7	23.6±0.0	23.6
2050	03/02/2010	96	37º36.21W	24º5.07N	37.5	23.6	37.6±0.0	37.5	23.6±0.0	23.6
1440	04/02/2010	98	35º55.67W	24º21.30N	37.5	23.5	37.6±0.1	37.5	23.5±0.0	23.5
1125	05/02/2010	100	34º24.90W	24º29.64N	37.5	22.8	37.6±0.1	37.5	22.8±0.0	22.8
1550	05/02/2010	202	34º02.95W	24º30.54N	37.6	23.2	37.6±0.0	37.6	23.3±0.0	23.2
2025	05/02/2010	101	33º43.90W	24º29.88N	37.6	23.1	37.6±0.0	37.6	23.1±0.0	23.1
1225	06/02/2010	103	33º21.28W	24º29.37N	37.4	23	37.5±0.1	37.4	23.1±0.1	23
1830	06/02/2010	104	31º41.12W	24º29.95N	37.4	23	37.5±0.0	37.4	22.9±0.0	23
1130	07/02/2010	106	30º19.29W	24º29.51N	37.3	22.85	37.4±0.0	37.3	22.9±0.0	22.85
2033	07/02/2010	107	29º39.42W	24º30.12N	37.5	23.3	37.4±0.0	37.5	23.4±0.0	23.3
1400	08/02/2010	109	28º16.82W	24º29.88N	37.3	22.8	37.3±0.0	37.3	22.8±0.1	22.8
0915	09/02/2010	111	26º55.18W	24º30.98N	37.3	23.2	37.2±0.0	37.3	23.3±0.0	23.2
1545	09/02/2010	112	26º13.40W	24º30.25N	37.2	23.2	37.1±0.1	37.2	23.2±0.0	23.2
1000	10/02/2010	114	24º50.82W	24º30.85	36.9	22.8	37.1±0.0	36.9	22.8±0.0	22.8
1620	10/02/2010	115	24º10.04W	24º30.14N	37.0	22.7	37.1±0.1	37.0	22.8±0.0	22.7
0920	11/02/2010	117	22º52.68W	24º43.25N	37.1	22.4	37.1±0.0	37.1	22.5±0.1	22.4
1515	11/02/2010	118	22º16.04W	24º55.16N	36.9	22.3	36.9±0.0	36.9	22.2±0.1	22.3
1155	12/02/2010	121	20º25.12W	25º32.78N	36.9	22.3	37.1±0.1	36.9	22.2±0.0	22.3
1800	12/02/2010	122	19º47.83W	25º44.58N	37.0	22.8	37±0.1	37.0	22.1±0.2	22.8
1315	13/02/2010	125	17º57.5W	26º22.59N	36.9	21.45	37±0.0	36.9	21.5±0.1	21.45
1935	13/02/2010	126	17º20.08W	26º34.60N	37.1	21.5	37±0.0	37.1	21.5±0.1	21.5
0910	14/02/2010	128	16º5.73W	26º59.13N	37.0	20.8	37±0.0	37.0	20.9±0.0	20.8
1357	14/02/2010	129	15º28.89W	27º12.12N	36.9	20.3	36.9±0.0	36.9	20.4±0.0	20.3
1045	15/02/2010	133	13º33.38W	27º52.01N	36.6	19.4	36.8±0.1	36.6	19.4±0.0	19.4
1325	15/02/2010	134	13º24.55W	27º54.66N	36.5	19.5	36.8±0.0	36.5	19.5±0.0	19.5
1540	15/02/2010	135	13º22.14W	27º55.65N	36.5	19.6	36.8±0.0	36.5	19.5±0.0	19.6

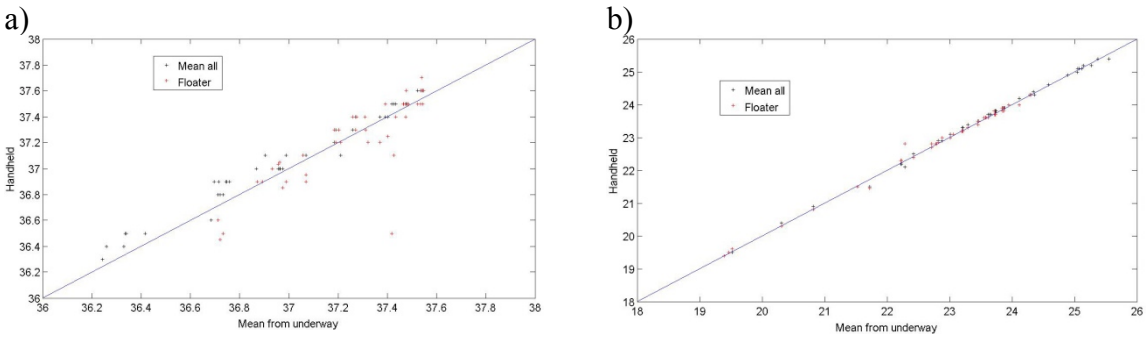

Figure 68: Scatterplots of mean a) SSS and b) SST from the TSG versus results from the handheld CT probe for all deployments. The solid line is the reference line showing equality.

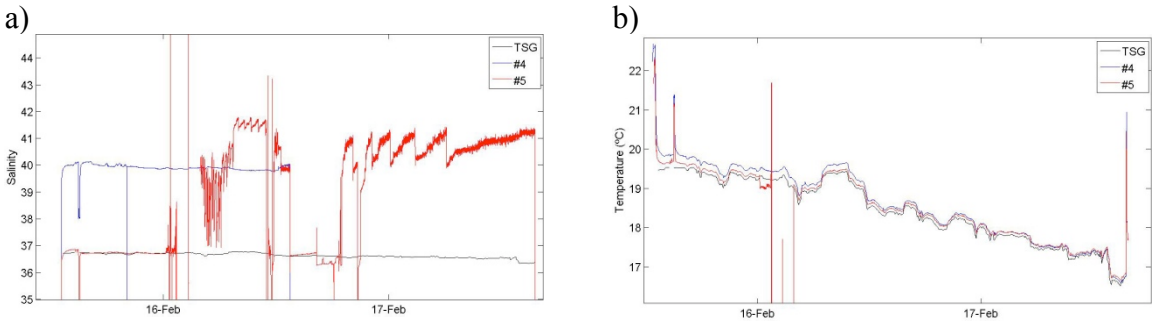

Figure 69: Comparison of a) salinity and b) temperature of water from non-toxic supply in the WBA and from sensors #4 and #5.

Chris Banks

Appendix: Details of Stations Sampled during Cruise D346

										Number of Bottle Samples					
Stn	**Date**	**Time**	**Latitute**	**Longitude**	**Water Dep Corr (m)**	**Max CTD Dep (m)**	**Min Ht off Bot (m)**	**Max Wire-out (m)**	**Max CTD Press (db)**	**Dep**	**Sal**	**Oxy**	**Nut**	**CO2**	**CFC**
	06/01/10	1649													
1	06/01/10	1720	27 50.10	78 50.41	-999	837	15	1851	845	8	19	20	0	12	0
	06/01/10	1758													
	07/01/10	0419													
2	07/01/10	0432	27 20.29	79 56.85	113	103	8	-3	103	3	3	17	3	3	4
	07/01/10	0444													
	07/01/10	0554													
3	07/01/10	0609	27 20.74	79 51.10	265	258	5	-2	260	4	4	19	4	4	4
	07/01/10	0627													
	07/01/10	0751													
4	07/01/10	0815	27 21.11	79 45.29	407	396	9	-2	399	6	6	6	6	6	5
	07/01/10	0840													
	07/01/10	1004													
5	07/01/10	1031	27 20.41	79 40.45	554	541	11	-2	545	7	7	7	7	7	7
	07/01/10	1102													
	07/01/10	1241													
6	07/01/10	1316	27 20.64	79 34.67	741	731	9	-1	737	9	9	9	9	9	9
	07/01/10	1355													
	07/01/10	1533													
7	07/01/10	1552	27 20.66	79 30.14	725	713	10	-2	719	9	9	9	9	9	10
	07/01/10	1626													
	07/01/10	1753													
8	07/01/10	1818	27 20.83	79 25.01	678	662	14	-2	667	9	9	9	9	9	10
	07/01/10	1902													
	07/01/10	2023													
9	07/01/10	2042	27 20.01	79 20.14	587	578	7	-1	583	8	7	7	7	7	6
	07/01/10	2114													
	07/01/10	2231													
10	07/01/10	2247	27 19.94	79 15.03	449	435	12	-2	439	6	6	6	0	6	8
	07/01/10	2307													
	08/01/10	0016													
11	08/01/10	0035	27 20.11	79 12.50	362	350	9	-3	353	5	5	5	5	5	6
	08/01/10	0053													
	08/01/10	0204													
12	08/01/10	0214	27 20.29	79 11.02	256	242	9	-4	244	4	4	4	4	4	5
	08/01/10	0229													
	08/01/10	0401													
13	08/01/10	0408	27 20.08	79 10.45	177	167	7	-4	168	3	3	3	3	3	3
	08/01/10	0418													
14	08/01/10	1854													
	08/01/10	1903	26 30.07	76 56.05	249	246	9	6	248	8	8	8	8	7	7

	08/01/10	1925													
	08/01/10	2035													
15	08/01/10	2109	26 29.94	76 51.89	1318	1221	79	-19	1232	14	14	14	15	9	9
	08/01/10	2208													
	08/01/10	2327													
16	09/01/10	0006	26 31.97	76 48.97	1689	1591	77	-21	1607	16	16	16	16	0	9
	09/01/10	0130													
	09/01/10	0313													
17	09/01/10	0407	26 30.19	76 46.93	2289	2281	80	72	2308	18	16	16	15	10	8
	09/01/10	0525													
	09/01/10	0655													
18	09/01/10	0737	26 29.93	76 48.05	1501	1493	5	-2	1508	15	11	11	11	9	9
	09/01/10	0848													
	09/01/10	1002													
19	09/01/10	1140	26 29.74	76 45.68	3778	3763	3	-12	3822	24	24	23	24	14	15
	09/01/10	1405													
	09/01/10	1612													
20	09/01/10	1743	26 29.95	76 40.96	4574	4561	11	-3	4641	22	21	21	21	14	14
	09/01/10	2028													
	09/01/10	2315													
21	10/01/10	0100	26 29.83	76 37.79	4698	4686	10	-2	4769	22	20	20	20	16	17
	10/01/10	0314													
	10/01/10	0521													
22	10/01/10	0652	26 29.76	76 32.28	4839	4831	7	-2	4919	22	19	20	18	14	13
	10/01/10	0903													
	10/01/10	1348													
23	10/01/10	1522	26 29.02	76 26.60	4837	4826	9	-2	4914	22	23	23	21	16	18
	10/01/10	1748													
	10/01/10	1947													
24	10/01/10	2129	26 29.75	76 18.18	4835	4821	11	-2	4909	22	21	23	24	17	20
	10/01/10	2356													
	11/01/10	0149													
25	11/01/10	0333	26 29.22	76 13.50	4810	4805	4	-1	4892	24	23	21	24	4	18
	11/01/10	0551													
	11/01/10	1350													
26	11/01/10	1520	26 29.75	76 06.52	4805	4794	9	-2	4881	22	23	23	24	17	18
	11/01/10	1745													
	11/01/10	1954													
27	11/01/10	2140	26 30.11	75 54.53	4746	4733	11	-2	4818	24	24	24	24	16	21
	11/01/10	2356													
	12/01/10	0211													
28	12/01/10	0349	26 29.91	75 43.56	4696	4684	9	-3	4768	23	22	22	24	3	4
	12/01/10	0553													
	12/01/10	0756													
29	12/01/10	0928	26 30.03	75 30.53	4687	4677	7	-3	4760	22	21	21	20	16	18
	12/01/10	1136													
	12/01/10	1326													
30	12/01/10	1501	26 29.81	75 18.72	4642	4631	9	-3	4713	23	23	23	22	15	19
	12/01/10	1713													
31	12/01/10	1912													
	12/01/10	2042	26 30.19	75 04.38	4605	4594	9	-2	4675	23	23	24	24	2	5

	12/01/10	2252													
	13/01/10	0051													
32	13/01/10	0224	26 29.80	74 48.25	4538	4526	10	-2	4605	23	23	24	23	16	18
	13/01/10	0437													
	13/01/10	0637													
33	13/01/10	0805	26 29.88	74 31.01	4496	4484	9	-2	4562	24	23	23	23	16	19
	13/01/10	1010													
	13/01/10	1217													
34	13/01/10	1342	26 29.88	74 14.52	4542	4530	10	-2	4609	22	21	21	21	0	1
	13/01/10	1546													
	13/01/10	1801													
35	13/01/10	1935	26 30.98	73 35.14	4918	4901	12	-4	4991	23	21	21	21	16	19
	13/01/10	2148													
	14/01/10	0023													
36	14/01/10	0203	26 30.98	73 35.14	4918	4901	12	-4	4991	23	23	23	23	16	18
	14/01/10	0414													
	14/01/10	0700													
37	14/01/10	0832	26 30.61	73 12.33	5043	5031	10	-2	5125	23	22	21	23	0	6
	14/01/10	1046													
	14/01/10	1320													
38	14/01/10	1501	26 30.35	72 50.49	5132	5123	7	-1	5220	23	23	23	0	17	19
	14/01/10	1718													
	14/01/10	2004													
39	14/01/10	2145	26 30.46	72 27.83	5140	5130	8	-2	5227	23	22	22	22	15	17
	15/01/10	0009													
	15/01/10	0246													
40	15/01/10	0430	26 30.81	72 06.40	5269	5256	11	-2	5356	23	23	22	22	0	0
	15/01/10	0651													
	15/01/10	0936													
41	15/01/10	1117	26 30.82	71 43.13	5378	5364	11	-3	5468	24	24	24	24	16	16
	15/01/10	1415													
	15/01/10	1639													
42	15/01/10	1818	26 29.75	71 21.69	5481	5471	8	-1	5579	23	23	24	24	16	20
	15/01/10	2043													
	15/01/10	2314													
43	16/01/10	0115	26 28.54	71 00.25	5489	5476	11	-2	5584	24	20	20	20	0	5
	16/01/10	0343													
	16/01/10	0715													
44	16/01/10	0856	26 06.16	70 38.03	5503	5489	12	-3	5597	24	24	24	24	16	19
	16/01/10	1141													
	16/01/10	1526													
45	16/01/10	1710	25 41.94	70 15.94	5513	5502	9	-2	5610	23	21	22	21	14	20
	16/01/10	1934													
	16/01/10	2315													
46	17/01/10	0101	25 18.31	69 54.16	5501	5488	10	-3	5595	23	23	23	23	0	10
	17/01/10	0303													
	17/01/10	0658													
47	17/01/10	0842	24 54.27	69 32.15	5593	5583	9	-2	5693	24	24	24	24	17	18
	17/01/10	1049													
48	17/01/10	1435													
	17/01/10	1615	24 30.30	69 09.17	5637	5627	9	-1	5738	23	23	23	22	16	19

	17/01/10	1820													
	17/01/10	2307													
49	18/01/10	0055	24 30.56	68 24.43	5711	5700	9	-2	5815	24	24	24	24	0	0
	18/01/10	0304													
	18/01/10	0804													
50	18/01/10	0946	24 30.50	67 40.20	5716	5705	9	-2	5819	24	23	24	23	17	19
	18/01/10	1154													
	18/01/10	1605													
51	18/01/10	1754	24 29.99	66 56.35	5699	5686	10	-3	5800	24	24	24	24	16	21
	18/01/10	2001													
	19/01/10	0015													
52	19/01/10	0147	24 29.94	66 12.63	5135	5123	11	-2	5218	23	23	23	24	0	8
	19/01/10	0342													
	19/01/10	0757													
53	19/01/10	0958	24 30.10	65 29.36	-999	5436	5	6439	5541	23	23	23	23	16	17
	19/01/10	1204													
	19/01/10	1643													
54	19/01/10	1844	24 29.94	64 46.06	5940	5925	11	-3	6047	24	19	23	23	16	20
	19/01/10	2102													
	20/01/10	0150													
55	20/01/10	0331	24 30.82	64 00.97	5628	5615	11	-2	5727	24	22	22	22	0	15
	20/01/10	0533													
	20/01/10	1006													
56	20/01/10	1142	24 29.73	63 17.51	5802	5789	11	-2	5907	24	24	24	24	17	21
	20/01/10	1341													
	20/01/10	1806													
57	20/01/10	1954	24 30.07	62 33.35	5912	5901	10	-1	6022	24	23	23	23	16	20
	20/01/10	2210													
	21/01/10	0246													
58	21/01/10	0422	24 30.50	61 48.38	5649	5639	9	-2	5751	24	24	24	24	0	4
	21/01/10	0623													
	21/01/10	1024													
59	21/01/10	1203	24 30.10	61 05.07	5882	5871	10	-1	5991	24	24	24	24	16	19
	21/01/10	1407													
	21/01/10	1817													
60	21/01/10	2007	24 29.97	60 20.82	5819	5806	10	-2	5924	24	21	21	21	14	18
	21/01/10	2227													
	22/01/10	0245													
61	22/01/10	0429	24 30.37	59 37.69	5784	5773	8	-2	5890	24	24	24	24	2	3
	22/01/10	0635													
	22/01/10	1959													
62	22/01/10	2138	24 29.88	58 53.78	5851	5839	10	-2	5958	24	23	22	22	17	20
	22/01/10	2341													
	22/01/10	1959													
63	22/01/10	2138	24 30.11	58 09.03	5663	5653	9	-2	5766	24	22	21	22	15	19
	22/01/10	2341													
	23/01/10	0434													
64	23/01/10	0625	24 30.12	57 23.91	6273	6265	9	1	6399	24	24	24	24	5	1
	23/01/10	0900													
200	23/01/10	1120													
	23/01/10	1307	24 29.80	57 03.03	6228	6218	10	0	6350	1	24	24	0	0	0

	23/01/10	1729													
	23/01/10	1957													
65	23/01/10	2148	24 29.35	56 41.38	5840	5821	15	-3	5940	24	24	24	24	16	20
	24/01/10	0023													
	24/01/10	0535													
66	24/01/10	0742	24 28.79	55 56.62	6461	6451	11	1	6592	24	24	24	24	17	20
	24/01/10	1051													
	24/01/10	1834													
67	24/01/10	2026	24 29.78	55 14.33	6107	6097	11	1	6225	24	24	23	24	4	7
	24/01/10	2307													
	25/01/10	0552													
68	25/01/10	0830	24 30.58	54 27.17	5292	5270	21	0	5371	23	23	22	22	17	19
	25/01/10	1047													
	25/01/10	1508													
69	25/01/10	1711	24 30.60	53 56.28	6155	6147	9	1	6277	24	24	24	24	16	21
	25/01/10	1959													
	26/01/10	0046													
70	26/01/10	0251	24 50.35	53 23.96	5931	5919	12	0	6041	24	23	23	24	3	20
	26/01/10	0523													
	26/01/10	0938													
71	26/01/10	1143	25 06.65	52 50.43	5859	5707	18	-134	5821	24	21	20	20	15	18
	26/01/10	1406													
	26/01/10	1730													
72	26/01/10	1926	25 04.80	52 17.41	5529	5517	13	0	5625	23	20	23	22	16	19
	26/01/10	2138													
	27/01/10	1218													
73	27/01/10	1410	25 01.33	51 45.19	6038	6026	10	-1	6152	24	24	23	24	3	0
	27/01/10	1700													
	27/01/10	2032													
74	27/01/10	2212	24 56.24	51 11.11	5784	5768	14	-2	5885	24	23	23	23	15	20
	28/01/10	0022													
	28/01/10	0337													
75	28/01/10	0515	24 47.90	50 37.92	5138	5171	13	1	5268	23	24	24	24	18	21
	28/01/10	0718													
	28/01/10	1038													
76	28/01/10	1232	24 40.12	50 05.40	5593	5581	10	-2	5692	23	21	21	21	1	17
	28/01/10	1450													
	28/01/10	1816													
77	28/01/10	2022	24 31.24	49 32.05	5956	5944	10	-2	6066	24	23	23	23	16	19
	28/01/10	2300													
	29/01/10	0226													
78	29/01/10	0409	24 20.94	49 00.49	5390	5380	8	-2	5484	24	23	23	23	17	17
	29/01/10	0612													
	29/01/10	0937													
79	29/01/10	1115	24 11.76	48 28.38	5287	5274	11	-2	5375	24	21	22	21	2	19
	29/01/10	1312													
	29/01/10	1630													
80	29/01/10	1831	24 03.97	47 56.56	5302	5290	10	-3	5391	24	23	23	23	16	19
	29/01/10	2032													
81	29/01/10	2357													
	30/01/10	0122	23 58.53	47 24.52	4564	4550	99	85	4629	23	21	21	21	0	8

	30/01/10	0343													
	30/01/10	0739													
82	30/01/10	0924	23 53.95	46 52.56	4910	4853	26	-31	4940	23	24	24	24	16	19
	30/01/10	1139													
	30/01/10	1519													
83	30/01/10	1712	23 52.43	46 20.02	5059	5064	6	12	5158	23	21	22	22	15	19
	30/01/10	1908													
	30/01/10	2251													
84	31/01/10	0020	23 46.02	45 48.12	4529	4512	15	-2	4590	22	24	24	24	2	13
	31/01/10	0208													
	31/01/10	0527													
85	31/01/10	0654	23 43.95	45 16.20	4469	4447	21	-1	4523	22	22	22	21	16	15
	31/01/10	0840													
	31/01/10	1232													
86	31/01/10	1401	23 38.13	44 44.12	4419	4407	13	1	4482	21	22	23	22	15	19
	31/01/10	1545													
	31/01/10	1919													
87	31/01/10	2050	23 32.12	44 12.54	4862	4842	15	-5	4929	24	23	23	23	2	16
	31/01/10	2246													
	01/02/10	0218													
88	01/02/10	0401	23 27.00	43 40.31	4870	4854	13	-3	4942	22	24	24	24	17	20
	01/02/10	0554													
	01/02/10	0921													
89	01/02/10	1057	23 22.36	43 08.49	4904	4892	11	-1	4980	22	23	23	23	16	19
	01/02/10	1255													
	01/02/10	1618													
90	01/02/10	1814	23 15.02	42 36.03	5405	5391	12	-2	5495	23	24	24	24	3	7
	01/02/10	2031													
	02/02/10	0144													
91	02/02/10	0312	23 23.08	41 46.14	4593	4518	11	-1	4661	22	24	23	24	15	19
	02/02/10	0504													
	02/02/10	1005													
92	02/02/10	1131	23 31.23	40 56.66	4740	4729	11	0	4813	22	24	24	24	16	20
	02/02/10	1322													
	02/02/10	1830													
93	02/02/10	2017	23 40.03	40 06.50	5421	5410	6	-5	5514	23	21	22	24	3	10
	02/02/10	2219													
	03/02/10	0318													
94	03/02/10	0457	23 47.96	39 15.73	5444	5431	10	-3	5536	23	24	24	24	16	20
	03/02/10	0659													
	03/02/10	1154													
95	03/02/10	1335	23 56.09	38 25.99	5728	5715	10	-3	5829	23	24	23	24	10	18
	03/02/10	1557													
	03/02/10	2050													
96	03/02/10	2235	24 05.37	37 36.66	5238	5227	13	2	5326	22	22	22	24	3	13
	03/02/10	0030													
	04/02/10	0531													
97	04/02/10	0709	24 13.16	36 46.19	5140	5127	10	-3	5223	23	24	24	24	16	20
	04/02/10	0911													
98	04/02/10	1354													

	04/02/10	1542	24 21.80	35 55.64	5766	5753	11	-2	5869	22	23	23	23	16	20
	04/02/10	1755													
	05/02/10	0052													
99	05/02/10	0238	24 30.37	35 05.10	5756	5746	9	-2	5862	24	24	23	24	2	15
	05/02/10	0448													
	05/20/10	0839													
100	05/02/10	1028	24 29.73	34 25.00	6096	6001	76	-19	6125	23	22	21	23	18	20
	05/02/10	1318													
	05/02/10	1534													
202	05/02/10	1639	24 30.37	34 02.78	5968	3500	76	-2392	3552	1	0	24	0	0	0
	05/02/10	1738													
	05/02/10	1928													
101	05/02/10	2106	24 29.77	33 43.71	5350	5347	4	1	5449	24	24	24	24	15	20
	05/02/10	2311													
	06/02/10	0251													
102	06/02/10	0435	24 30.01	33 02.69	5732	5716	13	-2	5831	23	24	24	24	3	8
	06/02/10	0644													
	06/02/10	1035													
103	06/02/10	1218	24 29.64	32 21.44	5649	5632	14	-3	5744	23	20	20	21	14	17
	06/02/10	1425													
	06/02/10	1804													
104	06/02/10	1957	24 29.86	31 40.85	5674	5661	11	-3	5774	24	24	24	24	17	21
	06/02/10	2224													
	07/02/10	0221													
105	07/02/10	0410	24 29.78	31 00.16	5909	5892	14	-2	6013	24	23	23	24	3	0
	07/02/10	0630													
	07/02/10	1039													
106	07/02/10	1229	24 29.52	30 19.29	5409	5398	10	-2	5502	22	22	22	24	15	19
	07/02/10	1512													
	07/02/10	1930													
107	07/02/10	2127	24 30.17	29 39.50	5409	5399	7	-3	5503	24	22	22	20	15	18
	07/02/10	2350													
	08/02/10	0413													
108	08/02/10	0618	24 30.05	28 57.65	5674	5659	12	-3	5772	24	24	24	24	1	6
	08/02/10	0847													
	08/02/10	1303													
109	08/02/10	1523	24 30.05	28 17.27	5645	5633	10	-2	5745	24	24	24	24	13	21
	08/02/10	1750													
	08/02/10	2215													
110	09/02/10	0001	24 29.50	27 35.96	5577	5562	13	-2	5671	24	23	23	24	15	19
	09/02/10	0229													
	09/02/10	0637													
111	09/02/10	0821	24 30.72	26 54.71	5489	5479	8	-2	5586	24	23	23	24	1	11
	09/02/10	1049													
	09/02/10	1502													
112	09/02/10	1643	24 30.60	26 13.50	5390	5377	11	-2	5480	23	23	22	24	14	19
	09/02/10	1904													
	09/02/10	2328													
113	10/02/10	0125	24 30.67	25 32.49	5310	5297	12	-2	5398	23	23	24	23	14	19
	10/02/10	0343													
114	10/02/10	0811													

	10/02/10	0950	24 30.85	24 50.82	5226	5214	10	-2	5312	23	23	23	23	1	0
	10/02/10	1155													
	10/02/10	1558													
115	10/02/10	1739	24 29.99	24 09.88	5128	5117	10	-2	5212	23	22	22	22	11	19
	10/02/10	1940													
	10/02/10	2329													
116	11/02/10	0102	24 29.65	23 30.06	5013	5001	10	-2	5093	23	22	24	20	12	16
	11/02/10	0305													
	11/02/10	0651													
117	11/02/10	0821	24 42.85	22 53.05	4910	4899	9	-2	4989	23	23	23	24	1	12
	11/02/10	1024													
	11/02/10	1407													
118	11/02/10	1537	24 55.12	22 15.94	4767	4756	9	-2	4841	22	23	21	23	13	18
	11/02/10	1728													
	11/02/10	2109													
119	11/02/10	2230	25 08.20	21 39.14	4650	4638	10	-2	4720	23	20	22	22	14	19
	12/02/10	0016													
	12/02/10	0351													
120	12/02/10	0512	25 20.08	21 01.82	4457	4444	9	-4	4520	22	21	21	20	1	13
	12/02/10	0658													
	12/02/10	1032													
121	12/02/10	1148	25 32.75	20 25.11	4284	4271	11	-2	4343	21	21	22	22	13	10
	12/02/10	1334													
	12/02/10	1710													
122	12/02/10	1824	25 44.55	19 47.81	3922	3909	10	-2	3971	22	21	22	21	10	0
	12/02/10	2001													
	12/02/10	2339													
123	13/02/10	0045	25 57.74	19 11.31	3545	3532	10	-2	3586	21	21	20	21	1	0
	13/02/10	0212													
	13/02/10	0553													
124	13/02/10	0658	26 10.06	18 34.43	3442	3431	9	-1	3482	21	23	23	23	12	1
	13/02/10	0832													
	13/02/10	1212													
125	13/02/10	1319	26 22.58	17 57.54	3639	3628	9	-2	3683	22	22	22	22	6	0
	13/02/10	1458													
	13/02/10	1840													
126	13/02/10	1949	26 34.58	17 20.06	3628	3617	9	-1	3673	21	24	24	24	1	0
	13/02/10	2116													
	14/02/10	0105													
127	14/02/10	0214	26 47.39	16 42.90	3617	3608	8	-2	3663	22	24	24	24	5	0
	14/02/10	0349													
	14/02/10	0720													
128	14/02/10	0826	26 59.31	16 05.81	3481	3468	10	-3	3520	21	23	24	24	0	0
	14/02/10	0959													
	14/02/10	1338													
129	14/02/10	1444	27 11.83	15 28.98	3104	3092	10	-2	3136	22	21	22	21	1	0
	14/02/10	1611													
	14/02/10	1950													
130	14/02/10	2047	27 24.87	14 52.12	2605	2594	9	-2	2628	20	24	24	24	0	0
	14/02/10	2203													
131	15/02/10	0149													

	15/02/10	0231	27 37.37	14 14.21	2034	2023	9	-2	2046	18	18	24	24	0	0
	15/02/10	0332													
132	15/02/10	0632													
	15/02/10	0704	27 47.37	13 46.63	1446	1435	9	-2	1449	16	14	22	22	0	0
	15/02/10	0815													
133	15/02/10	1015													
	15/02/10	1040	27 52.00	13 33.37	1120	1107	11	-2	1118	14	14	22	22	0	0
	15/02/10	1122													
134	15/02/10	1302													
	15/02/10	1320	27 54.68	13 24.61	555	542	11	-2	546	10	10	15	20	0	0
	15/02/10	1348													
135	15/02/10	1525													
	15/02/10	1541	27 55.65	13 22.15	356	343	11	-2	345	8	8	15	24	0	0
	15/02/10	1601													